



## Durham E-Theses

---

# *An Evaluation of a Hydrological Model Used to Predict the Impact of Flow Attenuation on Downstream Flood Flows*

PORTER, ROBERT,ANDREW,I-HSIEN

### How to cite:

---

PORTER, ROBERT,ANDREW,I-HSIEN (2011) *An Evaluation of a Hydrological Model Used to Predict the Impact of Flow Attenuation on Downstream Flood Flows* , Durham theses, Durham University.  
Available at Durham E-Theses Online: <http://etheses.dur.ac.uk/813/>

### Use policy

---

The full-text may be used and/or reproduced, and given to third parties in any format or medium, without prior permission or charge, for personal research or study, educational, or not-for-profit purposes provided that:

- a full bibliographic reference is made to the original source
- a [link](#) is made to the metadata record in Durham E-Theses
- the full-text is not changed in any way

The full-text must not be sold in any format or medium without the formal permission of the copyright holders.

Please consult the [full Durham E-Theses policy](#) for further details.

---

Academic Support Office, Durham University, University Office, Old Elvet, Durham DH1 3HP  
e-mail: [e-theses.admin@dur.ac.uk](mailto:e-theses.admin@dur.ac.uk) Tel: +44 0191 334 6107  
<http://etheses.dur.ac.uk>

**An Evaluation of a Hydrological Model Used to Predict  
the Impact of Flow Attenuation on Downstream Flood Flows.**

Robert Andrew I-Hsien Porter

Thesis submitted for the degree of Master of Science by research.

Department of Geography, University of Durham.

May, 2011. 1 volume.

# **An Evaluation of a Hydrological Model Used to Predict the Impact of Flow Attenuation on Downstream Flood Flows.**

I-Hsien Porter

## **Abstract**

A number of recent high magnitude events have shown that fluvial flooding has increasingly detrimental impacts on people and properties. There is a perception that flood risk is increasing due to several factors, including urbanisation of floodplains and climate change. This has created a need to assess the potential of using the natural function of floodplains, to slow and temporarily store water, as a means of mitigating downstream flooding.

This project applied and assessed a reduced complexity hydrological model called *Overflow*, which was used to predict the impact of flow attenuation on downstream flood flows. The model behaviour was theoretically consistent with physical processes, allowing it to be calibrated for the River Seven, North Yorkshire for a flood event in June 2007.

At the catchment scale, multiple, spatially distributed flow attenuation measures were shown to reduce downstream peak flood flows. However, any individual intervention could have a positive, neutral or negative impact on downstream flooding by affecting the timing and synchronicity of hydrographs from different tributaries. This demonstrated the importance of the specific geographic location of interventions.

The results were compared with a hydraulic model, HEC-RAS, which is a standard tool for flood hazard prediction in the UK. HEC-RAS is not without its own uncertainties however, so the aim of the model comparison was to benchmark *Overflow* against an established model, rather than validating the model with respect to reality. At the reach scale, *Overflow* was less sensitive to an increase in flow resistance than HEC-RAS, so it will under-predict the effects of flow attenuation. However, *Overflow* predicted higher magnitude hydrographs than HEC-RAS. This was due to the inclusion of lateral overland flow routing in *Overflow*, which could not be simulated in HEC-RAS. Further model development is required to integrate *Overflow's* predictions of overland flow with boundary conditions for hydraulic models.

This thesis therefore provides a framework for the assessment of flow attenuation as a flood risk management tool, in the case of an extreme event, on the River Seven, North Yorkshire.

## Contents

List of Tables .....	vii
List of Figures .....	viii
List of Equations.....	x
List of Abbreviations and Symbols .....	xi
Statement of copyright .....	xiii
Acknowledgements.....	xiv
1. Introduction .....	1
1.1. Overview .....	1
1.2. Flood management in the UK .....	1
1.3. Project justification .....	4
1.4. Substantive research objectives .....	7
1.4.1. The impact of flow attenuation .....	7
1.4.2. Numerical model evaluation.....	11
1.5. Thesis structure.....	13
2. Numerical modelling.....	15
2.1. Summary .....	15
2.2. Justification .....	16
2.3. General assumptions and limitations .....	18
2.4. Model choice.....	19
2.5. Overflow.....	21
2.5.1. Model background .....	21
2.5.2. Assumptions and limitations.....	21
2.5.3. Model description .....	23
2.6. Summary .....	32
3. Test case: the River Seven and June 2007 flood.....	33
3.1. Summary .....	33
3.2. The River Seven Catchment .....	33
3.2.1. Catchment description.....	33

---

3.2.2.	Justification of choice of catchment .....	38
3.3.	Flood research in Ryedale .....	38
3.4.	The June 2007 Flood .....	39
3.4.1.	Justification of choice of event .....	42
3.4.2.	Justification of choice of rain gauge.....	43
3.5.	Summary .....	45
4.	Model evaluation .....	46
4.1.	Summary .....	46
4.2.	Introduction to sensitivity analysis, calibration and uncertainty analysis.....	47
4.2.1.	Sensitivity analysis .....	47
4.2.2.	Calibration.....	47
4.2.3.	Uncertainty analysis.....	48
4.3.	Sensitivity analysis .....	49
4.3.1.	Model output .....	49
4.3.2.	Overview of sensitivity analysis methods.....	51
4.4.	Local sensitivity analysis.....	53
4.4.1.	Method.....	53
4.4.2.	Results.....	56
4.4.3	Local sensitivity analysis summary.....	63
4.5.	Global sensitivity analysis .....	64
4.5.1.	Method.....	64
4.5.2.	Results.....	66
4.6.	Discussion of sensitivity analysis.....	77
4.7.	Calibration.....	78
4.8.	Conclusion.....	81
5.	Catchment response to intervention measures .....	83
5.1.	Summary .....	83
5.2.	Catchment riparian intervention measures (CRIMS).....	84
5.2.1.	Introduction .....	84

---

5.2.2.	Large woody debris (LWD) dams .....	85
5.2.3.	Riparian buffer strips .....	86
5.2.4.	Representing CRIMS in the model .....	86
5.3.	Experiment design .....	88
5.3.1.	Individual CRIM impacts.....	90
5.3.2.	Combined effects test.....	91
5.3.3.	Removal of negative reaches.....	91
5.4.	Results.....	93
5.4.1.	Individual CRIM test.....	93
5.4.2.	Combined effects.....	94
5.4.3.	Removal of negative reaches.....	97
5.4.4.	Location of the interventions.....	99
5.5.	Uncertainty analysis.....	100
5.5.1.	Method.....	100
5.5.2.	Results.....	102
5.6.	Discussion.....	107
5.7.	Conclusion.....	108
6.	Model comparison .....	110
6.1.	Summary .....	110
6.2.	Justification of model comparison.....	111
6.3.	HEC-RAS .....	114
6.3.1.	Background .....	114
6.3.2.	Process representation .....	114
6.3.3.	Parameters.....	116
6.3.4.	Key assumptions .....	116
6.4.	Method .....	117
6.4.1.	Model construction.....	117
6.4.2.	Sensitivity analysis .....	118
6.4.3.	Calibration.....	120

---

6.4.4.	Comparison with <i>Overflow</i> .....	121
6.5.	Results.....	124
6.5.1.	HEC-RAS validation and calibration .....	124
6.5.2.	Comparison with <i>Overflow</i> .....	128
6.6.	Discussion.....	139
6.7.	Conclusion.....	140
7.	Summary and conclusions .....	141
7.1.	Thesis summary .....	142
7.1.1.	Quantify the impact of flow attenuation measures in isolation.....	143
7.1.2.	Understand the combined effects of multiple, spatially distributed interventions.....	144
7.1.3.	Assess the uncertainty in the results resulting from the selection of parameter values to represent flow attenuation measures (CRIMS).....	145
7.1.4.	Assess <i>Overflow's</i> representation of physical processes in relation to observed data, theoretical understanding of catchment processes and a different model conceptualisation, HEC-RAS.....	145
7.2.	Project limitations .....	147
7.2.1.	Manning's $n$ and flow attenuation.....	147
7.2.2.	Wider applicability of the results.....	148
7.3.	Overall conclusions .....	149
	References .....	152
	Appendix 1: Index of Manning's $n$ values .....	162
	Appendix 2: Frequently used terms and definitions.....	164



## List of Tables

Table 2.1 Key parameters and a description of their roles.....	31
Table 3.1 Summary catchment characteristics.....	35
Table 3.2 Peak-over-threshold series .....	37
Table 3.3 Recorded rainfall for the 24 hours from midnight, 25 <sup>th</sup> June 2007 .....	40
Table 3.4 Comparison of rain gauge and discharge observations for the June 2007 flood. ....	44
Table 4.1 Parameters and the values used in the local sensitivity analysis.....	53
Table 4.2 Dimensionless sensitivity index results.....	63
Table 4.3 Summary model responses for global sensitivity analysis.....	66
Table 4.4 Summary model responses for global sensitivity analysis with constant rainfall rate	68
Table 5.1 Flow attenuation interventions and their representation in <i>Overflow</i> . ....	90
Table 5.2 Reaches that caused a reduction or no change in peak discharge downstream.....	93
Table 5.3 Peak discharge reduction achieved with all reaches used in combination.....	97
Table 5.4 Summary results for each type of intervention .....	103
Table 5.5 Confidence intervals due to $n$ value uncertainty .....	104
Table 5.6 Percentage confidence intervals due to $n$ value uncertainty .....	104
Table 5.7 Confidence intervals due to rainfall rate and runoff rate uncertainty .....	105
Table 5.8 Peak discharge reduction, with confidence intervals .....	106
Table 6.1 Summary of characteristics of the reaches tested in HEC-RAS.....	122
Table 6.2 Confidence intervals due to $n$ value uncertainty .....	128
Table 6.3 Difference in peak discharge between <i>Overflow</i> and HEC-RAS .....	133
Table 6.4 Change in peak discharge downstream. ....	133
Table 6.5 Analysis of peak discharge at reach inlet and outlets in <i>Overflow</i> .....	135
Table 6.6 Difference in peak discharge between the two models, with flow attenuation .....	137

## List of Figures

Figure 1.1 A hypothetical flood hydrograph .....	5
Figure 2.1 Flow chart summarising the overall method .....	16
Figure 2.2 Conceptual diagram showing the different routing algorithms. ....	26
Figure 2.3 A hypothetical time map.....	28
Figure 2.4 Time maps to demonstrate the effect of the rainfall rate parameter.....	28
Figure 2.5 Contributing areas of the catchment.....	30
Figure 3.1 Sketch map of the catchment of the River Seven to Normanby .....	34
Figure 3.2 Daily rainfall totals recorded at the Brown Howe rain gauge.....	40
Figure 3.3 Hourly rainfalls for the 25 <sup>th</sup> June 2007 storm .....	41
Figure 3.4 Stage hydrograph recorded at Normanby for 25th June 2007 flood. ....	42
Figure 4.1 A hypothetical discharge hydrograph.....	50
Figure 4.2 The River Seven at Sinnington .....	54
Figure 4.3 Hydrographs and measures of model response to channel Manning's n. ....	57
Figure 4.4 Hydrographs and measures of model response to land cover Manning's n. ....	57
Figure 4.5 Hydrographs and measures of model response to rainfall rate .....	59
Figure 4.6 Hydrographs and measures of model response to runoff rate. ....	60
Figure 4.7 Hydrographs and measures of model response to multiples of channel depth. ....	61
Figure 4.8 Hydrographs and measures of model response to multiples of channel width.....	61
Figure 4.9 Nash Sutcliffe Efficiency for each parameter.....	62
Figure 4.10 Peak discharge response.....	69
Figure 4.11 Time to peak response.....	70
Figure 4.12 Overbank flood volume response.....	71
Figure 4.13 Nash Sutcliffe Efficiency index and its response.....	72
Figure 4.14 Peak discharge response with constant rainfall rate.....	73
Figure 4.15 Time to peak response with constant rainfall rate.....	74
Figure 4.16 Overbank flood volume response with constant rainfall rate .....	75
Figure 4.17 Nash Sutcliffe Efficiency and its response with constant rainfall rate.....	76
Figure 4.18 Calibrated model hydrograph.....	80
Figure 4.19 Input rainfall rates and the sequence of rainfall rate parameters .....	81
Figure 5.1 Artificially constructed large woody debris dam. ....	85
Figure 5.2 The River Seven drainage network .....	89
Figure 5.3 Hypothetical results for CRIMS applied to a combination of reaches.....	92
Figure 5.4 Reaches that, individually, had a positive, neutral or negative impact.....	93
Figure 5.5 Results of the combined effects test .....	96

---

Figure 5.6 Cumulative effects of interventions.....	97
Figure 5.7 Results of the combined effects test once negative reaches had been removed.....	98
Figure 5.8 Location of the reaches tested in combination with each other.....	98
Figure 5.9 Ranking of interventions.....	119
Figure 6.1 Reaches modelled in the HEC-RAS sensitivity analysis.....	133
Figure 6.2 Discharge hydrograph for the tributary above Normanby.....	119
Figure 6.3 Location of the reaches tested in HEC-RAS.....	121
Figure 6.4 Sketch maps of the reaches and cross sections modelled in HEC-RAS.....	123
Figure 6.5 Summary statistics of HEC-RAS hydrograph sensitivity.....	127
Figure 6.6 Response of hydrographs to variations in Manning's $n$ .....	127
Figure 6.7 Calibrated HEC-RAS hydrograph.....	128
Figure 6.8 Hydrographs at the reach inlets and outlets.....	131
Figure 6.9 Hydrographs at the reach inlets and outlets with flow attenuation measures.....	132
Figure 6.10 Downstream hydrographs predicted by each model.....	138

## List of Equations

Standard notation has been used and is defined in the relevant captions. A list of frequently used abbreviations and symbols is given in the next section for reference.

Equation 1.1 Continuity equation.....	3
Equation 1.2 Manning equation .....	8
Equation 2.1 Empirical relationship between width and discharge.....	25
Equation 2.2 Empirical relationship between depth and discharge.....	25
Equation 2.3 Continuity equation.....	27
Equation 2.4 Manning equation .....	27
Equation 2.5 Combination of the continuity and Manning equations. ....	27
Equation 2.6 Rearrangement of Equation 2.5 to make depth the subject.....	27
Equation 2.7 Manning equation, with depth substituted for hydraulic radius. ....	27
Equation 2.8 Total discharge at a point .....	29
Equation 4.1 Dimensionless Nash Sutcliffe Efficiency ( <i>NSE</i> ).....	50
Equation 4.2 The sensitivity index, <i>SI</i> . ....	55
Equation 4.3 Calculation of a probability density function ( <i>PDF</i> ). ....	65
Equation 5.1 Expression of a value with confidence intervals. ....	101
Equation 5.2 Standard error. ....	101
Equation 5.3 Statement of a confidence interval. ....	101
Equation 5.4 Confidence interval with uncertainty from two sources.....	102
Equation 6.1 The continuity equation, in the form taken in the Saint Venant equations.....	114
Equation 6.2 The dynamic equation, in the form taken in the Saint Venant equations. ....	115
Equation 6.3 Friction slope .....	115
Equation 6.4 Energy head loss, $h_e$ .....	115
Equation 6.5 Statement of a confidence interval .....	124

## List of Abbreviations and Symbols

The meaning of each abbreviation or symbol is also defined at the relevant point in the text. Page numbers refer to the first appearance of each symbol in the thesis.

For some abbreviations, units are not applicable (n/a). Likewise, some symbols are used to refer to a generic measured quantity (e.g. a model response), so units depend on the exact application (denoted by '-').

Frequently used terminology is defined in Appendix 2.

Symbol	Meaning	Units	Page number
$A$	Area	$m^2$	27
$A_t$	Area of the catchment time map within time bands 0 to $t$	$m^2$	27
Cumecs	Cubic Metres per Second	$m^3s^{-1}$	3
CRIMS	Catchment Riparian Intervention Measures	n/a	84
$d$	Depth	m	3
Defra	Department for the Environment Food and Rural Affairs	n/a	1
DEM	Digital Elevation Model	n/a	23
EU	European Union	n/a	4
LWD	Large Woody Debris	n/a	9
$n$	Manning's roughness parameter	$sm^{-1/3}$ , but considered dimensionless	27
$N$	Number of observations or simulations	n/a	101
$NSE$	Nash Sutcliffe Efficiency	dimensionless	50
$O$	Empirical observation	-	50
OAT	One at a time (sampling)	n/a	53
OD	Ordnance Datum	n/a	33
$P$	Model prediction	-	50
PDF	Probability Density Function	n/a	65
$Q$	Discharge	$m^3s^{-1}$	3
$Q_t$	Discharge at time $t$	$m^3s^{-1}$	29
$R$	Hydraulic radius	m	27
$r$	Rainfall	mm	29

$r_t$	Rainfall falling over $t$ hours after the start of the event.	mm	29
$S$	Slope	dimensionless	27
$SI$	Sensitivity Index	dimensionless	55
$t$	Time	hours or seconds, depending on application	29
$v$	Velocity	$\text{ms}^{-1}$	3
$w$	Width	m	3
$x$	A continuous random variable	-	65
$x_{best}$	Mean and best estimate of a variable	-	101
$y$	A continuous random variable	-	102
$\delta x$	Change in the continuous random variable, $x$	Same units as $x$	101
$\sigma_x$	Sample standard deviation	Same units as the dataset	101

## **Statement of copyright**

The copyright of this thesis rests with the author. No quotation from it should be published without the prior written consent and information derived from it should be acknowledged.

---

## Acknowledgements

Thanks are due to a number of people for their help throughout this project.

Primarily, I would like to thank my supervisors, Prof. Stuart Lane and Dr. Richard Hardy of the Department of Geography, Durham University, for their continued guidance and support. Thanks are also due to Dr. Nick Odoni, also of Durham University, for developing the *Overflow* model and his advice throughout this project.

Likewise, I am grateful for data and other information provided by Forest Research and Environment Agency staff working on the Forestry Commission's *Slowing the Flow at Pickering* project, and also to the U.S. Army Corps of Engineers for developing and making available the HEC-RAS model.

Finally, I would like to thank my parents, family, friends and the students and staff of St John's College for their generous support throughout my time at Durham.

The research was funded through a bursary of The Institute of Hazard, Risk and Resilience, Durham University.



## 1. Introduction

### 1.1. Overview

In the UK, numerical modelling is the standard method for making predictions about fluvial flood risk (Tayefi et al., 2007). In recent years, increasing emphasis has been placed on flood management strategies that make use of the natural function of river floodplains in slowing and storing floodwater (Fleming, 2002; Defra, 2004). This requires models that are capable of simulating the effect of multiple, interacting interventions over large spatial scales (Ivanović and Freer, 2009). However, simplifications in process representation and limitations on data availability at such scales result in uncertainty in model outputs. As a result, uncertainties exist in both the impact of flow attenuation on downstream flooding and the accuracy of the models used to simulate these effects.

The aim of this project was to evaluate a hydrological model, which was used to predict the impact of flow attenuation on downstream flood flows. Four specific objectives presented themselves:

- (1) Quantify the impact of flow attenuation measures in isolation.
- (2) Understand the combined effects of multiple interventions.
- (3) Assess the uncertainty in the results resulting from the selection of parameter values to represent flow attenuation.
- (4) Assess the model representation of physical processes in relation to observed data, theoretical understanding of catchment processes and a different model conceptualisation, HEC-RAS.

This introductory chapter discusses the rationale and aims of this project. A general review of the literature is undertaken in relation to the research aims. However, further specific literature reviews are included in later chapters where relevant to the research. This chapter begins by discussing flooding and the pressures facing flood management in the UK. This is further developed into the motivation for the project and four specific research objectives. Finally, the structure of the rest of the thesis is outlined.

### 1.2. Flood management in the UK

River flooding is a natural process, but one that has increasingly detrimental impacts on human lives and livelihoods. After a number of recent high magnitude events, such as in Boscastle (2004),

Carlisle (2005), Yorkshire and the Midlands (2007) and Cockermouth (2009), there is a perception that the risk posed by flooding is increasing (Pitt, 2008).

Flood risk is a product of the consequences of a flood and the probability of a flood event occurring (Alexander, 2002). In recent decades, the potential consequences of flooding have increased. Urban development on river floodplains is exposing greater numbers of people and properties to flooding (Crichton, 2005): for example, one-quarter of properties inundated in severe floods in June-July 2007 were built within the past 25 years (Pitt, 2008). This has led to disruption, some loss of life and rising economic damages: the 2007 floods are estimated to have caused over £3 billion of insured damage (Pitt, 2008; Environment Agency, 2010b). In the future, the probability of flood events occurring is forecast to increase. The magnitude and frequency of flooding in the UK is expected to rise in response to long term climate change (Thorne et al., 2006). Various studies have predicted that winter precipitation totals and summer precipitation intensity will increase (Arnell, 1998; Hulme et al., 2002; Murphy et al., 2009), raising the prospect of increases in flood magnitude of up to 20 % by 2050 (Wheater, 2006). This thesis focuses on techniques to reduce flood magnitude, hence the probability of a flood of a given size occurring.

The physical processes by which a flood event occurs can be conceptualised into sources, pathways and receptors (Evans et al., 2004). This conceptual framework links the weather-related source events that input water into the system, through the pathways by which water is transferred, to the built and natural assets that are affected by flooding.

The conventional approach to flood management focuses on defending flood receptors: in the UK, this was initially agricultural land to protect food supplies, but subsequently people, homes and businesses on the floodplain (Brown and Damery, 2002). This is in line with flood policies that were formerly predominantly preventative, urban-focused and politically visible (Johnson et al., 2007). Engineered structures are used to accommodate the additional discharge of a flood event within river channels by increasing their depth (e.g. building embankments able to accommodate high water levels) or by increasing the rate at which excess water is conveyed away from the area at risk (e.g. artificially straightening river reaches) (von Lany and Palmer, 2007).

However, although hard engineering has been largely successful in protecting receptors of flood risk (Werritty, 2006), the damage caused by recent flood events has demonstrated that this is not always the case. In the summer 2007 floods, of the flood defences that were affected by flooding, 50 % were overtopped because they had not been built to accommodate the extreme magnitude of the event (Pitt, 2008). These events, alongside increases in flood risk due to climate change (Evans et al., 2004) and floodplain development have called into question the cost-benefit ratio of conventional approaches to flood management. The cost of engineered defences can be very high, although they may only benefit relatively few people (Environment Agency, 2009).

Engineered defences are difficult to sustain and many are nearing the end of their designed lifespan (Brown and Damery, 2002). Modifying river channels to cope with rare flood events (such as a 1:100 year flood) takes the channel out of equilibrium with normal flow regimes. This may disrupt sediment transport; for example, widening channels reduces stream power per unit bed area. Consequently, the ability of the river to entrain and transport sediment is reduced, leading to aggradation and a rise in bed level (Brookes, 1997). As a result, hard engineered approaches often need continual maintenance, which generates additional economic costs and disturbance to the local environment. While engineered defences may be successful in locally reducing flood risk, the Environment Agency estimates that there are 2.4 million properties at risk of river and coastal flooding in England and Wales (Environment Agency, 2009). It is not viable, due to their economic and environmental cost, to introduce engineered flood defences everywhere (Atkins, 2005). For example, for 2010-11, the Environment Agency has allocated £570 million (71% of its annual spending on flood and coastal risk management) to build and maintain flood defences (Environment Agency, 2009).

An additional drawback of hard engineering is that by conveying floodwater away from a locality more rapidly, flood problems are transferred downstream (Fleming, 2002). Engineered defences cause an increase in local flow velocity, since water is more likely to be contained within the channel by embankments or straightened sections of river, where there is less resistance to flow. Given that if the mass of water is to be conserved, the continuity equation (Ferguson, 1986) states that:

$$Q = w d v$$

**Equation 1.1 Continuity equation**

where  $Q$  = discharge ( $\text{m}^3\text{s}^{-1}$  or 'cumecs'),  $w$  = width (m),  $d$  = depth (m) and  $v$  = velocity ( $\text{ms}^{-1}$ ), an increase in velocity must lead to a local reduction in width or depth, reducing the risk of overbank flooding. However, this increase in velocity implies a reduction in flow attenuation, so the peak discharge at a point downstream rises. This may increase the magnitude and duration of overbank flows downstream, in turn necessitating further flood management interventions.

The tendency for engineered defences to have detrimental impacts on downstream flood risk can be problematic given the rising number of properties on floodplains, particularly in areas where settlements are dispersed throughout the catchment (Crichton, 2005). More recent paradigms in flood policy have therefore been driven by a need for flood mitigation that is cost-effective and that can manage flooding over large areas of land, with consideration of the effects of interventions on the wider catchment (Fleming, 2002).

These priorities have led to a shift away from seeing defence-orientated solutions as the only strategy to manage flood problems. Hard engineering is often successful in defending local areas

from flooding and is likely to continue to play a part in flood management (Fleming, 2002). However, a range of options must be considered to find flood risk management strategies that are appropriate to particular contexts. Current policy now focuses on; (1) making space for water – restoring the natural function of floodplains to provide flood protection elsewhere; and (2) living with the impacts of flooding, where the costs of interventions in the river system outweigh the associated benefits for flood risk reduction (Johnson et al., 2007). The Department of Environment, Food and Rural Affairs' *Making Space for Water* policy emphasises flood risk management that is 'integrated' with both these objectives – upstream-downstream linkages in the drainage network and wider policy (Defra, 2004). Given increasing pressures on floodplain land for urban development and the impacts of individual defence schemes on the wider drainage network, flood management cannot solely depend on localised defences, but must integrate local needs with catchment scale planning and management (Fleming, 2002). This is promoted by legislation such as the Flood and Water Management Act (2010), which creates new responsibilities for the Environment Agency to manage flooding at a national level (Defra, 2010). Legislation such as the EU Water Framework Directive and Habitat Directive also drives a need to reconcile flood management with the multiple needs of all river users and stakeholders, such as conservation, recreation and ecology (Lane et al., 2007b).

There is therefore a need to mitigate flooding in a way that is cost-effective and sustainable, that benefits large numbers of people and recognises the potential for detrimental effects downstream, and that is compatible with the other uses of rivers such as recreation or ecological habitat. Historically, hard engineering has been reactive to flood events or the perceived threat of flooding. In a dynamic environment, in which changes in flood magnitude and the potential consequences of flooding are uncertain, engineered responses are therefore difficult to sustain (Sear et al., 1995). If flood management is to be integrated across river catchments and with multiple policy objectives, it must be proactive in mitigating the causes of flooding, rather than reacting to flood impacts alone (von Lany and Palmer, 2007). This has created a need for research to better understand the processes that cause flooding and how floods can be mitigated. This must also incorporate an understanding of how interventions in one part of a river catchment impact upon areas further downstream (Fleming, 2002).

### 1.3. Project justification

Floods occur when water levels exceed the local capacity of the river channel (Lane et al., 2007a). Flood hazard is therefore a product of water level, which in turn is controlled by; (1) the volume of water entering a river reach, from upstream precipitation and catchment runoff (the flood source); and (2) the capacity of the channel to contain that discharge (as a flood pathway).

A number of studies have focused on flood sources, such as climate change impacts on extreme precipitation events (Wheater, 2006), and hydrological pathways, notably the role of land use in generating and conveying runoff to the drainage network (Posthumus et al., 2008; Parrott et al., 2009). Clearly, without a source event to act as a trigger and mechanisms to deliver water to rivers, river flooding would not occur. However, there has been less research into the impact of hydraulic pathways on flood risk (Raven et al., 2009), despite empirical (Burt, 1989; Stover and Montgomery, 2001; Pinter and Heine, 2005) and modelling evidence (Acreman et al., 2003) of their importance in controlling local flooding and transmitting flood risk downstream. For example, on the Lower Missouri River, Pinter and Heine (2005) found, for a given discharge, a rising trend in flow stages over time. This indicates that it is not only the magnitude of source events that controls water stage and hence the likelihood and extent of overbank flow. Since Pinter and Heine's (2005) analysis was for an equal discharge, the variability in stage was attributed to the effect of changes in channel morphology on the way that water is partitioned between flow depth, width and velocity. Similarly, on the Skokomish River, Washington, Stover and Montgomery (2001) observed that despite dam-regulated flows, overbank flood frequency increased coincidentally with changes in channel morphology. This example highlights that interventions to regulate the amount of water entering a reach from upstream are still modified by local processes operating throughout the river pathway.

If, as discussed, engineered flood defences add to problems downstream by speeding up river flow (Fleming et al., 2001), then it might be possible to mitigate flood problems downstream by slowing, or attenuating, flow. The aim of attenuating water upstream, such that the passage of flood water takes place over a much longer time period, is to reduce the magnitude of the peak discharge at critical points further down the river network (Shaw, 1994), Figure 1.1.

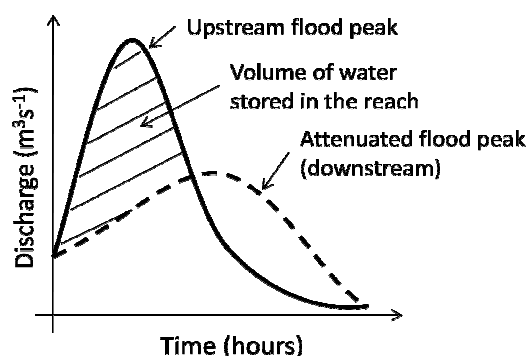


**Figure 1.1** A hypothetical flood hydrograph. The solid line shows the hydrograph as it enters the river network, the dotted line shows the attenuated hydrograph at a point downstream. The total discharge (the area under the curves) is the same for the upstream and downstream hydrographs, but in the case of the attenuated hydrograph it has been distributed over a longer period of time, so the peak magnitude is lower. The shaded area shows the volume of water that is stored within the river network over time.

A number of approaches have been considered (Defra, 2004), but all operate on the basis of reducing the magnitude of the flood peak by storing water or slowing the downstream passage of the flood hydrograph (Thomas and Nisbet, 2007). One approach is to temporarily store water in floodplain areas where flooding is acceptable (e.g. low value pasture land) for the duration of a flood event, in preference to areas of land where flooding is not acceptable (e.g. towns and cities) (Lane et al., 2007b). However, such an approach requires water levels to be sufficiently high for floodwater to be transferred onto the floodplain in flood-acceptable areas. This can be achieved by increasing flow resistance, causing a reduction in flow velocity and hence increasing flood attenuation. The continuity equation (Equation 1.1) states that, for a given discharge, any reduction in velocity must lead to an increase in width or depth. Since flow width is limited by the width of the channel, a reduction in velocity will primarily lead to an increase in flow depth for a given discharge. This reduces the discharge required for an overbank flow to occur. For example, in one modelling study on the River Cherwell in Oxfordshire, Acreman et al. (2003) compared modelled water levels for a given discharge, in the presence and absence of flow attenuation. It was found that floodplain water levels rose by 0.6 – 1.5 metres in response to channel restoration and flow attenuation. Higher water levels suggest an increase in the probability and extent of overbank flow, and Acreman et al.'s study indicates that this may be attributed to a reduction in flow velocity.

Floodplain storage has additional ecological benefits. In the event of an overbank flow, allowing rivers to reconnect to their floodplains generates temporary low velocity floodplain habitats, which provide refugia for aquatic animals during high velocity in-channel flood flows (Wydoski and Wick, 2000). Managing rivers for ecological objectives, such as under the EU Habitats Directive, often involves measures to promote habitat diversity that also serve to increase resistance to flow. For example in the restoration of the River Idle, Nottinghamshire, flow deflectors, bankside vegetation and riffles were imported to increase flow variability and habitat diversity (Downs and Thorne, 2000). As a result, the water depth associated with a given discharge increased; hence overbank flow (flood) frequency also increased (Downs and Thorne, 2000). Understanding how activities that reduce flow velocity can also be used to manage flood risk allows multiple policy objectives to be achieved simultaneously.

If floodplain storage is given, particularly in the case of a permanent impoundment or reservoir, some reduction in downstream flood magnitude can be expected. Attenuation of flood water throughout the river channel network may also contribute to reductions in downstream peak flows, even in the absence of overbank flows and floodplain storage (Lane and Thorne, 2007). There is therefore a need for interventions that attenuate floodwater flow, by reducing flow velocity. Natural processes that slow the flow tend to be dispersed throughout the catchment and, individually, have a low impact on catchment scale flow characteristics (Lane et al., 2007b).

The magnitude of the impact of flow attenuation on downstream flows increases as these multiple small scale effects are accumulated throughout the catchment (Parrott et al., 2009). However, due to a large number of processes operating throughout catchment flow pathways (Lane, 2003a), it is difficult to relate interventions that are widely dispersed across the catchment to flood risk downstream (Jackson et al., 2008). The uncertainties involved have, so far, limited the use of flow attenuation as a practical flood management tool (Thomas and Nisbet, 2007).

In summary, river flood management now considers the sources and pathways that cause flooding, rather than only defending receptors. Flow attenuation is one approach that can be used to reduce peak flow magnitudes downstream. However, the magnitude of these reductions is uncertain due to the river pathway processes that modify the flood hydrograph between where reductions in flow velocity take place and downstream receptors (Lane et al., 2007b). It is still, nonetheless, the reduction in water levels at flood receptors that is of concern in flood management. This project aims to evaluate the impact of flow attenuation interventions on downstream flood flows, and to evaluate the uncertainties in a numerical model used to predict these impacts.

#### **1.4. Substantive research objectives**

The research objectives of this project are to:

- (1) Quantify the impact of flow attenuation measures in isolation.
- (2) Understand the combined effects of multiple interventions.
- (3) Assess the uncertainty in the results resulting from the selection of parameter values to represent flow attenuation.
- (4) Assess the model representation of physical processes in relation to observed data, theoretical understanding of catchment processes and a different modelling approach, using HEC-RAS.

Research objectives (1) and (2) relate to understanding the impact of flow attenuation on downstream flood flows so are justified together in the next section (section 1.4.1). Objectives (3) and (4) involve an evaluation of the model, so are discussed separately in section 1.4.2.

##### **1.4.1. The impact of flow attenuation**

The previous section has established the need for interventions that increase flow attenuation by reducing flow velocity. Flow velocity is understood to a high level of detail in the three spatial dimension and time (Hardy, 2008). However, at the scale of a river catchment and flood event,

there is often a lack of observed data required to describe flow in such detail (Lane et al., 1999). A number of equations have been developed to relate flow velocity to other hydraulic characteristics, which can be easily measured; for example, the Chezy, Darcy-Weisbach and Manning equations (see Knighton, 1998). Of these, the Manning equation (Equation 1.2) has been widely used in flood modelling studies and commercial modelling software due to its relatively straightforward relationship with other hydraulic variables (Whatmore and Landström, 2009).

The Manning equation (Manning, 1891) relates flow velocity to the hydraulic radius of flow, water surface slope and a roughness parameter:

$$v = \frac{R^{2/3} S^{1/2}}{n}$$

**Equation 1.2 Manning equation**

Where  $v$  = velocity ( $\text{ms}^{-1}$ ),  $R$  = hydraulic radius (m),  $S$  = slope and  $n$  = Manning's roughness parameter. Manning's  $n$  has theoretical units of  $\text{sm}^{-1/3}$  (seconds multiplied by metres to the power of  $-\frac{1}{3}$ ) but for practical purposes these have no real physical meaning. Throughout this project, Manning's  $n$  is considered dimensionless. Strictly speaking, hydraulic radius is the cross sectional area divided by wetted perimeter of the flow (Evans et al., 2008). However, in channels that are relatively wide for their depth, such as many rivers in the UK, the width component of cross sectional area and the width component of the wetted perimeter approximately cancel out, so hydraulic radius can be assumed to be approximately equal to flow depth (Yu and Lane, 2006a).

The Manning equation is not without its shortcomings. For example, if  $n$  is considered dimensionless (as is frequently the case in flood studies), the equation is not dimensionally balanced (Ferguson, 1986). The Manning equation has also been criticised as a simplification of many interacting physical processes (e.g. Lane, 2005). However, this study considers catchment scale flooding. This requires a means of understanding flow characteristics in the absence of a complete knowledge of small-scale variations in related parameters. It is the ability of the Manning equation to provide reliable, albeit approximations, of flow characteristics on easy to measure data that has led to its frequent use in practical studies of flooding and hydraulic engineering (Whatmore and Landström, 2009).

Equation 2.1 shows that in order to achieve a reduction in flow velocity and flow attenuation, hydraulic radius ( $\approx$  depth) or slope must decrease, or roughness must increase. The first two of these options are not practical solutions for flood management. A change in channel geometry to either; (1) reduce flow depth (by increasing channel width to accommodate more water) or, (2) reduce channel slope, would require extensive engineering. This would have subsequent detrimental effects on sedimentation: in both cases the ability of the river to entrain and transport sediment would be reduced (Brookes, 1997). On the assumption that channel width is



fixed over the timescale of a flood event, the continuity equation (Equation 1.1) implies that a simultaneous reduction in flow depth and velocity could only occur if discharge were reduced. However, to reduce the discharge delivered to the channel network would require attenuation and storage across the catchment land surface. While some studies have shown the potential benefits of land use in attenuating flow before it is delivered to rivers (e.g. Posthumus et al., 2008; Parrott et al., 2009; Hess et al., 2010), such interventions require the cooperation of a large number of land owners and may be costly to implement. As a result, this project focuses on flow attenuation by reductions in flow velocity within the river channel itself. To this end and on the assumption that the Manning equation is a reasonable approximation of flow velocity, the most practical way to reduce river flow velocity is by measures that increase the roughness parameter, Manning's  $n$ .

Manning's  $n$  represents the resistance to flow and consequent energy loss and flow attenuation caused by skin friction, form drag or obstructions, often referred to as channel 'roughness' (Lane, 2005; Lane and Thorne, 2007). Sources of flow resistance are found naturally in rivers in the form of irregularities of the channel bed surface, variation in channel width or depth, obstructions, vegetation or channel meandering (Cowan, 1956). Any combination of these factors can therefore be used to influence flow attenuation (Odoni and Lane, 2010). However, at high flows, small scale sources of roughness take up a smaller proportion of the flow and hence make a lower contribution to flow resistance and attenuation (Ferguson, 2007). This may be the case in large channels where high flows can 'submerge' the effects of roughness (Ferguson, 2007). However, the Manning equation shows that the effects of roughness are related to both flow velocity and hydraulic radius (Equation 1.2). In smaller, upland channels velocity and hydraulic radius tend to be smaller. As a result, flow resistance due to roughness is important in smaller channels and could be used a method to attenuate flows in, for example, upland tributaries to a main river (Evans et al., 2008).

For the purposes of flood flow attenuation, it is necessary to implement measures that cause flow resistance at high flows. Larger scale sources of resistance, such as vegetation and other obstructions, are therefore considered. For example, both vegetation (Darby, 1999) and large woody debris dams (Wilcox et al., 2006; Wilcox and Wohl, 2006) attenuate flow by form drag or by generating turbulence (Lane and Thorne, 2007). This can be achieved at low cost, for example, by the reduction of channel maintenance. Large woody debris (LWD) refers to large tree branches that fall into or across the channel and trap sediment and smaller debris, forming a semi-permeable 'dam'. Although river vegetation and LWD dams occur naturally, they have also been reinstated and trialled as a means for reducing downstream flood magnitude. A series of studies have established their potential contribution. A demonstration site on the River Devon, Scotland showed that LWD and riparian vegetation could reduce flow velocity by up to 13 % and result in

the equivalent of 34 % more water storage (Johnson, 2007). In another study that looked at how flow attenuation was transmitted downstream, Acreman et al. (2003) found that when flow was attenuated, peak flows downstream were reduced by 10–15% (Acreman et al., 2003). Flow attenuation can therefore be successfully implemented to store excess water during a flood event and reduce downstream flood magnitude.

However, despite research demonstrating the impact of flow attenuation on downstream flood magnitude, challenges remain as to where to locate such interventions within a river catchment. Even in relatively small catchments, there are many potential locations for channel interventions. The extent to which LWD attenuates flood water is dependent on site-specific features of the river channel and floodplain, such as the existing channel size and morphology (its ability to contain high discharges) and floodplain topography (which controls flow routing and hence areas that water can flow into). Some locations may therefore be more effective at attenuating and temporarily storing floodwater than others.

Flow attenuation also affects the timing of the flood wave, so attenuation of a flood wave in one tributary or sub-catchment may be countered by flows arriving in the main river from other sub-catchments (Lane et al., 2007b). For example, Lane (2003a) demonstrated by a statistical analysis of flood records on the River Ouse, Yorkshire, that the relative timings of flood hydrograph contributions from tributary sub-catchments impacted on peak discharge and water levels further downstream at York. If flow attenuation interventions were sited such that they synchronised the arrival of flood waves from different tributaries, they may increase water levels and hence flood magnitude downstream (Odoni and Lane, 2010). Thus it is not only the type or amount of management interventions that affects flood risk, but also their location within the catchment, alongside the location and intensity of precipitation events (Lane, 2003a; Lane, 2008).

It is therefore necessary to identify the optimum locations in the catchment network where flow attenuation will have the most beneficial impact on downstream flood risk, in terms of reducing peak water levels. This must also recognise that, due to the possibility of coincident flood waves, any combination of interventions may increase, decrease or have no effect on downstream flood magnitude (Odoni and Lane, 2010).

However, it is also recognised that different rainfall events do not necessarily have the same spatial properties. This is particularly the case for large catchments with many sub-catchments. As a result, there is uncertainty associated with the potential impact of flow attenuation in a given combination of river reaches, in different events. One of the limitations of the modelling approach used in this project is the assumption that rainfall can be applied homogeneously across the catchment (the reasons for this assumption are discussed further in 2.5.2). This may mask some of the uncertainty arising from spatial variability in rainfall. However, it is still informative to

compare change due to flow attenuation interventions, albeit with limitations on the applicability of the findings to different rainfall events.

#### 1.4.2. Numerical model evaluation

The research objectives discussed in the previous section require a large number of combinations of interventions to be tested. Since the number of possible interventions is large and flood events in any given river are relatively rare, it is not possible to make direct measurements of the impact of different interventions during a flood event. Also, it is the interaction of many interventions throughout the drainage network that is of interest, which would require an extensive measurement programme across the catchment. Since it is not practical to use direct observations, these objectives must be addressed using a numerical model. Models incorporate an understanding of flow processes, using mathematical equations to represent flow behaviour (Lane, 1998). This allows the prediction of flow characteristics, such as peak water levels during a flood, at the scale of a river catchment and in response to many combinations of interventions (Lane and Bates, 2000).

In the physical sciences, the 'real world' is understood as governed by a set of laws; for example, the continuity of mass or momentum (Saltelli et al., 2008). The role of a numerical model is to represent this behaviour through numerical rules or equations. However, there are many methods by which laws governing the 'real world' can be translated into numerical equations in a model (Saltelli et al., 2008). As a result, it is possible to construct many different model representations of a physical system. It is therefore possible to arrive at the same conclusions by many different routes (Beven, 1996). Often, the modelling approach is dictated by the purpose for which the model will be used, resulting in limitations to or assumptions about how physical processes are represented. These assumptions may limit the amount of information that can be gleaned from model predictions; for example, the precision with which results can be interpreted, or their wider applicability to different places or times. Chapter 2 discusses the purpose for which the model used in this project has been designed, and the simplifications of physical processes that have been in model construction.

Although the theoretical behaviour of river flows is well understood and can be represented with a high level of complexity (Lane, 1998; Hardy, 2008), much of this detail is not relevant to predicting flood risk at the catchment scale. It therefore does not justify the increase in computational resources and work required to collect additional boundary condition data (Lane et al., 1999). As a result, it is common for practical applications of flood research to use models that are based on a theoretical understanding of flow, but are simplified in some way (Tayefi et al.,

2007). Faster computation times allow a large number of interventions to be tested. Since this project aimed to test a large number of interventions, a reduced complexity model was used.

In 2008, Durham University were contracted by Forest Research (the research division of the UK Forestry Commission) to develop a reduced complexity model to test multiple interventions at the scale of a river catchment (Odoni and Lane, 2010). It is this model, *Overflow*, that will be used in this project. The simplified process representation means that the model requires limited boundary condition data and has faster computation times, allowing multiple scenario testing.

However, by reducing the level of detail that is explicitly represented in the model's constituent equations, it becomes necessary to introduce parameters. Parameters are constants in the model equations, which aim to account for a loss of complexity. One parameter of particular significance in this study is Manning's  $n$  (Equation 1.2). Manning's  $n$  is used to represent the impact of flow attenuation, without needing to explicitly represent the complexities of flow around large woody debris and other features. The selection of parameter values is uncertain, often based on the subjective personal experience of the researcher involved (Evans et al., 2001) or by calibration of model predictions to an observed case (Bates and Anderson, 2001). There can then be a range of acceptable parameter values, which generate a range of acceptable model results (Beven, 1989). However, by comparing the results with an observed flood event, it is possible to establish whether the model parameter values are representative of known physical processes (Bates et al., 1996).

However, calibrating parameter values to one event does not necessarily validate the model to predict the results of subsequent changes to parameter values. As a result, information on the expected physical behaviour of the catchment is required to inform whether variations in parameter values can be used to generate a model response that is representative of the real world.

The third and fourth research objectives of this project are to evaluate model behaviour. First, a sensitivity analysis was undertaken. The model was run multiple times and parameter values were varied between each successive simulation. The results were used to assess whether model behaviour was theoretically representative of expected 'real world' behaviour, in response to variation in the physical processes represented by those parameters. A further discussion of the physical processes operating in the catchment is given in the context of the study site, in Chapter 3. The sensitivity analysis was used to indicate whether varying parameter values could allow the model to be used predicatively; namely to predict the impact of flow attenuation measures.

Second, model predictions were compared to observed data. This assessed the accuracy with which the model replicated an observed event. The comparison of modelled to observed data allowed the calibration of parameter values to represent the 'baseline' scenario, i.e. the catchment at the time of the observed flood event. The impact of attenuation measures were

assessed relative to this base case. However, this process does not validate the model's ability to predict change. Following an analysis of the effect of interventions to slow flood flows, model uncertainty was examined. The aim of this investigation was to assess the level of model precision and the relative significance of flow attenuation.

## 1.5. Thesis structure

In this introductory chapter, the background and objectives of the project have been introduced. Flood risk needs to be managed in a way that is cost-effective and can benefit large numbers of people, without detrimental environmental impacts. One method that has already been trialled is the use of large woody debris and vegetation to attenuate river flow and reduce downstream flood magnitude. However, uncertainties remain in establishing the optimum locations for flow attenuation in a given catchment. A numerical model, *Overflow*, was used to test the impact of different combinations of interventions on downstream flood magnitude. However, the simplified process representation requires the model to be compared to observed data to establish the validity of the results. In order to verify the mathematical equations used to represent flow behaviour, *Overflow* will also be compared to another model with different constituent equations that include a higher level of process representation.

Chapter 2 discusses the need for numerical modelling and the limitations of such an approach. The rationale, conceptual basis and constituent equations of the *Overflow* model are described in greater detail.

Chapter 3 introduces the catchment that was investigated in this project: the River Seven, North Yorkshire. A review of recent flood research in the area is given. Chapter 3 also describes the available data from a flood event during June 2007, which will be used as the 'test scenario' for the model.

Chapter 4 addresses research objective (1). First, the process of model evaluation is introduced. *Overflow* was tested against observed data to ensure that it is capable of replicating observed flow behaviour and to optimise the selection of parameter values. The optimum parameter values were then selected to represent the River Seven during the June 2007 flood. This provided the base case against which the impact of attenuation measures could be assessed.

In Chapter 5, the model was applied to answer research objectives (2) and (3). The chapter gives a discussion of measures that can be implemented to attenuate flow and how they are represented in the model, with reference to the relevant literature. *Overflow* was used to predict the impact of individual flow attenuation interventions on downstream flood flows was predicted. Next, the combined effect of interventions was examined. This information was used to map the optimum locations within the catchment for flow attenuation. Finally, in answer to research objective (4),

an uncertainty analysis on the parameter values used to represent flow attenuation was undertaken to quantify the level of error in the results.

Chapter 6 develops the model evaluation further by comparing a sample of results from *Overflow* against a model with a greater level of process complexity (HEC-RAS). The aim was to establish whether the reduced complexity model *Overflow* has a sufficient level of process representation to accurately represent the processes of relevance during this catchment and event.

The results of this study are discussed in Chapter 7, with the purpose of drawing conclusions in answer to the research objectives. The limitations of this study and the methods used are examined and, in light of this, overall conclusions to the project are presented.

## 2. Numerical modelling

### 2.1. Summary

Floods are rare events and hence difficult to observe. The research objectives stated in Chapter 1 require a method to predict the impact of interventions during a flood event in the absence of direct empirical measurements. This chapter introduces numerical modelling as the method for answering the research aims and objectives.

The chapter begins with a discussion of numerical modelling as a method for achieving the aims of this project, with reference to its methodological limitations. Next, the objectives of the study (Chapter 1) were used to justify the choice of *Overflow*, a hydrological model, for use in this project. The background, data needs and operation of the model is described. It is the aim of this section to describe the functions of *Overflow* in a way that is relevant to this research. The model is still under development and a fuller description of the numerical scheme may be found in Odoni and Lane (Forthcoming).

It is concluded that, despite a number of simplifying assumptions, numerical modelling is the only practical method for undertaking catchment scale research in flooding and spatially distributed interventions. Due to the uncertainty associated with model simplifications, two models based on different representations of physical processes were selected for use in this project. Details of how the models were applied to a specific catchment and flood event to test the effects of interventions are given in later chapters. The purpose of this chapter is to introduce the methodological approach and the models used in this research.

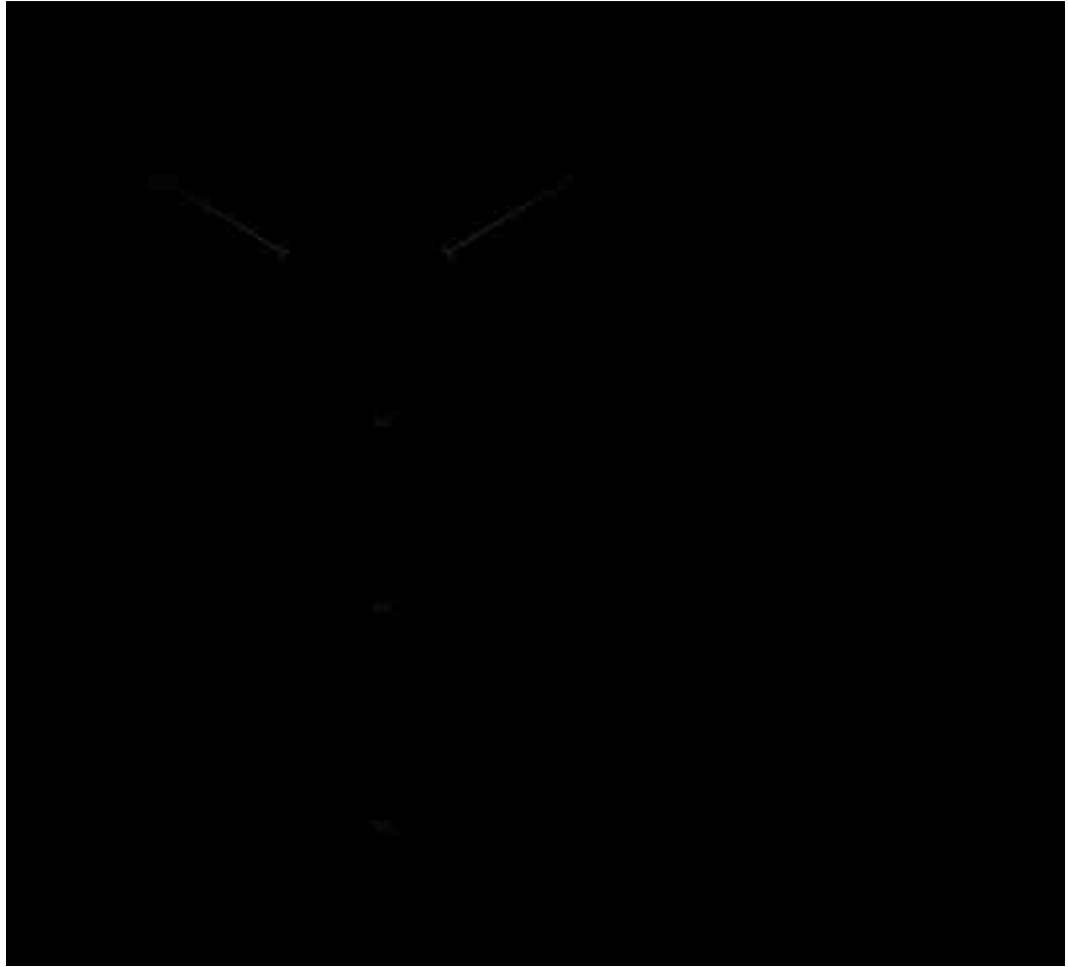


**Figure 2.1** Flow chart summarising the overall method for the research project, in answer to the research objectives in Chapter 1.

## 2.2. Justification

In order to answer the research questions, a relationship between intervention measures in any given reach and downstream flood risk is required. Many catchments in the UK do not have sufficient density of empirical data to describe the spatial distribution of hydrological processes and where data collection does take place, it is often limited to point-based measurements (Beven, 2000; Marks and Bates, 2000). Measuring individual processes and features may not allow generalisations to any point in the catchment. Nor may it be representative of the interaction of multiple processes at the catchment scale. Numerical modelling can supplement empirical measurements, since physical laws allow flow characteristics to be calculated at any point in space and can take account of the interaction of processes at larger scales (Lane and Bates, 2000). Finally, if the purpose of the study is to identify reaches where effective interventions can be made for flood management, modelling is necessary for predictive purposes because empirical experiments with controlled conditions are not possible in real rivers or at the catchment scale (Mulligan, 2002).



Typically in science, theoretical statements that describe the properties of or interactions between objects are used to generate hypotheses that can be directly tested by observations (Rhoads and Thorn, 1996). However, at the catchment scale, the natural environment is too complex to be managed in this way, so it must be reduced or simplified. In this sense, a model is a simplified description of the real world that can be used to replicate natural processes (Thorn, 2003).

Many studies have used statistical relationships between observations of variables as a means of elucidating cause and effect (Burt, 1989; Lane, 2003a; Pinter and Heine, 2005). For the purposes of explaining the statistical patterns, these observations may be related to pre-existing theories. However, statistical relationships cannot be reliably extrapolated to situations that are not represented by the datasets on which they are based. Since floods are extreme events, and hence rare, in many catchments there are a lack of long, consistently measured datasets on which statistical generalisations can be made. Since hydrological measurements tend to be point-based and hence biased to conditions at a particular place, observations may not be representative of the wider catchment (Beven, 2000). For example, in the UK, rain gauges tend to be located near to settlements for functional purposes (Kirchner, 2006).

Even if it were possible to fully observe the system at every point in space and time, the complexity of the natural environment might introduce noise and uncertainty that is not fully understood, which makes the observations difficult to interpret (Richards, 1996; Young et al., 1996). In hydrology, variables are often autocorrelated: for example, a flood event may be influenced by ground saturation resulting from preceding flood events. This causes difficulties in directly relating changes in flood risk to the unique combination of processes operating in a particular catchment and event (Jackson et al., 2008).

If observations are scarce or difficult to interpret, then a model must be based on physical laws that govern the behaviour of the system (Young et al., 1996). These physical laws are expressed as mathematical equations that can be solved to make predictions about the response of particular outputs of the system (e.g. water levels in a river channel) to inputs or forcing factors (e.g. a rainfall event).

Process based numerical models are necessary in flood research due to their predictive ability, in the sense that they allow a researcher to understand and make statements about the probable behaviour of the natural environment, without needing complete empirical evidence. In this project, numerical models are necessary as they allow:

1. Experiments to predict the effect of individual processes in isolation (Mulligan and Wainwright, 2002). In the case of this project, the impact of an intervention on downstream flood risk can be assessed in isolation from other variables such as the size and intensity of rainfall, antecedent conditions etc.

2. Predictions about how processes interact over large scales, where empirical measurements are not sufficient (Lane and Bates, 2000). For example, understanding how much an intervention might slow floodwaters in a particular tributary does not inform us whether floodwater arriving from several tributaries might become synchronised and worsen flooding downstream (Lane et al., 2007b).
3. Predictions about events that have not yet happened – we cannot test interventions in real life as it would be too costly and time consuming to experiment with interventions in different combinations of reaches, nor would the controlling factors of successive observed flood events be identical (Mulligan 2004).
4. Predictions about the response of the system at any point in space – flow and rain gauges are relatively sparse so it is not possible to make observations of flooding at the density required (Marks and Bates, 2000).

However, empirical data are still required to make physical models and their mathematical equations representative of a particular place and time; in particular, the conditions used to define the boundary conditions, such as the input of water from rainfall or flow from upstream. The processes that generate rainfall or flow outside the system are not explicitly modelled, but are specified from observations to define a particular event. Physical numerical models are therefore not independent of empirical data. Thus the role of modelling is to mediate between the observations that are available (e.g. the discharge recorded entering and leaving a river reach) and theoretical knowledge (e.g. the conservation of mass) (Morton, 1993). However, empirical observations are often uncertain and affected by the complexities of the real world. Since it is this information that is also used to constrain numerical models, uncertainties in observed data also have implications for uncertainties in model predictions. The accuracy and precision of model results are therefore dependant on the quality of observed input data. Issues relating to data availability and quality are further discussed in the context of the test catchment, in Chapter 3.

### 2.3. General assumptions and limitations

Constructing a model representation of a natural system involves simplifications, which requires decisions to include or exclude processes. These decisions are dependent on perceptions of what is important in a particular catchment and for the purposes of a particular study. Consequently, it may not be possible to generalise model results to other catchments or events, since they are partly an artefact of the decisions about which processes to include (Lane, 2003b).

If models are to be used to make predictions about places or events because it is not possible to make empirical measurements, then there are no empirical measurements by which we can establish whether the model is giving correct answers (Konikow and Bredehoeft, 1992). A

necessary part of a modelling study is therefore to assess uncertainty in the model results: the variability in model predictions caused by the existence of a range of possible model boundary conditions and parameter values.

In numerical models, there are therefore significant uncertainties in both the representation of processes and the representation a real world setting in which those processes operate. Given this uncertainty, the results of this study are not prescriptive solutions for managing flood risk. Nor are the results intended to be generalised beyond the test case of the River Seven; modelling is not a substitute for empirical data collection, since empirical data is required to provide the model with boundary conditions that describe the specific catchment under investigation. However, by assessing the model sensitivity to individual causal processes at a range of scales, the research will contribute to the scientific understanding of flow attenuation as a means to mitigate river flooding.

## 2.4. Model choice

In the UK, under section 105 of the Water Resources Act 1991, the Environment Agency undertakes flood risk mapping for all rivers in England and Wales, in order to inform flood management policies (Hamer and Mocke, 2002). For example, the UK government's *Planning Policy Statement 25* states that local and regional planning authorities must undertake flood risk assessments at all stages in the process of planning developments as an essential pre-requisite for flood risk management and reduction (HMSO, 2006). Numerical models form an important part of this approach as they allow the prediction of future flooding under different scenarios (e.g. climate change), or in areas where there is no measured flood data (Lane, 2003b). This has driven the development of a wide range of software packages and methods that can be used in flood risk assessment (Evans et al., 2001).

Despite the range of models available, there is no real consensus as to the level of complexity required to adequately represent a catchment for the purpose of flood risk management (Tayefi et al., 2007). This is not because of limitations in process understanding, as the physical laws that control flow are well understood and have been established in the form of the Navier-Stokes equations since the nineteenth century (Hardy, 2008). However, to apply these equations in three or even just two dimensions requires long computation times and excessive amounts of data (e.g. of river geometry), so it is unfeasible for modelling at the scales of river catchments. The uncertainty associated with selecting parameter values to account for this lack of observed data is such that little predictive ability is lost in simpler representations of the system (Romanowicz and Beven, 1998; Perrin et al., 2001). Thus reduced complexity models may still be sufficiently realistic

for predictive purposes, while also allowing greater clarity in understanding processes and the response of the system (Young et al., 1996).

A distinction is drawn between hydrological models, which represent how flow is routed over the land surface after falling as rain, and hydraulic models, which represent the behaviour of water once it is channelled into rivers. Hydraulic flow can be represented by the Navier-Stokes equations or simplifications thereof. In practice, hydrologic models are used to determine the probability of events of different magnitudes, while hydraulic models use this information to transform flows into water levels that can be used to estimate inundation extent (Odoni and Lane, In preparation).

In this project, testing the effects of flow attenuation on downstream flood risk necessitates catchment scale modelling, in order to predict how interventions in a combination of reaches interact (Lane and Bates, 2000). Because there are many possible combinations of interventions, this project requires a model that has a short run time and is easy to set up for each simulation, allowing multiple scenarios to be tested. The available boundary condition data are collected at a low spatial density, since rain and flow gauges tend to be sparse in comparison to the processes that must be modelled (Beven, 2000). For a catchment scale study, the only available data to characterise the input of water to the model are rainfall data. It is rare for flow gauges to be located in the upper reaches of a catchment at a density required to characterise the contributions of many separate tributaries (Kirchner, 2006). The required output is a measure of flow characteristics at the downstream location, which is commensurate with the observed gauge data so that model predictions can be compared to an empirical measurement (Chapter 4).

A hydrologic model is necessary to represent how rainfall is routed overland and into river channels. A number of well-established hydrologic models could have been used, such as CRUM3 (Lane et al., 2009) or TOPMODEL (Beven et al., 1984). However, CRUM3 must be set up manually for each set of interventions and has long run times of several hours per simulation (Odoni and Lane, 2010). In TOPMODEL, topographic data is lumped at the scale of sub-catchments, so the model cannot simulate small scale spatially distributed interventions (Beven et al., 1984). These models are therefore ill-suited to testing many combinations of flow attenuation interventions. A reduced complexity hydrologic model, *Overflow* (Odoni and Lane, 2010), was selected as it was able to perform rapid catchment scale simulations on the basis of limited data and predict a discharge hydrograph at any point in the catchment (Ryedale Flood Research Group, 2008).

## 2.5. Overflow

### 2.5.1. Model background

*Overflow* is a MATLAB-based hydrologic routing model, developed at Durham University by Dr. Nick Odoni. The model was created as part of the Rural Economy and Land Use Programme *Knowledge Controversies* project, 2007 – 2010, to enable affected residents and stakeholders to participate in the decision making process surrounding flood management (Ryedale Flood Research Group, 2008).

As a result, the model development was informed by problems and solutions relating to flood management in specific rural catchments. *Overflow* was therefore developed to run with minimum information requirements, but to be capable of modelling a wide range of management options.

The main aims of *Overflow* are to be:

1. Quick to run and able to allow simple implementation of different interventions, in response to suggestions made by competency group members involved in the *Knowledge Controversies* project.
2. Able to simulate out-of-bank diffusive flow routing, so that floodplain flow effects in response to land management can be modelled.
3. Spatially distributed over two dimensions, but able to simulate a flood hydrograph at any point in the catchment.

*Overflow* has minimal data requirements so the necessary topographic and flow data are readily available as a result of previous work as part of the *Knowledge Controversies* project. Unlike many generic modelling software programmes, *Overflow* was developed specifically to test the catchment scale impact of land and river management options on flood routing, in upland rural catchments. As a result, decisions about the processes that have been included or excluded from the model representation of the system have been made with a similar catchment and purpose to this project in mind. The model's reduced complexity and low computational demands allow fast catchment scale simulations.

The impact of flood management interventions will be assessed in terms of their impact on the flood hydrograph at a downstream location.

### 2.5.2. Assumptions and limitations

In the UK, high river flows usually begin with high rainfall; in particular, frontal and orographic storms in winter and convective storms in summer (Newson, 1975). As a rainfall event progresses, the catchment land surface becomes saturated and overland flow begins. The time taken for the

land surface to become saturated depends on variables such as soil and geological characteristics, antecedent conditions and precipitation intensity (Burt, 1989). Surface runoff is then routed, under gravity, into river channels.

Overflow was designed for short, high flow (flood) events in wet catchments, such as upland catchments that experience frequent rainfall (Odoni and Lane 2010). As a result, a number of assumptions about hydrological behaviour can be made. However, these assumptions limit the applicability of the model to other situations.

In wet catchments, the soil is likely to be already highly saturated before the start of a rainfall event. As a result, overland flow will begin soon after the start of a rainstorm. Upland catchments in particular are also characterised by steep topography, which increases the speed at which surface runoff is conveyed, under gravity. Consequently, the catchments for which *Overflow* was designed tend to have a rapid 'flashy' response to rainfall events (a steep rise and fall in the downstream flood hydrograph).

Since groundwater flow responds more slowly than surface runoff, groundwater is unlikely to contribute significantly to the peak of the flood hydrograph downstream. Additionally, in wet catchments, the proportion of rainfall that is lost to infiltration or groundwater flow is likely to be small. It is therefore assumed that all flows are overland. Groundwater flow is not explicitly represented, although losses to groundwater flow by infiltration and percolation may be accounted for by adjustments to a runoff rate parameter. Although this assumption is reasonable for single events, as in this project, it limits the applicability of the model to situations in which groundwater flow may be an important component of the hydrograph; for example, long duration or series of events.

The spatial characteristics of rainfall are variable. They may also be expected to change between events and during a single event. However, rainfall observations tend to be point based, at rain gauges, so data characterising the spatial variability of rainfall are rare (CEH, 2008). As *Overflow* was initially designed to allow the input of local knowledge into a flood modelling study, it was designed with moderately sized catchments (a few hundred square kilometres) in mind. As such, the spatial variability of rainfall is likely to be limited in comparison to a large catchment system. The model assumes that rainfall is spatially homogenous. It is acknowledged that this is a generalised representation of the rainfall conditions. In particular, there may be inaccuracies in the timing and magnitude of flow contributions from sub-catchments or tributaries. However, this project aims to predict the impact of flow attenuation relative to a base case scenario. As a result, the way in which the rainfall input is represented is of less concern than the ability of the model to represent the processes by which that rainfall is routed overland. As a reduced complexity model, one of the principal aims of *Overflow* was to be of practical use in situations such as these, where there is limited data availability. However, there would be greater uncertainties if the

model were applied for the purpose of predicting the spatial distribution of flood water. In Chapter 3, the available data is assessed in relation to river gauging within the study catchment.

These assumptions allow a reduced level of process representation in *Overflow*, resulting in lower computational requirements. However, this necessitates the use of parameters, constant numbers in the model's constituent equations, to account for processes and information that are not otherwise explicitly represented. The selection of parameter values generates uncertainty in the model outputs.

### 2.5.3. Model description

#### 2.5.3.1. Overview of data needs

*Overflow* calculates flow routing using hydrological routing algorithms and equations for the continuity of mass and flow velocity. To perform these calculations, the model requires information about the catchment elevations and gradients, volumes of water entering the catchment as rain and parameters that account for flow resistance and runoff. In this project, *Overflow* was applied to the case of River Seven, North Yorkshire and the June 2007 flood, which is described and justified in Chapter 3. The purpose of this section is to introduce the processes involved in the model set-up and flow routing.

To characterise the catchment land surface, the model requires topographic data in the form of a Digital Elevation Model (DEM), a raster grid where cells of a given size are assigned an elevation value. The water input to the model is given by point-based rain gauge records, which are multiplied by the area of each model grid cell and applied to every cell across the catchment. A number of parameters must also be specified in order to perform the flow routing calculations and to account for processes that are not explicitly represented (e.g. losses to infiltration). As it is impractical to directly measure parameters for every grid cell of the catchment, their values can be selected by calibration of model predictions to observed data. To do so, observed data is required at the outlet of the catchment in the form of a measured flow hydrograph.

Previous work for the *Knowledge Controversies* project had generated a large amount of data characterising the River Seven catchment (Ryedale Flood Research Group, 2008), which is described throughout the explanation of the model operation below. As part of this previous work, the *Overflow* model topography and hydraulic geometry (described in sections 2.4.3.3. and 2.5.3.3.) had already been set up in advance of the research undertaken in this thesis. Nonetheless, a description of the operations involved in setting up catchment topography and hydraulic geometry is included, in order to provide a full description of the operations involved in setting up and running *Overflow*.

### 2.5.3.2. Topography

The user is required to supply a DEM to describe catchment topography. In the UK, Ordnance Survey map data is currently the only widely available source of topographic information with national coverage (Marks and Bates, 2000). This project uses a raster grid of 20 m resolution, which was resampled from 5 m resolution NEXTMAP data (Odoni and Lane, 2010).

Topography directly controls flow direction and velocity (which is dependant on slope), so the DEM quality is important in accurately calculating overland flow routing. NEXTMAP data, which is collected by synthetic aperture radar and has an accuracy of  $\pm 1$  m (Intermap, 2011), was considered sufficiently accurate to represent the catchment for this purpose. It is recognised that the resolution of the grid inhibits more detailed analysis of flow routing, which might be of interest in settlements or areas of complex topography where flow routes operate on a scale of less than a 20 m grid (see, for example, Yu and Lane, 2006a). However, the primary aim of this project is to assess model parameter sensitivity and the impact of flow attenuation at a point downstream (the impact of attenuation on the downstream flood hydrograph). As a result, the precision with which flow routing can be mapped within the catchment is of less importance than the ability to undertake multiple scenario testing.

The DEM was processed to remove pits and depressions using an algorithm developed by Planchon and Darboux (2001), so that downhill flow routing could occur from any point in the catchment.

### 2.5.3.3. Channel network and hydraulic geometry

A numerical algorithm was applied to predict the location of the channel network based on topography. A cell is defined as a channel cell where a critical discharge is exceeded; in this project, critical discharge is specified as  $0.06 \text{ m}^3\text{s}^{-1}$ , which was found to be representative of small, rural catchments for which *Overflow* was designed (Odoni and Lane, Forthcoming). Therefore, the number of channel cells depends on the selection of a rainfall input that is thought to represent bankfull conditions.

A spatially homogenous and temporally invariable rainfall rate, which was equivalent to bankfull discharge conditions, was routed through the model. In the case of the River Seven, bankfull discharge is known from gauging station cross-sectional surveys (JBA Consulting, 2008b). In a process of trial and error, different rainfall rates were routed through the model until the modelled discharge at the gauging station approximated bankfull discharge. Bankfull discharge conditions at the gauging station were replicated in response to a rainfall rate of 38 mm/day. The



resulting discharges for each cell under the 38 mm/day rainfall rate were used to calculate the width and depths of river channels. This is not to say that the same value of bankfull discharge was extrapolated throughout the catchment. Rather, the conditions that resulted in an approximation to bankfull discharge at the gauging station were used to estimate bankfull discharge at unmeasured locations. Although a potential source of error, the reason for this assumption was that it was not possible to survey river channel geometry throughout the catchment. The calculation of channel dimensions was based on Leopold and Maddock's (1953) empirical equations for hydraulic geometry. In *Overflow*, these were taken to be:

$$w = 1.4 Q^{0.45}$$

**Equation 2.1 Empirical relationship between width and discharge.**

$$d = Q^{0.32}$$

**Equation 2.2 Empirical relationship between depth and discharge.**

where  $w$  = width (m),  $d$  = depth (m) and  $Q$  = discharge ( $\text{m}^3\text{s}^{-1}$ ) (Leopold and Maddock, 1953). The constants and exponents of the original hydraulic geometry equations proposed by Leopold and Maddock have been found to vary under different conditions (Ferguson, 1986). As a result, the precise values were selected by a process of optimisation to surveyed stream geometry at the gauging station (Nick Odoni, 2010, personal communication).

At this stage, the model has the topographic boundary conditions (including channel geometry) required to represent the catchment during a flood event. This was the extent to which the River Seven model had been set up as part of previous work for the *Knowledge Controversies* project.

#### **2.5.3.4. Flow routing**

The direction of flow routing is defined by the difference in altitude between one grid cell of the DEM and its neighbouring grid cells (Mulligan, 2002). In *Overflow*, two routing algorithms were used according to whether a cell was classified as a 'channel cell' or 'non-channel' (i.e. any other land type in the catchment).

In channel cells, flow is routed using the D8 algorithm (O'Callaghan and Mark, 1984). The D8 algorithm calculates the gradient between a cell and each of its neighbours, then routes all water by the steepest downslope path only.

In all other cells, flow is routed diffusively using an algorithm based on the MF (multiple-flow) algorithm (Quinn et al., 1991). The MF algorithm routes flow to all downhill neighbouring cells, with flow apportioned between each cell according to the relative gradient of each (Mulligan, 2002).

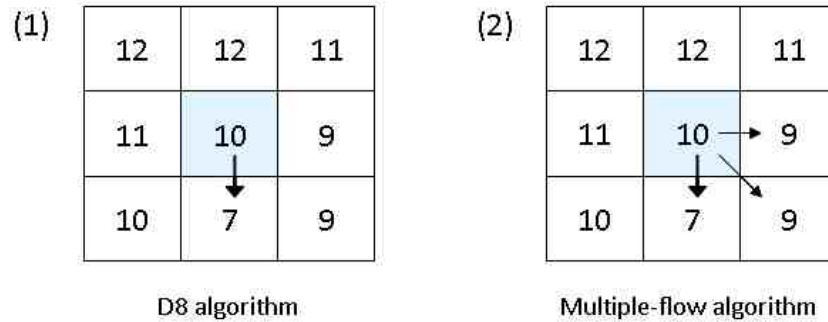


**Figure 2.2** Conceptual diagram showing the different routing algorithms used. Each shows a raster grid, in which elevations have been assigned to each cell. In both algorithms, the gradient from a cell to each of its neighbours is calculated. In the D8 algorithm (1) flow occurs along the steepest gradient only, hence all flow is routed into the lowest neighbouring cell. In the MF algorithm (2), flow is routed to all lower neighbouring cells, but is apportioned according to the gradients of each. This process is repeated for each cell in the DEM.

The precision with which channel cells can be identified is limited by the resolution of the DEM. For example, in many locations, topographic data is of a coarser resolution than the size of the channel. Therefore a channel cell will also contain an area of floodplain, although it is assumed that channel flow dominates the cell.

### 2.5.3.5. Flow hydrographs

There are two stages to routing a flow hydrograph through the catchment. The flow velocity, hence travel time of water through the catchment, is calculated based on a theoretical rainfall rate parameter. As with other model parameters, the value of this rainfall rate is selected by a process of optimisation, which is discussed in Chapter 4. The parameter is intended to approximate flow velocity over the catchment throughout the whole of the event. In a second, separate step, this information on flow velocity is used to calculate the routing of an actual observed rainfall event through the model. This two-stage process allows a single flow velocity to be applied to each grid cell for the whole event. This allows much faster model run times than if the velocity were based on the input rainfall timeseries, and hence updated at every timestep of the event. However, in reality, flow velocities would change throughout a rain storm as the land surface becomes wetter and flows become deeper. The implications of this assumption are explored in Chapter 4. The remainder of this section describes the calculation of flow velocity and the separate, subsequent flow hydrograph routing.

First, flow velocities across each cell of the catchment are calculated. A theoretical rainfall rate, in mm/hour, was multiplied by the area of each grid cell (20 m) and then converted into discharge ( $\text{m}^3\text{s}^{-1}$ ). For each grid cell, this discharge is then applied and the subsequent flow depth and velocity are solved.

The calculation of flow depth and velocity are based on equations for the distribution of discharge between flow width, depth and velocity (assuming that in order to conserve mass, discharge must remain constant)

$$Q = wdv$$

### Equation 2.3 Continuity equation

and the Manning equation

$$v = \frac{R^{\frac{2}{3}} S^{\frac{1}{2}}}{n}$$

### Equation 2.4 Manning equation

where  $Q$  = discharge ( $\text{m}^3\text{s}^{-1}$ ),  $w$  = width (m),  $d$  = depth (m),  $v$  = velocity ( $\text{ms}^{-1}$ ),  $R$  = hydraulic radius (m),  $S$  = slope and  $n$  = the roughness parameter Manning's  $n$  (Cowan, 1956).

Hydraulic radius is assumed to be approximately equivalent to depth (see discussion in Section 1.4.1), since the cross section of overland flow in particular is very wide for its depth (Emmett, 1978; Yu and Lane, 2006a). On the assumption that  $R \approx d$ , Equation 2.3 and Equation 2.4 can be combined to give

$$Q = \frac{1}{n} w d^{\frac{5}{3}} S^{\frac{1}{2}}$$

### Equation 2.5 Combination of the continuity and Manning equations.

which can be rearranged for depth

$$d = \left( \frac{nQ}{wS^{\frac{1}{2}}} \right)^{\frac{3}{5}}$$

### Equation 2.6 Rearrangement of Equation 2.5 to make depth the subject.

Equation 2.6 can be substituted into the Manning equation (Equation 2.4) in place of  $R$  (Emmett, 1978). This gives the equation

$$v = \frac{d^{\frac{2}{3}} S^{\frac{1}{2}}}{n}$$

### Equation 2.7 Manning equation, with depth substituted for hydraulic radius.

where  $d$  = Equation 2.6.

The catchment DEM allows the calculation of slope ( $S$ ) from the difference between adjacent grid cells. Discharge ( $Q$ ) is calculated from the rainfall rate. At this stage of the modelling, width ( $w$ ) is

the grid cell width. After selection of an appropriate Manning's  $n$  value, Equation 2.7 can be used to calculate velocity and hence the travel time of water across each grid cell, for a given discharge.

These times are accumulated throughout the catchment to generate a 'time map' – the travel time of water from each cell in the catchment to a reference point where the flood hydrograph will be calculated (Figure 2.3). For this project, the time map is divided into one hour intervals. This will form the basis for generating the flood hydrograph. One hour intervals are considered to give adequate temporal resolution of a flood event.

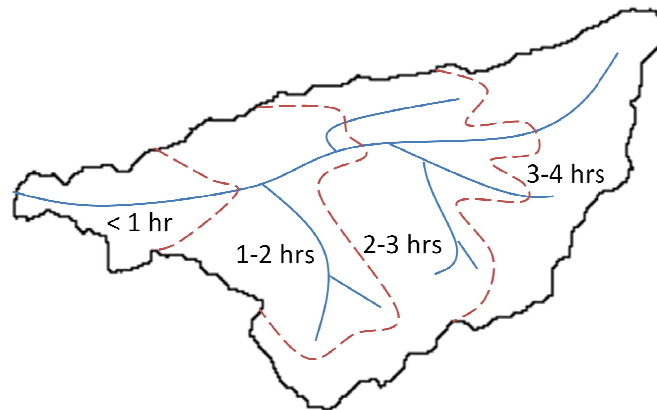


**Figure 2.3** A hypothetical time map for illustrative purposes. Bold lines show the catchment outline and river network. Dotted lines show the division of the catchment into time-bands, given by the numbers. Thus any precipitation falling within the first time band (on the left) would be expected to reach the catchment outlet within one hour. Flow is expected to be faster in channels than elsewhere, so the boundaries of the time bands follow the channels further upstream (Odoni and Lane, Forthcoming).

A change to the value of the rainfall rate parameter will generate a different time map. Higher rainfall rates result in a higher discharge, since more water is applied to the catchment. In turn, this results in greater flow velocities. Therefore the travel time through the catchment is reduced and a larger area lies within a given travel time of the downstream reference point.

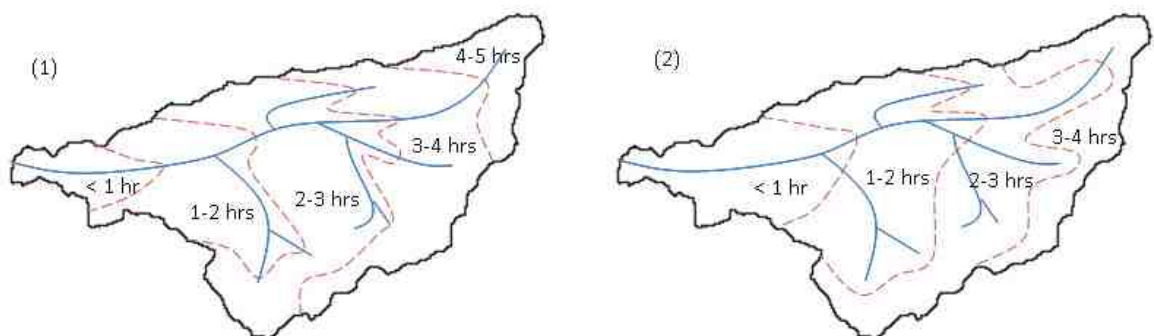


**Figure 2.4** Illustrative time maps to demonstrate the effect of changing the rainfall rate parameter. In (2), a higher rainfall rate has been selected, so a higher discharge was applied to the model grid. This leads to greater flow velocities, so the travel time from a given point in the catchment to the catchment outlet is less.

Overland flow velocities are controlled by a number of factors that may vary between catchments and flood events. The level of soil saturation will affect the volume of overland flow, which is in turn dependent on antecedent conditions and the magnitude of rainfall. The rainfall rate parameter is designed to account for these processes, allowing flow velocity to be generalised for the whole, or large portions of, an event. In Chapter 4, the model was tested using a range of different approximations of cell flow velocities, by selecting range of different rainfall rate parameter values. In order to generate a map of cell flow velocities that were representative of the 'real' catchment during a specific flood event, rainfall rate values were selected by the optimisation of model predictions to gauging station measurements.

However, in reality flow velocity may also vary within the timescale of an event. For example, as a storm event progresses, the catchment will become progressively wetter and more saturated, and hence overland flow velocity will increase (Wilson, 1990). As the rainfall rate parameter only provides an approximation of the 'average' conditions throughout an event, detailed changes in flow velocity over time are not explicitly calculated. This is a simplification that is intended to allow more efficient computation.

At this stage in the model set-up, the model is an approximation of the catchment at the start of the rainfall event. The rainfall rate parameter is used solely to calculate flow travel times across the catchment. However, the estimated flow velocities are used to calculate a flow hydrograph for a downstream reference point. The user is required to supply an actual rainfall hyetograph based on observed rain gauge data. This project used rain gauge data for a storm on 25<sup>th</sup> – 28<sup>th</sup> June 2007 (discussed in more detail in Chapter 3).

At any given moment in time, the discharge at the downstream reference point is the sum of precipitation that has fallen on different parts of the catchment at different times:

$$Q_t = \sum A_t r_t$$

#### Equation 2.8 Total discharge at a point

The discharge,  $Q$  ( $\text{m}^3\text{s}^{-1}$ ), at time  $t$  (hours) after the start of a rainfall event, is found by the area,  $a$  ( $\text{m}^2$ ) of the catchment that lies within time bands 0 to  $t$ , multiplied by the rainfall,  $r$ , falling in that time (Odoni and Lane, Forthcoming). This calculation is repeated at each model time-step to generate a series of discharges which form the flood hydrograph. On a 2.10 GHz computer processor, each model run takes approximately ten minutes.

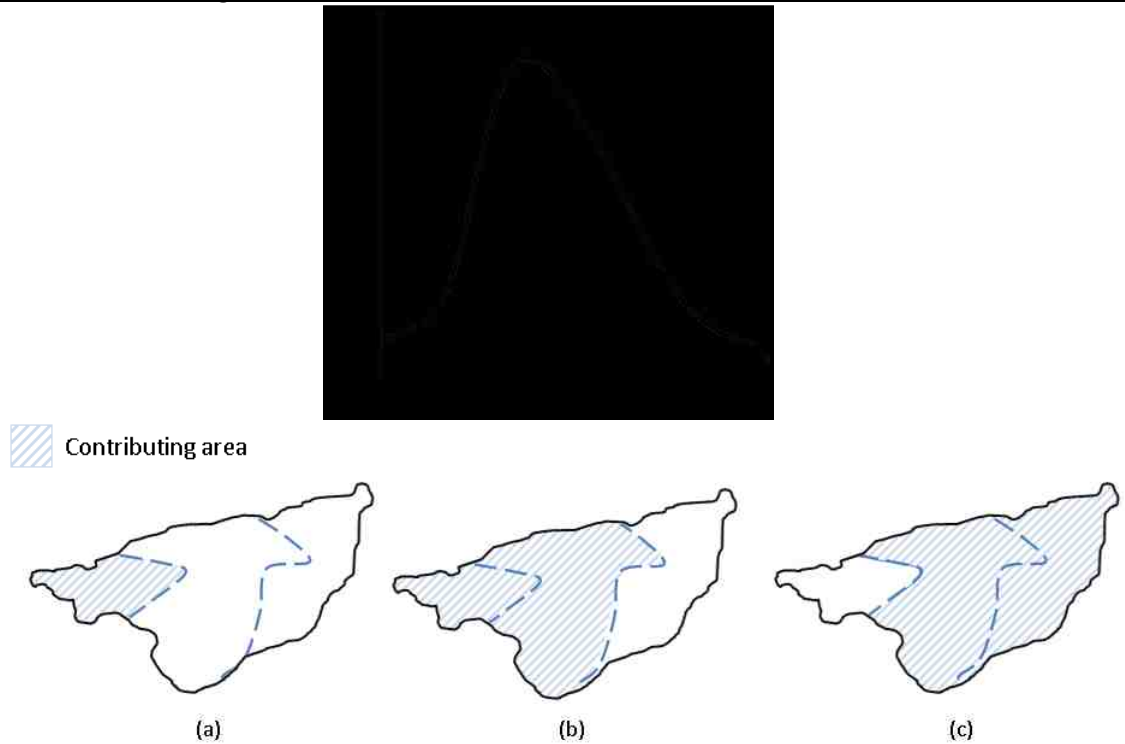


**Figure 2.5** Flow at time  $t$  is related to the area of the catchment with a travel time within  $t$  hours. Thus, when  $t = 1$ , the catchment area within 0 to 1 hours travel time away contributes rainfall to the flood hydrograph (a). When  $t = 2$ , the contributing area is that between 0 to 2 hours travel time (b) etc. When rainfall ceases at the end of the event, the time map operates in reverse. Rainfall falling within the first time band drains first, so that the contributing area is that which is greater than 1 hour travel time (c).

It should be noted that the rainfall rate used to calculate flow velocities across the catchment and the observed rainfall input are different quantities. Thus there are two distinct stages in generating a downstream flow hydrograph from a rainfall input. In the first stage, flow velocities for each cell are calculated for a rainfall rate (the value of which is selected on the basis of calibration to observations). To repeat this calculation for every grid cell at every model time step would be computationally demanding, resulting in longer run times. Instead, the flow velocities of each grid cell are used to divide the catchment into areas of similar cell flow passage times (e.g. one-hour intervals as in Figure 2.3). At a downstream reference point, the discharge at a point in time is related to the catchment area that could have contributed to flow, until that point in time.

Using the same cell flow velocities throughout the rainfall event makes the assumption that the wetness of the catchment does not change as more rainfall is applied, so the model is particularly suited to simulating catchments that are highly saturated. Chapter 3 describes a flood event for which this is a reasonable assumption. This is because of high runoff rates during the event, which is implied by a comparison of rain gauge and downstream flow gauge data (section 3.4). In addition, wet conditions recorded in the month prior to the event (Figure 3.2). It is likely that under these conditions, the catchment land surface was already heavily saturated, therefore could not get any wetter over the course of the event. However, the value taken by the constant

rainfall rate used to calculate cell flow velocities requires careful selection, which will be investigated in Chapter 4.

### 2.5.3.6. Parameters

In the discussion above, the operation of *Overflow* has involved five parameters, which are summarised in Table 2.1 and subjected to further analysis in Chapter 4.

Parameter	Description of role in <i>Overflow</i>
Critical discharge for channel formation	Used to designate some cells as channel cells.
Constants and exponents in calculation of channel width and depth	Values of the constants and exponents used in Leopold and Maddock's calculation of channel bankfull widths and depths.
Manning's $n$	Flow velocities in the formation of the time maps are calculated using Manning's equation, which requires the use of the constant, $n$ .  Ultimately, MATLAB allows $n$ to be specified for every cell in the catchment. However, in this application there is not enough information to specify $n$ in such detail, so a distinction will only be made between channel and land cover (i.e. non-channel) $n$ .
Rainfall rates for flow velocity calculations (mm/day)	Rainfall rate used for calculation of flow velocity for each model grid cell. In reality, this might vary depending on antecedent conditions and throughout a rainfall event.
Runoff rate (percent)	To account for water losses to evaporation, infiltration, groundwater and baseflow (likely to be negligible in a high flow event).

**Table 2.1 Key parameters and a description of their roles.**

All parameters are assumed to be spatially uniform, with the exception of Manning's  $n$ , where a distinction is made between the channel and non-channel grid cells. This is consistent with other modelling approaches, where data limitations prevent physically meaningful  $n$  values being specified for individual grid cells (Bates et al., 1998). To specify parameter values locally would also unnecessarily complicate an assessment of the uncertainty caused by parameter selection. This is particularly the case in the River Seven catchment, where observed gauging station data is not available at a great enough density to validate parameter selection at the scale of less than the whole catchment. However, the ability of *Overflow* to separately specify parameter values for each grid cell of the DEM will be used later to represent interventions for individual river reaches.

Since these parameters are used to represent processes for which there is no directly observed measurement, they must be selected by a process of optimisation. Parameter values are adjusted to match the modelled flow hydrograph with an observed flow hydrograph at the catchment outlet, measured by an objective statistical function. This process is described in Chapter 4.

## 2.6. Summary

This chapter has introduced the methodological approach of this project, that of numerical modelling, and the specific model that was used to answer the research questions. Modelling is necessary for this research as it allows predictions to be made about the effect of interventions in a flood event, without the need for direct observations. This allows a wide range of possible intervention sites to be tested. A hydrologic routing model, *Overflow*, was selected to assess the impact of multiple, spatially distributed flow attenuation interventions on flood risk. *Overflow* is well suited to this task as it makes use of a simplified process representation and requires limited boundary condition data. The model is therefore capable of fast run times and is easy to set up for different interventions, allowing multiple scenario testing.

Chapter 3 describes and justifies the specific catchment and flood event for which *Overflow* was used to test the effects of flow attenuation interventions. However, due to limited spatial distributed data and the demands placed on computational resources by catchment-scale simulations, there is a need to make assumptions and simplifications in the way the catchment is represented by parameters and boundary conditions (e.g. topography). Chapter 4 evaluates whether *Overflow* responds to these parameters in a theoretically realistic manner and identifies parameter values suitable to the River Seven and June 2007 flood. The uncertainty associated with the selection of parameter values to represent flow attenuation measures was assessed in Chapter 5. In Chapter 6, the flow routing equations used in *Overflow* were evaluated by comparison the results obtained by a hydraulic model for the same topographic and flow boundary conditions.



## 3. Test case: the River Seven and June 2007 flood

### 3.1. Summary

This chapter introduces the catchment and flood event that was investigated in this project. First, the geography of the catchment is described. Next, the wider context of previous research and flood management strategies in the area is reviewed. This has been used to inform the methodological approach taken in the project. Finally, the 'test scenario' for the models, a flood event of June 2007, is discussed alongside the available data.

Chapter 1 outlined the aims of this project, which are to apply a numerical model to assess the impact of flow attenuation on downstream flood flows. Chapter 2 justified the choice of a reduced complexity hydrological model, *Overflow*, and described the model operation and data needs. This chapter concludes that the River Seven, North Yorkshire is a suitable catchment in which investigate the impact of flow attenuation, and that a flood event in June 2007 provides a suitable test scenario to do so. Data is also available for this event and catchment with which the model can be evaluated.

### 3.2. The River Seven Catchment

#### 3.2.1. Catchment description

The River Seven drains part of the North York Moors National Park and is a tributary of the River Rye at Little Habton, north of Malton. The catchment has a total area of approximately 122 km<sup>2</sup> at the town of Normanby, south of Sinnington, with a length of 21 km and a maximum width of 10 km. The land is predominantly rural, with large areas of forestry, the management of which can significantly affect overland flow routing (Forestry Commission, 2007). The geology is varied and consists of limestone, sandstone, siltstone and mudstone.

Altitude varies from 493 m to 21 m Ordnance Datum (OD). The River Seven therefore has a relatively steep gradient, with a drop in elevation of around 270 m (from 296 m to 26 m OD) along the length of the river channel itself. As a result, the river is fast flowing and responds rapidly to rainfall, giving little advance warning of floods to people living downstream. The catchment is also relatively wide and has several large tributaries draining into the main river along its length, increasing the volume of water that is delivered downstream during a flood.

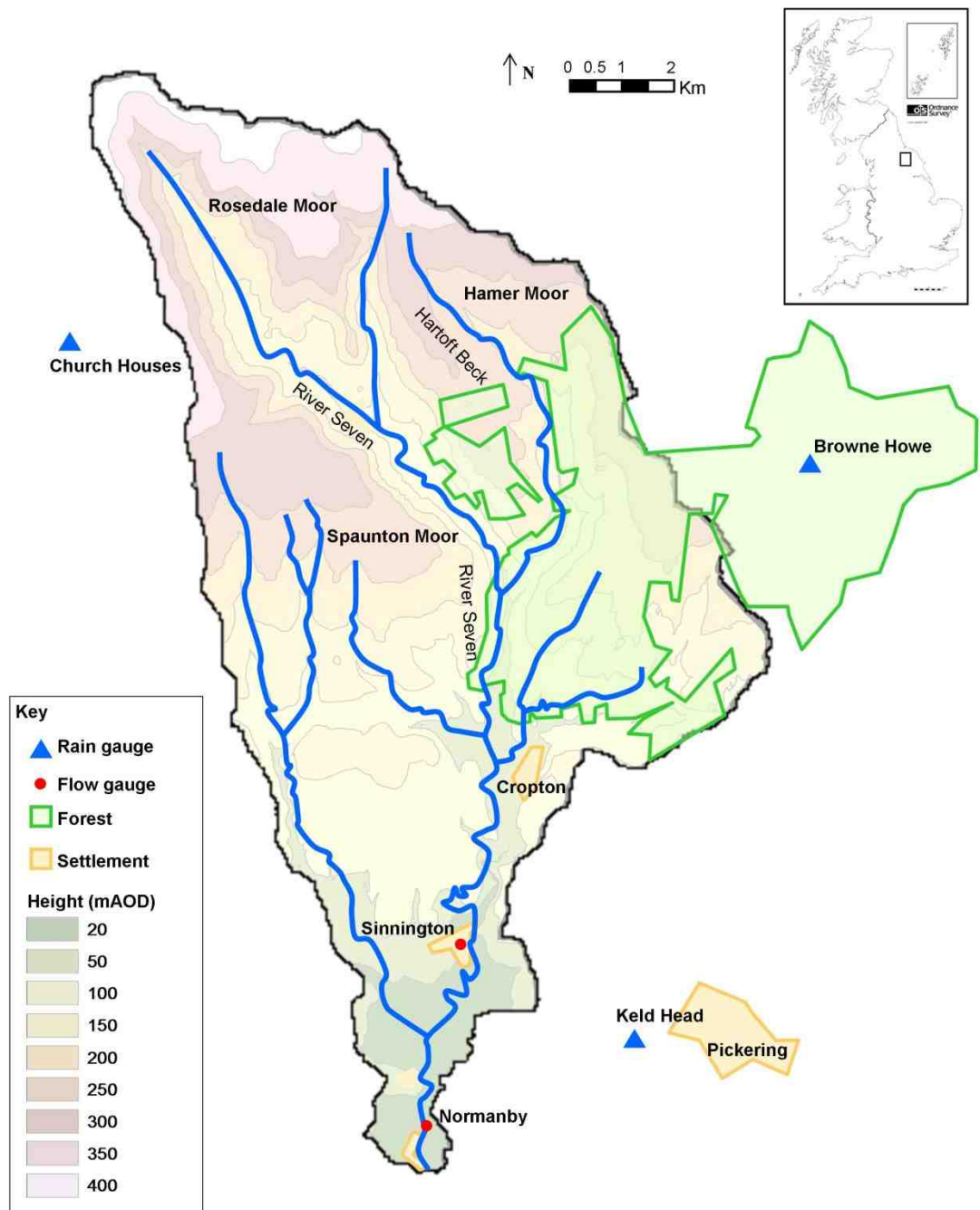


Figure 3.1 Sketch map of the catchment of the River Seven to Normanby showing gauging sites, the River Seven and its main tributaries. Flow gauges are located within the settlements of Sinnington and Normanby. The sketch map was based on Ordnance Survey 1:50,000 map data. (Inset: Great Britain location map reproduced from Ordnance Survey map data by permission of the Ordnance Survey.)

Catchment area	122 km <sup>2</sup>
Catchment altitude	493 m to 21 m above Ordnance Datum
Standard Average Annual Rainfall, 1961-1990*	875 mm
Drainage density	2.98 km per km <sup>2</sup>
Shreve stream order at Normanby**	118
Mean average flow at Normanby*	1.939 m <sup>3</sup> s <sup>-1</sup>
Soils and geology*	Jurassic limestone, shales and sandstone
Land cover*	34.4 % mountain/heath/bog/moorland
	28.9 % grassland
	18.5 % woodland
	14.6 % arable/horticultural
	0.3 % urban

**Table 3.1 Summary catchment characteristics. \*Figures from CEH, 2008. \*\*In Shreve stream ordering, the order of a stream is the sum of the orders of its upstream tributaries (Shreve, 1966).**

Rain and flow gauging has taken place in the catchment since the mid-1970s and the location of gauging stations is shown in Figure 3.1. Rainfall data are available from three gauges in the north-west, east and south-east of catchment (Church Houses, Brown Howe and Keld Head, respectively). These rain gauges are not within the catchment, so a further analysis of how representative they are of the catchment is undertaken in section 3.4.2. River flow is gauged at Normanby, at which point the river has a mean discharge of 1.94 m<sup>3</sup>s<sup>-1</sup> (CEH, 2008). The maximum recorded level at the Normanby gauge was observed in June 2007 as 4.24 m (JBA Consulting, 2008b). This project considers the catchment as far as Normanby, since this is the furthest downstream gauging station on the River Seven itself, before it joins the River Rye. In describing the River Seven throughout this project, the term ‘catchment’ refers to the area of land that drains through Normanby.

The river gauge at Normanby is the only observed data against which model predictions can be compared and calibrated. Its quality is therefore important in assessing model results. At the gauge, flows are contained within a relatively deep river channel (approximately 4m). This means that flows do not bypass the gauge (for example, by flooding upstream and being routed on the floodplain around the gauge), which would lead to underestimates of high flows (JBA Consulting, 2008b). However, although a large proportion of (if not all) flow passes through the gauge itself, there may be inaccuracies in measurements. For this project, there was not enough available data

to quantify measurement error at the gauge, but it is recognised as potential source of uncertainty when assessing model accuracy.

Sinnington and Normanby are among a number of low lying settlements located towards the south of the catchment. Throughout the catchment, the valley is relatively constrained with narrow floodplains. However, south (downstream) from Sinnington, the valley widens and the floodplain is particularly flat due to scour from glacial meltwater. Small changes in overbank flow depths can therefore cause inundation of large areas of the floodplain. The area has a long history of flooding and was particularly seriously affected in autumn 2000 and June 2007 (Environment Agency, 2007b). These events, alongside flooding in 1999, 2002, 2005, 2008 and 2009, have increased public demand for flood mitigation, although engineered defences have not been constructed due to their excessive cost (Ryedale Flood Research Group, 2008).

Date	Peak flood discharge ( $\text{m}^3 \text{s}^{-1}$ )
14/12/1979	103.599
15/08/1980	109.521
22/03/1981	103.443
04/01/1982	118.984
09/12/1983	126.943
21/05/1986	127.000
28/01/1990	109.895
14/09/1993	146.240
14/11/1993	131.058
11/04/1998	135.693
08/03/1999	114.539
30/10/2000	141.697
03/11/2000	122.881
08/11/2000	102.088
02/08/2002	148.775
03/11/2002	113.452
31/01/2004	122.937
25/06/2007	156.549
06/09/2008	154.083
13/12/2008	107.391
01/11/2009	106.068
30/11/2009	136.803
22/01/2010	100.741
26/02/2010	103.182

**Table 3.2 Peak-over-threshold series ( $\text{m}^3 \text{s}^{-1}$ ) of flood events at the Normanby gauging station, from the beginning of gauging in the 1970s until 2010. Events with peak discharge greater than  $100 \text{ m}^3 \text{ s}^{-1}$  are given, of which there were 24. Bankfull discharge is estimated as  $72.4 \text{ m}^3 \text{ s}^{-1}$  (JBA Consulting, 2008b).**

### 3.2.2. Justification of choice of catchment

The River Seven has been chosen for this study as it is a gauged catchment, providing observed data against which the model results can be validated. The presence of a number of rain gauges also allows the provision of input data to the flood model, *Overflow* (described in Chapter 2). As a result of previous research and the interest in flow attenuation as a means of mitigating downstream flood flows, relevant topographic data are also available. Thus the data required to construct and run model simulations, and to validate the model results, are readily available, allowing the aims and objectives of this project to be addressed.

Flood risk on the River Seven exists due to the likelihood of out-of-bank river flows and the presence of vulnerable properties on the floodplain. The small number and size of settlements on the floodplains of the River Seven mean that conventional, hard engineered approaches to flood risk management cannot be economically justified. Nonetheless, a number of properties have been damaged in previous floods and continue to be at risk of flooding (Environment Agency, 2007a; Environment Agency, 2007b). The dispersed nature of settlements (Figure 3.1) necessitates measures that can reduce the severity of flooding over a wide area. As a result, both recent research in a neighbouring catchment (Odoni and Lane, 2010) and local priorities in the River Seven catchment have led to a focus on upstream flow attenuation and storage as a means of reducing downstream flood magnitude (Ryedale Flood Research Group, 2008). The River Seven is therefore an area in which the changing focus of flood risk management considered in Chapter 1 has direct and current relevance.

### 3.3. Flood research in Ryedale

The management of flooding on the River Seven is guided by the Environment Agency's Catchment Flood Management Plan (CFMP) for the River Derwent, Yorkshire (Environment Agency, 2010a), of which the Rivers Rye and Seven are tributaries. The policy adopted in the CFMP is to:

“Seek opportunities to restore the natural flood storage by allowing the river to reconnect with the floodplain to slow the passage of water out of the area.”

(Environment Agency, 2010a: 12)

In 2007, the Ryedale Flood Research Group was established to undertake an eleven-month research project on flooding on Pickering Beck, which neighbours the River Seven catchment. The group consisted of academics from Durham, Newcastle and Oxford Universities alongside local residents from the area. The group used hydrologic and hydraulic models, informed by local knowledge. River channel vegetation growth and sedimentation (as a result of a lack of river

maintenance) were identified as causes of increased local flood risk. It was also found that storage of flood water upstream of the town of Pickering could significantly reduce flood risk downstream, in the town itself. These findings were published (Odoni and Lane, 2010) and have led to the agreement to construct several small 'bunds' in Pickering Beck. Bunds are permanent dam-like structures that allow the passage of low flows, but block higher flows, effectively limiting the peak discharge of the flood hydrograph.

As the River Seven catchment is mostly rural, it could also be suited to upstream attenuation and storage of floodwater on low value forestry or pasture land. Upstream storage has been identified by local residents as a socially acceptable option (Ryedale Flood Research Group, 2008). Since most of the land in the catchment is owned by relatively few landowners (much is owned by the Forestry Commission), there are also fewer stakeholders whose agreement is required in order to undertake flood attenuation schemes. Such an approach might contribute to a reduction in flood risk not only for settlements in the River Seven catchment, but also further downstream on the River Rye and River Derwent.

More recent research on flood mitigation in Ryedale (including the River Seven catchment) was undertaken by Forest Research, part of the Forestry Commission. Forest Research used GIS datasets to locate land that was in flood risk areas but unaffected by constraints to woodland planting (e.g. land ownership, detrimental impacts on local flood risk). Their work also allowed areas to be prioritised that generated additional benefits for conservation and water quality (Broadmeadow and Nisbet, 2009).

The series of recent flood events, alongside the work of the Ryedale Flood Research Group (2008) and Broadmeadow and Nisbet (2009), have resulted in a high availability of rainfall, discharge and topographic data, which can be used in this research. However, despite the interest in flood mitigation, it is not known where and to what extent upstream storage and slowing river flow might contribute to a reduction in flood risk in downstream settlements on the River Seven. This project attempts to address this problem specifically for Sinnington, where the less constrained river valley and larger floodplains cause a high probability of flooding.

### **3.4. The June 2007 Flood**

Heavy and prolonged rainfall in May, June and July 2007 led to widespread river and surface water flooding over large areas of the UK. Nationally, the floods resulted in 13 deaths, £3.2 billion insured damage and the inundation of approximately 55,300 properties (Pitt, 2008). At a national level, the scale of the flooding, its impacts and the emergency response required were called "unprecedented" (Pitt 2008: 3). In Ryedale, a number of properties were flooded. The seasonality of the flooding, which occurred during summer, was particularly disruptive to agriculture and

tourism. Rural business is heavily dependent on both farming and tourism, resulting in longer term impacts for the local economy (Morris et al., 2008b).

June 2007 was a very wet month. In some areas of the North York Moors, four times the average June rainfall fell during the month (Pitt, 2008). In particular, large volumes of rain fell on 15<sup>th</sup> and 20<sup>th</sup> June (Figure 3.2). Although this did not directly cause any significant flooding, it saturated the catchment land surface, contributing to a higher speed and volume of surface runoff during subsequent events.

The flood was triggered by an intense, localised rainfall event on 25<sup>th</sup> June. The recorded rainfalls are given in Table 3.3 and Figure 3.3. Figure 3.3 shows that the storm began suddenly but continued for up to 15 hours (at Brown Howe). In response, the River Seven rose rapidly, reaching its peak level of 4.24 m at about 9:15 pm on 25<sup>th</sup> June, after rising by around 3.65 m in the preceding 12 hours (Figure 3.4).

Rain gauge (see Figure 3.1)	Total rainfall (mm)	Peak rainfall rate (mm/hour)
Keld Head	47.8	4.6
Church Houses	55.6	7.4
Brown Howe	80.6	7.6

**Table 3.3 Recorded rainfall for the 24 hours from midnight, 25<sup>th</sup> June 2007. Total rainfall is the total depth of rainfall over the duration of the event (the sum of the hourly rainfall totals). Peak rainfall rate is the maximum rainfall depth recorded for any hour of the event.**

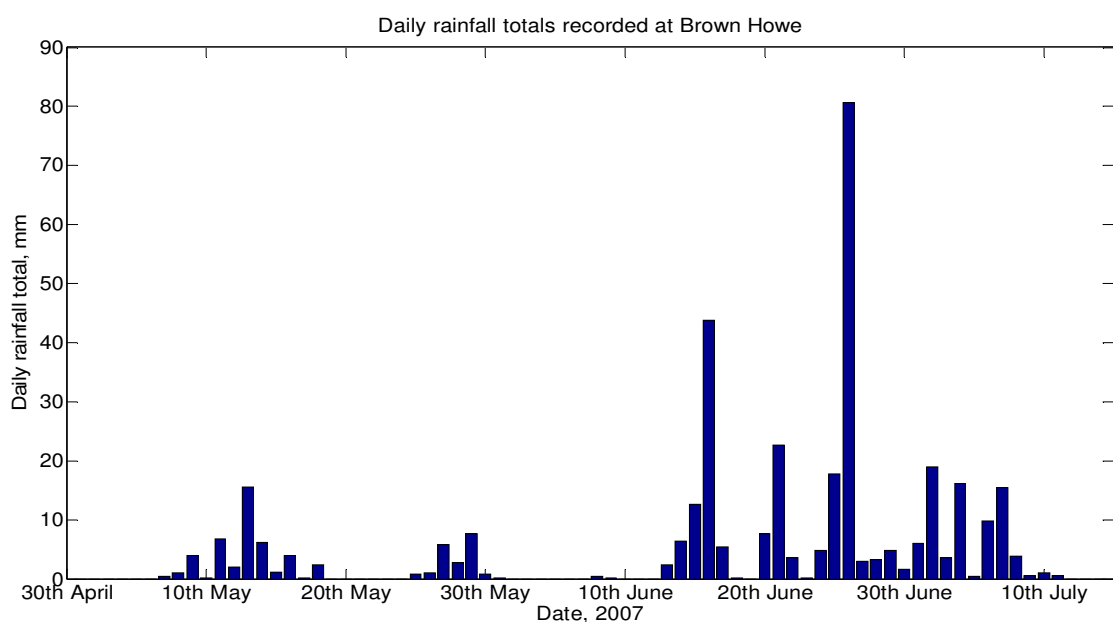


**Figure 3.2 Daily rainfall totals recorded at the Brown Howe rain gauge in the two months prior to the June 2007 flood.**



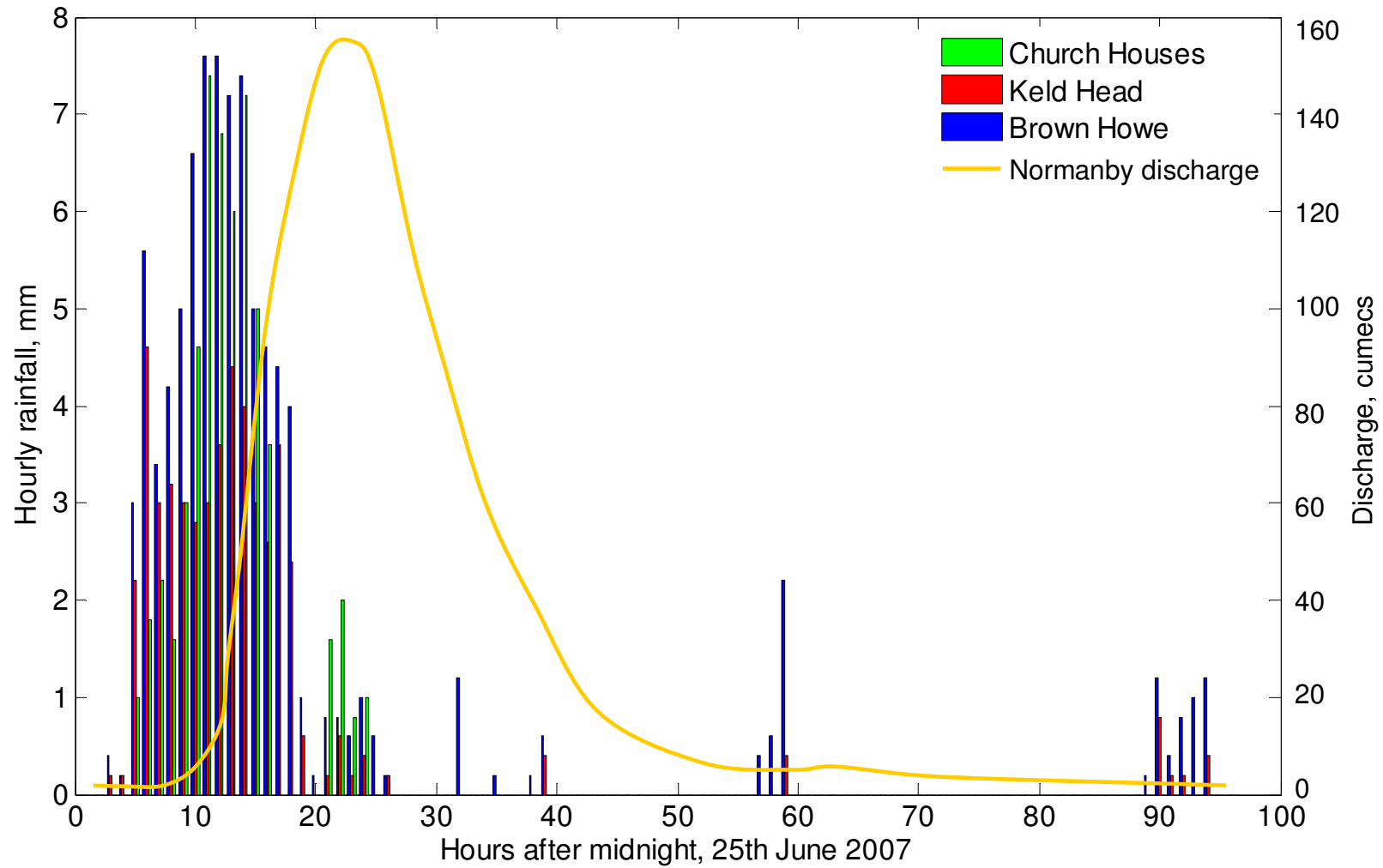


Figure 3.3 Hourly rainfalls for the 25<sup>th</sup> June 2007 storm, which resulted in the flood event, recorded from the three rain gauges around the River Seven catchment. See Figure 3.1 for locations.

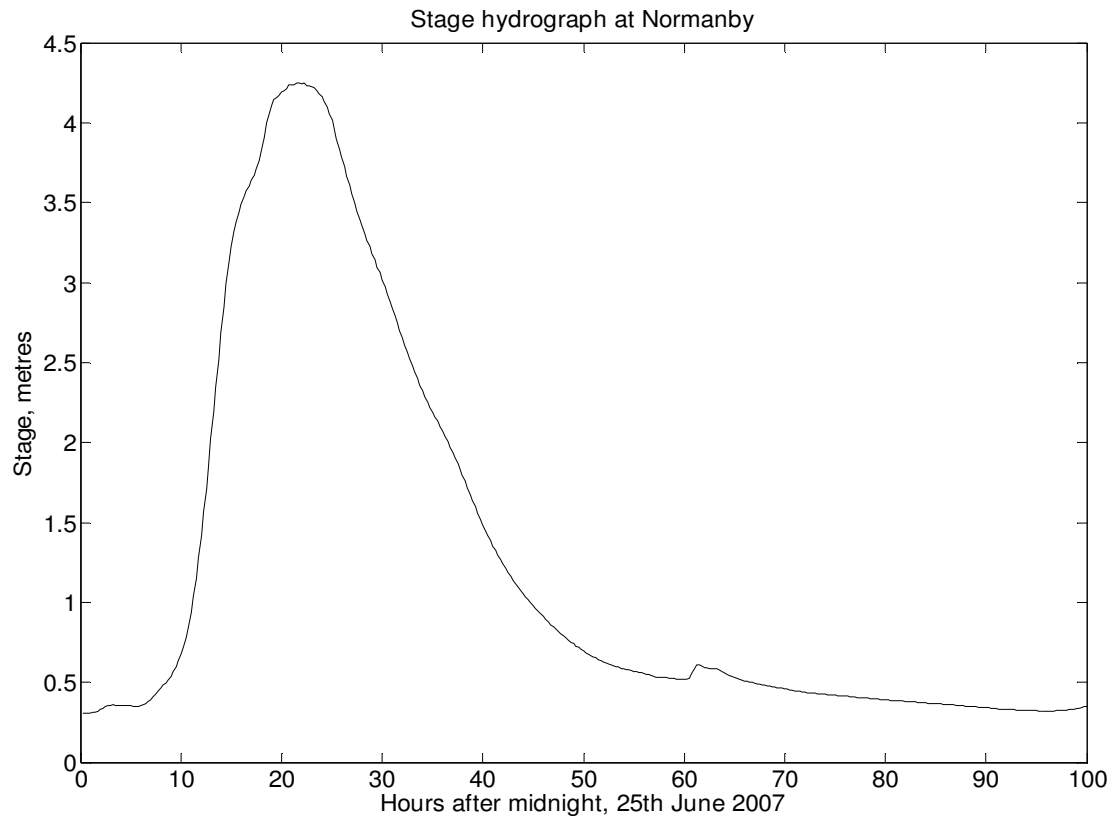


Figure 3.4 Stage hydrograph recorded at Normanby for 25th June 2007 flood.

#### 3.4.1. Justification of choice of event

The June 2007 flood is used as the boundary condition for the models in this study. Odoni and Lane (2010) found that the effect of increasing flow attenuation increased with the size of flood event. Higher flows increased the probability and magnitude of overbank flooding. As a result, larger events were more likely to interact with flow resistance measures on the adjacent floodplain. In comparison to within-channel flows, floodplain flows tend to have much wider flow widths and, consequently, shallower flow depths. Within the channel, flow width is constrained by channel geometry, so is unable to spread across a wide area. Floodplain flows therefore have a much higher wetted perimeter, so a greater proportion of flow interacts with attenuation measures. In response to attenuation measures, the attenuation and reduction in flood peak is expected to be greater at higher discharges (as a proportion of the flood peak magnitude). However, the actual flood peak may still be higher in higher magnitude events, despite interventions to increase attenuation.

The scale of this flood therefore makes it appropriate as a benchmark event (Pitt, 2008) to assess the response of the catchment under extreme conditions, when interventions in flow resistance might be expected to have the maximum impact. As a recent and serious flood, there is a comparatively large amount of data available to calibrate the model to this event.

### 3.4.2. Justification of choice of rain gauge

There are no rain gauges within the catchment itself (see Figure 3.1). Specifying model boundary conditions is therefore reliant on choosing representative conditions from the three nearby rain gauges. Applying rainfall across the catchment based on data measured at a point is uncertain. However, this is frequently the case for UK catchments and in order to reduce this uncertainty, rain gauge data must be compared to another related measurement. The rain gauge data was compared to the recorded discharge at Normanby, to assess how representative the rain gauges (the input to the model) were of the volume of water at the catchment outlet.

Figure 3.3 shows that qualitatively, the timing of the recorded rainfall at each gauge is relatively consistent; all three rain gauges show peaks between 11-14 hours after the start of the event. The hyetographs show similar event durations, beginning at around 2 hours after midnight and continuing until 20 hours, with a second small event recorded between 20 and 26 hours. This compares favourably to the shape of the flow hydrograph at Normanby, which suggests that the rain gauge and river gauge records relate to the same storm event. Data from any rain gauge may therefore be broadly representative of the timing of the event.

However, the magnitude of recorded rainfall differs at each gauge. The three gauges are distributed widely both geographically and in terms of altitude (Figure 3.1), which may cause the variation in precipitation measurements. Table 3.3 gives the total rainfall volume of rainfall recorded over the duration of the event. Brown Howe, to the north east, recorded a significantly larger volume of rainfall than Church Houses (to the north west) or Keld Held (to the south). Keld Head also recorded a significantly lower peak rainfall rate (in mm/hour), shown by a lower hyetograph peak in Figure 3.3. For these reasons, the selection of data that is representative of the magnitude of rainfall entering the catchment is uncertain. However, the widely distributed locations of the rain gauges suggest that data may encompass the geographical extremes of the catchment. Boundary conditions could be drawn from any of the three rain gauges or a combination of gauges. The selection of rainfall data was calibrated by comparison with gauging station data of water leaving the catchment. The catchment is known to respond rapidly to flood events: in the June 2007 event, the discharge hydrograph peaks within 10 hours of the peak rainfall. The discharge hydrograph also returns to its initial value within the observed timeseries. Consequently, it is assumed that storage of floodwater in the catchment over the duration of the event is negligible. Therefore, if mass is to be conserved, the volume of water observed leaving the catchment at Normanby must be approximately equivalent to the volume of water entering the catchment from rainfall.

A comparison of rain and river gauge volumes revealed that the volumes of rainfall recorded at the Keld Head and Church Houses gauges were 41.2 % and 23.0 % lower, respectively, than the volume of water recorded by the river gauging station at Normanby. That is to say, the volume of

water entering the drainage network as precipitation (measured at these two rain gauges) could not account for the volume of water that was observed leaving the drainage network at the Normanby gauging station. The same conclusions were drawn with rain data that was averaged between the rain gauges (Table 3.4). Given the wet antecedent conditions (Figure 3.2), it is likely that the ground was already heavily saturated at the time of the event, hence unable to store much additional water. It is unlikely that the difference in the volume of water recorded by the rain and flow gauges can be accounted for by storage within the catchment during the event.

Rain gauge	Total rainfall (mm)	Volume of observed rainfall, averaged over the catchment area (m <sup>3</sup> )	Volume of observed discharge (m <sup>3</sup> )	Percentage difference
Keld Head	50.4	6,098,400	10,374,210	- 41.2
Church Houses	55.6	7,986,000	10,374,210	- 23.0
Brown Howe	91.6	11,083,600	10,374,210	+ 6.8
Mean of Keld Head and Brown Howe	71.0	8,591,000	10,374,210	- 17.2
Mean of Church Houses and Brown Howe	73.6	9,534,800	10,374,210	- 8.1

**Table 3.4 Comparison of rain gauge and discharge observations for the June 2007 flood. The observed rainfall depths are given for 96 hours after midnight on 25<sup>th</sup> June 2007. This has been extended beyond the end of the main storm event to include rainfall during the whole duration of the flood hydrograph, including the recession. The rainfall depths have been converted to a catchment-averaged volume. This was calculated by multiplying the point based rain gauged measurements by the catchment area, then converting the volume into m<sup>3</sup> for comparison to the volume recorded at the gauging station. The percentage difference is the difference between the volume of rainfall and discharge, as a proportion of the volume of discharge. Discharge was recorded at the Normanby gauging station.**

It was found that only the Brown Howe rain gauge recorded a volume of rainfall that was comparable to the observed discharge at Normanby (a discrepancy of 6.8 %). The similarity in the Brown Howe record to the discharge at Normanby implies a high runoff rate, of almost 100 %. Because the ground surface was likely to be saturated prior to the event, a very high proportion of

rainfall falling on 25<sup>th</sup> June would have been rapidly routed through the catchment by overland flow, with little water lost to infiltration and groundwater.

The rain gauge record from Brown Howe is the most consistent with the gauged flow at Normanby. In light of the wet conditions leading up to the event, the implication of using rainfall recorded at Brown Howe (a high runoff rate) is a physically reasonable one. The rainfall recorded at Brown Howe was therefore selected as the input boundary condition to the model and the 'test case' on which model simulations were undertaken. There are uncertainties in the accuracy with which the available rainfall records characterise the River Seven catchment. This may have implications for the accuracy of the modelled hydrograph; in particular, whether adjusting parameter values to calibrate the model to observations may mask some potential measurement error. Model calibration is discussed further in Chapter 4. However, by selecting a rain gauge record on the basis of a comparison to river gauge measurements, this section has sought to make the most accurate and reasonable use of the available data.

### 3.5. Summary

For much of the River Seven catchment, steep sided valleys constrain the width of the floodplain and serve to contain flood flows. However, south from the village of Sinnington, the floodplain widens, increasing the risk of flood inundation over a large area. The steep gradient of the catchment means that the river responds rapidly to rainfall events, resulting in higher peak flood flows.

The River Seven is a catchment where a number of people and properties are at risk of flooding. However, conventional flood defences may have detrimental impacts downstream and cannot be justified on the grounds of expense. Recent research has identified flow attenuation upstream of settlements as a potential method for flood management in this catchment that is consistent with local priorities (Ryedale Flood Research Group, 2008) and regional policies (Environment Agency, 2007a). However, the best locations for such measures and the extent to which they may reduce downstream flood risk are unknown.

As discussed in Chapter 2, numerical models were used to predict the effect of interventions on flood response. The June 2007 flood was used as the boundary condition to the model since it allows the performance of flow attenuation and the model performance to be tested for an extreme event. Observed data is also available against which the model predictions can be validated.

However, in order to characterise the catchment and event, parameter values must be introduced into the model to account for unavailable data and process simplification. The next chapter evaluates model behaviour in relation to the River Seven and June 2007 flood.

## 4. Model evaluation

### 4.1. Summary

This chapter presents the results of a sensitivity analysis, which tested the sensitivity of the model response to variations in parameter values. This analysis assessed whether *Overflow's* behaviour was consistent with its constituent equations, and hence a realistic approximation of the physical processes operating in the catchment. The results of the sensitivity analysis allowed the model to be calibrated to the June 2007 flood event.

The assumptions involved in creating a model to represent a real world catchment were discussed in Chapter 2. Since a model is a simplification of reality, it is necessary to evaluate whether the model behaves realistically and how different it is to reality. This chapter begins with an introduction and justification of the need for model evaluation. Three aspects of model evaluation are introduced: sensitivity analysis, calibration and uncertainty analysis. Secondly, the method and results of an analysis of *Overflow's* sensitivity to parameter values are presented, which also allowed an examination of the relative importance of each parameter. Third, parameter values were adjusted to calibrate the model to the June 2007 flood by evaluating how accurately the model reproduced observations under different parameter sets. The aim of this chapter was to ensure that *Overflow* was a reasonable representation of the processes operating in the River Seven catchment during the June 2007 flood event. This was undertaken to ensure that the model could be used predicatively, to predict the impacts of flow attenuation, which is discussed in Chapter 5. Following the model application to assess the impact of interventions, in Chapter 5, the level of uncertainty and precision that could be associated with the results was quantified by an uncertainty analysis (Horritt, 2006).

The model responded to parameter variation in a way that could be explained by physical processes, represented in the model's constituent equations. Nothing was found that challenged the view that *Overflow's* response to variation in parameter values was a representative of the physical processes operating in the catchment (discussed in Chapter 3). Objective functions were used to assess the accuracy with which the model replicated gauging station observations. The results showed that accurate model predictions were made under a range of physically reasonable parameter sets. It is recognised that these tests cannot prove that the model is a completely true representation of the real world (Saltelli et al., 2008). However, the model was successfully corroborated with both observed data and an understanding of physical processes. It was concluded that the model was capable of representing the processes operating in the catchment and flood event, to a degree of accuracy that was sufficient for the purposes of this project – examining the impact of flow attenuation. Model sensitivity was greatest to the rainfall

rate and runoff rate parameter values. The model was calibrated using these parameter values, to carry out further investigations on flow attenuation in Chapter 5.

## 4.2. Introduction to sensitivity analysis, calibration and uncertainty analysis

### 4.2.1. Sensitivity analysis

A theoretical understanding of reality is often too complex to use for predictive purposes or at large scales. Numerical models simplify theoretical understanding by linking theory with the observable outcomes of environmental processes (Morton, 1993). Simplification of theoretical concepts into models that can be applied to specific situations requires the introduction of parameters and boundary conditions, in order to characterise the real world catchment (Beven, 1996). Parameters are a constant number in the mathematical equations that make up the model.

However, data are rarely available at the necessary scale to define parameter values by direct measurement (Beven, 2001) and in most cases, parameters are included to account for a lack of measured data. For example, Manning's  $n$  is, theoretically, used to account for topography smaller than that of the scale of measurement. In the case of *Overflow*, this is resistance to flow caused by topography or other features that occurs on scales of less than the 20 metre resolution DEM. If parameter values cannot be directly measured or inferred from other relevant observations, they must be selected by a process of optimisation, in which parameter values are used to fit model predictions to measurements (Beven, 1996). As a result, the values that parameters take may not have a real physical meaning. For example, in *Overflow*, while Manning's  $n$  might theoretically represent resistance to flow, it may also account for other processes that are not explicitly represented in the model.

A sensitivity analysis was therefore undertaken to assess whether the model behaved realistically in response to variations in parameter values. This was used to verify whether parameters represented the physical processes that they were intended to represent in the model's constituent equations. The sensitivity analysis also identified the parameters to which the model was most sensitive, where small changes in the input parameter value resulted in significant changes to the output.

### 4.2.2. Calibration

In this project, as in many UK catchments, data does not exist to define parameter values *a priori* or by direct empirical measurements (Marks and Bates, 2000). Parameter values are therefore

selected by optimisation of model predictions to an observed dataset. In this process, variables can be adjusted manually or using an automatic algorithm to obtain a 'better fit', measured by objective statistical functions, between modelled and observed results (Beven, 2001). Statistical techniques for quantifying 'goodness-of-fit' are discussed later, in section 4.3.

By comparing the results of the sensitivity analysis to empirical measurements, the model could be calibrated. This process allowed the selection of a set of parameter values that closely matched the June 2007 flood event. The differences between model predictions and reality were reduced by adjusting parameter values to obtain a better fit of model predictions to observations.

#### 4.2.3. Uncertainty analysis

While the sensitivity analysis assessed model response to the full range of parameter values, an uncertainty analysis also needed to be undertaken with respect to the parameter values used to represent flow attenuation interventions. This allowed an assessment of the uncertainty associated with the impact of flow attenuation interventions and is presented in Chapter 5.

If the model is calibrated by comparison with observations, then calibration against a different set of observations may result in the selection of different parameter values. The optimum parameter values may also depend on the scope and detail of observed datasets or the values taken by other parameters (Beven, 2000). For example, in a two dimensional model, Yu and Lane (2006a) found that coarsening the resolution of topographic data changed the predicted flood timing and inundation extent. Different parameter values were then required to optimise the model to observations. This was explained by different levels of topographic detail being explicitly represented at different resolutions, leading to varying levels of model dependence on roughness parameters (Yu and Lane, 2006a).

There may therefore be a range of parameter values that give accurate model predictions, depending on interactions with other components of the model, such as other parameters. For example, a parameter value that leads to inaccurate model results may subsequently predict accurate model results when other parameter values are varied (Beven, 2000). This situation, in which acceptable model results can be produced for a range of reasons, is called 'equifinality' (Beven, 1996). Equifinality causes difficulties in identifying the processes that give rise to a particular model response (Kirchner, 2006), which is problematic because this project aims to quantify the specific impact of flow attenuation on flood flows.

In Chapter 5, particular reaches of the river network were identified where flow attenuation reduced the magnitude of downstream flood flows. An analysis was undertaken to assess how the



uncertainty in selecting parameter values to represent flow attenuation (i.e. the range of values the parameter could realistically take) propagated through the model. This identified variability in the model output that was associated with particular processes (Hamby, 1994), allowing the calculation of the likely error margins arising from a particular set of parameter values.

The uncertainty analysis is closely related to the sensitivity analysis. However, the sensitivity analysis examines how the model output responds to changes in the model parameters or boundary conditions. Its purpose in this project is to determine if the model behaves realistically and to allow model calibration to take place, by assessing how accurately the model reproduces observations. The uncertainty analysis determines if, and by how much, uncertainty in parameters or boundary conditions generates variability and imprecision in the model outputs. Its purpose is to quantify the level of confidence that can be attached to modelled results (Smith and Smith, 2007).

### 4.3. Sensitivity analysis

#### 4.3.1. Model output

The sensitivity analysis assessed how model outputs responded to changes in parameter values. *Overflow* was used to calculate a discharge hydrograph at Normanby, from which a range of statistics were drawn to summarise the behaviour of the system. These were used to assess whether the model was responding to changes in parameter values in a theoretically realistic manner. The responses of most relevance to a flood inundation study are peak discharge magnitude, travel time of the flood hydrograph peak and overbank flood volume, which are shown in Figure 4.1.

Peak discharge magnitude indicates the maximum flow during the event. Peak discharge corresponds to the peak water depth and hence the magnitude of overbank flooding. Peak water depth can be calculated from rating curves (an empirical relationship between discharge and depth). However, this introduces additional uncertainties relating to gauging station measurement error and the extrapolation of empirical relationships to situations beyond the datasets on which they are based. As a result, peak discharge is used as the main measure of flood magnitude.

The travel time of the flood hydrograph peak is given as the number of hours after the start of the event at midnight on 25<sup>th</sup> June 2007. This can be used as a measure of the speed of overland flow and flow attenuation within the catchment.

Overbank flood volume is the volume of water above bankfull discharge, hence the volume of flood water on the floodplain. Bankfull discharge was taken to be  $72.4 \text{ m}^3\text{s}^{-1}$ , which corresponded to the bankfull stage of 3.96 m (JBA Consulting, 2008b). This bankfull discharge figure was based on a consultant's 1D hydraulic model of the location, which was developed for a flood risk mapping study and is the standard technique used for flood risk assessment in the UK (Lin et al., 2006; JBA Consulting, 2008b).

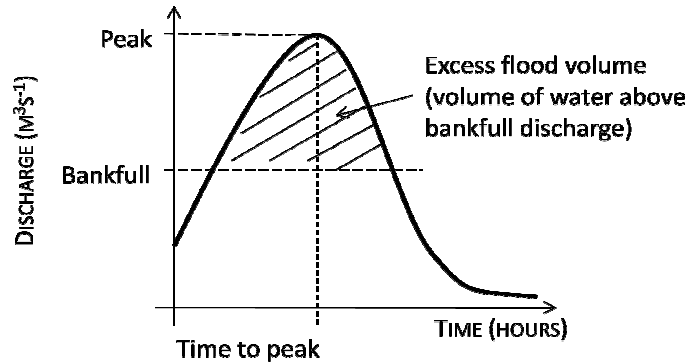


**Figure 4.1** A hypothetical discharge hydrograph, illustrating model responses assessed in the sensitivity analysis.

In addition, the whole hydrograph was compared to an observed hydrograph for the same event using an objective statistical function, the Nash Sutcliffe Efficiency Index (NSE). The NSE was used to assess whether the model was making accurate, not just theoretically realistic, predictions. However, the hydrograph peak, time-to-peak and overbank flood volume were still used to identify in which respects the model was accurate (Lane and Richards, 2001).

#### 4.3.1.1. Nash Sutcliffe Efficiency (NSE)

The NSE Index is widely used to compare model predictions and observations, in order to evaluate the 'goodness-of-fit' between the two (Nash and Sutcliffe, 1970; Green and Stephenson, 1986).

$$NSE = 1 - \frac{\sum_{i=1}^n (O_i - P_i)^2}{\sum_{i=1}^n (O_i - \bar{O})^2}$$

**Equation 4.1** Dimensionless Nash Sutcliffe Efficiency (NSE), which is based on three quantities: observed values of the variable ( $O$ ), the mean of the observations ( $\bar{O}$ ) and the values predicted by the model ( $P$ ). The Efficiency calculation is the ratio of variation in observations that are unexplained by the model (the numerator of the equation), to the total variation of observed values around the mean (the denominator of the equation), subtracted from 1.

An NSE value of 1 implies perfect model performance (where the numerator of the fraction, the observed variance unexplained by the model, equals 0). Values of greater than 0 imply that the model explains some of the observations. Values of less than 0 (where the unexplained variation in predictions is greater than total variation in the observations) imply that due to the amount of noise in the predictions, the model is no better than a set of random numbers (Beven, 2001).

A number of different objective functions exist to assess hydrographs. NSE was chosen as it is suited to assessing high flow hydrographs and comparing the goodness-of-fit between multiple hydrographs (Green and Stephenson, 1986). Unlike other techniques (e.g. the  $R^2$  correlation coefficient), NSE is sensitive to differences between the means and variances of observations and predictions. It is also dimensionless, so its value is not dependant on small differences in the magnitude of the hydrograph. Unlike measures based on the sum of errors or residuals, NSE is also independent of the number of values in the dataset. This allows NSE to be used to directly compare the goodness-of-fit of different hydrographs under different model boundary conditions or parameter selection.

Larger differences between observed and predicted results (the residuals) tend to occur around the hydrograph peaks (Beven, 2001). Since the residuals are squared, NSE is more sensitive to high flows than low flows and gives greater weight to errors at high flows (Legates and McCabe, 1999). For example, high NSE values can be found despite a poor fit between observations and predictions, if the variance of observations (the denominator of the fraction in Equation 4.1) is high (McCuen et al., 2006). NSE is consequently unsuited to assessing widely varying flows, e.g. a continuous simulation containing periods of extremely high and low flows. However, since this project is concerned with single flood events, the effects of variations in NSE sensitivity to large differences in flow magnitude are limited.

#### 4.3.2. Overview of sensitivity analysis methods

Two sensitivity analyses were undertaken: a local sensitivity analysis and a global sensitivity analysis. The local sensitivity analysis tested the model response to each parameter in turn, while all others were held constant. Any change in model response can therefore be attributed to a change in a particular parameter. This was used to establish whether the model responded to variations in parameters in a way that was consistent with its constituent equations and, in turn, an approximation of the physical environment. Section 4.4 describes the method used in the local sensitivity analysis, followed by the results and interpretation.

However, parameter values do not operate independently. A change in one parameter value may affect the model sensitivity to another parameter. In the global sensitivity analysis, the values of all parameters were varied simultaneously. This allowed an analysis of the effect of parameter

interdependence. By examining how the model responds to interactions between parameters, the relative importance of different parameters can be identified. The global sensitivity analysis was also a more efficient method of assessing parameter interdependence, allowing larger sample sizes. The limitations of this method are that the model response cannot be attributed to any one parameter. Therefore, it cannot be used to verify that the model responds to parameter variation in a way that can be explained with an understanding of physical processes. For this reason it is still necessary to undertake a local sensitivity analysis. Section 4.5 justifies the need for a global sensitivity analysis, followed by an explanation of the method, and then the results and interpretation.

As discussed in Chapter 3, the River Seven catchment topography and channel geometry had already been set up as part of previous work, so the sensitivity analysis is primarily concerned with using the model to perform flow routing calculations. As a result, the sensitivity analysis did not directly test the parameters involved in setting up the model geometry (e.g. constants and exponents in the Leopold and Maddock equations, section 2.5.3.3). However, the impact of channel geometry on flow routing was tested by varying the channel widths and depths within a representative range, which is discussed further in the local sensitivity analysis, section 4.4. Other parameters that were necessary for *Overflow's* flow routing calculations were also tested:

- Channel Manning's  $n$ , which was used in the Manning equation to calculate flow velocities in model grid cells designated as 'channel cells'.
- Land cover Manning's  $n$ , which was also used in the Manning equation to calculate flow velocities in 'non-channel' grid cells. River channels tend to offer less resistance to flow than catchment land cover, so it was important to distinguish channel and land cover Manning's  $n$  values. However, there was no spatially distributed data available to validate a further distinction between floodplain and general catchment land cover.
- Rainfall rate (mm/day), which was used to calculate the flow velocities of the model grid cells, for subsequent flow routing. Note that the rainfall input to the model, measured at a rain gauge, was not varied. Thus the input volume of water was the same in each model run. Varying the rainfall rate parameter affected the speed that flow was routed through the catchment (see section 2.5.3.5 for a fuller explanation).
- Runoff rate (%), which represented water losses to infiltration. This was achieved by subtracting an amount of water from the actual rainfall input to give an effective rainfall input.

## 4.4. Local sensitivity analysis

### 4.4.1. Method

The local sensitivity analysis assessed the sensitivity of the model response to each parameter, across the range of values that could feasibly be taken by those parameters (the parameter space). Although an element of subjectivity is introduced in deciding what constitutes a ‘feasible’ parameter value, the ranges were selected on the basis of widely used flood modelling literature and available measurements of the catchment. These ranges are defined in Table 4.1.

In the first stage of the sensitivity analysis, the parameters were sampled one-at-a-time (OAT) (Saltelli et al., 2008). This stage of the sensitivity analysis is called a local sensitivity analysis, because only one parameter changes in value between each successive simulation, while all others are held constant. Any change in the model output between each simulation can therefore only be attributed to the change in that parameter (Saltelli et al., 2008). The base case values for each parameter, which were taken when another parameter was under investigation, are given in Table 4.1. These values were intended as approximations of the catchment while other parameters were tested and were based on an understanding of physical processes from literature and previous work using the *Overflow* model in similar catchments.

The parameter values under investigation were sampled systematically to ensure coverage of the entire parameter space (Table 4.1). In each case, the relevant values in the model code were edited to take account of the new parameter value and flood routing was re-calculated, with all the parameter values applied throughout the duration of the event.

Parameter	Range of sampled values	Default value (taken when other parameters were under investigation)
Rainfall rate for time map	1 – 120 mm/day	20 mm/day
Runoff rate	30 – 100 % (Houghton-Carr, 1999)	100%
Manning’s $n$ (channel)	0.02 – 0.20 (Chow, 1959)	0.035
Manning’s $n$ (land)	0.02 – 0.20 (Chow, 1959)	0.060
Multiples of channel width	0.5 – 1.5	1.0
Multiples of channel depth	0.5 – 1.5	1.0

**Table 4.1 Parameters and the values used in the local sensitivity analysis.**



**Figure 4.2** The River Seven at Sinnington, looking upstream from near the Sinnington gauge, 28<sup>th</sup> November 2009. At this point the river channel is approximately 15 m wide and 3 m deep.

The range of runoff rates was based on measured values for UK catchments, given by Houghton-Carr (1999) in the Flood Estimation Handbook. Houghton-Carr estimated rainfall rates for 275 UK catchments in a series of flood events. The majority of runoff rates fell within the range 30 - 100%. This range was applied in the local sensitivity analysis. The default value for runoff rate was set at 100%. This implies that all rainfall was routed overland, with no losses to infiltration. Given the wet antecedent conditions of the June 2007 flood event, a high runoff rate is considered a realistic possibility. In previous work on the neighbouring Pickering Beck catchment (Odoni and Lane, 2010), these values were found to allow the model to accurately replicate observations.

Channel width and depth were derived from Leopold and Maddock's (1953) empirical equations, which relate channel geometry to discharge (Ferguson, 1986). Comparison of the derived channel geometry with stream channel surveys at the Normanby gauging station (JBA Consulting, 2008a; JBA Consulting, 2008b) reveals differences in width and depth of up to 44 % of the predicted values. The channel geometry was therefore varied within a range of  $\pm 50$  % from the initially derived widths and depths. In the base case, channel widths and depths were set as equivalent to the original values derived from the Leopold and Maddock equations.

The range of Manning's  $n$  values was based on an index by Chow (1959), which describes a variety of channels and floodplains and their associated  $n$  values. Relevant excerpts from the index are given in Appendix 1. Indexes, particularly Chow (1959), are widely used to estimate Manning's  $n$  values for flood modelling studies (Brunner, 2008). Manning's  $n$  is theoretically related to flow

depth and velocity by the Manning equation (Equation 2.4), so  $n$  could be calculated from direct measurements of flow. However, it is rare that such measurements are collected at high density, at the scale of entire catchments and during a flood event (Wohl, 1998). In most catchment scale flood modelling studies, it is therefore necessary to estimate  $n$  values from a suitable range. The base case Manning's  $n$  values correspond to a generally clean channel and light brush and trees overbank (Chow, 1959), which was mostly observed to be the case on the River Seven (Figure 4.2). Preliminary work using this default value these values showed that predicted hydrographs closely matched observations.

The base case value for rainfall rate was also based on prior experience with work on Pickering Beck for the same event (Odoni and Lane, 2010). A preliminary model simulation (using the default values for each parameter) showed that hydrographs predicted using this rainfall rate closely matched observations (with an NSE of 0.96). The rainfall rate parameter is intended to allow an approximation for flow velocity throughout the event. The range of rainfall rates tested was based on records from the three rain gauges surrounding the catchment. The recorded rainfall rate varied from 0 mm/day to the 80.6 mm/day (the maximum recorded daily rate at Brown Howe). Since the relationship between the rainfall rate parameter and flow velocity is uncertain, this range was expanded to include rainfall rates of up to 120 mm/day.

The model responses were then plotted against each parameter value and an index was calculated to compare the sensitivity to different parameters. The purpose of the local sensitivity analysis is to identify the change in model output in response to variations in parameters over a representative range (McCuen, 1973). It would not be appropriate to calculate a ratio of change in parameter to change in model output, since this measure would be affected by the magnitude of either parameter or output. Instead a sensitivity index is used, which expresses the difference in output value, when varying each input parameter across its entire range (Hamby, 1994; Smith and Smith, 2007).

$$SI = \frac{\text{output}_{\max} - \text{output}_{\min}}{\text{output}_{\max}}$$

**Equation 4.2** The sensitivity index,  $SI$ , where *output* refers to peak discharge, time to peak or overbank flood volume.  $\text{output}_{\max}$  is the maximum value and  $\text{output}_{\min}$  is the minimum value of the model response when parameter values are varied over their entire range. The index is standardised by dividing by the maximum value of the model output.  $SI$  can take any value between 0 and 1, with higher values meaning a more sensitive model response.

The limitation of this sensitivity measure is that it does not account for variability within the parameter space and assumes a linear relationship between variations in input and output, which is rarely the case in hydrological systems (Cheviron et al., 2010). The same applies to other



measures of the strength of a relationship between two variables, such as correlation coefficients or the gradient of a linear regression. These measures, which examine the change in output between every parameter value, are highly sensitive to the linearity of the results (Hamby, 1994). Therefore, the local sensitivity analysis is mainly qualitative, based on a graphical analysis of model responses against the output variable, which allows non-linearities and other details in the model behaviour to be identified. However, the sensitivity index is included to quantify the range of model sensitivity in response to parameter values at either extreme of the range.

The results of the local sensitivity analysis were used to assess whether the model behaved realistically and solved its constituent equations correctly.

#### 4.4.2. Results

##### 4.4.2.1. Manning's $n$

In *Overflow*,  $n$  is used in the Manning equation (Equation 2.4) to calculate flow velocities and depths in each model grid cell. The model response to catchment-wide variations of Manning's  $n$  was consistent with the Manning equation. As  $n$  increased, representing greater flow resistance, the hydrographs were attenuated and time-to-peak increased. Water therefore passed the catchment outlet over a longer period of time and, since mass must be conserved, this resulted in a lower peak discharge and hence a lower overbank flood volume. This suggests that increasing flow resistance and slowing flow within the catchment can have a beneficial impact on reductions in peak discharge and flood volume downstream.

The response to channel  $n$  and land cover  $n$  exhibited the same trend. However, sensitivity index values for the various summary measures of the hydrograph tended to be higher for channel  $n$  than land  $n$  (Table 4.2). NSE was significantly more sensitive to channel  $n$  than land  $n$  (SI = 0.76 and 0.05 respectively). This suggests that channel  $n$  may be a more important parameter when attempting to accurately reproduce the hydrograph.

Given that floodplain flows tend to be shallower than channel flows, it is perhaps surprising that variations in land cover  $n$  (Figure 4.4) appear to have less of an impact than variations in channel  $n$ . However, both these parameters are interdependent. For example, as channel  $n$  increases it causes greater flow attenuation and locally higher flow depths, thereby impacting on the volume of flow that interacts with the floodplain. The local sensitivity analysis of land cover  $n$  was carried out with a channel  $n$  value of 0.035 (relatively low attenuation). This may have allowed the channel network to convey flow more rapidly, leading to lower local flow depths and a reduction in the volume of overbank flow. While the overbank flood volumes at Normanby have been estimated, it was not possible to quantify the spatial distribution of out-of-bank flow.



As a result, the model results may be less sensitive to variations in land cover  $n$  than they would in combination with a higher value of channel  $n$ . This analysis therefore does not allow a comparison of model response between the two parameters, since the magnitude of attenuation is dependant on both parameter values.

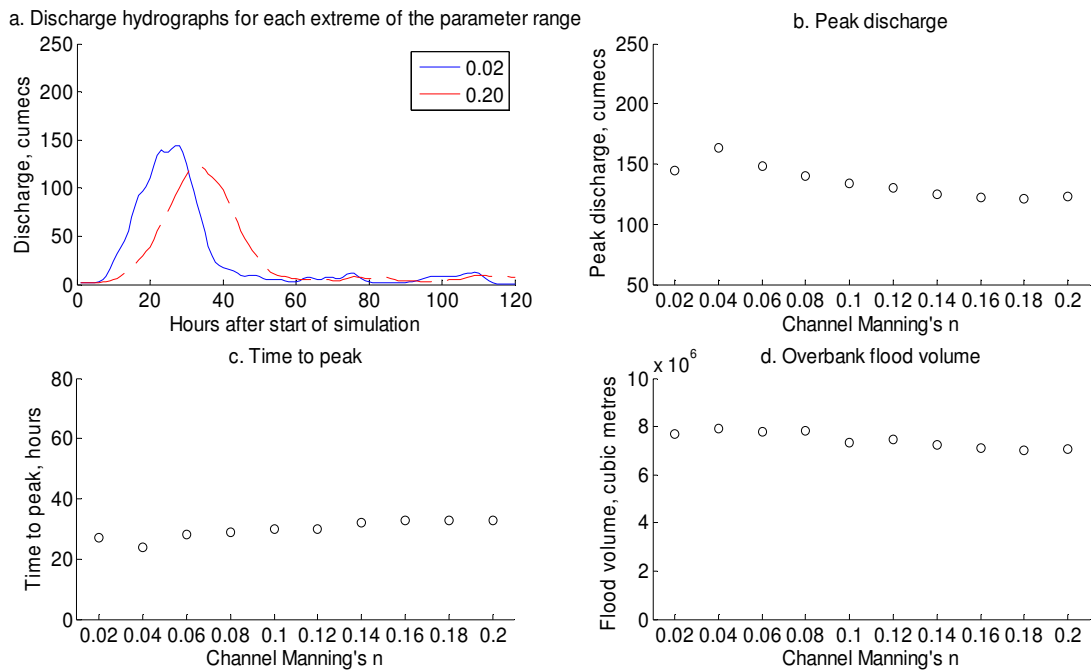


Figure 4.3 Hydrographs and measures of model response to channel Manning's  $n$ .

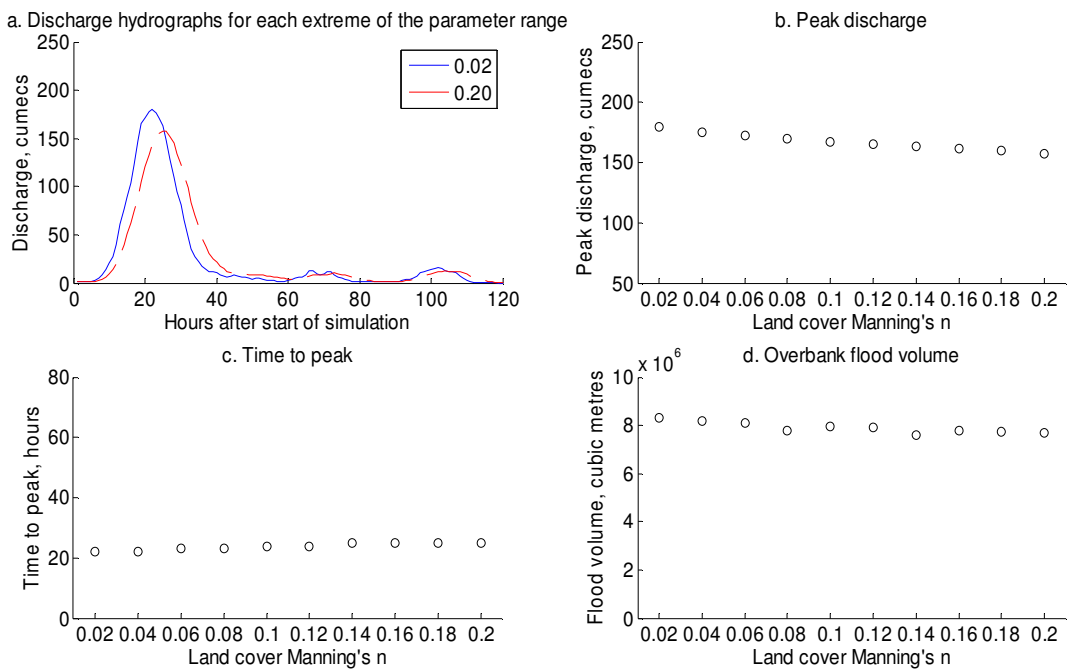


Figure 4.4 Hydrographs and measures of model response to land cover Manning's  $n$ .

#### 4.4.2.2. *Rainfall rates*

The operation of the rainfall rate parameter is discussed fully in section 2.5.3.2. The parameter is used as a means of estimating flow velocity over each model grid cell, which is subsequently used in hydrograph routing calculations. The shape of the hydrograph changed in response to variations in the parameter, and hence in response to flow velocity (Figure 4.5a). However, varying the rainfall rate parameter did not affect the input volume of rainfall, which in all cases was a rain gauge record of the June 2007 flood. Although the shape of the hydrograph changed, the area under the hydrograph remained the same in each simulation, since the same volume of water was routed through the model.

Before the observed event is routed through the model, the Manning and continuity equations are used to calculate flow velocity for a theoretical rainfall rate. Higher values for this rainfall rate result in higher discharges, leading to faster overland flow routing. As a result, hydrograph time-to-peak decreased as the value of the rainfall rate parameter increased. Faster overland flow routing results in a larger volume of water being routed downstream in a shorter period of time. This is reflected in increases in peak discharge and overbank flood volume with rainfall rate.

The response to rainfall rates is highly non-linear. Initially, small changes in rainfall rate result in large changes in all model responses. However, there is a marked increase in peak discharge at 18 – 20 mm/day. This corresponds to a point where overbank flood volume no longer increases and time-to-peak no longer decreases. Above rainfall rates of 20 mm/day the gradient of the trend in all model responses decreases. It is possible that a thresholding effect occurred, where given the boundary conditions and values of other parameters, water is being routed at its maximum velocity through the drainage network, regardless of any further increase in rainfall rate. This may be because the model explicitly represents the effects of parameters in its constituent equations. While further increases in model response might be expected, theoretically, from the model equations, additional increases may be physically unrealistic for the specific catchment and event.

In comparison to other parameters using the sensitivity index, the model is most sensitive to rainfall rate (e.g. peak discharge SI = 0.67). This suggests that variation in rainfall rate, with the consequent effect on flow velocities in each model grid cell, is the dominant control on the downstream hydrograph.

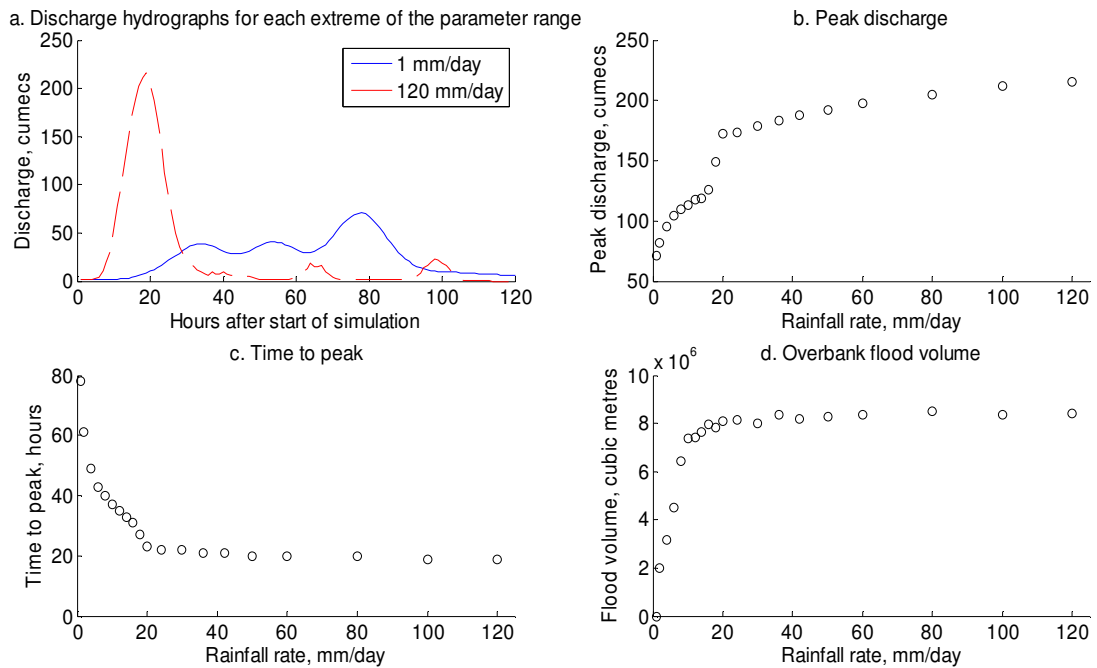


Figure 4.5 Hydrographs and measures of model response to rainfall rate, a parameter that was used for cell flow velocity calculations.

#### 4.4.2.3. Runoff rate

The response to runoff rate is, again, non-linear. Peak discharge and overbank flood volume are both positively correlated with runoff rate, while time to peak is negatively correlated. While the responses do not exhibit the same range as rainfall rate, the model is sensitive at all values of runoff rate, although there is little change in all responses between 90 % and 100 % runoff rate.

In *Overflow*, runoff rate represents the proportion of precipitation that is routed overland, minus losses to infiltration and groundwater flow, by subtracting an amount from the precipitation input. For example, a runoff rate of 90 % means that 90 % of the actual precipitation will be routed overland. The remainder of the water (losses to infiltration) is not explicitly modelled. *Overflow* is designed for the simulation of single flood events. Since infiltration and groundwater flow have much slower response times than overland flow, they are assumed not to impact significantly on the flood hydrograph over the timescale of the event. The runoff rate parameter is therefore essentially a loss function. The parameter directly controls the volume of water routed through the model, taking effect on the rainfall input rather than its subsequent routing through the catchment.

At higher runoff rates, a greater proportion of the input rainfall is routed through the catchment, so peak discharge and overbank flood volume both increase. The sensitivity index value for peak discharge is consequently very high (0.40), more so than Manning's  $n$ . As runoff rates increase, time to peak decreases. A greater volume of water causes an increase in flow depth and hydraulic

radius. According to the Manning equation (Equation 2.4), this causes an increase in flow velocity, leading to shorter hydrograph travel times. As a result, time-to-peak is also very sensitive (SI = 0.41). However, overbank flood volume is comparatively less sensitive to runoff rate (SI = 0.11), which suggests that the relationship between runoff volumes and overbank flood volumes downstream is not straightforward and may be affected by interactions with other processes.

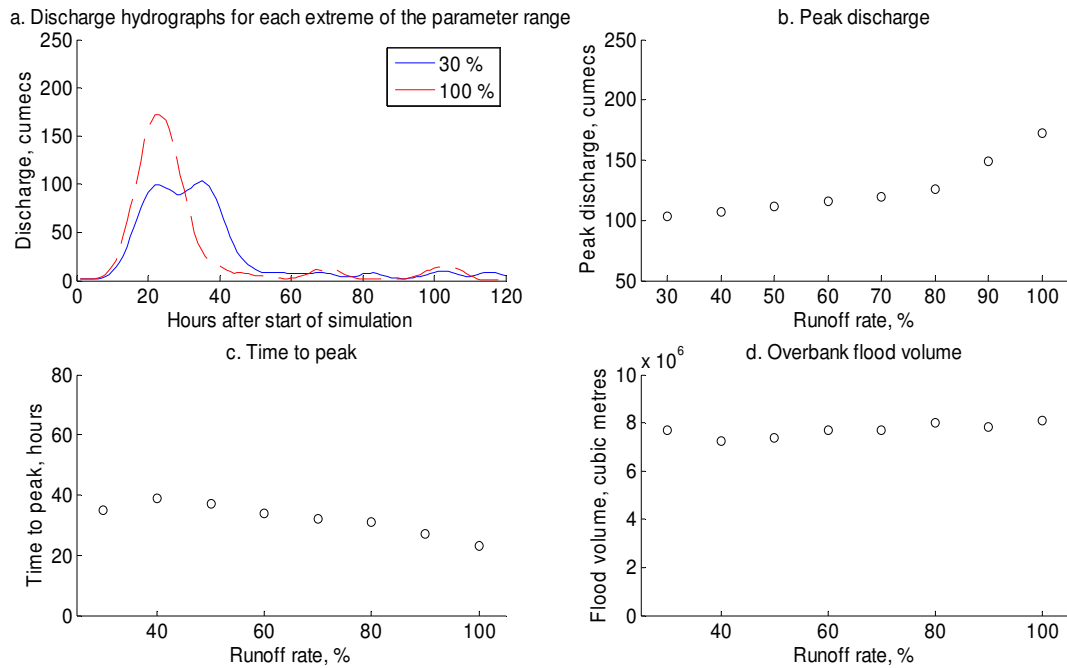


Figure 4.6 Hydrographs and measures of model response to runoff rate.

#### 4.4.2.4. Channel geometry

There was no consistent trend in the model response to channel geometry, shown in Figure 4.7 and Figure 4.8. The model showed little sensitivity to reductions in channel widths and depths from their original values. However, a more marked change occurred when the channel widths and depths were increased. Both wider and deeper channels were found to cause a decrease in peak discharge and an increase in the time to peak, implying greater flow attenuation.

If channel width or depth increases, then the area of flow in contact with the river bed or banks also increases. In turn, this leads to a decrease in hydraulic radius (the cross sectional area of flow divided by the wetted perimeter). The Manning equation (Equation 2.4) shows that a decrease in hydraulic radius causes a decrease in flow velocity. This results in flow attenuation, which accounts for a delayed flood peak and lower peak discharge. In physical terms, a greater area of flow is affected by the roughness of the channel surface, which increases flow resistance.

The SI values showed that all model responses were more sensitive to channel width than depth. The absolute values for channel width were much higher than depth, so adjusting channel geometry by multiplying these values led to a much higher absolute increase in width, resulting in a greater effect on flow behaviour.

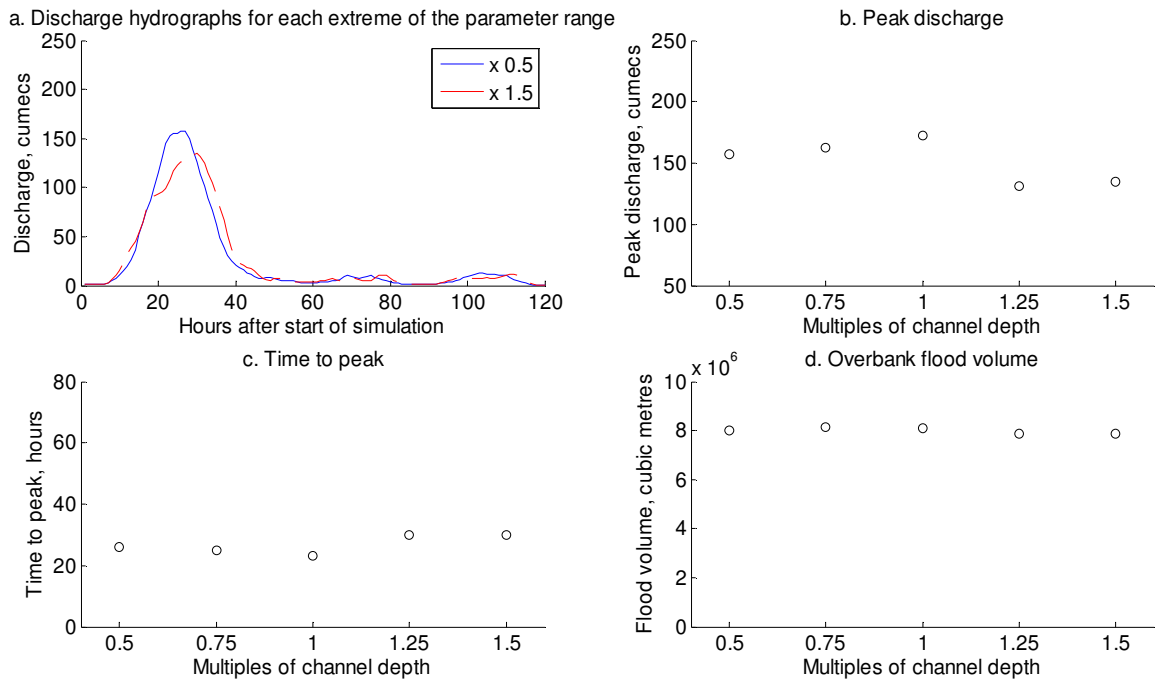


Figure 4.7 Hydrographs and measures of model response to multiples of channel depth.

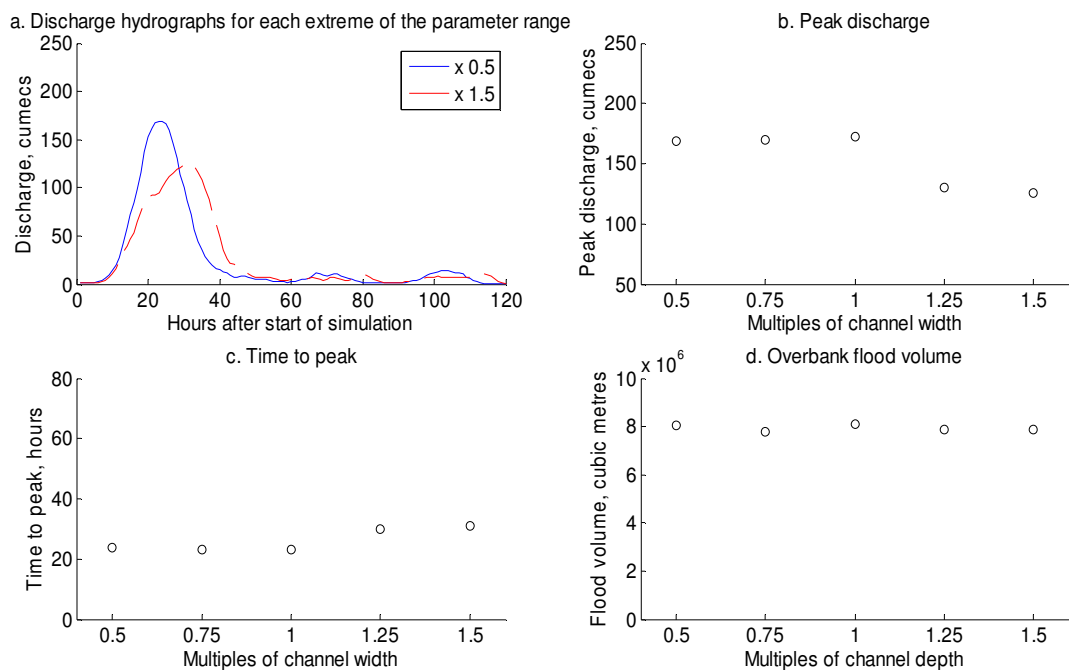


Figure 4.8 Hydrographs and measures of model response to multiples of channel width.

#### 4.4.2.5. Nash Sutcliffe Efficiency

A range of NSE values were predicted for each parameter. All the NSE values were greater than 0, which indicates that, for all the parameter values that were tested, the model captured at least some aspect of the observed hydrograph. All parameters, when adjusted, were capable of predicting a high NSE value, in which the model accurately replicated observations for the June 2007 event. There were a large range of NSE values for the model hydrographs in their response to rainfall rate, channel  $n$  and runoff rate (Figure 4.9), which had sensitivity index values of 1.42, 0.76 and 0.58 respectively. NSE was less sensitive to land cover  $n$ , channel depth and channel width, which had sensitivity index values of 0.05, 0.16 and 0.24 respectively. This was also the case when the response in Figure 4.9 was examined, which suggests that rainfall rate, channel  $n$  and runoff rate had a greater impact on the magnitude and timing of the flood hydrograph. This seems plausible since the rainfall rate parameter and channel  $n$  directly affect flow velocity calculations, while runoff rate controls the effective rainfall that is routed through the catchment. These are likely to be more important parameters in calibrating the model to the observed hydrograph.

NSE is used as a measure of how well the modelled hydrograph reproduces observations. However, it gives a limited insight into model behaviour in response to parameter values. For this, it is necessary to refer to other characteristics of the hydrograph, such as peak discharge, time to peak and overbank flood volume.

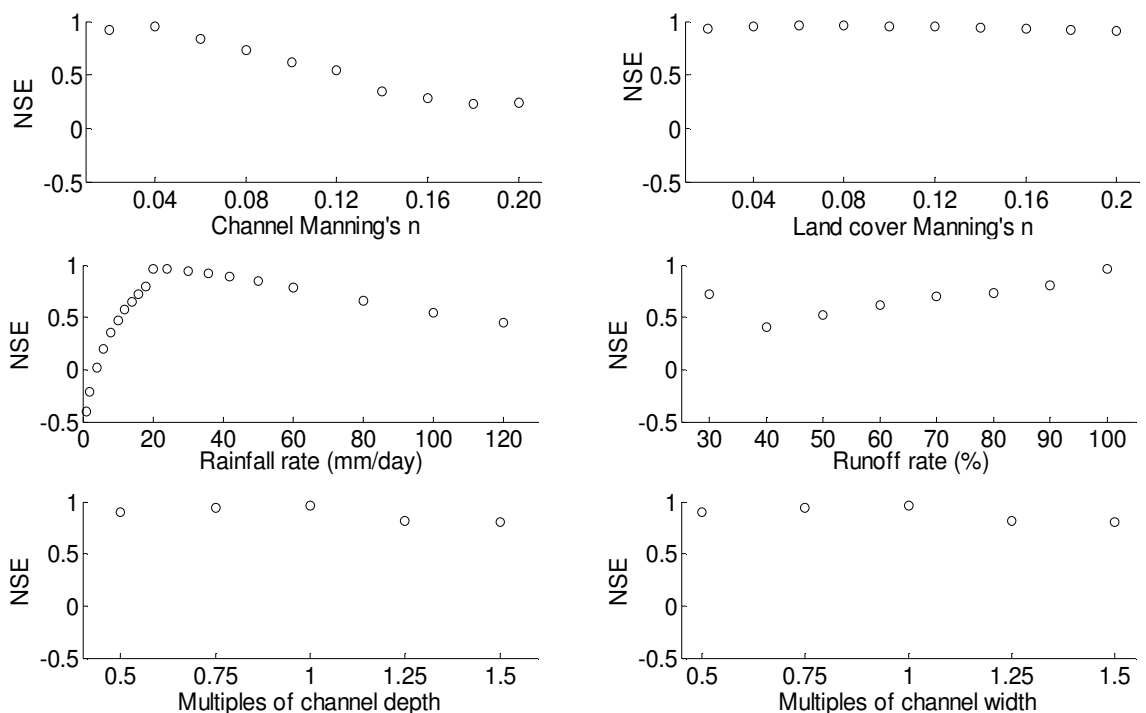


Figure 4.9 Nash Sutcliffe Efficiency for each parameter.

	Channel $n$	Land $n$	Rainfall	Runoff	Depth	Width
Peak discharge	0.26	0.12	0.67	0.40	0.24	0.27
Time to peak	0.27	0.12	0.76	0.41	0.23	0.26
Flood volume	0.11	0.09	1.00	0.11	0.04	0.04
NSE	0.76	0.05	1.42	0.58	0.16	0.24

**Table 4.2 Dimensionless sensitivity index results (see Equation 4.2) of parameters in local sensitivity analysis.**

#### 4.4.3 Local sensitivity analysis summary

The local sensitivity analysis showed variations in the modelled hydrograph in response to variation in individual parameters. The qualitative trends in the model response were explained theoretically in the context of the Manning equation, on which flow routing in *Overflow* is based. The model response to parameter variation was consistent with *Overflow's* constituent equations (see Chapter 2 for details). This suggests that the model was able to solve its constituent equations in a theoretically reasonable manner and, accordingly, was capable of replicating something of the physical processes on which those equations were based. Some parameter values also led to the prediction of hydrographs with a high NSE ( $> 0.98$ ). This implied that the model was capable of explaining a large part of the observed hydrograph.

The high NSE values suggest that given the appropriate selection of parameter values, accurate prediction of an observed flood event is possible. The results of the local sensitivity analysis also indicate that the model results are sensitive to changes in parameter values in a way that is theoretically consistent with *Overflow's* conceptual basis. This becomes significant for Chapter 5, in which parameter values are varied to represent increased flow attenuation. However, what is less clear from the local sensitivity analysis is whether the range of model responses is representative of the 'real world' processes operating in the catchment.

In the local sensitivity analysis, as one parameter was varied, all others remained constant (see Table 4.1 for the values used). This allowed variation in the model results to be attributed to specific parameters and was important in showing whether model response to each parameter was theoretically reasonable (i.e. consistent with physical process equations). However, the sensitivity of the model response to changes in parameters might also be affected by interactions with other parameter values. For example, higher channel Manning's  $n$  values within the catchment led to a reduction in overbank flow volume at the catchment outlet (Figure 4.3). As overbank flow volume decreased in response to channel Manning's  $n$ , a lower volume of water would interact with the floodplain. As a result, the model would appear less sensitive to land cover Manning's  $n$ . The local sensitivity analysis does not show the effects of parameter interaction and the relative importance of parameters when varied in combination with others. This is an issue that is dealt with in the global sensitivity analysis.

## 4.5. Global sensitivity analysis

### 4.5.1. Method

In reality, interaction or autocorrelation between parameters may allow different parameters sets to give equally accurate model outputs (Beven and Binley, 1992). An example of autocorrelated parameters in *Overflow* is that of rainfall rates and runoff rates. Both parameters are affected by the saturation of the catchment, which may lead to both a change in the volume of surface runoff (runoff rate) and overland flow velocities (calculated by selection of an appropriate theoretical rainfall rate). The effect of parameter interaction and autocorrelation is not detected in OAT sampling until all possible combinations of parameter values have been tested (Sanchez, 2006). It is therefore necessary to test parameters in combination, to give a more useful assessment of the sensitivity of the model results to parameter value selection and to assess the impact of equifinality (Beven, 2001).

However, the systematic OAT sampling used in the local sensitivity analysis would be an inefficient method to ensure coverage of the entire parameter space. To assess every possible combination of parameter values, for  $k$  parameters at  $m$  levels (the number of different values that can be taken by each parameter), would require  $m^k$  model runs (Sanchez, 2006; Saltelli et al., 2008). This method of sampling the six parameters used in the local sensitivity analysis with, for example, five levels for each parameter, would require  $5^6 = 15,625$  runs. Sampling methods are therefore needed that minimise the number of simulations. However, sampling must still take place at a great enough density across the whole parameter space to be representative. The approach taken in this research was to consider parameter values in combination with each other, on the premise that any parameter set may potentially give an accurate representation of the system (Beven and Binley, 1992; Freer et al., 1996). The results were analysed on the basis of the relative likelihood that a particular model response would be observed for a given parameter value. Unlike the local sensitivity analysis, this method does not allow model response to be attributed to a single parameter. However, it gives an indication of the role of parameter interaction in the model, allowing a more thorough assessment of model behaviour.

Monte Carlo simulations of *Overflow* were undertaken, in which the model was run multiple times with randomly sampled parameter sets (Beven, 2001). The parameter values were selected at random from a continuous uniform distribution across feasible ranges of each parameter (Table 4.1), using a random number generator. Random sampling gives an equal probability that any combination of parameter values will be chosen, precluding bias that may result from the researcher's subjective influence or because sample intervals coincide with the scale of some other systematic process (Rice, 2003). This minimises systematic errors or bias that cannot be



detected by statistical tests associated with the mean or variance of results, such as those used to calculate confidence intervals in the uncertainty analysis (section 5.5).

However, unlike systematic or stratified sampling, a random sample may not cover the entire sampling space. As sample values are selected at random, there may be gaps or clusters of values (Rice, 2003). As the sample size increases, these clusters of values even out (Saltelli et al., 2008). However, the ability of a sample to represent a given variable is limited by the sample size. A sample size that was representative of the variables of interest was estimated empirically. As the sample size increases, values of the statistics used to summarise the sample change, gradually achieving stability when the sample size becomes representative of the system (Rice, 2003). Statistics drawn from successive batches of five hundred model runs were compared and the sampling was curtailed when the sample statistics were similar. However, a relatively large number of runs would still be needed to ensure coverage of the full range of each parameter, as it would be possible for values to be randomly selected from the same area of the parameter space each time. Also, since all the parameters were tested in combination, it is difficult to identify each parameter's individual contribution to variation in the model response (Cheviron et al., 2010). In order to reduce the number of runs required and to make the results meaningful to interpret, only the parameters of most relevance to flow routing were tested. On the basis of the local sensitivity analysis, these were rainfall rate, runoff rate, channel  $n$  and land cover  $n$ .

Finally, to display the large number of results for each parameter and response, they were plotted as a probability density function (PDF). The PDF describes the probability that a particular value of the model response will occur in a particular region of the parameter space. Thus the sum of all the probabilities in the PDF equals 1. The probability of an output occurring for a given model response is given by the ratio of that model response to the total range of responses (Andrews and Phillips, 2003):

$$PDF = \frac{\delta F(x)}{\delta x}$$

**Equation 4.3 Calculation of a probability density function (PDF), where  $x$  is a continuous, random variable. The PDF is a ratio of  $\delta F(x)$ , the change in a function of  $x$ , to  $\delta x$ , a change in  $x$  (Andrews and Phillips, 2003).**

This calculation is undertaken for parameter values and the resulting model response. The results are plotted together as a two dimensional PDF. In other words, the PDF is a plot of the response surface – the relationship between parameter values and the model response (Wu and Hamada, 2000). The response surface was divided into a fifty by fifty grid and the probability of model outputs falling into each region of the grid was plotted. To aid comparison between plots, the PDFs were scaled from zero to the maximum value of the model response or parameter. Since not

all parameters were sampled as low as zero (for example, runoff rates below 30 % were thought unrealistic), some blank space appears on the PDFs as a result.

#### 4.5.2. Results

A total of 2000 model runs, each with a randomly selected parameter set were undertaken. Table 4.3 shows the summary statistics of each response. There is little variation in these statistics between each set of runs. For example, the average peak discharge had a range of  $0.48 \text{ m}^3\text{s}^{-1}$ , which is insignificant given the potential for measurement error in the observed data against which these results are compared. Therefore, sampling was curtailed after 2000 runs.

Model response	First 500 runs		First 1000 runs		First 2000 runs	
	Mean	Standard deviation	Mean	Standard deviation	Mean	Standard deviation
Peak discharge ( $\text{m}^3\text{s}^{-1}$ )	112.11	47.90	111.63	47.76	111.95	47.11
Time to peak (hours)	47.49	27.64	47.68	27.22	47.18	26.82
Overbank flood volume ( $\text{m}^3$ )	5,048,800	3,274,300	4,972,400	3,271,300	5,004,900	3,247,100
NSE	0.22	1.56	0.21	1.61	0.21	0.52

**Table 4.3 Mean and standard deviation of model responses for the first 500, 1000 and 2000 Monte Carlo runs of the global sensitivity analysis. NSE values are given to 4 decimal places to allow differences between the sets of values to be better distinguished.**

Figures 4.10 to 4.13 shows the PDFs of the response of peak discharge (Figure 4.10), time to peak (Figure 4.11), overbank flood volume (Figure 4.12) and Nash Sutcliffe efficiency (Figure 4.13) to the four parameters, channel Manning's  $n$ , land cover Manning's  $n$ , rainfall rate and runoff rate. The results are for all 2000 model runs.

In all three responses, rainfall rate showed the clearest trend. Peak discharge and overbank flood volume increased with rainfall rate. The increase was rapid at low rainfall rates, but then declined in gradient. Rainfall rate was also negatively correlated with time-to-peak; again, the trend was initially rapid but declined in gradient as rainfall rate increased. The sensitivity to rainfall rate showed the clearest trend and greatest density of results in model responses for a given

parameter value. This implies that rainfall rate is the parameter with the least equifinality (Beven and Freer, 2001). There is not a large range of parameter values that lead to the prediction of a particular model response, in comparison to model sensitivity to other parameters.

Rainfall rates were used in the calculation of cell flow velocities, which were accumulated through the catchment into a time map (section 2.5.3.5). To reduce model computation time, time maps were calculated for a series of discrete theoretical rainfall rates (Table 4.1) as part of the model set-up for the catchment. The global sensitivity analysis selected at random from these pre-calculated time maps. This caused many model responses to be predicted at particular discrete intervals in rainfall rate (Figure 4.10).

The sensitivity to channel  $n$ , land cover  $n$  and runoff rate did not show distinct trends. In terms of peak discharge (Figure 4.10), there was little clustering of parameter values. This suggests that any given value of peak discharge may result from many different combinations of parameter values. However, there was a slight clustering of values in the model response to time-to-peak (Figure 4.11) and overbank flow volume (Figure 4.12). At all values of channel  $n$ , land  $n$  and runoff rate, there was a higher probability of predicting a low time-to-peak and high flow volumes. However, as this clustering extended across the full range of the parameter space, it suggested that there may be many possible parameter sets that result in very similar model predictions.

Conversely, the lack of a distinct pattern in response to channel  $n$ , land  $n$  and runoff rate, particularly in the case of peak discharge (Figure 4.10), implies that any given parameter value may result in a wide range of model predictions. This could only be the case if the response was also controlled by variations in another parameter. Given the strong trend of sensitivity to rainfall rate in the global sensitivity analysis, it was thought that the control exerted by rainfall rate overwhelmed the model sensitivity to any other parameter.

However, the local sensitivity analysis showed that the model was sensitive to channel  $n$ , land cover  $n$  and runoff rate. These parameters were further explored. Another set of Monte Carlo simulations were undertaken, in which rainfall rate took a constant value, but the values of other parameters were selected at random, as in the previous test. The PDF of NSE values in response to rainfall rate showed that high NSE values were obtained most frequently with a rainfall rate of 18 mm/day. Consequently, the model was run again with an optimised rainfall rate of 18 mm/day. This allowed the removal of noise related to rainfall rate from the response to other variables. These results, again for 2000 model runs, are given in figures 4.14 to 4.17. The statistics used to curtail sampling after 2000 runs are given in Table 4.4, which shows little variation between each set of simulations. For example, average peak discharge had a range of  $0.86 \text{ m}^3\text{s}^{-1}$ , which is again within the potential uncertainty caused by measurement error in observations.

Model response	First 500 runs		First 1000 runs		First 2000 runs	
	Mean	Standard deviation	Mean	Standard deviation	Mean	Standard deviation
Peak discharge ( $\text{m}^3\text{s}^{-1}$ )	104.10	18.39	104.96	19.96	104.53	19.72
Time to peak (hours)	38.80	8.20	38.48	8.22	38.67	8.42
Overbank flood volume ( $\text{m}^3$ )	5,917,200	1,726,200	5,991,500	1,707,900	5,971,200	1,733,000
NSE	0.13	0.32	0.14	0.34	0.13	0.34

**Table 4.4 Mean and standard deviation of model responses for the first 500, 1000 and 2000 Monte Carlo runs of the global sensitivity analysis when rainfall rate was held constant. NSE values are given to 4 decimal places to allow differences between the sets of values to be better distinguished.**

Figures 4.14 to 4.17 show that trends in model response to channel  $n$ , land cover  $n$  and runoff rate are the same as in the local sensitivity analysis. The model outputs were most sensitive to runoff rate, as this showed the strongest degree of clustering in the PDFs. This suggests that it is easier to identify runoff rate values as there is a more limited range of values that can lead to a particular model response.

In the global sensitivity analysis without variations in rainfall rate, results for channel  $n$  and land cover  $n$  cluster in particular areas of the parameter space to a greater degree than previously. Channel  $n$  is more clearly identifiable than land  $n$ , because for each value taken by channel  $n$ , a greater number of simulations fall within a smaller range. However, both channel and land  $n$  show a stronger level of equifinality than rainfall rate and runoff rate, as a larger range of  $n$  values can result in any one model response.

The global sensitivity analysis shows that the model is most sensitive to the rainfall rate parameter, followed by runoff rate. The implication is that flow behaviour and the model accuracy are highly dependent on the accurate specification of rainfall rate and runoff rate.

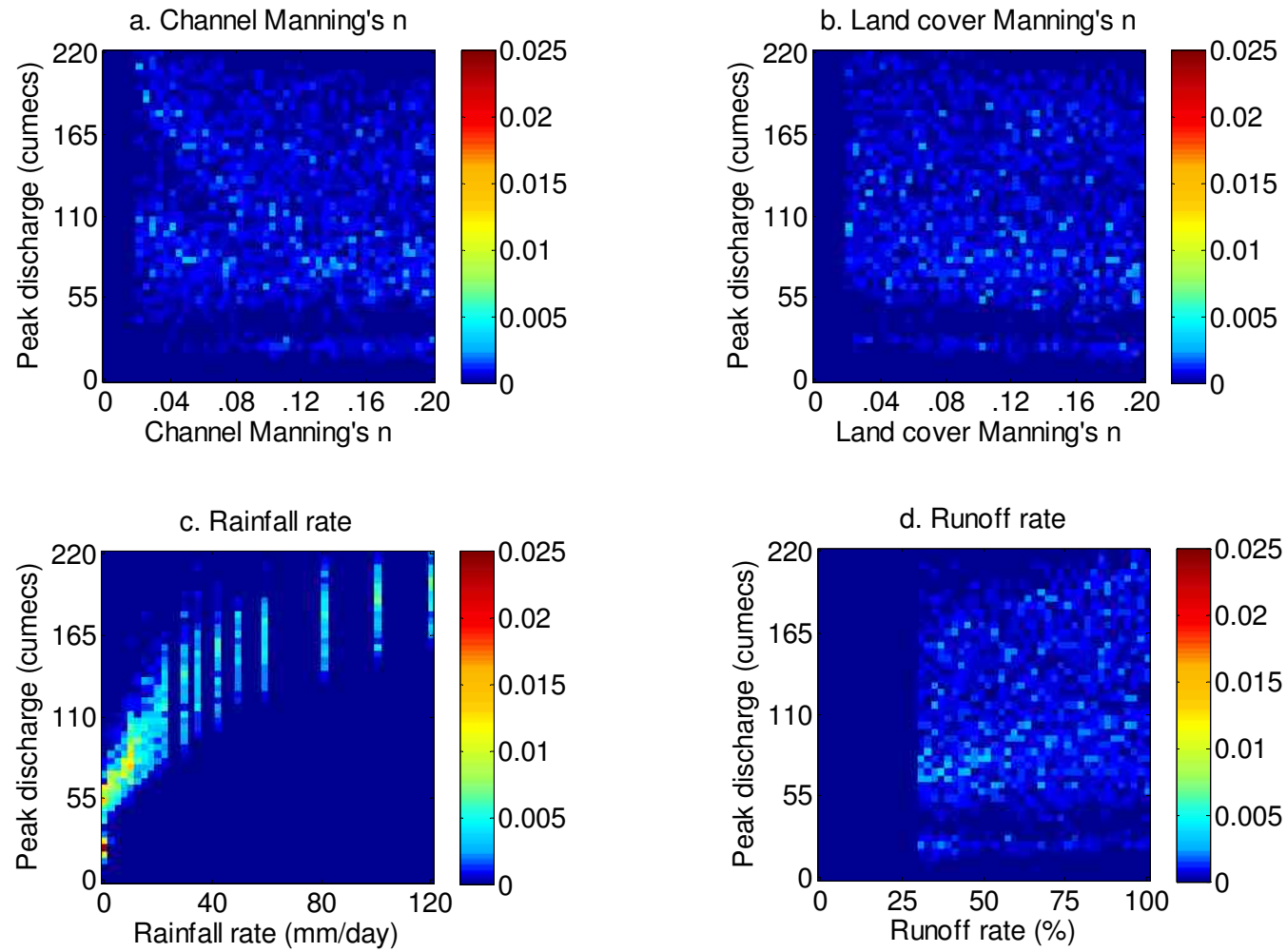


Figure 4.10 Peak discharge response to; a. Channel Manning's  $n$ , b. Land cover Manning's  $n$ , c. Rainfall rate and, d. Runoff rate. Colours to the higher (red) end of the colour bar indicate a higher probability of model responses occurring in that region of the response surface.

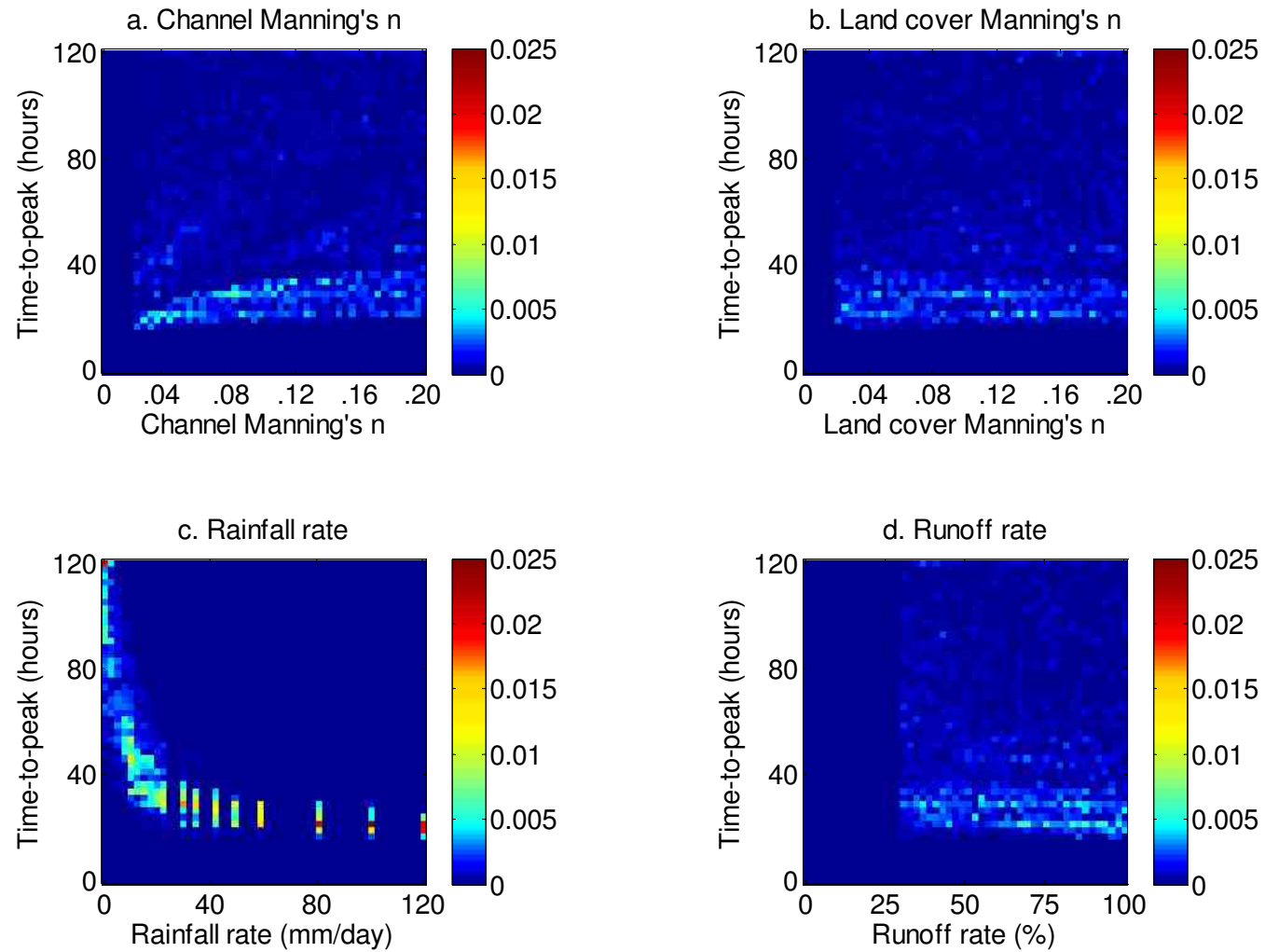


Figure 4.11 Time to peak response to; a. Channel Manning's  $n$ , b. Land cover Manning's  $n$ , c. Rainfall rate and, d. Runoff rate. Colours to the higher (red) end of the colour bar indicate a higher probability of model responses occurring in that region of the response surface.

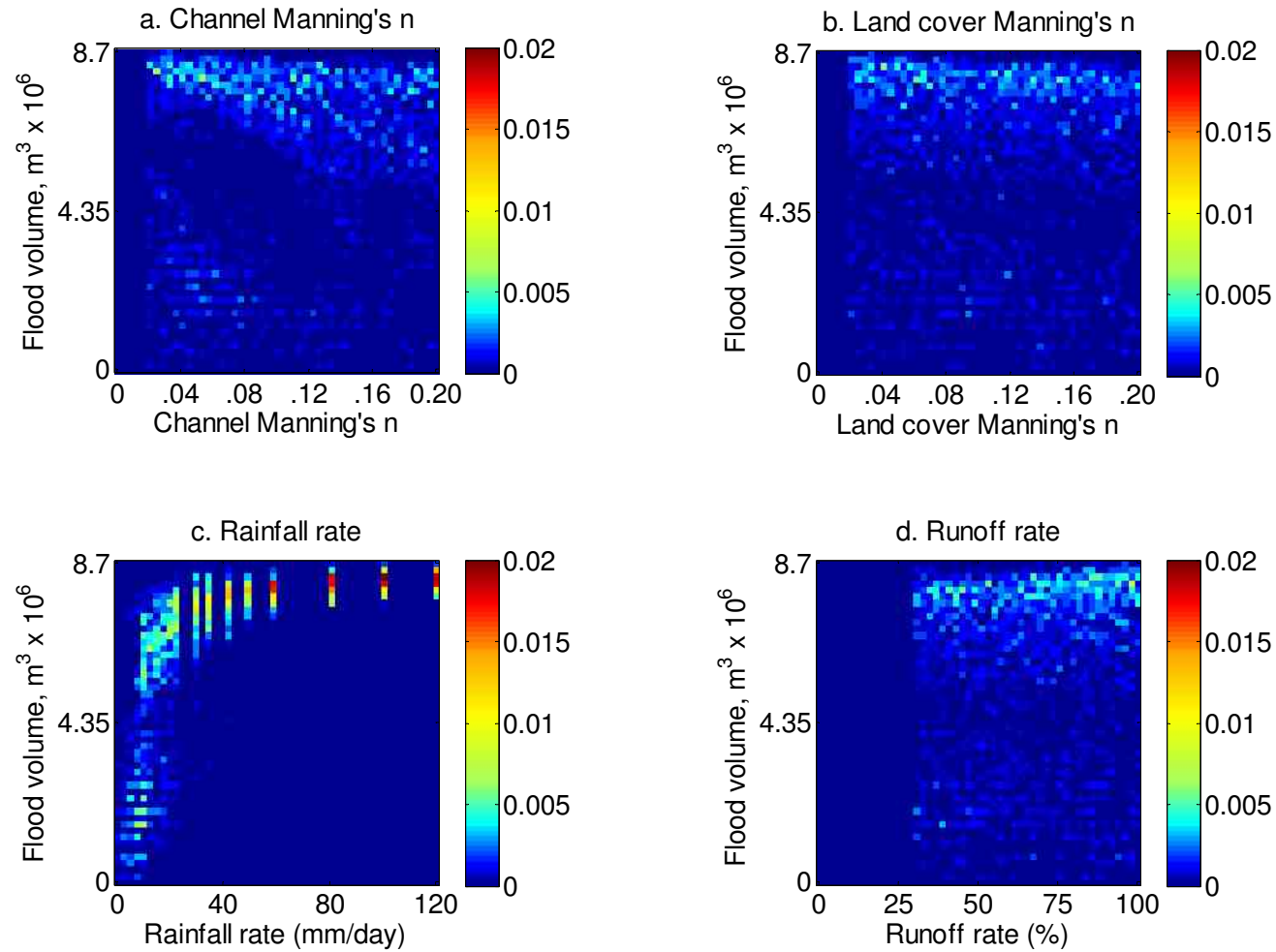


Figure 4.12 Overbank flood volume response to; a. Channel Manning's  $n$ , b. Land cover Manning's  $n$ , c. Rainfall rate and, d. Runoff rate. Colours to the higher (red) end of the colour bar indicate a higher probability of model responses occurring in that region of the response surface.

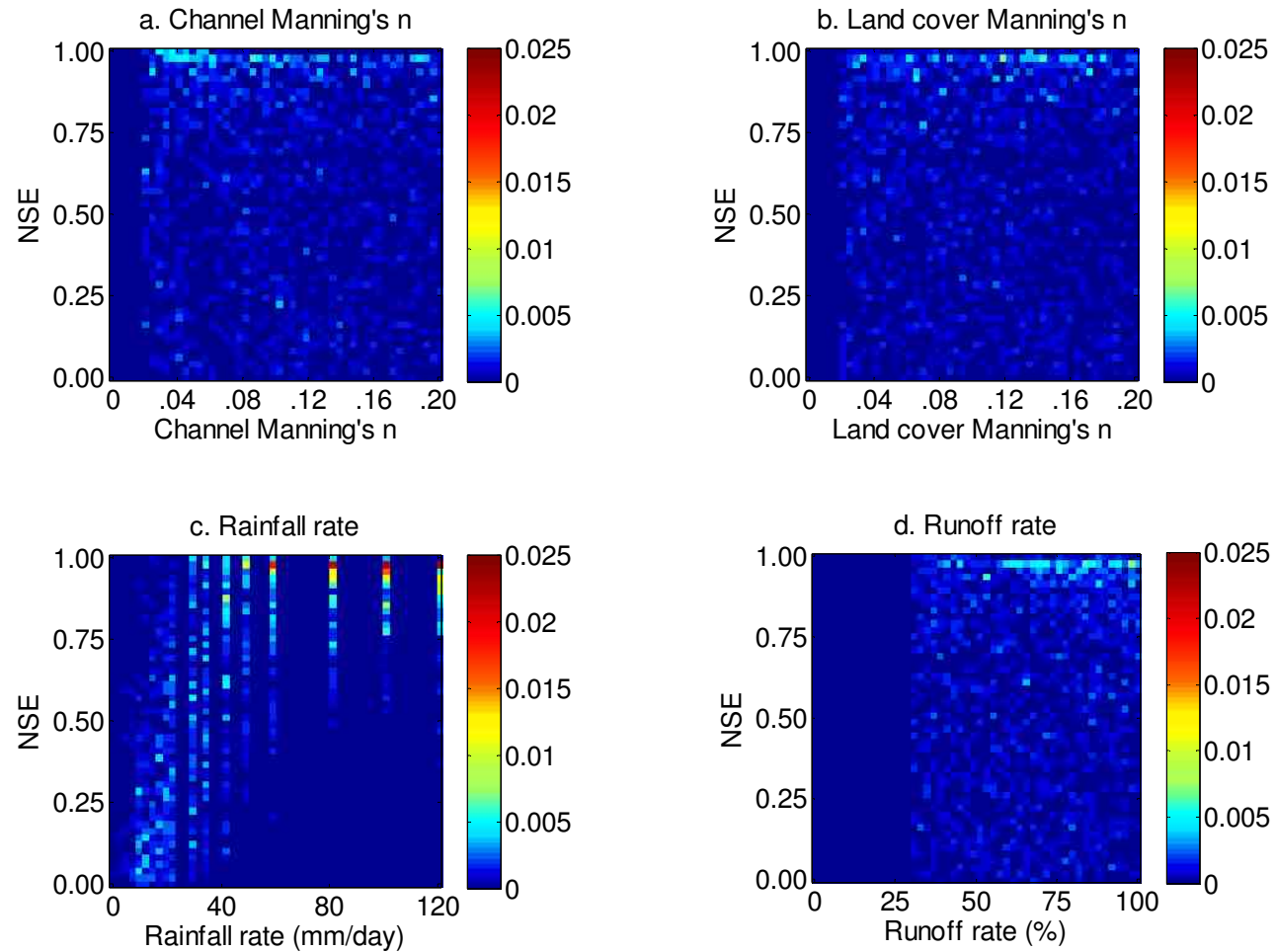


Figure 4.13 Nash Sutcliffe Efficiency index and its response to; a. Channel Manning's  $n$ , b. Land cover Manning's  $n$ , c. Rainfall rate and, d. Runoff rate. Colours to the higher (red) end of the colour bar indicate a higher probability of model responses occurring in that region of the response surface.



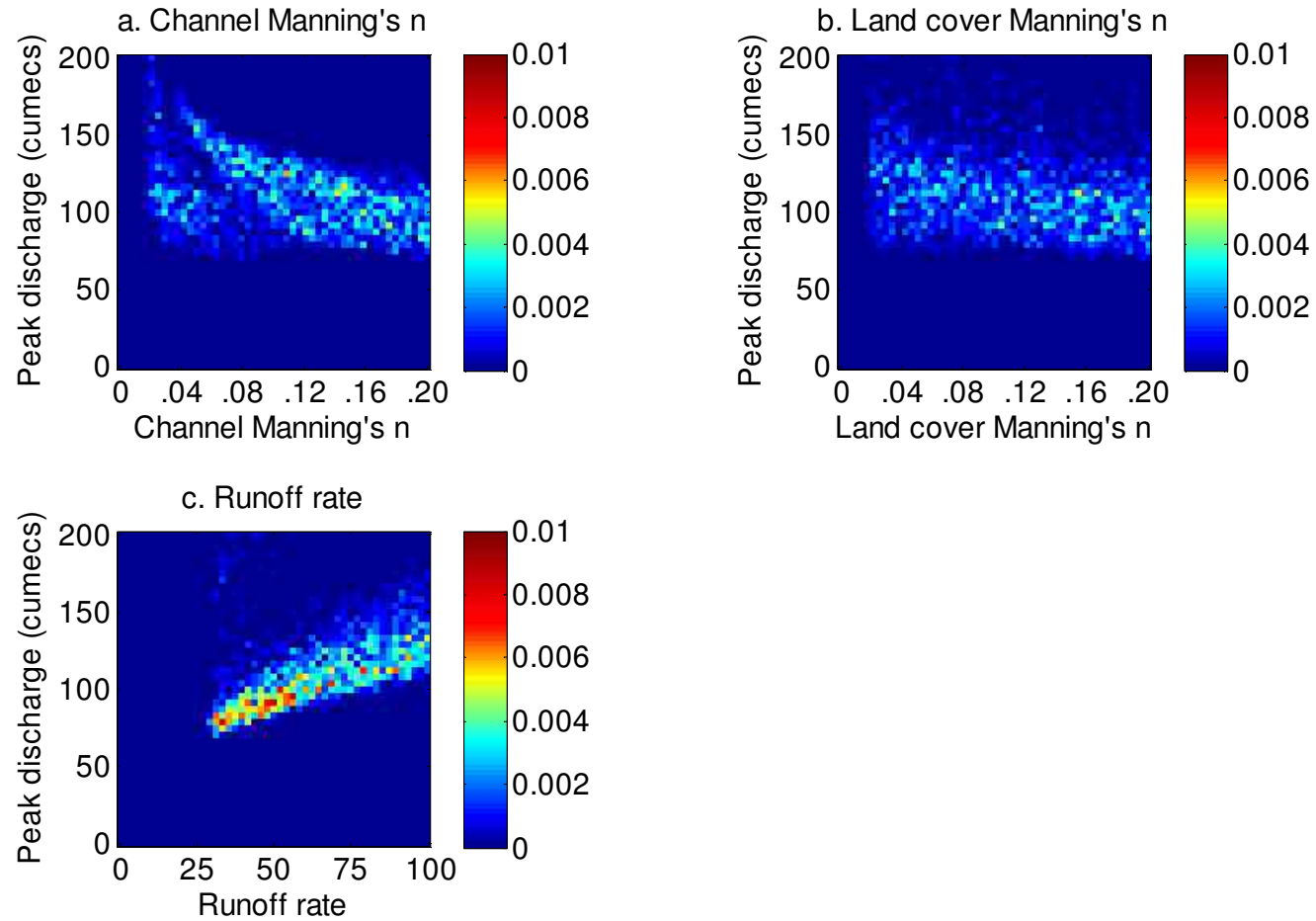


Figure 4.14 Peak discharge response to; a. Channel Manning's  $n$ , b. Land cover Manning's  $n$  and, c. Runoff rate, all when rainfall rate was held constant. Colours to the higher (red) end of the colour bar indicate a higher probability of model responses occurring in that region of the response surface.

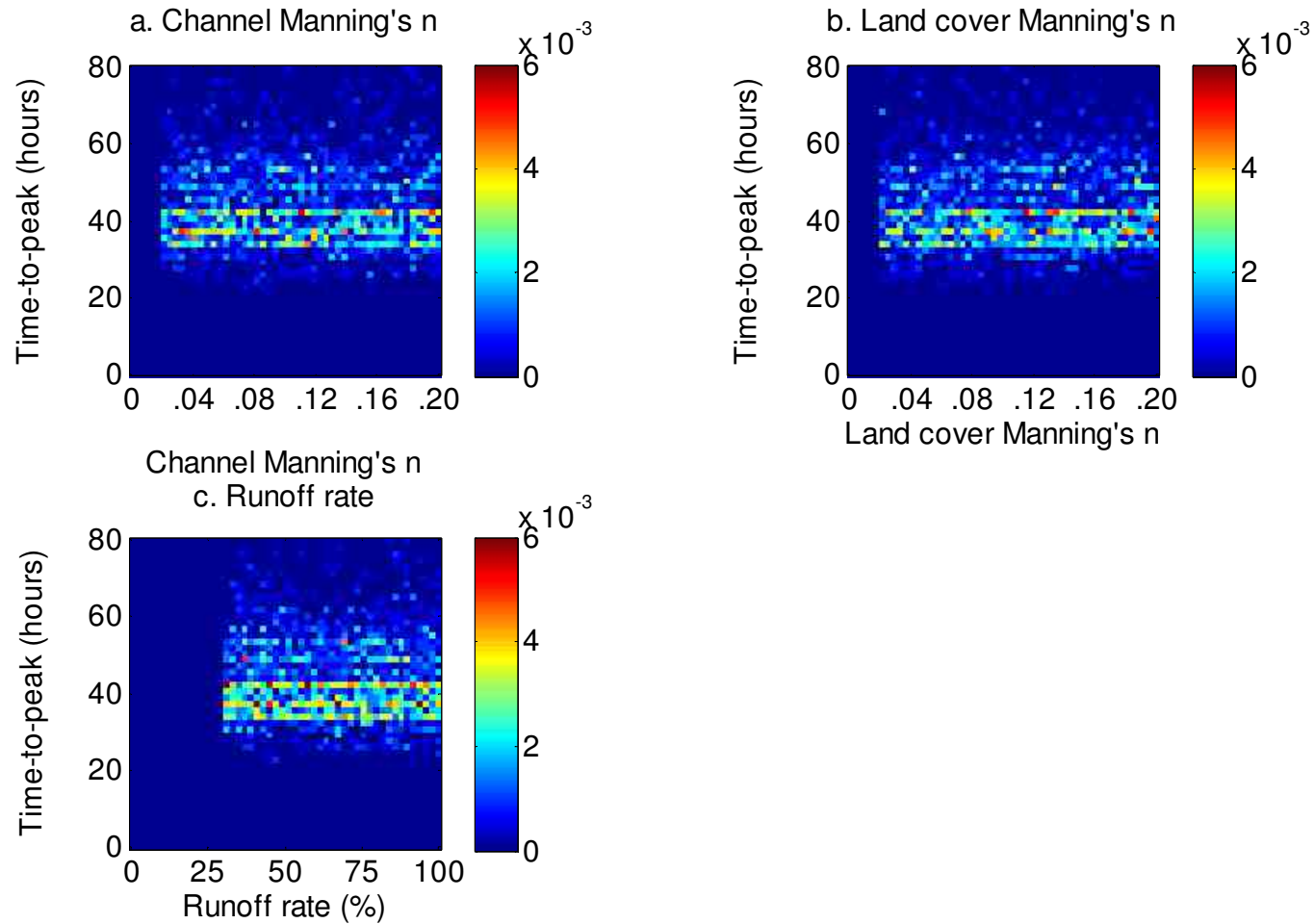


Figure 4.15 Time to peak response to; a. Channel Manning's  $n$ , b. Land cover Manning's  $n$  and, c. Runoff rate, all when rainfall rate was held constant. Colours to the higher (red) end of the colour bar indicate a higher probability of model responses occurring in that region of the response surface.

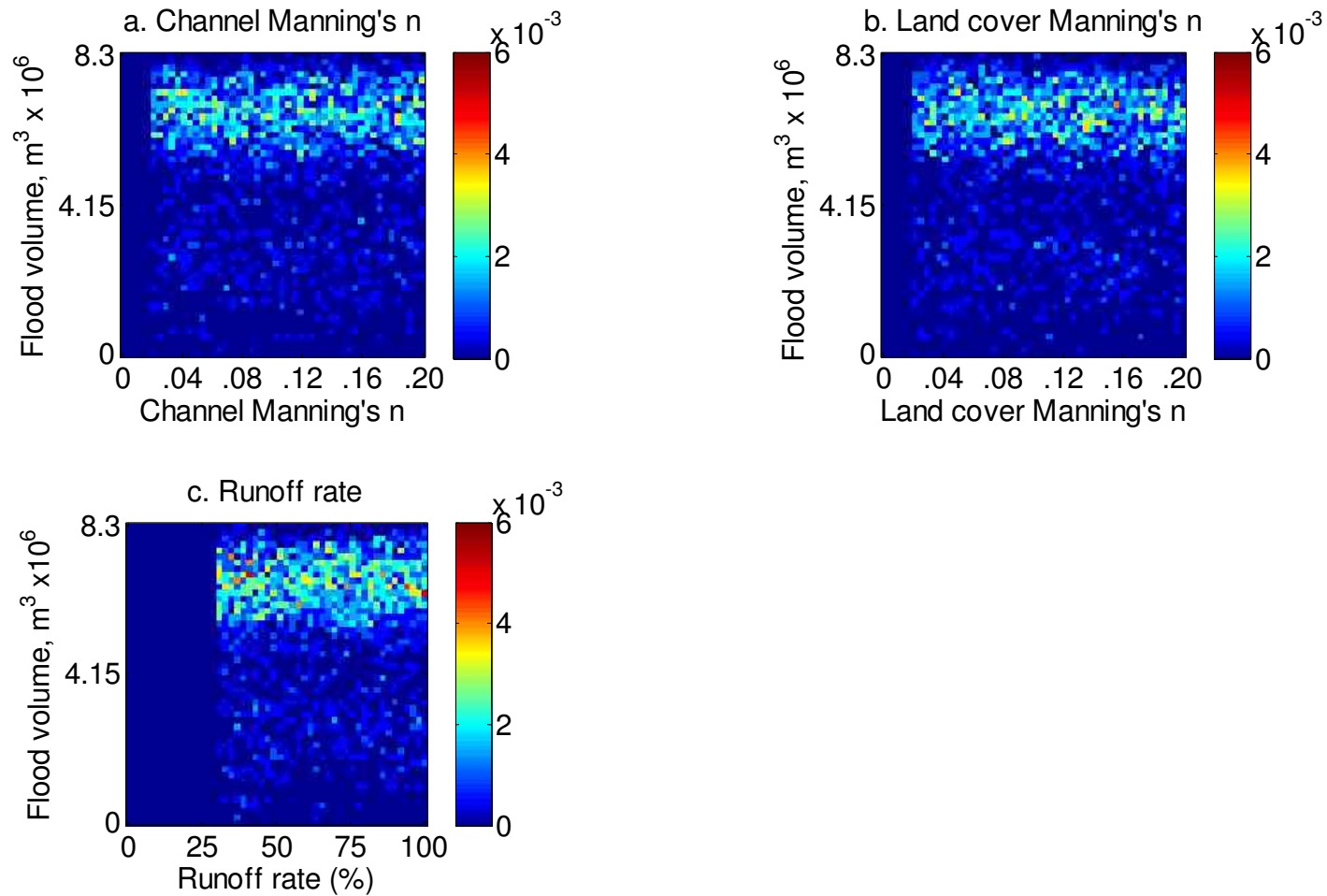


Figure 4.16 Overbank flood volume response to; a. Channel Manning's  $n$ , b. Land cover Manning's  $n$  and, c. Runoff rate, all when rainfall rate was held constant. Colours to the higher (red) end of the colour bar indicate a higher probability of model responses occurring in that region of the response surface.

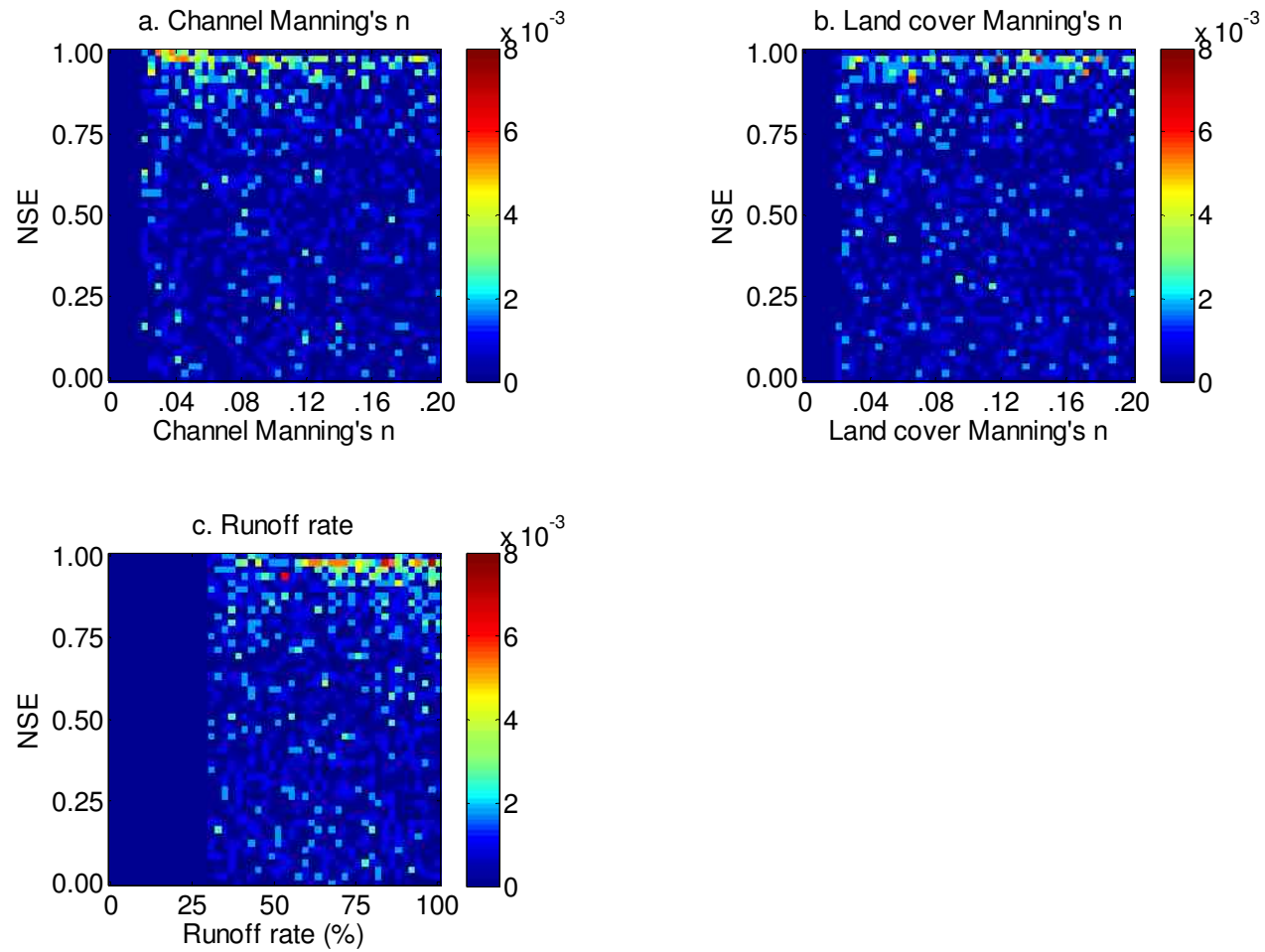


Figure 4.17 Nash Sutcliffe Efficiency and its response to; a. Channel Manning's  $n$ , b. Land cover Manning's  $n$  and, c. Runoff rate, all when rainfall rate was held constant. Colours to the higher (red) end of the colour bar indicate a higher probability of model responses occurring in that region of the response surface.

## 4.6. Discussion of sensitivity analysis

This project aims to assess the impact of slowing the flow on downstream flood magnitude, using a reduced complexity model as a means of testing the impact of flow attenuation. To this end, the time to peak response was indicative of slowing the flow, while peak discharge and overbank flood volume were indicative of the magnitude of the flood hazard. The local sensitivity analysis shows that in the case of every parameter, an increase in time to peak correlates with a reduction in peak discharge and overbank flood volume. Hence, slowing the flow within the catchment is associated with a reduction in downstream flood risk at the catchment outlet. However, it should be noted that these results were taken from the catchment outlet and are not necessarily representative of the internal response at any point within the catchment.

In the local sensitivity analysis, the model outputs responded to changes in parameters in a way that was consistent with *Overflow's* constituent equations. The sensitivity analysis therefore suggests that the model is capable of replicating the behaviour of its numerical equations, which are in turn an approximation of the physical environment. As discussed in the local sensitivity analysis, these results can be explained in physical terms. Increasing the value of Manning's  $n$  increases the level of flow resistance. Likewise, higher values for channel widths and depths lead to a greater area of flow being exposed to flow resistance. This reduces flow velocities, leading to a greater time-to-peak. The resulting flow attenuation leads to lower peak discharges and overbank flood volumes. Increases to the rainfall rate parameter increases the speed at which water is routed through the catchment and consequently has the opposite effect. Likewise, higher runoff rates lead to a larger volume of effective rainfall. The analysis has therefore found nothing that challenges the belief that *Overflow* behaves in a theoretically realistic manner.

The global sensitivity analysis tested model sensitivity to variation in a parameter values simultaneously. The trends that were observed were consistent with the local sensitivity analysis and the model's constituent equations. *Overflow* was most sensitive to rainfall rate and runoff rate, as these parameters showed the greatest amount of clustering in the PDFs for all model responses, hence exerted the greatest control over model predictions.

In both the local and global sensitivity analyses, comparisons with an observed hydrograph resulted in a wide range of NSE values. A high level of variability is to be expected when varying parameters across the entire range of physically possible values that they could take. However, some parameter sets resulted in very high NSE values (of around to 0.98). This indicates that the model is capable of accurately predicting flow hydrographs in the River Seven catchment for the June 2007 event. By comparison with the observed hydrograph, it is possible to select parameter set that gives an accurate prediction the June 2007 flood; hence a parameter set that is representative of flow processes in the River Seven catchment. This process of calibration is presented in the next section.

## 4.7. Calibration

By the optimisation of parameter values and using observations and information about the catchment (Chapter 3), the model was calibrated to produce acceptable simulations of the River Seven and June 2007 flood.

The aim of model calibration is to select parameters that allow the model to accurately predict the observed event, so that the effect of interventions on downstream flood magnitude can be predicted in comparison to the flood magnitude with no interventions. The model was repeatedly run with different parameter sets. The resulting hydrographs were compared with the observed hydrograph for the June 2007 event and the NSE was used to evaluate how well the model predictions fitted the observations.

Based on the results of the global sensitivity analysis, rainfall and runoff rates exerted the greatest control over model responses. They also demonstrated the least equifinality, so there was a smaller range of possible rainfall and runoff values that gave acceptable predictions of the observed hydrographs. Rainfall rates and runoff rates were therefore given the most attention in order to improve how well the modelled hydrograph fitted the observed hydrograph (Beven, 2001). It was decided not to calibrate the model using parameters that would affect flow pathways (such as channel geometry and Manning's  $n$ ), since the purpose of the investigation was to examine the impact of changes to local flow velocity on downstream flood magnitude. In particular, Manning's  $n$  values were subsequently varied to represent the effect of interventions on flow attenuation (Chapter 5). The lack of a consistent trend in model response to channel geometry also limited its usefulness in model calibration.

The rainfall rate parameter is used to calculate flow velocities, on which subsequent routing of the flow hydrograph takes place (see section 2.5.3). Runoff rate controls the proportion of rainfall that is routed overland, with the remainder assumed to be 'lost' to infiltration. In reality, flow velocities and runoff rates are not constant throughout a storm event. They change as the event progresses and the catchment becomes wetter and more saturated. Therefore, it would potentially be difficult to approximate catchment characteristics during the event by selecting a single value for rainfall and runoff rates. In order to reflect this, rainfall and runoff rates did not remain constant throughout the modelled event, but were varied at hourly intervals. Hence, each model run made use of a different sequence of rainfall and runoff rates for the event. The rainfall rates were used to re-calculate flow velocities across the catchment at intervals during the event. The subsequent routing of the flow hydrograph was based on these periodically updated flow velocities.

A numerical algorithm (Odoni and Lane, 2010) was used to generate flow hydrographs for different combinations of time-varying rainfall rate and runoff rate parameter values. The algorithm calculated two NSE values: one for the rising limb of the flood hydrograph, from the beginning of the event until the peak, and one for the falling limb, from the peak until the end of the recorded event. Only parameter sets that resulted in high NSE values for both the rising and falling limb of the hydrograph were considered acceptable (Odoni and Lane, 2010).

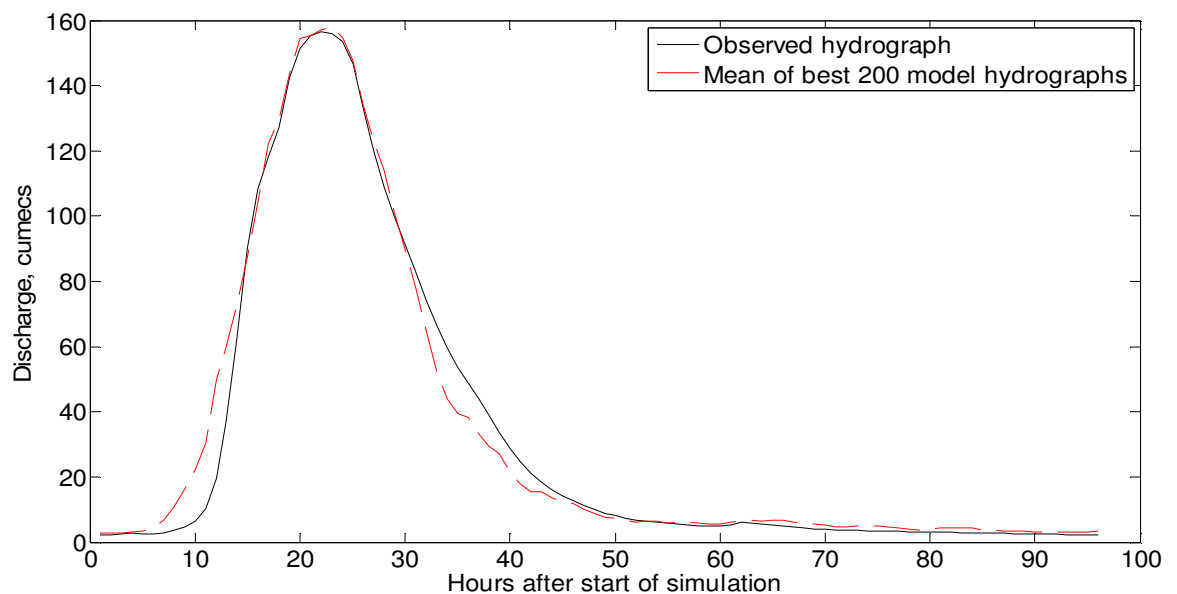
Since many parameter sets may give 'good fits', it is difficult to identify a single parameter set that gives a 'best fit' (Beven, 2001). Rather than assume a single 'best' parameter set, a region of the parameter space with parameter values that produced accurate model predictions was identified. These were ranked by the NSE values they predicted for the hydrograph and the parameter sets with the highest NSE values were used in the calibrated model. The two hundred parameter sets with the highest NSE values were included, on the basis that these parameter sets displayed little variation in NSE, and hence had a high level of equifinality. To 2 decimal places, the best two hundred parameter sets had an NSE of 0.98. To 4 decimal places, the NSE values of these parameter sets ranged from 0.9808 to 0.9826. It was therefore difficult to select a single optimum parameter set from this range. Each run of the calibrated model made use of these two hundred parameter sets, thereby predicting two hundred hydrographs. The mean of these hydrographs was taken as the final calibrated model output (Figure 4.18) and itself has a NSE value of 0.9822.

Figure 4.19 shows the mean of the sequence of rainfall rate parameter values (in mm/day). The purpose of the rainfall rate parameter is to calculate cell flow velocities, representative of the antecedent conditions and the changing wetness of the catchment throughout the event. Rather than recalculating cell flow velocities at every model timestep, the input rainfall is specified separately and routed through the catchment based on these generalised flow velocities. Thus the input rain gauge data is still specified explicitly and the sequence of rainfall rate parameter values is not intended to replicate this. Instead, the rainfall rate parameter can be viewed as an indication of overland flow velocities.

The calibrated model simulation begins with high flow velocities. This was based on a relatively wet catchment, using rainfall rate of approximately 40 mm/day to calculate overland flow velocities. This seems acceptable given the prolonged rainfall prior to the event (section 3.4). There is a marked increase in the rainfall rate parameter between 23-28 hours after the start of the event (up to 200 mm/day), indicating faster overland flow velocities at this time. This represents a time lag of approximately 20 hours after the peak of the observed rainfall, but corresponds to the peak of the discharge hydrograph. As this time lag also occurs in the observed rain and discharge, it may relate to the time taken for the catchment to respond to the event (Wilson, 1990). However, it may also relate to errors resulting from the rainfall rate parameter accounting for other processes that are not explicitly represented in the model. The duration for

which the high rainfall rate parameter is applied, before returning to a value roughly equivalent to its initial value (40 mm/day) is similar to the duration of the flood hydrograph (about 30 hours). This is indicative of the greater flow velocities that would result from greater flow depths during a high flow event.

The flow hydrograph predicted by the calibrated model accurately replicated the observed hydrograph. It has been noted that there is a time lag in the response of the sequence of rainfall rate parameter values after the peak of the observed rainfall. However, the parameter is used in the calculation of flow velocity across the land surface and not to represent the volume of rainfall entering the catchment during the event itself (see section 2.5.3). For that reason, the parameter accounts for a range of processes that influence overland flow velocity. Since the parameter values are not direct measurements, but are selected on the basis of calibrating the resulting of model predictions to observations, there is a degree of uncertainty in the choice of parameter values. The variability in the 200 model hydrographs resulting from each parameter set was assessed in Chapter 5, in the context of its implications for the predicted impact of flow attenuation interventions.



**Figure 4.18** Discharge hydrographs at Normanby showing the observed hydrograph and the calibrated model hydrograph (the mean of 200 model hydrographs with the highest NSE values).



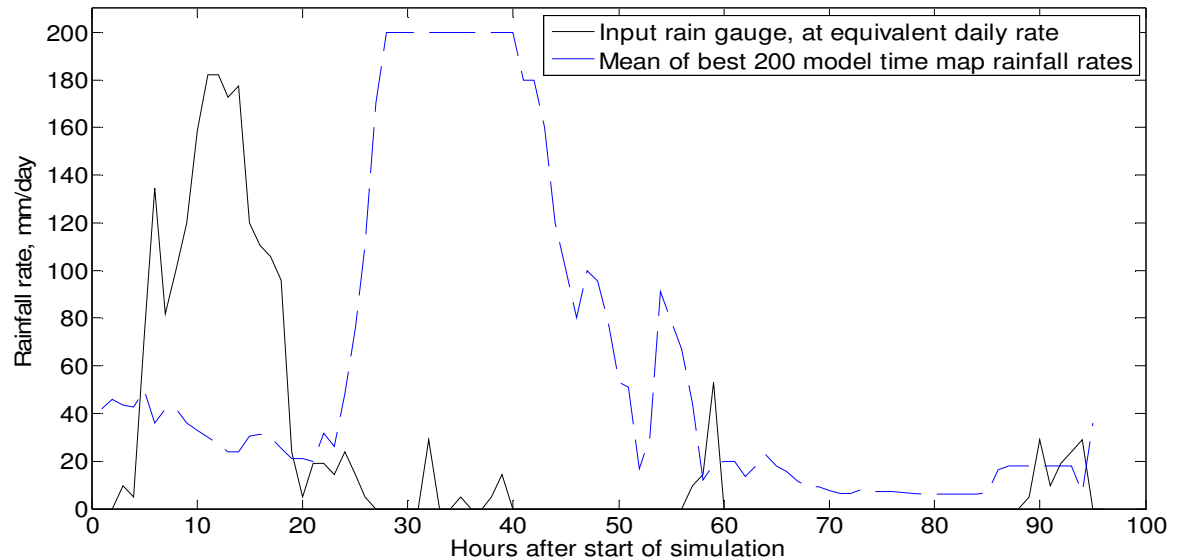


**Figure 4.19** Input rainfall rates measured at the Brown Howe gauge and the mean of the 200 different sequences of rainfall rate parameters, which were used in the calibrated model. The Brown Howe rain gauge data was measured in mm/hour so was multiplied by 24 to give the equivalent rate in mm/day.

The results show that it is possible to calibrate *Overflow* to a high level of accuracy, as measured by NSE values of over 0.98, for the River Seven and June 2007 flood. Further work could be undertaken to investigate the robustness of the model when calibrated for different magnitudes and types of flood. For example, floods following dry antecedent conditions (in contrast to June 2007) might be expected to exhibit a longer time to peak, since it might take longer for soil to saturate and overland flow to begin. Floods in which there was a greater or lesser amount of floodplain inundation might be expected to exhibit different degrees of sensitivity to land cover Manning's  $n$ . However, the June 2007 flood was selected as it was expected to generate river flows with a high likelihood of interacting with flow attenuation interventions. In Chapter 5, the focus of the research is on how flow attenuation causes flood flows to change relative to this baseline scenario.

#### 4.8. Conclusion

This chapter has evaluated *Overflow* by comparison to observed data of the June 2007 flood. The local sensitivity analysis indicates that the model is solving its constituent equations correctly. In terms of peak discharge, time-to-peak and overbank flow volume, the model response could be explained in physical terms so there is nothing to suggest that the model behaves in a theoretically unrealistic manner.

The global sensitivity analysis tested the parameters in combination and identified interaction effects. The parameters with the least equifinality were rainfall rate and runoff rate. As there were fewer values of rainfall and runoff rate that could give rise to any individual model result,

these parameters became the focus of model calibration. *Overflow* hydrographs were calibrated to observed hydrographs of the June 2007 flood by selecting parameter values through a process of optimisation. High NSE values ( $> 0.98$ ) confirm that model accurately represents the behaviour of flow in the River Seven during a flood event.

The local sensitivity analysis showed that the model is sensitive to the effects of increased flow resistance (Manning's  $n$ ). The resulting impact on flow attenuation leads to a reduction in the magnitude of flood flows downstream. This is consistent with the model's constituent equations and has a physical explanation in terms of how the 'real world' catchment operates. Using the calibrated model, Chapter 5 uses variations in Manning's  $n$  to explore the impact of flow attenuation on downstream flood flows.

## 5. Catchment response to intervention measures

### 5.1. Summary

In Chapter 4, the model was subjected to a sensitivity analysis to assess its response to parameter variation. Varying Manning's  $n$  values to represent flow attenuation measures caused the model to respond in a way that was qualitatively consistent with the Manning equation. As Manning's  $n$  increased, flow velocity decreased. Consequently, attenuation (measured by peak discharge and time to peak) increased. On the assumption that Manning equation is a reliable approximation of physical processes, this supports the idea that flow resistance measures could be used to cause attenuation of the flood hydrograph. The model was calibrated by optimising the values of rainfall and runoff rate parameters. This allowed the model to reproduce the June 2007 flood for the River Seven catchment as a baseline against which the impact of flow attenuation measures could be compared. The aim of this chapter is to use *Overflow* to predict the impact of flow attenuation measures on downstream flood flows and to assess the uncertainty related to the selection of parameters to represent flow attenuation.

First, the means by which flow can be attenuated are described in greater detail. Flow attenuation is discussed both in terms of the form that such measures take in the real world, and how these measures were represented in *Overflow*. Next, *Overflow* was used to investigate the impact of flow attenuation interventions individually and in combination with each other. The optimum location for flow attenuation interventions tended to be in the upper catchment. Finally, an uncertainty analysis was also undertaken to evaluate the extent to which uncertainty in the selection of  $n$  values propagates through the model calculations to uncertainty in the results (Smith and Smith, 2007). The selection of exact Manning's  $n$  values to represent intervention measures is uncertain as there is no observed data against which to optimise the selection of such values. As discussed in Chapter 4, the calibrated model also made use of 200 rainfall rate and runoff rate parameter sets for each simulation. The model uncertainty resulting from rainfall and runoff rate selection was added to the uncertainty caused by Manning's  $n$  value selection. It was found that although the selection of parameter values caused some variability in the results, the combined impact of attenuation measures on downstream flood flows was large enough to be distinguished from the uncertainty.

In Chapter 4, the model was calibrated to observations at the Normanby gauging station, which is the furthest downstream gauging station in the catchment. However, the village of Sinnington, upstream of Normanby, also experiences flooding. Flow attenuation increases local water levels, which leads to a locally higher probability of overbank flooding. This may also increase flooding for a distance of several hundred metres upstream of interventions, due to

'backwater' effects, as flow cannot be conveyed downstream as rapidly through the intervention (Thomas and Nisbet, 2007). Due to the potential for flow attenuation to increase local flood risk, interventions should not be sited at or immediately downstream of settlements (Broadmeadow and Nisbet, 2009). The effect of flow attenuation measures was assessed at Sinnington as it is a location where flood mitigation is of interest. Although flow attenuation measures further downstream may benefit Normanby, they may also have detrimental effects at Sinnington, so were not tested.

## 5.2. Catchment riparian intervention measures (CRIMS)

### 5.2.1. Introduction

In this project, measures for increasing resistance to river flow are grouped under the heading of Catchment Riparian Intervention Measures (CRIMS) (Odoni and Lane, 2010). A number of methods can be used to increase flow resistance. These include changes to channel width, depth or meandering and obstructions, vegetation or irregularities in the channel or floodplain surface (Cowan, 1956). However, changes to the channel geometry and planform would require intensive and possibly repeated engineering operations (e.g. dredging), which would be disruptive to river habitats and lower flows. In practice, less intensive and smaller scale interventions, such as placing obstructions to flow in river channels, might be preferred as they are less costly to introduce and maintain. Rather than exhaustively test all possible characteristics that could affect flow behaviour, this project explores two main measures that cause flow attenuation, which were considered as part of work by Durham University and Forest Research on the neighbouring Pickering Beck catchment (Odoni and Lane, 2010). These were tested in each reach of the catchment and their impact on downstream flood risk was modelled.

The methods of flow attenuation that were examined were: (1) large woody debris (LWD) dams within the river channel itself and; (2) riparian buffer strips of trees or other vegetation adjacent to the channels. Both occur naturally in rivers, but in some areas have been removed as a means of local flood mitigation, by increasing the ability of the river channel to convey floodwater downstream (Forestry Commission, 2010). However, it is possible to artificially construct debris dams and to reinstate river-bank vegetation. These activities have additional ecological benefits (e.g. greater habitat diversity as a result of flow variability caused by debris dams). In accordance with the EU Water Framework Directive, these techniques are increasingly promoted as a method for sustainable management of rivers (Birol et al., 2009). This chapter aims to investigate the effect of riparian vegetation and LWD dams on downstream flood risk, both individually and when multiple interventions are tested.

### 5.2.2. Large woody debris (LWD) dams

Large woody debris refers to branches, tree stems and logs of a diameter greater than 10 cm (Marrington, 2010). LWD dams occur naturally in woodland streams. They may also be artificially constructed with the purpose of slowing flood flows, resulting in an increase in flood depth and the transfer of water onto the floodplain. Floodplains have a lower ability than river channels to convey water, so transferring water onto the floodplain results in attenuation of the flood hydrograph and a delayed release of floodwater downstream (Lane et al., 2007b). In turn, this may reduce downstream peak discharge. The local and global sensitivity analyses in Chapter 4 demonstrated this effect when channel Manning's  $n$  values were increased.

Unlike permanent storage structures, such as reservoirs or engineered dams, LWD dams do not interrupt low flows or the movement of fish and other river organisms. They are therefore a tool for flood risk management that is compatible with other objectives, such as ecology.



Figure 5.1 An artificially constructed large woody debris dam, in a river channel at low flow, Cropton, north of Sinnington, 25<sup>th</sup> March 2010. The logs and branches that make up the dam have been wedged against trees to reduce the chance of being washed downstream in a flood. Vertical stakes can also be driven into the river bed in front of the dam for the same purpose (Forestry Commission, 2010). Photograph by Dr. Nick Odoni, Durham University.

However, there are a number of constraints on their construction, which limits the reaches where they may be located. In the past, LWD dams have been actively removed from river channels due to concerns over debris being washed downstream and blocking bridges, weirs or other structures (Forestry Commission, 2010). As a result, LWD dams should not be constructed immediately above or below river structures. Likewise, dam construction is restricted to channels of less than 5 m width because wider river channels and flow width reduce the stability of dams and increase the risk of debris being washed downstream (Marrington, 2010). This allows a number of reaches to be immediately excluded as potential CRIM sites.

### 5.2.3. Riparian buffer strips

A riparian buffer strip refers to trees or other vegetation that occurs alongside the river channel. Riparian vegetation contributes to the natural formation of LWD dams and tree branches that overhang the river channel may also slow flow (Chow, 1959). More importantly, once water is transferred onto the floodplain (as a result of LWD dams) vegetation offers a greater resistance to flow and allows more water to be retained on the floodplain (Lane and Thorne, 2007). Riparian vegetation has a wide range of benefits, such as shelter and shade for river organisms or reducing erosion by strengthening river banks through rooting (Forestry Commission, 2007).

Due to cost and the complexities of land ownership, it is unlikely that riparian vegetation could be planted across the entire floodplain (Broadmeadow and Nisbet, 2009). Previous research identified that riparian buffer strips of 30 m width on each side of the river channel are most likely interact with flood flows and supply woody debris to the channel (Nisbet and Broadmeadow, 2003; Broadmeadow and Nisbet, 2009; Odoni and Lane, 2010). However, the DEM used in the *Overflow* model for the River Seven has a resolution of 20 m. In order to be commensurate with the model resolution, the riparian buffer strips are assumed to extend for 20 m (i.e. one model grid cell) either side of the channel. Since interventions are only being considered for channels of less than 5 m width, each cell designated as a 'channel cell' will not be occupied entirely by the river channel, but will also contain an area of floodplain. A buffer strip applied to an overbank section of 20 m width, in addition to LWD dams within the channel, is therefore a reasonable approximation to the total width of flow attenuation measures.

### 5.2.4. Representing CRIMS in the model

The parameters investigated in Chapter 4 suggested three general approaches to attenuate the flood hydrograph and reduce downstream peak discharges and overbank flood volumes.

- (1) Channel Manning's  $n$ , representing in-channel interventions to slow river flow, such as vegetation, irregular channel surfaces or other obstructions.
- (2) Land cover Manning's  $n$ , representing land uses or land cover types that slow overland flow, such as forestry.
- (3) Runoff rates, representing the ability of the land surface to absorb precipitation and hence the volume of overland flow generated by a rainfall event.

The rainfall rate for flow velocity calculations could also be used to represent catchment-wide land cover types and their effect on flow velocity. However, conceptually, this parameter relates to antecedent conditions and the influence of ground wetness on overland flow. In the current treatment of the model, it can also only be applied on the scale of the entire catchment. As such, land cover Manning's  $n$  is better suited to representing the effect of riparian buffer strips and LWD dams on flow velocity.

Since the runoff rate parameter affects flood risk by controlling the volume of water rather than its routing, it does not physically represent flow attenuation interventions and how they impact upon flood pathways. Channel and land cover Manning's  $n$  were therefore used to represent the effects of interventions that aim to slow river flow.

LWD dams were represented by a Manning's  $n$  value of 0.14 and riparian buffer strips by an  $n$  value of 0.16 for the grid cells of the selected reach. The Manning's  $n$  values are based on those agreed with Forest Research during previous work using the *Overflow* model (Odoni and Lane, 2010) and Chow's (1959) index, which is commonly used in operational flood modelling studies (Brunner, 2008). According to Chow (1959), these values correspond to dense vegetation or timber in the channel and densely planted trees on the floodplain with flow through the branches. Other indexes of Manning's  $n$  values are relatively consistent in assigning similar values to in-channel woody debris and overbank forestry (e.g. Fasken, 1963; Barnes, 1967). A study by Thomas and Nisbet (2007) used a similar  $n$  value for riparian woodland (0.15) in 1D and 2D models of a 2.2 km reach of the River Parrett, Somerset. They found that this caused a reduction in water velocity of 50 %, which compares favourably with reductions in velocity observed in empirical field studies (Limerinos, 1970). However, an uncertainty analysis was also undertaken to quantify the variability in model results resulting from uncertainty in the selection of Manning's  $n$  values. In the uncertainty analysis,  $n$  values were selected from a range that was representative of CRIMS, which is further discussed in section 5.5.

Naturally occurring LWD dams tend to be spaced at 7-10 times the channel width (Odoni and Lane, 2010), so there will be several LWD dams in each reach. Riparian buffer strips can be planted along the length of an entire reach. In order to simulate this, the higher Manning's  $n$  values were applied to the whole reach. However, changes to Manning's  $n$  could only take place at the scale of each grid cell, so the precision with which increases in  $n$  could be applied was



limited by the resolution of the DEM. Increases in  $n$  were applied across the full 20m width of each cell. In reality, large woody debris dams may not occupy the full 20m x 20m area of the catchment that is represented by each model grid cell. Increasing Manning's  $n$  is therefore intended as an approximation of the flow attenuation that would occur within each grid cell in response to interventions. Although a simplification of flow around large woody debris and riparian buffer strips, for the purposes assessing CRIM impacts on flood risk at the catchment scale, it is considered acceptable to represent the impact of woody debris and vegetation using Manning's  $n$ .

In the *Overflow* model, the physical meaning of an increase in Manning's  $n$  is an increase in flow resistance. This results in a lower flow velocity, as calculated through the Manning equation (section 2.5). The sensitivity analysis in Chapter 4 showed that, qualitatively, the model response to Manning's  $n$  was theoretically correct: as  $n$  increased, the model predicted greater flow attenuation. This implied reduced flow velocities in response to increases in flow resistance, which is consistent with the physical processes operating in a 'real' catchment. However, the analysis did not allow a validation of the magnitude of model response to  $n$  value variation. Because  $n$  is a dimensionless parameter (see section 1.4.1), it is difficult to directly measure  $n$  in the field or laboratory, in order to relate it to other flow observations. Uncertainties therefore result from both (1) the selection of  $n$  values to represent CRIMS, and; (2) the magnitude of model response to a change in  $n$ . The sensitivity analysis suggests a limited reduction in peak discharge in response to the likely range of Manning's  $n$  (e.g. around a 10% reduction in peak discharge in response to extremes of channel  $n$ , Figure 4.4). For these reasons, this chapter aims not only to identify potential CRIM locations (sections 5.3 and 5.4), but also to assess whether the magnitude of flow attenuation in response to CRIMS is discernable from parameter uncertainty (section 5.5).

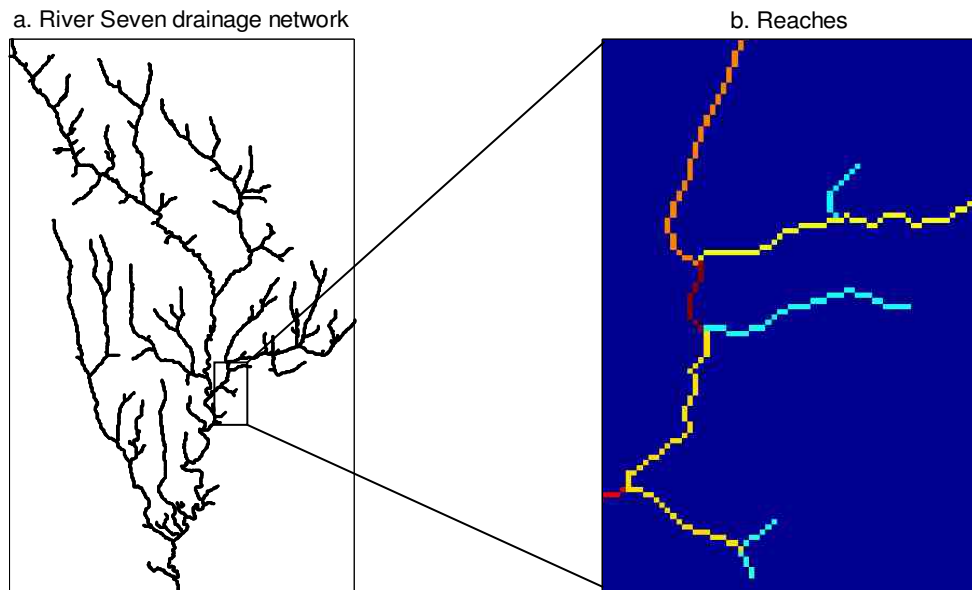
### 5.3. Experiment design

Floods occur when the depth of water exceeds the capacity of the river channel (Lane et al., 2007a). To quantify downstream flood risk, the model response of most interest is peak discharge, which is indicative of the peak water depth. As the flood magnitude is of most concern, rather than the time taken for the drainage network to respond to a rainfall event, the time to hydrograph peak is not considered relevant. The impact of CRIMS was therefore assessed in terms of peak discharge at Sinnington.

Each reach, including those of tributaries to the main River Seven, was given a separate, unique identification number. The reaches were identified along the same principles as stream ordering, (e.g. Shreve, 1966). Thus a reach is defined as the stretch of river channel between its source or



the upstream confluence with a tributary and the next confluence downstream. On this basis, a numerical algorithm was used to divide the river into 214 separate reaches as far as Sinnington.

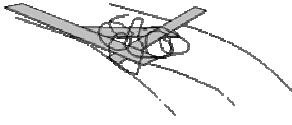
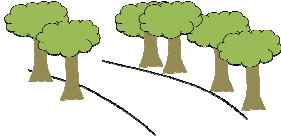
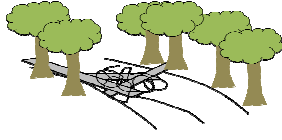
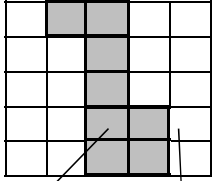
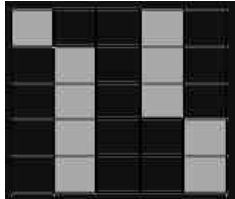
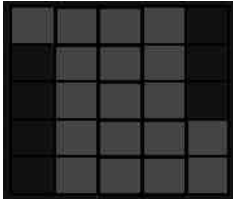


**Figure 5.2** The River Seven drainage network to Normanby (a), with a detail (b) showing how the drainage network is subdivided into reaches. Each reach is coloured separately.

LWD dams cannot be installed in channels greater than 5 m wide (Marrington, 2010). Reaches greater than 5 m in width were therefore not considered possible intervention sites. These reaches were screened out from further analysis on the basis of the channel geometry defined in the model set-up (section 2.5.3.3). There were 186 reaches as far as Sinnington of less than 5 m width, which were considered possible CRIM sites.

The experiment, described below, was repeated for three possible types of intervention:

1. A higher Manning's  $n$  in channel cells only (representing in-channel LWD dams).
2. A higher Manning's  $n$  only in the overbank section immediately adjacent to the reach, of one cell width on each bank (representing a riparian buffer strip of 20 m width on each bank).
3. A higher Manning's  $n$  in both channel and adjacent overbank cells simultaneously.

	1	2	3
<b>'Real world' intervention</b>			
	Large woody debris dam	Riparian buffer strip	LWD dam and buffer strip
<b>Representation in <i>Overflow</i></b>			
	<input type="checkbox"/> Default value <input checked="" type="checkbox"/> Increased $n$		
<b>Description</b>	A higher Manning's $n$ (0.14) in channel cells only.	A higher Manning's $n$ (0.16) only in the overbank section immediately adjacent to the reach, of one cell width on each bank.	A higher Manning's $n$ in channel and adjacent overbank cells simultaneously (0.14 for channel, 0.16 for overbank).

**Table 5.1** Flow attenuation interventions and their representation in *Overflow*.

### 5.3.1. Individual CRIM impacts

Results from the sensitivity analysis (Chapter 4) suggest that flow attenuation will reduce downstream peak discharges. However, it is impractical to attenuate flow everywhere in the catchment at once, so individual reaches must be selected on the basis of the magnitude of their reduction of peak discharge.

An individual CRIM test was undertaken on each reach in turn. A CRIM was modelled in each individual reach by increasing Manning's  $n$  to a value of 0.14 for the channel cells and 0.16 for the adjacent floodplain cells. The impact of the CRIM on the downstream flood hydrograph was assessed. This was quantified in terms of peak discharge at Sinnington. This and the later CRIM experiments made use of the 200 best calibrated parameter sets discussed in the model calibration (section 4.7), which were averaged to give a single hydrograph in response the inclusion of a CRIM. Between each successive run of the calibrated model, all other parameters

were kept constant, so any change in peak discharge between each successive simulation could only be attributed to the CRIM in that particular reach.

The results allowed potential CRIM sites to be located and reaches that had no beneficial impact on downstream flood risk could be excluded from further analysis. Where peak discharge increased in response to a CRIM being added to a particular reach (i.e. it had a negative impact on downstream flood risk), that reach was excluded as a potential CRIM site. If there was a reduction in peak discharge in response to a CRIM (i.e. a positive impact on flood risk), the reach was included as a potential CRIM site. Where there was no significant impact on the downstream peak discharge (a 'neutral' site), the reach was also included, since it might still have a beneficial impact in combination with another reach.

### 5.3.2. Combined effects test

Flow attenuation affects the timing of the flood hydrograph in different tributaries, which might cause the arrival of floodwater in the main river to become synchronised, leading to an increase in peak discharge (Lane et al., 2007b). As a result, any reach might have a positive, neutral or negative impact on peak discharge when used in combination with others (Odoni and Lane, 2010).

Next, all reaches that, individually, had a positive or neutral impact on peak discharge were ranked by the magnitude of that impact. The model was then run with interventions in all these positive or neutral reaches at once. In each successive model run, the CRIM in the least beneficial reach was removed, until only one reach (the most individually beneficial reach) remained.

The results therefore consisted of a peak discharge for an intervention in the single most beneficial reach, followed by the second most beneficial reach in combination with the first, and so on. The ranking of the reaches was not altered between each model run, since the purpose was to assess the impact of every potential CRIM site in combination with the others.

### 5.3.3. Removal of negative reaches

Due to the possibility of flood hydrographs becoming synchronised, reaches that, on their own, had a positive impact on peak discharge reduction, might have a negative impact when used in combination with other reaches. These reaches were screened out from further analysis based on the combined effects test. Reaches that had a negative impact on peak discharge were identified by calculating the difference in peak discharge between one model simulation and the next. Where the inclusion of a reach resulted in a higher peak discharge than if that reach was not included, the reach was excluded from subsequent simulations. The combined effects test was then re-run with CRIMS applied to all the remaining reaches, with the least beneficial reach

removed in each successive model run. This process was repeated to remove all reaches with a negative impact on peak discharge when used in combination with other reaches.

This procedure left only those reaches where flow attenuation reduced downstream peak discharges, ranked by the magnitude of the peak discharge reduction.

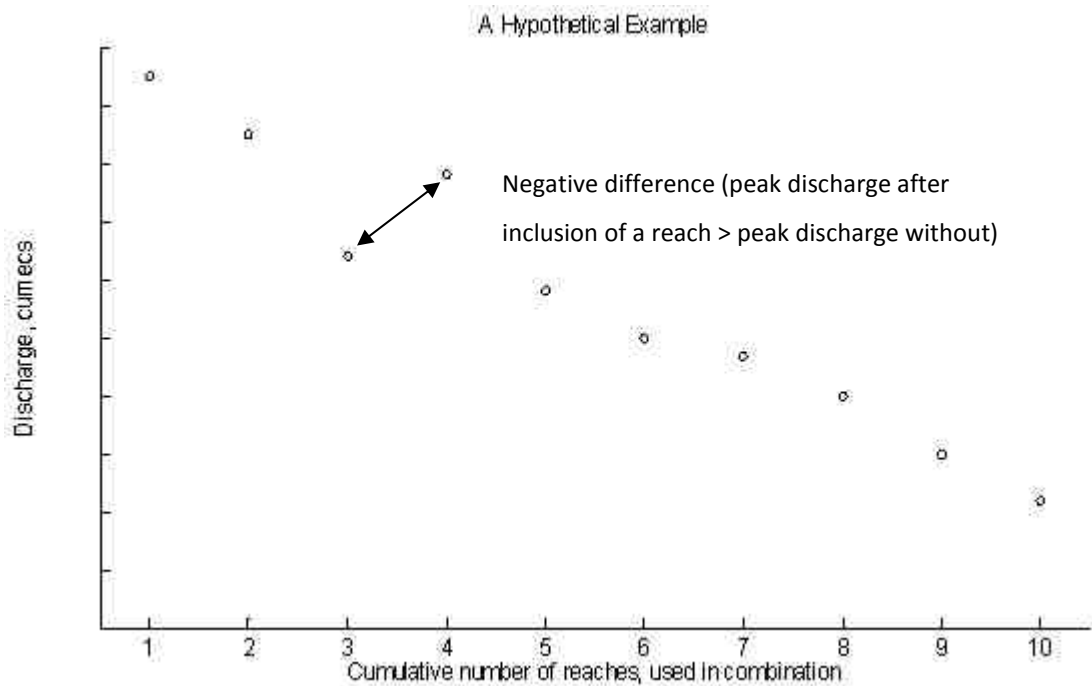


**Figure 5.3** An illustration of results for CRIMS applied to a combination of reaches, to demonstrate the method. In this example, the inclusion of the fourth reach results in a higher peak discharge than with three reaches alone. Consequently, this reach will be removed from subsequent model runs and the simulation will be repeated for the remaining nine reaches in combination.

The entire experiment (Section 5.3.1 to Section 5.3.3) was repeated for each of the types of intervention described in Table 5.1: an intervention in the channel only, an intervention in adjacent overbank floodplain only, or an intervention in both the channel and the adjacent floodplain cells. Where a ‘channel’ intervention was considered, a Manning’s  $n$  value of 0.14 was applied to all the channel cells of the reach in question. Where an ‘overbank’ intervention was considered, a Manning’s  $n$  value of 0.16 was applied to the floodplain cells immediately adjacent to the channel. Where interventions were not under consideration, Manning’s  $n$  values of 0.35 for the channel and 0.06 for the floodplain were assumed. These were the  $n$  values taken when the model was calibrated (Section 4.7) and correspond to a theoretically reasonable ‘baseline’ representation of the catchment.

## 5.4. Results

### 5.4.1. Individual CRIM test

Of the 186 reaches identified as far as Sinnington, 118 were found to have a positive or neutral impact on peak discharge in the case of simultaneous channel and overbank interventions, 119 were positive or neutral in the case of a channel intervention only, and 102 were positive or neutral in the case of overbank interventions only. In all cases, therefore, the majority of reaches had a beneficial or neutral impact on downstream peak discharge.

Intervention	Number of positive/neutral	Percentage of reaches positive/neutral
Channel and overbank	118	63.4
Channel only	119	63.9
Overbank only	102	54.8

**Table 5.2** Number of reaches that individually caused a reduction or no change in peak discharge downstream.

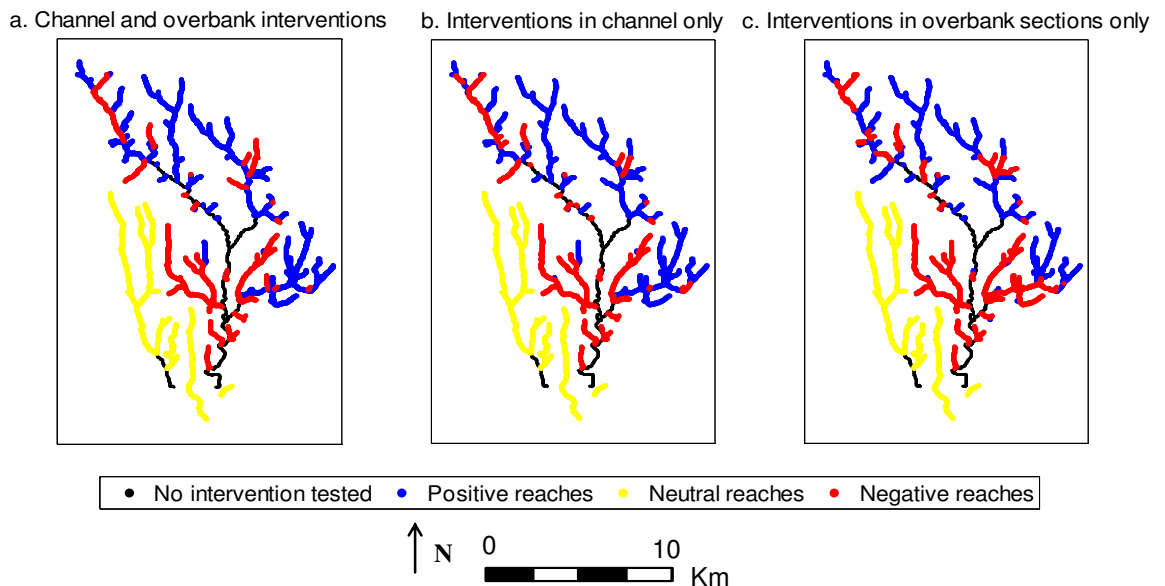


**Figure 5.4** Plot showing reaches that, individually, had a positive, neutral or negative impact on peak discharge at Sinnington. Reaches with a width of greater than 5 metres were not tested as they were considered unsuitable for LWD dams. These are shown by the thinner, black line.

The map of the reaches (Figure 5.4) shows that positive reaches tended to occur towards the source areas of the tributaries of the River Seven, in the upper and eastern part of the catchment. This might be expected because they have greater potential to attenuate flow before it arrives in the lower catchment at Sinnington (Odoni and Lane, 2010). Reaches in the lower part of the catchment tended to be negative. It is possible that flow attenuation may not reduce peak discharge magnitude over short distances. However, a number of negative reaches are also located in the upper catchment. The reasons for this cannot be immediately established from the individual CRIM test, but it may be that flow attenuation in these reaches causes the peak of the flood hydrograph to coincide with the arrival of floodwater from other tributaries. In addition to reducing the peak discharge, flow attenuation also extends the duration of the hydrograph (Thomas and Nisbet, 2007). Attenuation may increase the likelihood of flood hydrographs becoming synchronised as the peak of the hydrograph is extended over a longer duration.

Tributaries in the western part of the catchment, shown in yellow in Figure 5.4, appear to be neutral in terms of their impact on peak discharge at Sinnington. However, these tributaries join the River Seven downstream of Sinnington, so can have no impact on flow at Sinnington itself. These tributaries were included because some portion of their length, they lie in the area of the catchment above Sinnington and there was no straightforward way to remove the reaches from the individual CRIM test. The reaches were still included the model, since precipitation falling on hillslopes in that part of the catchment would still be routed out of the catchment by those reaches, rather than being routed diffusively across the land surface and joining the main river. However, since they were shown to have no impact on the flood hydrograph at Sinnington, they did not influence the results of the combined effects test.

All reaches upstream of Sinnington that were tested had some impact (positive or negative) on peak discharge downstream. In the combined effects test, the reaches were ranked by their effectiveness on reducing peak discharge. This allowed both neutral reaches and positive reaches that had a minimal impact on peak discharge reduction to be removed from further consideration.

#### 5.4.2. Combined effects

Starting from the most beneficial reach, as interventions were added to additional reaches, there was a reduction in the rate of decrease in peak discharge (Figure 5.5). Figure 5.6 shows that a large proportion of the reduction in peak discharge could be achieved with a small number of reaches.

In the case of channel and overbank sections combined, the most effective reach contributed to a reduction in peak discharge of 0.72 % ( $0.92 \text{ m}^3\text{s}^{-1}$ ) on its own. This accounted for 13.5 % of the

total reduction in peak discharge achieved by all the reaches. The first five reaches together contributed to a peak discharge reduction of 2.59 % ( $3.31 \text{ m}^3\text{s}^{-1}$ ), which was almost half of the total peak discharge reduction (48.7 %). The 78 least beneficial reaches only contributed a peak discharge reduction of 0.87 % ( $1.12 \text{ m}^3\text{s}^{-1}$ ), which was 10 % of the total peak discharge reduction achieved.

In the case of interventions in the channel only, the first reach resulted in a peak discharge reduction of 0.64 % ( $0.81 \text{ m}^3\text{s}^{-1}$ ), which was 13.7 % of the total peak discharge reduction for all reaches. The first five reaches contributed to a 2.20 % ( $2.82 \text{ m}^3\text{s}^{-1}$ ) reduction in the flood peak. This was almost half (47.6 %) the total reduction achieved. The final 10 % of the total peak discharge reduction required interventions in the 82 least effective reaches. These reaches collectively gave a peak discharge reduction of 1.82 % ( $2.32 \text{ m}^3\text{s}^{-1}$ ).

For interventions in the overbank section only, the first reach caused a peak discharge reduction of 0.75 % ( $0.96 \text{ m}^3\text{s}^{-1}$ ). This was a large proportion (60.6 %) of the total reduction. The 70 least effective reaches only reduced the flood peak by 0.13 % ( $0.17 \text{ m}^3\text{s}^{-1}$ ), or 10 % of the total reduction. Different reaches therefore had a different magnitude of impact on peak discharge reduction. This was analysed in terms of their location within the catchment, in section 5.4.4.

It is also possible to compare the different types of intervention. The greatest reduction in peak discharge was achieved with interventions in channel and overbank sections simultaneously, followed by interventions in the channel only (Table 5.3). The addition of increased Manning's  $n$  in the overbank cells adjacent to the reach has a greater impact on downstream peak discharge than channel cells alone, since a greater reduction in flow velocity can be expected. Interventions in the overbank sections only, or conversely, failing to intervene in the channel has a significantly lower impact on peak discharge reduction than interventions in only the channel, or channel and overbank sections. Interventions in the channel therefore appear the main driver of reduction in peak discharges.

Once floodwater has entered the river network and is contained within channels of (over the timescale of a flood) fixed width, reductions in flow velocity within the channel must be taken up by an increase in flow depth. Without a reduction in within-channel velocity, the flow depth may not exceed the depth of the channel. In this situation, any interventions designed to slow the flow on the floodplain adjacent to the channel would have little or no effect, since the flow would not interact with the interventions. Increasing the Manning's  $n$  value of the channel, in order to reduce flow velocity, therefore has a much greater impact on downstream peak discharge, since there is a greater likelihood that flow would interact with within-channel interventions. This explanation is consistent with the similar patterns observed between channel-and-overbank and channel-only interventions in Figure 5.5 and Figure 5.6, while overbank-only interventions exhibits a different response.

This highlights the importance of considering flow attenuation in channel and overbank sections simultaneously. Without flow attenuation within the channel, water may not be transferred onto the floodplain where it can interact with overbank interventions (Lane and Thorne, 2007). However, as flow depth increases, within-channel interventions affect a smaller proportion of flow and hence become less important in attenuation (Ferguson, 2007). Once flows are out-of-bank, the floodplain contributes to a large part of attenuation since floodplain flow depths, no longer constrained by channel width, tend to be shallower (Ervin et al., 1993). This maintains the importance of attenuating flow on the floodplain, in addition to within the channel.

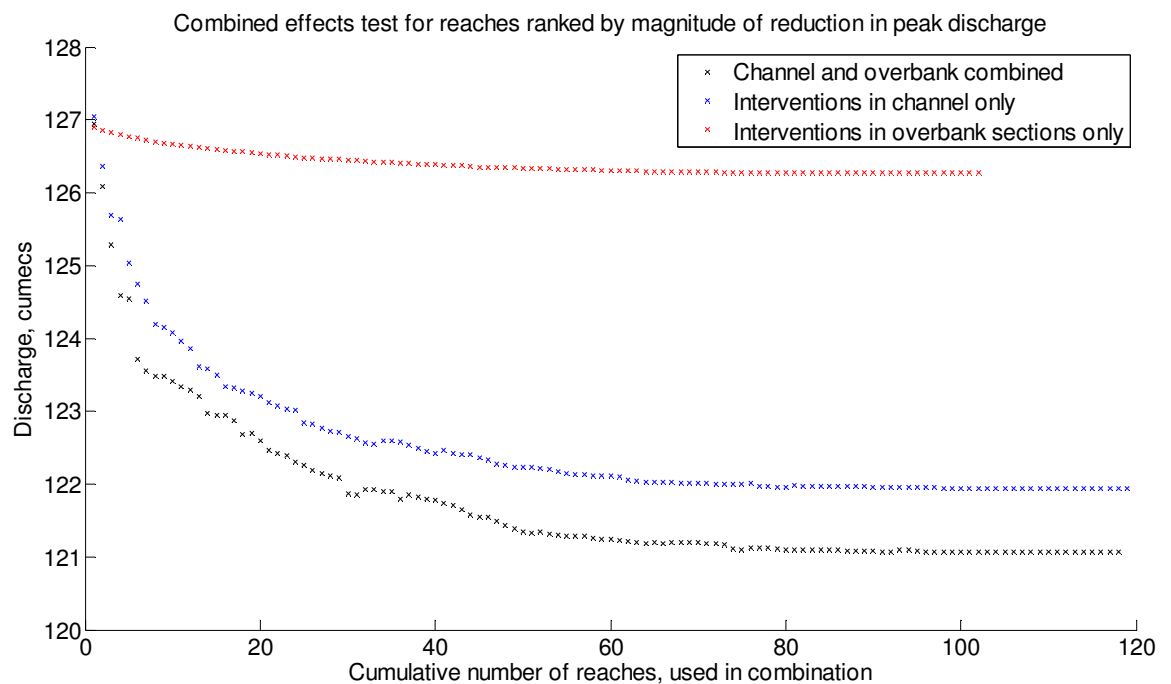


**Figure 5.5** Results of the combined effects test, for interventions in the channel and overbank sections of each reach simultaneously (black), the channel only (blue) and the overbank sections only (red). The reaches were ranked based on their impact on peak discharge in the main effects test, so each point does not necessarily refer to the same reach between each type of intervention. Each point relates to the average of the 200 parameter sets used in the calibrated model. The uncertainty associated with these results is discussed in Section 5.5.



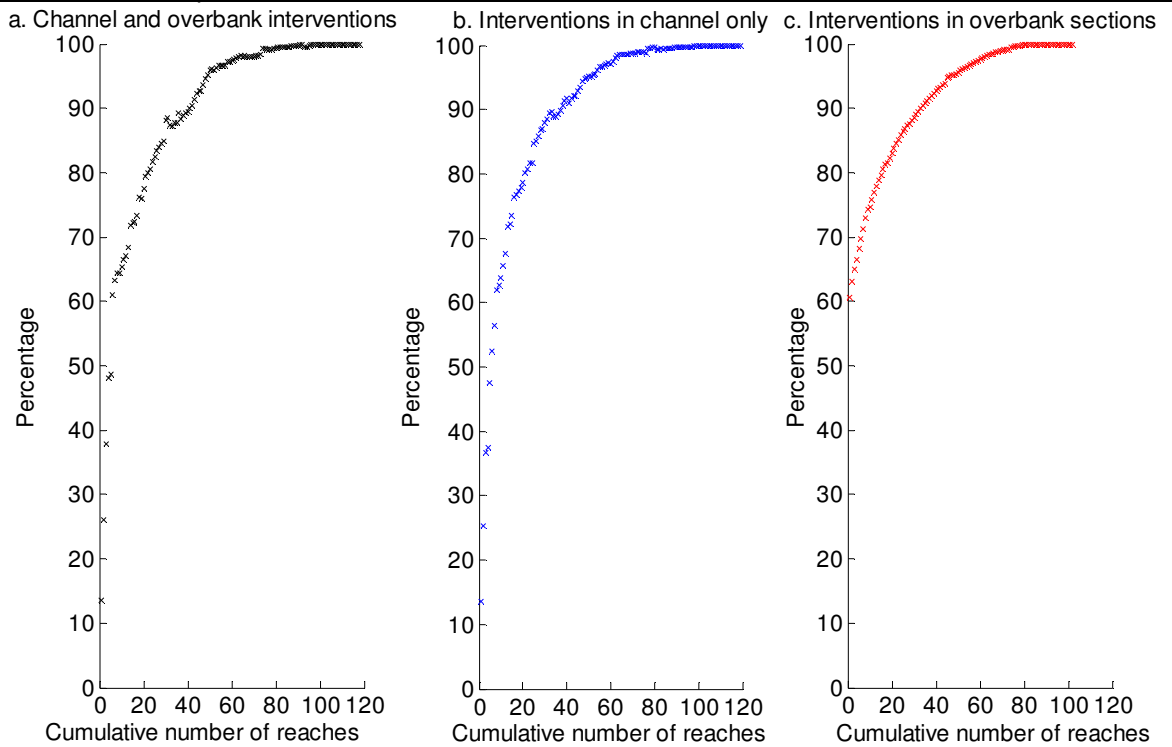


Figure 5.6 The percentage of the total reduction in peak discharge (for each type of intervention) achieved by the cumulative number of reaches. The ‘total reduction’ in peak discharge refers to the maximum reduction in peak discharge when all reaches were used in combination, in comparison to the peak discharge predicted by the calibrated model, in each of the three types of intervention. A summary of absolute values are given in Table 5.3.

Intervention	Minimum peak discharge ( $\text{m}^3\text{s}^{-1}$ ), i.e. with all reaches in combination	Reduction of peak discharge as a percentage of the model ‘base case’ with no interventions
Channel and overbank	121.06	5.31
Channel only	121.94	4.62
Overbank only	126.27	1.24

Table 5.3 Peak discharge reduction achieved with all reaches used in combination. The ‘base case’ peak discharge predicted by the model when no interventions were modelled was  $127.86 \text{ m}^3\text{s}^{-1}$ .

#### 5.4.3. Removal of negative reaches

From Figure 5.4 a number of individual reaches that have a negative impact when used in combination with other reaches can be identified. However, in the case of interventions in the overbank sections only, no reaches were found to have a negative impact on peak discharge in

combination with other reaches. No more reaches were removed from the overbank test, leaving 102 positive or neutral reaches.

Removing reaches that had a negative impact on peak discharge left 105 positive and neutral reaches where an intervention was made only in the channel and 98 positive and neutral reaches where an intervention was made in the channel and adjacent overbank section simultaneously.

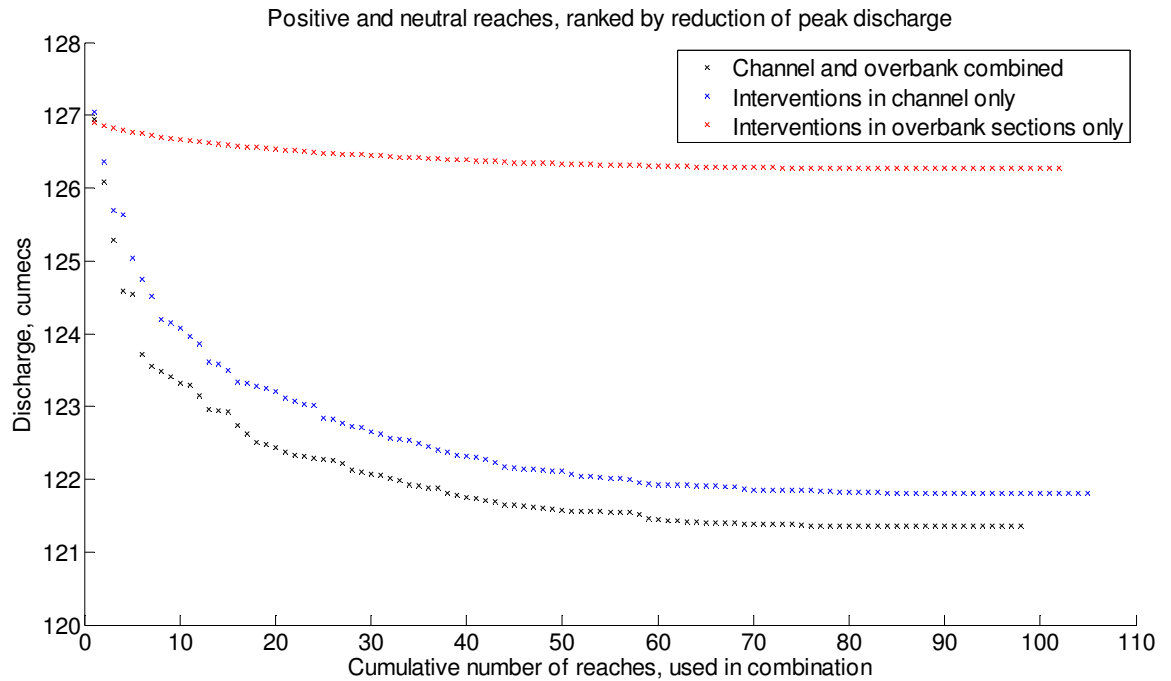


Figure 5.7 Results of the combined effects test once negative reaches had been removed throughout.

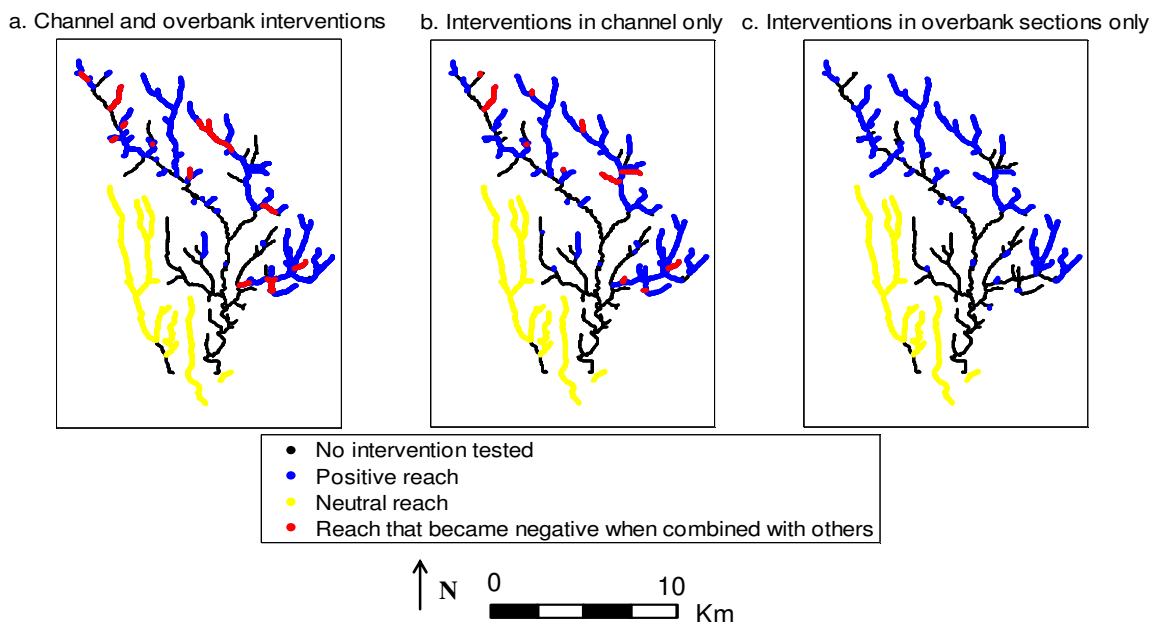
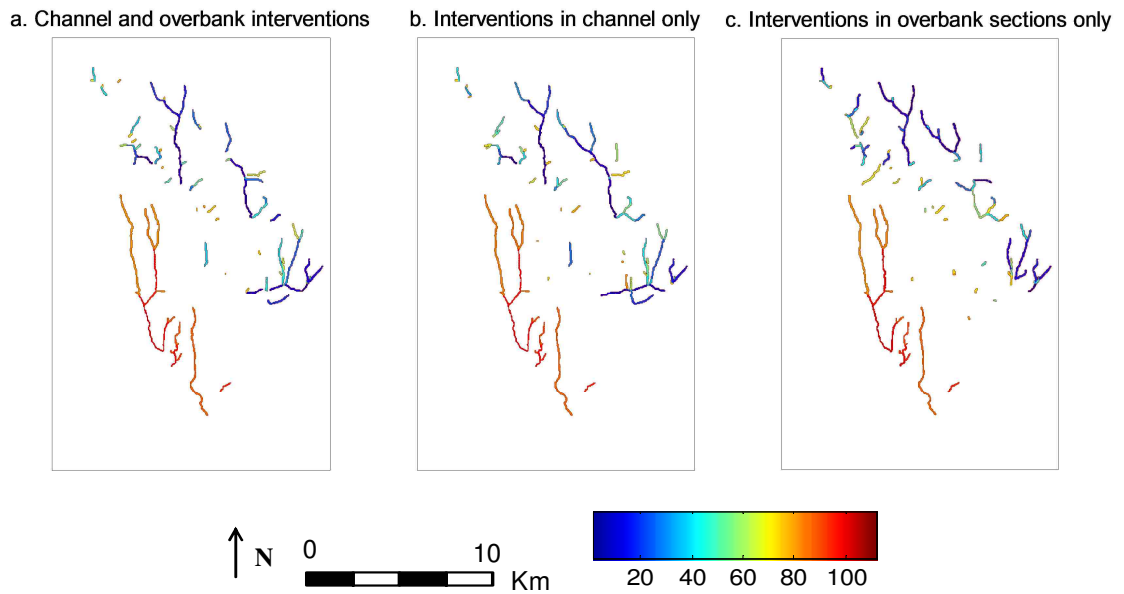


Figure 5.8 Location of the reaches tested in combination with each other, showing positive and neutral reaches and individually positive reaches that became negative when combined with others. Reaches that were individually negative were not tested in combination with others, so have been omitted from this plot for clarity.

#### 5.4.4. Location of the interventions



**Figure 5.9** Interventions after they were ranked and negative reaches were removed. A higher ranking (lower number) indicates the most positive reaches (those that caused the greatest reduction in peak discharge at Sinnington). Neutral reaches have also been included. The colour bar refers to the order in which the reaches were ranked, with 1 the most effective.

The most positive reaches under each set of interventions are located in the upper catchment. In smaller streams, interventions to increase channel roughness have a proportionally larger impact on flow attenuation, since flow depth is typically much lower, so interventions take up a larger proportion of the flow (Ferguson, 2007; Lane and Thorne, 2007). In terms of the Manning equation (Equation 2.4), hydraulic radius (or flow depth) tends to be much lower in smaller streams, which in itself leads to lower flow velocities for a given Manning's  $n$ .

Many positive reaches are also located along the length of relatively long tributaries. These sites have the potential to attenuate water from a larger area and over a longer distance, thereby contributing to a greater reduction to downstream peak discharge.

These results have used a single Manning's  $n$  value to represent LWD dams and riparian buffer strips. There is no directly observable data to validate these measurements, so the selection of precise  $n$  values is uncertain. The uncertainty that this causes in the results is quantified in the next section.

## 5.5. Uncertainty analysis

The purpose of the uncertainty analysis is to assess how uncertainty in the selection of a Manning's  $n$  value to represent CRIMS (from a range of possible  $n$  values) is propagated through the model calculations to variability in the results. The uncertainty analysis will allow a level of confidence to be assigned to the model results. The variability of peak discharge caused by selecting CRIM  $n$  values at random will then be compared to the variability in peak discharge caused by implementing CRIMS in different reaches. This will establish whether the reduction in peak discharge achieved by CRIMS is discernable from the uncertainty in parameter selection.

### 5.5.1. Method

#### 5.5.1.1. Experiment design

CRIMS are represented by a change to Manning's  $n$  only; no alterations are made to the rainfall rate, runoff rate or general catchment Manning's  $n$  in the calibrated model. Therefore, only two parameters (Manning's  $n$  of the channel and the adjacent overbank section for the CRIMS of interest) need to be tested in order to determine the uncertainty associated with how CRIMS are represented in the model. The other model parameters, which were calibrated to the June 2007 flood event, took the same values in each successive simulation.

A global uncertainty analysis was undertaken on the results of the combined effects test with negative reaches removed. The uncertainty analysis was designed along the same lines as the global sensitivity analysis (section 4.5). Monte Carlo simulations were undertaken, using Manning's  $n$  values selected using a random number generator. The Manning's  $n$  values were selected from within a realistic range that they could take to represent CRIMS and were applied to the reaches under investigation. The ranges that Manning's  $n$  values could take were specified as 0.05 – 0.15 for the channel (LWD dams) and 0.08 – 0.20 for the adjacent overbank cells (riparian buffer strips). These ranges were based on values suggested by indexes of Manning's  $n$  values (Chow, 1959; Barnes, 1967) and are broadly representative of the upper and lower working values used in modelling studies undertaken for Forest Research (Odoni and Lane, 2010).

Three separate uncertainty analyses were undertaken in which CRIMS were simulated in the most positive twenty, forty and sixty reaches (based on their impact on peak discharge in the combined effects test). This was repeated for the three types of intervention: channel and overbank, channel only and overbank only. In each run, a new Manning's  $n$  value was randomly selected and applied to all the reaches under investigation.

However, each model simulation used of 200 different calibrated rainfall rate and runoff rate parameter sets. The resulting 200 hydrographs were averaged to give one 'best' predicted

hydrograph for each set of interventions. Uncertainty was therefore also introduced into the results for each model run by variability in rainfall and runoff rates. The total uncertainty caused by parameter selection was calculated by taking the sum of uncertainty resulting from Manning's  $n$  values and uncertainty resulting from the 200 rainfall and runoff rate parameter sets.

### 5.5.1.2. Calculation of confidence margins

Uncertainty in parameter selection may result in a range of acceptable model responses. Parameter uncertainty must be quantified by confidence intervals to ensure that, firstly, the confidence intervals are not so large that any possible model result could fall within the intervals and, secondly, to ensure that any signal in flood response caused by the introduction of CRIMS is greater than, hence distinguishable from, the uncertainty of parameter selection.

Confidence intervals are expressed as a 'best estimate' of the variable of interest ( $x_{best}$ ), bounded by the highest and lowest probable values ( $\delta x$ ):

$$x_{best} \pm \delta x$$

**Equation 5.1 Expression of a value with confidence intervals (Taylor, 1982).**

$x_{best}$  is given by the mean average of the sampled model response.  $\delta x$  is given by the sample standard deviation, also known as the standard error:

$$\frac{1}{\sqrt{N}} \cdot \sqrt{\frac{1}{N-1} \cdot \sum_{i=1}^n (x_i - \bar{x})^2} = \frac{\sigma_x}{\sqrt{N}}$$

**Equation 5.2 The standard error of the variable  $x$  is given by the sample standard deviation  $\sigma_x$  divided by the root of the number of observations  $N$  (Taylor, 1982). Where  $x_i$  is the  $i$ th observed value and  $\bar{x}$  is the mean of the observations.**

A large sample of measurements tends to follow a normal distribution. Because the normal distribution is known, the probabilities of measurements falling into a given range are known. For any point, there is a 95 % probability that it will fall within 1.96 standard errors of the mean (Mendenhall et al., 2009). Therefore, at a 95 % confidence level, the model response falls within the confidence interval:

$$x_{best} \pm \delta x = \bar{x} \pm 1.96 \frac{\sigma_x}{\sqrt{N}}$$

**Equation 5.3 Statement of a confidence interval (Taylor, 1982; Mendenhall et al., 2009).**

The combined effect of uncertainty in all parameters was found by the sum of the confidence intervals resulting from Manning's  $n$  uncertainty and the confidence intervals due to the use of different rainfall and runoff rate parameter sets (Taylor, 1982):

$$x_{best} \pm (\delta x + \delta y)$$

**Equation 5.4 A confidence interval with uncertainty from two sources, where  $\delta x$  = highest and lowest probable values of  $x_{best}$  due to Manning's  $n$  uncertainty and  $\delta y$  = highest and lowest probable values of  $x_{best}$  due to rainfall rate and runoff rate uncertainty (Taylor, 1982).**

### 5.5.2. Results

First, the necessary sample size was identified. Next, uncertainty resulting solely from the selection of Manning's  $n$  values to represent flow attenuation was examined. Finally, the total parameter uncertainty (including that resulting from rainfall and runoff rates) was calculated. The implications of parameter uncertainty for the impact of CRIMS on downstream flood flows are then discussed.

#### 5.5.2.1. Sample size

The necessary sample size was assessed empirically, as in the global sensitivity analysis (section 4.5). Sampling was curtailed after 1000 runs for each set of interventions, when successive sets of simulations gave similar mean peak discharge values and standard deviations (Table 5.4). Fewer model runs were needed than in the global sensitivity analysis, since only two, rather than four, parameters were tested and these were tested over a smaller range, representing the intervention measures rather than the full range of possible  $n$  values.

Intervention type	Number of reaches tested	First 250 runs ( $\text{m}^3\text{s}^{-1}$ )		First 500 runs ( $\text{m}^3\text{s}^{-1}$ )		1000 runs ( $\text{m}^3\text{s}^{-1}$ )	
		Average	Standard deviation	Average	Standard deviation	Average	Standard deviation
Channel and overbank	Best 20	123.72	1.45	123.62	1.45	123.57	1.45
	Best 40	123.06	1.57	123.09	1.57	123.07	1.55
	Best 60	123.14	1.56	122.98	1.53	122.96	1.63
Channel only	Best 20	124.19	1.45	124.22	1.45	124.20	1.11
	Best 40	123.82	1.40	123.76	1.39	123.71	1.38
	Best 60	123.50	1.56	123.42	1.53	123.50	1.51
Overbank only	Best 20	126.75	0.31	126.74	0.31	126.73	0.31
	Best 40	126.59	0.34	126.61	0.34	126.59	0.34
	Best 60	124.69	0.69	124.70	0.70	125.63	1.09

**Table 5.4 Mean average peak discharge and standard deviation of the results ( $\text{m}^3\text{s}^{-1}$ ) for each type of intervention. Results should be read across the table; the intention of this analysis is to assess that the mean and standard deviation of the results are stable with respect to the number of model runs.**

### 5.5.2.2. Manning's $n$ uncertainty

Table 5.5 lists the confidence intervals for each set of interventions. The absolute confidence intervals (in  $\text{m}^3\text{s}^{-1}$ ) were smallest for interventions in overbank sections only and largest for interventions in the channel and overbank sections simultaneously. This reflects the higher model sensitivity to variation in channel Manning's  $n$  than land cover  $n$  (Chapter 4). For each intervention type, the absolute confidence intervals also became slightly larger as more reaches were included, from the best twenty to sixty reaches, because inclusion of more reaches introduced more points in the catchment where the selection of Manning's  $n$  values was uncertain.

However, as more reaches were included and as channel interventions were included, the impact on downstream peak discharge also increased. As a result, the confidence interval as a percentage of peak discharge was fairly stable (most values were around 2%). While the absolute confidence intervals varied for different interventions and different numbers of reaches, the importance of the confidence intervals as a proportion of peak discharge remained relatively constant.

Intervention type	First 20 reaches ( $\text{m}^3\text{s}^{-1}$ )	First 40 reaches ( $\text{m}^3\text{s}^{-1}$ )	First 60 reaches ( $\text{m}^3\text{s}^{-1}$ )
Channel and overbank	$\pm 0.09$	$\pm 0.10$	$\pm 0.10$
Channel only	$\pm 0.07$	$\pm 0.09$	$\pm 0.09$
Overbank only	$\pm 0.02$	$\pm 0.02$	$\pm 0.07$

**Table 5.5 Confidence intervals around the mean peak discharge due to  $n$  value uncertainty, to 1 significant figure (Equation 5.3). The confidence intervals express how variability in the selection of Manning's  $n$  values to represent CRIMS generates uncertainty in the resulting peak discharge.**

Intervention type	First 20 reaches (%)	First 40 reaches (%)	First 60 reaches (%)
Channel and overbank	$\pm 2.10$	$\pm 2.10$	$\pm 2.04$
Channel only	$\pm 1.91$	$\pm 2.17$	$\pm 2.06$
Overbank only	$\pm 1.77$	$\pm 1.57$	$\pm 3.14$

**Table 5.6 Percentage confidence intervals around the mean peak discharge due to  $n$  value uncertainty. The confidence intervals express the uncertainty as a percentage of the reduction in peak discharge achieved under each set of interventions, for comparative purposes.**



### 5.5.2.3. Total parameter uncertainty

Chapter 4 illustrated the potential for parameter interactions, where model sensitivity to one parameter also depended on the value of other parameters. A variation in Manning's  $n$  to represent different types or numbers of CRIMS could have an effect on model sensitivity to rainfall and runoff rates. A confidence interval for rainfall and runoff rate uncertainty was calculated for each set of interventions (Table 5.7). This was based on the range of model results given by the 200 different calibrated runs, each of which used a different sequence of runoff and rainfall rate parameter values (see section 4.7).

Intervention type	First 20 reaches ( $\text{m}^3\text{s}^{-1}$ )	First 40 reaches ( $\text{m}^3\text{s}^{-1}$ )	First 60 reaches ( $\text{m}^3\text{s}^{-1}$ )
Channel and overbank	$\pm 0.12$	$\pm 0.10$	$\pm 0.10$
Channel only	$\pm 0.24$	$\pm 0.15$	$\pm 0.15$
Overbank only	$\pm 0.06$	$\pm 0.07$	$\pm 0.04$

**Table 5.7 Confidence intervals around the mean of the results due to rainfall rate and runoff rate uncertainty, to 1 significant figure (Equation 5.3). The confidence intervals express how variability in the 200 rainfall rate and runoff rate parameters for each model run generates uncertainty in the resulting peak discharge.**

The sum of uncertainty due to Manning's  $n$  (Table 5.5) and the uncertainty due to rainfall and runoff rates (Table 5.7) gave a confidence interval that represented the total parameter uncertainty. The reduction in peak discharge that could be achieved by each set of interventions, with the associated confidence intervals, is given in Table 5.8.

Any one CRIM used in isolation has a low impact. Figure 5.5 shows that the individual contribution of many reaches is of a similar magnitude to the uncertainty caused by the selection of parameters to represent the CRIMS. With the exception of the few 'most positive' reaches, the individual contribution of a CRIM is unclear.

However, in the case of multiple CRIMS, the predicted reduction in peak discharge is greater than the uncertainty caused by selection of Manning's  $n$  values to represent the intervention. Therefore, a combination of CRIMS reduces peak discharge to an extent that can be distinguished from variability in the results caused by parameter uncertainty. As a proportion of the reduction in peak discharge, this signal is most distinct where interventions are carried out in channel and overbank sections simultaneously and for a larger number of reaches.

Intervention type	Number of reaches tested	Mean peak discharge based on 1000 model runs for each set of interventions ( $\text{m}^3 \text{s}^{-1}$ )	Absolute reduction in peak discharge ( $\text{m}^3 \text{s}^{-1}$ )	Confidence interval ( $\text{m}^3 \text{s}^{-1}$ )	Confidence interval (as a percentage of reduction in peak discharge)
Channel and overbank	Best 20	123.57	4.29	$\pm 0.21$	$\pm 4.90$
	Best 40	123.07	4.79	$\pm 0.20$	$\pm 4.18$
	Best 60	122.96	4.90	$\pm 0.20$	$\pm 4.08$
Channel only	Best 20	124.20	3.66	$\pm 0.31$	$\pm 8.47$
	Best 40	123.71	4.15	$\pm 0.24$	$\pm 5.78$
	Best 60	123.50	4.36	$\pm 0.24$	$\pm 5.50$
Overbank only	Best 20	126.73	1.13	$\pm 0.08$	$\pm 7.08$
	Best 40	126.59	1.27	$\pm 0.09$	$\pm 7.09$
	Best 60	125.63	2.23	$\pm 0.11$	$\pm 4.93$

Table 5.8 Peak discharge reduction ( $\text{m}^3 \text{s}^{-1}$ ) in comparison to the peak discharge predicted at Sinnington with no interventions ( $127.86 \text{ m}^3 \text{ s}^{-1}$ ), with confidence intervals at the 95% level of confidence. Therefore, with 95% confidence, each reduction in peak discharge falls within  $\pm$  the confidence interval.

## 5.6. Discussion

This chapter applied the calibrated *Overflow* model to predict the impact of flow attenuation measures on peak discharge in the River Seven catchment. The interventions that were tested consisted of large woody debris dams in the channel, and forested buffer strips overbank.

Increasing Manning's  $n$  (to represent attenuation) in the river channel on its own was found to have a much greater impact on peak discharge than increasing  $n$  in the overbank area immediately adjacent to the reach. Interventions in the channel only for all reaches led to a peak discharge reduction of 4.62 %. Interventions in overbank sections only for all reaches led to a peak discharge reduction of 1.24 %. However, combining increases in  $n$  in the river channel and overbank areas led to a further reduction in peak discharge (5.31 % for all reaches). This suggests that interventions in both (in the form of LWD dams and riparian buffer strips) offer the greatest opportunity to influence downstream flood risk.

When CRIMS were tested individually, it was found that the magnitude of the impact on downstream peak discharge varied for different reaches. The most positive reaches tended to be in the upper part of the catchment, while negative reaches tended to be in the main river or further downstream. It is likely that CRIMS in the upper half of the catchment have greater potential for attenuating flow and desynchronising the contribution of floodwater from different tributaries (Odoni and Lane, 2010). On the other hand, CRIMS in the lower half of the catchment may not be a sufficient distance from Sinnington for flow attenuation to have a beneficial effect. Alternatively, they may cause flood hydrographs from different tributaries to become synchronised (Lane et al., 2007b). However, most reaches had a relatively low impact on downstream peak discharge (at most a 0.72 % or  $0.92 \text{ m}^3\text{s}^{-1}$  reduction, depending on the type of intervention and number of reaches tested). An uncertainty analysis showed that the individual impact of CRIMS in these reaches could not be easily discerned from parameter uncertainty (up to  $\pm 0.31 \text{ m}^3\text{s}^{-1}$ ).

In combination, CRIMS had a much greater effect on downstream peak discharge, to the extent that the impact was distinct from parameter uncertainty. Channel and overbank CRIMS in the best 20 reaches led to a reduction in peak discharge of  $4.29 \text{ m}^3\text{s}^{-1}$  (3.35 %) at Sinnington. CRIMS in all positive and neutral reaches resulted in a reduction in peak discharge of  $6.58 \text{ m}^3\text{s}^{-1}$  (5.30 %). However, it was also found that some reaches that were individually positive, had negative impact when used in combination with other reaches. Since these reaches only became negative on interaction with others, this suggests that flow attenuation in one tributary may cause the timing of the flood hydrograph to coincide with contributions from another tributary, leading to an overall increase in peak discharge downstream (Lane et al., 2007b).

However, in light of the extent of changes to Manning's  $n$ , these results show a limited change in peak discharge in response to the scale of flood attenuation interventions. Manning's  $n$  is used to represent a wide range of sources of flow resistance. However,  $n$  only affects the magnitude of momentum loss (Lane, 2005). Obstructions, such as large woody debris dams, may also block and route flow (Yu and Lane, 2006b). Blockage is not explicitly represented in the Manning equation, although in this project,  $n$  is still used to account for these effects. This assumption, which has been made to allow *Overflow* to conduct fast, catchment scale simulations, may therefore lead to uncertainty in quantifying the magnitude of flow attenuation. However, since the sensitivity analysis (Chapter 4) showed that *Overflow* responds to variation in Manning's  $n$  in a way that is consistent with theoretical understanding of the physical processes, the results may still be used to understand the catchment scale behaviour of the system.

Further research may be required to evaluate different methods for representing flow resistance in flood models. Alternative methods have been developed; for example, Yu and Lane (2006b) explicitly include flow blockage in a flood model. Three dimensional modelling also allows the impact of sources of flow resistance to be understood in high spatial and temporal resolution (Hardy, 2008). However, additional levels of complexity require greater computation time and greater levels of observed data to specify sources of flow resistance. It is recognised that the use of Manning's  $n$  to represent flow resistance is a limitation of the model. However, it is one that represents a trade-off between explicit representation of physical processes and the demands for additional data and computation. One of *Overflow's* design aims was to allow the model to be applied with limited data collection (Odoni and Lane, 2010).

## 5.7. Conclusion

This chapter has demonstrated that flow attenuation can reduce downstream flood risk and has identified locations in the River Seven that might be suitable for flow attenuation measures. Catchment Riparian Interventions Measures (CRIMS), which were used to attenuate flow, consisted of large woody debris dams and riparian buffer strips. CRIMS increase flow resistance by generating form drag and obstructions to flow. They were represented in the model by increased Manning's  $n$  values for the reach of interest. A value of 0.14 was used for the channel and 0.16 for the floodplain. An individual CRIM in any one reach has a low impact; at most, a 0.72 % or  $0.92 \text{ m}^3\text{s}^{-1}$  reduction in flood peak. This is of similar magnitude to total parameter uncertainty (up to  $\pm 0.31 \text{ m}^3\text{s}^{-1}$ ). Thus it is difficult to discern the impact of an individual CRIM from uncertainty in parameter value selection. However, the impact of multiple CRIMS throughout the catchment accumulates to an effect that is distinct from uncertainty in the selection of parameter values. A reduction in flood peak of up to  $6.80 \text{ m}^3\text{s}^{-1}$  (5.31 %) was predicted for the most effective case (increasing Manning's  $n$  in the channel and overbank simultaneously).

CRIMS reduced flow velocity and thus increased attenuation. Overall, this led to a reduction in downstream peak discharge. However, in some reaches, CRIMS increased peak discharge. This may be due to the effect of flow attenuation on the timing of the flood hydrograph peak, which can cause hydrographs from several tributaries to arrive coincidentally at a point further downstream. Therefore, the impact of CRIMS on downstream flood flows is also influenced by the location of the reach within the catchment. The most positive reaches tended to be in the upper catchment, where there was greater potential for flow attenuation to desynchronise the contribution of different tributaries and mitigate downstream flood flows.

In terms of the Manning equation, the physical meaning of increasing  $n$  is to increase flow resistance, thereby slowing flow velocity. Although the sensitivity analysis (Chapter 4) showed that *Overflow* behaved in this way, there is no empirical data against which the magnitude of this response can be compared. The next chapter assesses flow behaviour at a scale that is internal to the model. *Overflow* is compared to a hydraulic model with a different method of process representation, designed for flow predictions at the reach-scale.

## 6. Model comparison

### 6.1. Summary

*Overflow's* reduced complexity means that it can be used to model at the scale of the entire catchment with short run times, allowing multiple scenario testing. However, this comes at a cost of simplifications to how physical processes are represented in the model's numerical equations. In order to make these simplifications it was necessary to make assumptions about the behaviour of physical processes. These assumptions represent judgements about the relevant processes operating in specific types of catchments and types of flood, for which *Overflow* was designed (see section 2.5).

For the purpose of flood modelling, there are a number of ways of simplifying the equations that describe physical processes (Hunter et al., 2007). A large number of different models and software packages are used in flood studies in the UK (Evans et al., 2001), which illustrates that the method of process representation may vary with the application of the model and is ultimately uncertain (Hunter et al., 2008). For example, Manning's  $n$  was used to represent flow resistance measures, which were used to cause flow attenuation. *Overflow* responded to Manning's  $n$  (and other parameter values) in a way that was theoretically consistent with physical processes, represented by the model's constituent equations. However, the analysis has so far done little to inform about how simplifications made in *Overflow* affects the predicted magnitude of flow attenuation, in comparison to alternative approaches. However, by comparing results from different models, it is possible to determine the effect of different levels of detail and equations by which physical processes are represented (Bates and Anderson, 2001).

The aim of this chapter is to compare results given by *Overflow* with those of a hydraulic model, HEC-RAS, which has a conceptually different process representation. This was undertaken to assess the effect of different methods of process representation, for the same topographic and boundary condition data. *Overflow* was used to predict discharge hydrographs at the inlet to a sample of reaches within the catchment. These hydrographs were used as the input to HEC-RAS, which modelled the reach of interest using the same topographic data as *Overflow*. The hydrographs that were predicted by each model at the downstream outlet of the reach were compared.

First, the chapter explains and justifies the process of benchmarking results from one model against another. Second, the constituent equations and operation of the HEC-RAS model is described. Next, the method by which the HEC-RAS model is constructed of the River Seven, calibrated and compared to *Overflow* is outlined. The results of the model benchmarking are

given. Finally, the results are discussed with reference to the practicalities of using each model and possible areas for future work.

For each model and reach, the downstream output hydrograph was compared to the input boundary condition hydrograph. This was used as a measure of how the model process equations modified the input hydrograph as it was routed downstream. The results showed that HEC-RAS predicted a peak discharge and flood volume that was similar in magnitude to the input hydrograph. On the other hand, *Overflow* predicted a higher peak discharge and flood volume at the reach outlet than could be accounted for by the input hydrograph. It is likely that the inclusion of floodplain flow in *Overflow* resulted in water arriving downstream by overland flow routes other than the channel. This water was not accounted for by the upstream hydrograph at the reach inlet, so did not appear in the HEC-RAS model, which routes flow in one dimension only based on an upstream boundary condition. In the current version of *Overflow*, floodplain flow is routed diffusively and it is not possible to isolate the downstream component of flow from lateral flows. The chapter concludes that future work may be required to integrate floodplain flow predictions from *Overflow* as a boundary condition to hydraulic models for further testing.

Reach-scale testing of model predictions is important to ensure that *Overflow* is not overcalibrated to gauging station observations at the catchment outlet using parameters, at a cost of representing flow processes within the model domain (Hamilton, 2007).

## 6.2. Justification of model comparison

This project has used a reduced complexity model, *Overflow*. Due to the simplifications and assumptions involved in producing a model representation of reality, throughout this project it has been necessary to evaluate how well *Overflow* replicates physical processes.

In Chapter 4, a sensitivity analysis was undertaken to ensure that the model behaved in a manner that was theoretically consistent with physical processes. The model was then calibrated by adjusting parameter values to reduce the difference between model predictions and observed data. In Chapter 5, the model was applied to predict suitable reaches for intervention measures. An uncertainty analysis was undertaken to quantify how variability in parameters was propagated to uncertainty in the model output. It was concluded that *Overflow* was capable of reproducing observed flow hydrographs accurately, that model sensitivity to parameter values was consistent with the physical processes known to operate in the catchment and that the results were sufficiently precise for the impact of CRIMS, when used in combination, to be detected. From these tests it appears that *Overflow* is capable of approximating processes operating in the River Seven catchment for the June 2007 flood, for the purpose of predicting the impact of flow attenuation on downstream flood risk.

However, in Chapter 4, the model was assessed and calibrated using catchment-wide parameter values and a comparison to a gauging station at the catchment outlet. Although this resulted in a calibrated model that predicted the June 2007 flood event with a high degree of accuracy (NSE values  $> 0.98$ ), it does not necessarily imply that the model parameter values are physically meaningful at any given point within the catchment (Hardy et al., 2003). This is problematic because CRIMS were spatially distributed and specified at the scale of river reaches within the catchment. Chapter 5 found that the low magnitude of an individual CRIM impact in any one reach could not be distinguished from parameter uncertainty, so flow behaviour in response to an individual CRIM is uncertain. Therefore the impact of assumptions and simplifications made in model process representation are uncertain.

The effect of multiple CRIMS was quantified in terms of their combined impact on a downstream flow hydrograph. However, the global sensitivity analysis in Chapter 4 showed that there was the potential for equifinality in Manning's  $n$ . Due to parameter interactions, many different parameter sets could result in equivalent model predictions (Aronica et al., 1998). Thus it might be possible for *Overflow* to make accurate predictions of the flood hydrograph, using theoretically unrealistic parameter values at any point within the catchment. At the catchment scale, a reduced complexity hydrological model could reproduce lumped flow observations at the catchment outlet to the same level of accuracy as a more complex model, by the selection of parameter values that cause the predicted and observed hydrographs to match (Bates and Anderson, 2001).

As a result, it is uncertain whether the downstream impact of CRIMS is solely a result of the increase in Manning's  $n$  values used to represent attenuation, or whether it is affected by interactions with other spatially distributed parameter values. In assessing the impact of reach-scale interventions, it is important that the model is capable of representing flow behaviour in response to an intervention at the reach scale, rather than including influences from interactions with other processes and parameter values elsewhere in the catchment (Bates and Anderson, 2001).

Model results were examined at the scale of individual river reaches. Chapters 4 and 5 have compared the model to observed data, with the purpose of evaluating how well the model reproduces observations at a point in the lower part of the catchment, where reducing flood magnitude is of interest. This chapter investigates whether the model is producing these results for physically meaningful reasons at a scale internal to the modelled catchment (Kirchner, 2006).

However, as there is no observed gauge data for the River Seven other than at the outlet of the catchment, *Overflow's* reach scale predictions could not be validated by comparison to observations. As an alternative, numerous studies have compared results from several models of the same observed event (Horritt and Bates, 2002; Chau et al., 2005; Tayefi et al., 2007; Apel et al., 2009). This approach does not validate models with respect to reality because, in the absence



of complete and comprehensive observations, all models contain a degree of simplification to account for a lack of measured data. However, the process of corroborating results from different models can be used to infer the impact of different levels of process representation and boundary condition detail. *Overflow* was compared to predictions from a conceptually different model, which uses a different method of process representation.

Despite the high levels of complexity that can be achieved through two- or three-dimensional models derived from the Navier-Stokes equations, the standard and accepted method for operational flood modelling in the UK is the use of one dimensional (1D) models, which benefit from shorter computation times and lower data requirements (Tayefi et al., 2007). A 1D hydraulic model, HEC-RAS was used to corroborate the results from the hydrological routing model, *Overflow*. HEC-RAS calculates characteristics of flow using the one dimensional Saint Venant equations.

Since flood models are intended to simplify physical processes to enable flood prediction, all models are subject to uncertainty (Saltelli et al., 2008). *Overflow* therefore cannot be 'validated' by a comparison of results to HEC-RAS. In particular, HEC-RAS is not without its own uncertainties when applied to upland catchments (Tayefi et al., 2007). HEC-RAS also represents topographic and flow data in a way that is conceptually different to *Overflow* (described in section 6.3).

The intention of corroborating *Overflow* predictions with those of HEC-RAS is to demonstrate the impact of different methods process representation on the model predictions. By basing the HEC-RAS model on the same topographic data and boundary conditions used in *Overflow*, any difference in the model results can be attributed to the way in which physical processes are represented in each model. As such, this chapter is intended as a more robust test of the predicted impact of flow attenuation interventions and the associated uncertainty, by comparing the effect of two different numerical representations.

HEC-RAS was selected since it does not require any additional boundary condition or topographic information beyond what was available for *Overflow*. The model comparison is therefore a comparison of the process and boundary condition representation within each model. It is not influenced by any additional 'external' information. It is informative to make comparisons to HEC-RAS, because HEC-RAS has also been used previously to predict the impact of flow attenuation interventions by Forest Research (Thomas and Nisbet, 2007).

### 6.3. HEC-RAS

#### 6.3.1. Background

HEC-RAS 4.0 (Hydraulic Engineering Centre River Analysis System) was developed by the Hydraulic Engineering Centre of the U.S. Army Corps of Engineers and may be freely downloaded from the internet (<http://www.hec.usace.army.mil/software/hecras/>). HEC-RAS is widely used by consultants and researchers for one-dimensional prediction of river flows in flood, sediment transport and water quality modelling studies (Pappenberger et al., 2005; Brunner, 2008). In particular, HEC-RAS is one of a number of models used extensively by the Environment Agency for Section 105 flood risk mapping and is a standard tool for flood prediction in the UK (Evans et al., 2001).

HEC-RAS was chosen for this study due to its availability, ease of use and short computation time, allowing large numbers of predictions for multiple scenarios. It is possible to implement the model with minimal field work and with boundary conditions provided by *Overflow*.

#### 6.3.2. Process representation

In HEC-RAS, river channel and floodplain topography are represented by a series of cross-sections, perpendicular to flow direction and which extend across the floodplain. At the upstream boundary of the model, the user inputs steady flow (i.e. a constant discharge rate) or unsteady flow (i.e. a discharge hydrograph) data. In this project, cross sections were based on the same DEM as *Overflow* and boundary condition data was given by flow hydrograph predictions from *Overflow*. This allowed a comparison of the flow routing calculations for the same boundary conditions and topography. A more detailed description of how the data requirements were met and how HEC-RAS was applied is given in section 6.4.

HEC-RAS then solves the 1D Saint Venant equations. The Saint Venant equations consist of terms for the conservation of mass and the conservation of momentum. The conservation of mass is given by the continuity equation (Equation 6.1), which maintains that the rate of flow into the reach equals the sum of the rate of flow out of the reach plus any change in storage within the reach. The conservation of momentum is given by the dynamic equation (Equation 6.2), which balances the forces of pressure, gravity, friction and inertia (Lopes et al., 2004). The dynamic equation is derived from the three dimensional Navier-Stokes equations. In HEC-RAS, these equations are given in the form:

$$\frac{\partial A}{\partial t} + \frac{\partial Q}{\partial X} - q_1 = 0$$

**Equation 6.1** The continuity equation, in the form taken in the Saint Venant equations.

$$\frac{\partial Q}{\partial t} + \frac{\partial Qv}{\partial X} + gA \left( \frac{\partial z}{\partial X} + S_f \right) = 0$$

**Equation 6.2** The dynamic equation, in the form taken in the Saint Venant equations.

$$\text{Where the friction slope, } S_f = \frac{(Q|Q|n^2)}{2.208R^{4/3}A^2}$$

**Equation 6.3** Friction slope

Where  $A$  = cross sectional area of flow ( $m^2$ ),  $t$  = time (s),  $Q$  = discharge ( $m^3s^{-1}$ ),  $X$  = length of the reach (m),  $q_1$  = lateral inflow discharge per unit length ( $m^3s^{-1}m^{-1}$ ),  $v$  = velocity ( $ms^{-1}$ ),  $g$  = gravitational acceleration of  $9.81$  ( $ms^{-2}$ ),  $z$  = height of the water surface (m),  $R$  = hydraulic radius (m),  $n$  = Manning's friction coefficient (Bathurst, 1988; Brunner, 2008).

The equations are solved iteratively at each cross section to calculate flow characteristics, such as water level (Horritt and Bates, 2002). In an unsteady flow event, these calculations are repeated at each model timestep to calculate a hydrograph at each cross section (Haestad Methods et al., 2003). To calculate the change in momentum between each cross section as the water flows downstream, a term representing energy loss ( $h_e$ ) is included:

$$h_e = LS_f + C \left[ \frac{a_2 v_2^2}{2g} - \frac{a_1 v_1^2}{2g} \right]$$

**Equation 6.4** Energy head loss,  $h_e$

Where  $L$  = reach length weighted by discharge,  $S_f$  = friction slope (Equation 6.3),  $C$  = a coefficient representing energy loss due to expansion or contraction,  $v_1$  and  $v_2$  = average velocity at subsequent cross sections ( $ms^{-1}$ ),  $a_1$  and  $a_2$  = velocity weighting coefficients and  $g$  = gravitational acceleration ( $ms^{-2}$ ) (Brunner, 2008).

A final boundary condition at the downstream cross section allows HEC-RAS to construct a rating curve relationship between discharge and water level, to calculate water depths at each cross section. This can be provided by a stage hydrograph or a water surface slope, from which water level can be calculated using the Manning equation. As an additional final step, the inundation extent or overbank flood volume can be estimated by interpolating values for water depth between cross sections and overlain on a DEM (Tayefi et al., 2007).

### 6.3.3. Parameters

Since HEC-RAS is limited to the prediction of hydraulic flows in surveyed sections of river channel, there are fewer parameters required to represent unmeasured catchment characteristics than in hydrological models such as *Overflow*.

Like *Overflow*, HEC-RAS uses Manning's  $n$  to represent resistance to flow and the consequent energy loss in the friction slope term, Equation 6.3 (Pappenberger et al., 2005). However, in HEC-RAS, a 1D hydraulic representation of the river channel,  $n$  is used to represent energy loss at the scale of cross-sections and due to two-dimensional variables, such as variation in river planform. In *Overflow*,  $n$  represents resistance to flow across each two-dimensional, 20 metre square grid cell. As a result, Manning's  $n$  values have a different physical meaning in each model and cannot be absolutely compared (Horritt and Bates, 2002).

HEC-RAS allows an unlimited number of Manning's  $n$  values to be specified across each cross section at user-defined intervals. However, in many flood modelling studies, Manning's  $n$  is not directly calculated, but estimated from index tables, photographs or researchers' personal experience (Evans et al., 2001), so locally specific  $n$  values have questionable physical basis. As with the specification of parameters in *Overflow*, only two  $n$  values were specified: one for the channel and one for the floodplain.

### 6.3.4. Key assumptions

In 1D modelling, a number of simplifications are made. Key assumptions of relevance to this project are discussed here to identify limitations in the process of model comparison.

In a 1D model, it is assumed that flow and variations in velocity occur in one dimension only – downstream. Furthermore, the water depth cannot vary across a model cross section. For the purpose of modelling flood flows within river channels, lateral and vertical flow variations are insignificant in comparison to the downstream component of flow (Tayefi et al., 2007). However, on the floodplain, the lateral movement of water is of greater interest. Floodplain flows tend to be shallower, so floodplain topography is able to have greater influence on flow routing (Yu and Lane 2006a). In this respect, the ability of a 1D model to simulate overland flow routing compares poorly to a routing model such as *Overflow*.

In some respects, HEC-RAS is less complex than *Overflow*. For example, boundary conditions to HEC-RAS must be specified as a (hydraulic) flow hydrograph; the model is not capable of estimating flood flows based on (hydrological) rain gauge observations. However, HEC-RAS does make use of a higher level of process representation of within-channel flows. It is therefore informative to compare model predictions at the reach-scale; in particular, how each model responds to increases in flow resistance associated with CRIMS (section 5.2).

## 6.4. Method

HEC-RAS was used to model a sample of reaches of the River Seven. The flow hydrographs predicted by HEC-RAS for the downstream outlet of each reach were compared with hydrographs predicted by *Overflow* for the same point. The same topographic data and upstream flow hydrograph inputs were used in each case, so that any difference between the hydrographs predicted by each model could only be attributed to differences in the constituent equations used to route the hydrographs through the reach.

### 6.4.1. Model construction

HEC-RAS requires information about the topography of the channel and floodplain, and boundary condition data about the flow conditions.

Topography is discretised as a series of cross sections, across the channel and floodplain, perpendicular to flow direction. In order for the model results to be compared on the basis of process representation rather than topographic representation, the cross sections were extracted from the same 20 m resolution DEM data as was used in the *Overflow* model. For each cross section, floodplain heights were sampled at 20 m intervals, from each successive cell in a cross section perpendicular to the channel. Information about the channel width and depth had already been predicted using the Leopold and Maddock (1953) equations for flow routing calculations in *Overflow* (see section 2.5.3.3). This information was used to specify the channel geometry within each cross section. The resulting data were entered manually into HEC-RAS.

To begin with, cross sections were taken at systematic intervals of 100 m along the channel, every five grid cells of the DEM, following recommendations by Samuels (1990) and to give a density of topographic data that was comparable to other hydraulic models used for research purposes (Horritt and Bates, 2002; Tayefi et al., 2007). Each cross section ran perpendicular to the channel across the full extent of the floodplain. However, in HEC-RAS, successive cross sections must not overlap (i.e. the same topographic data must not be entered in more than one cross section). In some cases, where the reach meandered, some cells falling within the cross section were also channel cells, which limited the width of the floodplain data and created the risk of cross sections overlapping. In this situation, cross sections were sampled before and after the meander where possible. However, in many cases the only way of avoiding overlapping cross sections was to increase cross sectional spacing. Given the available data and the resolution of the DEM, the cross sections were limited in characterising small scale variations in the channel and floodplain (e.g. at meander bends). However, the purpose of constructing the HEC-RAS model was to compare the impact of the different flow routing equations used in HEC-RAS and *Overflow*. The HEC-RAS model

was therefore broadly representative of the same topographic and channel geometry data that was used in *Overflow*, even if it was not possible to represent small scale topographic or channel geometry detail of the real catchment.

The flow input to the HEC-RAS model was a discharge hydrograph, predicted by *Overflow* for the model grid cell that corresponded to the upstream cross section of the reach in HEC-RAS. HEC-RAS also requires a downstream boundary condition of either a stage hydrograph or water surface slope in order to calculate the model initial conditions and water levels throughout the event. Observed stage hydrographs were only available for the downstream gauging stations. However, if an *Overflow* hydrograph was used as the downstream boundary condition at the reach outlet, it would not be very informative to compare the HEC-RAS hydrograph predicted at the reach outlet with the same *Overflow* hydrograph. Instead, water surface slopes were used as the downstream boundary condition. In HEC-RAS, these are referred to as 'normal depths' (Brunner, 2008). Specifying a water surface slope allowed HEC-RAS to calculate water depths based on the Manning equation (Equation 2.4). Slopes were approximated by averaging the gradients between successive channel cells in the DEM.

#### 6.4.2. Sensitivity analysis

First, a sensitivity analysis to Manning's  $n$  values was undertaken. This tested whether HEC-RAS responded to changes in parameter values in a way that was consistent with its constituent equations, and hence in a manner that approximated reality. The results of the sensitivity analysis allowed the model to be calibrated to observations of the June 2007 flood by optimising the parameter values. The reach upstream of Normanby was modelled in order to make a comparison of the HEC-RAS predictions to gauging station data (Figure 6.1). The predicted hydrographs were summarised using the peak discharge, time to peak, overbank flood volume and Nash Sutcliffe Efficiency (NSE), as in the sensitivity analysis of *Overflow* (Chapter 4).

The *Overflow* model and examination of aerial photographs and Ordnance Survey maps showed that an unnamed tributary joined the main River Seven within the reach, approximately 500 m upstream of the Normanby gauge. However, an *Overflow* prediction of the hydrograph at the outlet of this tributary during the June 2007 flood (Figure 6.2) showed that the tributary contributed a peak discharge of  $1.75 \text{ m}^3\text{s}^{-1}$  and a total volume of water of  $104,840 \text{ m}^3$ , in comparison to  $156.50 \text{ m}^3\text{s}^{-1}$  and  $11,105,000 \text{ m}^3$  observed in the main River Seven at Normanby. Given the scale of the event, it was concluded that this tributary contributed a negligible amount of water (0.94 % of the total volume of water measured at Normanby). This tributary was not included in the HEC-RAS model. A total of 23 cross sections were used along the 2500 m reach of the main River Seven above Normanby.

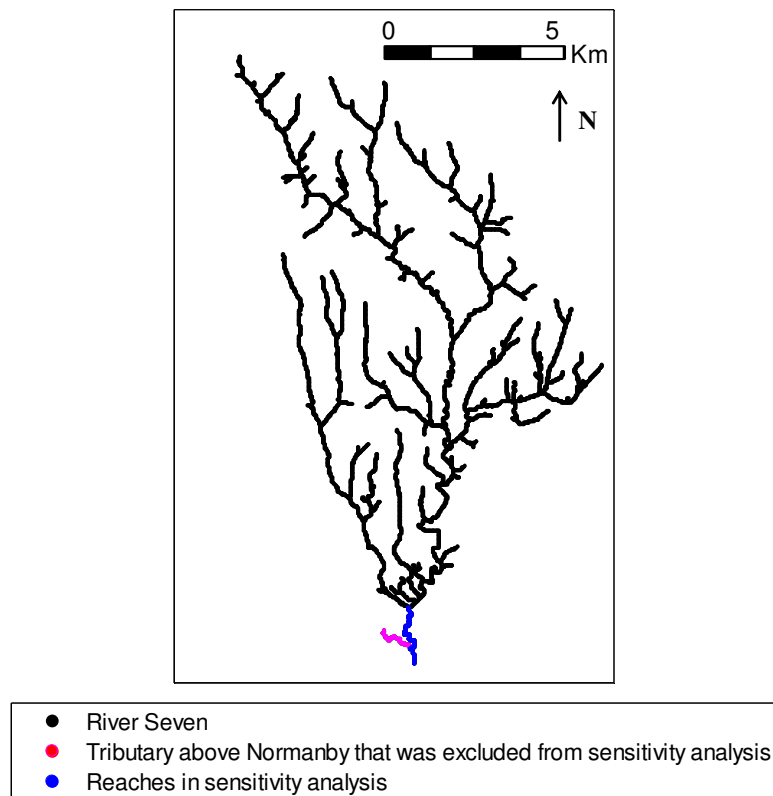


Figure 6.1 Reaches modelled in the HEC-RAS sensitivity analysis, which was used to calibrate the HEC-RAS model. The diagram also shows the tributary, which was not included in the HEC-RAS model.

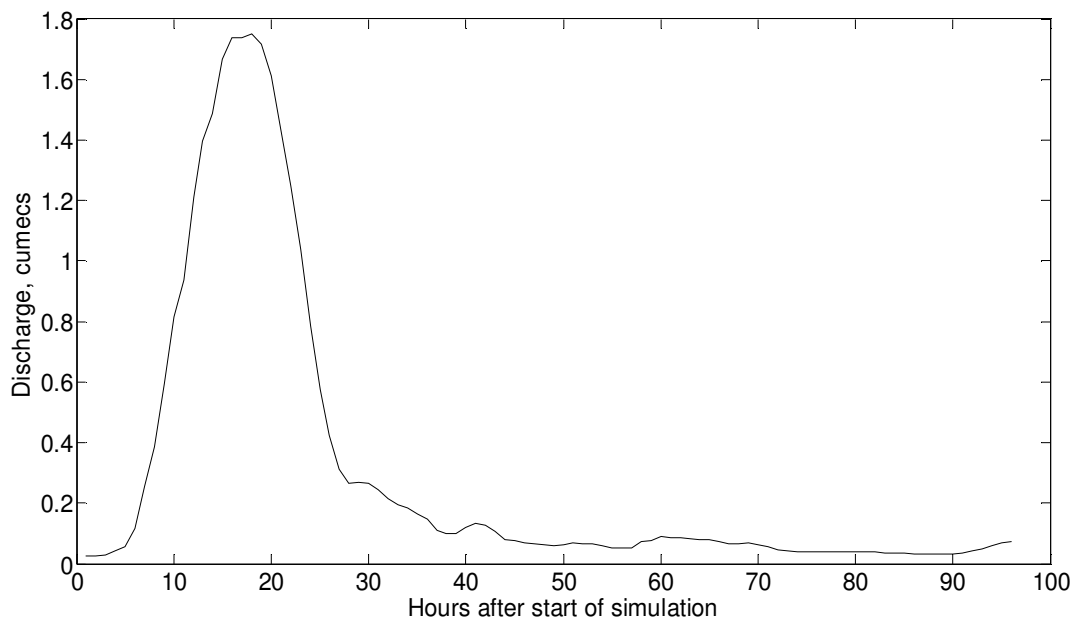


Figure 6.2 Discharge hydrograph for the tributary above Normanby, at its confluence with the main River Seven.

A systematic sample of Manning's  $n$  values was used across a theoretically realistic range that  $n$  could take. This range was 0.02 to 0.20 for each of the channel and the floodplain, as discussed in the *Overflow* sensitivity analysis (section 4.4.1) and based on Chow (1959). The range of Manning's  $n$  values is intended to encompass physically reasonable values, including values that

were considered representative of CRIMS (0.14 for the channel and 0.16 for the floodplain, which is discussed in section 6.5.2.2). The values were varied one-at-a-time at intervals of 0.02 until the model had been run for every possible combination of channel and floodplain  $n$  values within the sample. Simulations were therefore undertaken for every combination of 10 values for the channel (0.02, 0.04, 0.06, 0.08, 0.10, 0.12, 0.14, 0.16, 0.18 and 0.20) and the same 10 values for the floodplain (0.02, 0.04, 0.06, 0.08, 0.10, 0.12, 0.14, 0.16, 0.18 and 0.20). Hence 100 model runs were undertaken. Despite the risk of bias introduced in systematic sampling (Rice, 2003),  $n$  values were selected in this way to ensure full coverage of the parameter space in the minimum number of runs. A random sample, for example, requires hundreds of runs to avoid repeatedly selecting similar values from the parameter space (Odoni, 2007). Minimising the number of runs required was particularly important for HEC-RAS since the user is required to input values manually between each successive model run.

### 6.4.3. Calibration

The model calibrated to observations by selecting the parameter sets that resulted in a high level of fit between predicted and observed hydrographs, as measured by the NSE, peak discharge error and time to peak error.

Manning's  $n$  is used to represent a range of different sources of flow resistance. In different models, different sources of flow resistance may be represented explicitly by boundary conditions or process equations. Thus in different models, Manning's  $n$  may be used to account for different levels of unmeasured data (Hunter et al., 2007) and hence different physical quantities (see section 6.3.3). Additionally, *Overflow* was calibrated on the basis of rainfall and runoff rates, while  $n$  was varied to represent flow attenuation measures. Therefore,  $n$  values cannot be directly compared between different models (Horritt and Bates, 2002), so the  $n$  values used in the *Overflow* model cannot be directly transferred into HEC-RAS. HEC-RAS must therefore be calibrated separately.

HEC-RAS was calibrated on the basis of comparing discharge, rather than stage, hydrographs. This was because *Overflow* directly predicts discharge hydrographs, although water stage can be subsequently calculated using the Manning equation (Equation 2.4). In the sensitivity analysis and calibration it was therefore important to ensure that discharge hydrographs predicted by HEC-RAS responded realistically.



#### 6.4.4. Comparison with *Overflow*

##### 6.4.4.1. Model set-up

Given the amount of information required to construct a hydraulic model (section 6.3), setting up HEC-RAS with cross sections and boundary conditions for the entire catchment would be a time consuming process. To test the *Overflow* predictions, three reaches of interest were selected. These were a reach that had a clear positive impact, a reach with a slightly positive impact (of low magnitude) and a reach with a clear negative impact, measured by the reduction in downstream peak discharge when used with flow attenuation measures (Chapter 5). The characteristics of each reach are summarised in Table 6.1.

Since only a sample of reaches could be tested, the method of model comparison cannot assess the reach-scale accuracy of *Overflow* throughout the whole River Seven catchment. The model comparison is intended, therefore, to benchmark the process representation used in *Overflow* against an established flood model, HEC-RAS.

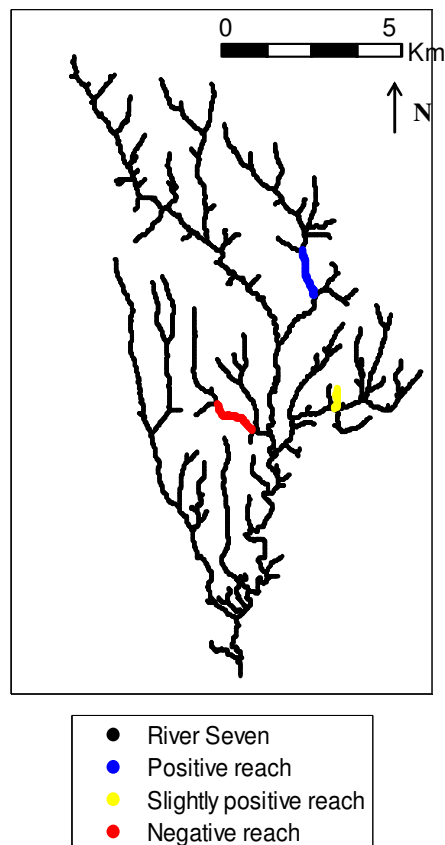


Figure 6.3 Map of the River Seven drainage network and the reaches tested in HEC-RAS.

Reach	Positive reach	Slightly positive reach	Negative reach
Reach length (m)	1480	710	1440
Average depth (m)	1.60	0.53	1.24
Average width (m)	4.87	0.47	2.55
Peak discharge upstream ( $\text{m}^3\text{s}^{-1}$ )	20.70	0.30	6.31
Water surface slope	0.02	0.05	0.02
Number of cross sections	15	7	15

**Table 6.1 Summary of characteristics of the reaches tested in HEC-RAS. Reach length was measured along the channel thalweg. Average depth and width are the mean of HEC-RAS cross sections. The peak discharge upstream was predicted by *Overflow* as the peak of the hydrograph used as the upstream boundary condition for HEC-RAS. Water surface slope downstream was calculated within *Overflow* by the Manning equation (Equation 2.4) and was the downstream boundary condition for HEC-RAS.**

The positive reach was in a narrow and steep sided valley. The river channel bed was at 127 m OD at the downstream cross section, while the valley rose to around 170 m OD within 200 metres to the north east. The reach was located in a forested area to the north east of the catchment with a contributing area predicted by *Overflow* of 720,940  $\text{m}^2$ . A CRIM in this reach, on its own, was predicted to lead to a peak discharge reduction of 0.80  $\text{m}^3\text{s}^{-1}$  at Sinnington.

The slightly positive reach was selected on the basis that it was comparatively small and contributed only a 0.02  $\text{m}^3\text{s}^{-1}$  peak discharge reduction at Sinnington. The reach was a first order stream that drained a mostly forested area of 15,520  $\text{m}^2$  to the north east of the catchment. It drained down the slope of the valley into Sutherland Beck, a tributary of the River Seven approximately 4 km above Sinnington. As it drained downslope across the valley contours, the channel had a steep gradient: bed level fell from 140 m to 120 m OD along its 710 m length.

The negative reach had a contributing area of 265,300  $\text{m}^2$  and fed into the River Seven approximately 4.5 km above Sinnington. This reach was for the most part situated within a narrow and steep sided valley, although towards its confluence with the River Seven, the valley sides were less steep, allowing the formation of a floodplain. The river channel bed level was 172 m OD at the downstream cross section of the reach. The negative reach was predicted to increase peak discharge at Sinnington by 0.56  $\text{m}^3\text{s}^{-1}$  when a CRIM was included.

Again, cross sections were taken at approximately 100 m intervals, with adjustments to cross section position made where there was a danger of cross sections overlapping.

**Key for all maps**  
 — River  
 - - Cross section  
 ■ Forest

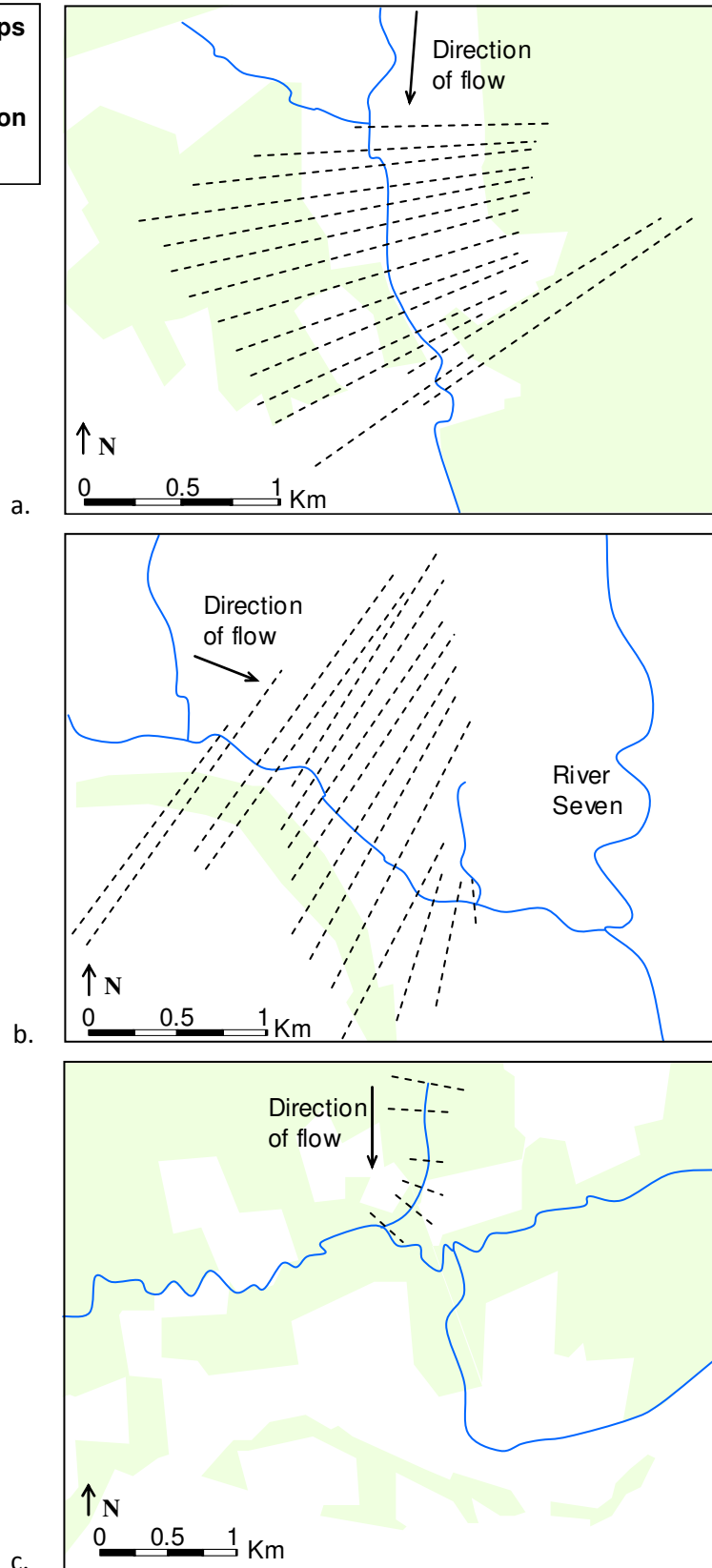


Figure 6.4 Sketch maps of the reaches and cross sections modelled in HEC-RAS for (a) positive reach, (b) slightly positive reach and (c) negative reach. Based on 1:50,000 Ordnance Survey map data.

Discharge hydrographs predicted at the outlet of each reach within the HEC-RAS and *Overflow* models could then be compared. This comparison, where hydrographs are assessed within the

model domain, is intended to provide information on *Overflow* model predictions at a point internal to the model domain where its constituent equations are being solved, rather than just at the catchment outlet.

#### 6.4.4.2. Method for comparison with *Overflow*

First, a global sensitivity analysis of the calibrated *Overflow* model to Manning's  $n$  values was undertaken. The same sample of  $n$  values was used and the same reaches above Normanby were modelled as in the HEC-RAS sensitivity analysis. This allowed confidence intervals to be calculated on the basis of comparison with gauging station data at Normanby and allowed comparison of the results with that of the HEC-RAS sensitivity analysis. The results from the HEC-RAS and *Overflow* sensitivity analyses were used to calculate confidence margins with respect to parameter selection at the 95% confidence level, using Equation 6.5 (Taylor, 1982). This allowed a comparison of the sensitivity of each model to variation in Manning's  $n$  values and the resulting uncertainty in the model response.

$$x_{best} \pm \delta x = \bar{x} \pm 1.96 \frac{\sigma_x}{\sqrt{n}}$$

**Equation 6.5 Statement of a confidence interval (Taylor, 1982; Mendenhall et al., 2009).**

In previous chapters, the model was compared to observed data on the assumption that the observed measurements are 'correct' and the modelled hydrograph is in error; the purpose of calibration, for example, is to select parameter values that minimise this error. Since hydrographs predicted by *Overflow* and HEC-RAS both have some level of error in comparison to observations, it would not be appropriate to compare one hydrograph to another, on the assumption that all errors occur in one modelled hydrograph (Van Huffel and Vandewalle, 1991).

In addition, comparing each modelled hydrograph does not necessarily identify in what respects the different levels of process representation cause differences (if any) between the modelled results. In order to better understand the effects of the different approaches to process representation, the upstream and downstream hydrographs were compared for each model, reach and intervention and used to infer the effect of different process representation.

## 6.5. Results

### 6.5.1. HEC-RAS validation and calibration

Peak discharge (Figure 6.5a) predicted by HEC-RAS at Normanby ranged from 139 to 157 m<sup>3</sup>s<sup>-1</sup>. In general, as channel and floodplain Manning's  $n$  values increased, the predicted peak discharge

decreased. Peak discharge was sensitive to values of channel  $n$  across the full range of  $n$  values. However, at low channel  $n$  values (0.02 and 0.04), the model was insensitive to floodplain  $n$ . Examining the cross section geometry and peak water levels in the HEC-RAS program showed that this was because at low channel  $n$  values, the flow did not go out of bank and interact with the floodplain, so floodplain  $n$  had no impact on the model results.

Time to peak (Figure 6.5b) ranged from 21 to 24 hours after the start of the model simulation, although as the model is run in hourly timesteps to correspond with the observed rainfall input, the results are not very detailed. The pattern of hydrograph peak times in response to variations in Manning's  $n$  was broadly similar to that of peak discharge. Faster response times occurred tended to occur at lower  $n$  values. Again, when channel  $n = 0.02$  or  $0.04$ , the model was insensitive to variations in floodplain  $n$ . Higher  $n$  values result greater energy loss and flow attenuation, causing a reduction in flow velocity, which leads to a later time to peak and a reduction in peak discharge as water is released downstream over a longer period of time.

Overbank flood volume (Figure 6.5c) was calculated from the area of the flood hydrograph that exceeded a bankfull discharge of  $72.4 \text{ m}^3\text{s}^{-1}$ , which corresponded to a bankfull depth of 3.96 m at Normanby. This is the same value as was used in the *Overflow* sensitivity analysis (section 4.3.1). Bankfull discharge was estimated in previous work for the Environment Agency, using a 1D hydraulic model at Normanby (JBA Consulting, 2008b). It should be noted that there are uncertainties in relating measured bankfull depth to a value for discharge. In this case, a model was used to generate a stage-discharge relationship to estimate bankfull discharge. The trend in flood volume in response to Manning's  $n$  was less distinct, but generally similar to peak discharge. However, higher flood volumes tended to occur when both channel and floodplain  $n$  values were high, while lower flood volumes tended to occur at low channel  $n$  values.

In summary, the sensitivity analysis found nothing to show that, in response to variation in Manning's  $n$  values, HEC-RAS did not behave in a manner that was consistent with its constituent equations and hence theoretical knowledge about physical processes. The predicted hydrographs were compared with the observed hydrograph to calculate the peak discharge percentage error (Figure 6.6a), time to peak percentage error (Figure 6.6b) and overbank flood volume percentage error (Figure 6.6c). The NSE (Figure 6.6d) was also calculated to compare each modelled hydrograph with the gauging station observations. All modelled hydrographs performed well in comparison with the observed hydrographs (all had NSE values of greater than 0.90). Peak discharge error ranged from -11.44 % to 0.62 %, time to peak error ranged from -4.54 % to 9.09 % and overbank flood volume error ranged from -29.90 % to -37.87 %. These results suggest that the model is capable of reproducing observations. Since model behaviour in response to change in parameters was theoretically reasonable, the model was applied to predict flow in other reaches.

However, Figure 6.6 shows that the results for each statistic are not distributed consistently across the parameter space. Peak discharge error was lowest at channel  $n$  values of 0.02. However, time to peak error was at its lowest for either; a low floodplain  $n$  (0.04) and any value of channel  $n$ , or; a low channel  $n$  (0.04) and any value of floodplain  $n$ . NSE is sensitive to both the magnitude and timing of the flood hydrograph. For this reason, the highest NSE values (over 0.98) occurred at high channel  $n$  and low floodplain  $n$  values. The lowest NSE values were consistent with high discharge and timing errors, at high channel and floodplain  $n$  values. However, the variation in NSE values in response to varying Manning's  $n$  was small. No NSE values were less than 0.90 (which corresponds to a very accurate prediction of the observed hydrograph). Given that NSE values were high and peak discharge error was no greater than -11.44 % (equivalent to  $17.90 \text{ m}^3\text{s}^{-1}$ ), a compromise was sought between the different objective functions in order to select Manning's  $n$  values that would optimise the model predictions to available observations.

On this basis, a channel Manning's  $n$  of 0.04 and a floodplain Manning's  $n$  of 0.06 were selected to represent the catchment. This corresponds to a channel that is generally clean, but meandering with some vegetation and a floodplain that consists of some trees and vegetation (Chow, 1959). Since the sensitivity analysis shows that it is possible to make predictions that match observations using a wide range of  $n$  values, these  $n$  values were also selected on the basis of the physical realism with which they represented the channel and floodplain (Beck and Chen, 2000). For the HEC-RAS model of the reach above Normanby during the June 2007 flood, these  $n$  values gave a predicted hydrograph with an NSE value of 0.96, peak discharge error of -0.52 %, time to peak error of 0 % and flood volume error of -31.38 %. Given the range of model responses to Manning's  $n$ , these were considered acceptable predictions of the hydrograph at the Normanby gauging station. These  $n$  values are not identical to those used in the calibrated *Overflow* model, since Manning's  $n$  takes different physical meanings in each model (section 6.3.3). However, the values also corresponded to theoretically realistic characteristics of the River Seven and its floodplain (see Chow, 1959).

Figure 6.7 shows the observed hydrograph and the HEC-RAS hydrograph for these Manning's  $n$  values. Although the rising and falling limbs of the HEC-RAS hydrograph begin slightly earlier than the gauging station measurement, HEC-RAS accurately reproduces the peak area of the hydrograph (everything above  $100 \text{ m}^3\text{s}^{-1}$ ), which is of greatest concern in the prediction of flood flows.

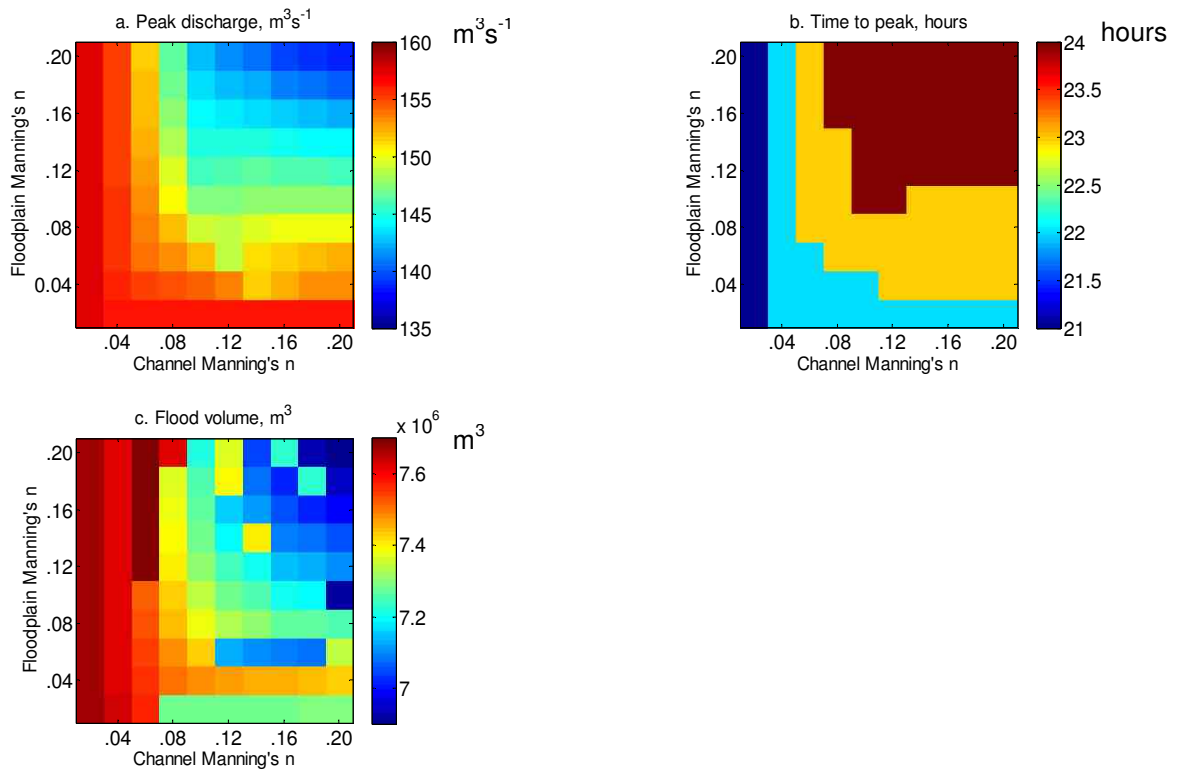


Figure 6.5 Summary statistics of HEC-RAS hydrograph sensitivity to variation in channel and floodplain Manning's  $n$ : (a) Peak discharge ( $m^3s^{-1}$ ), (b) Time to peak (hours after start of simulation) and (c) Overbank flood volume ( $m^3$ ). Values are given by the colour bar on the right of each plot.

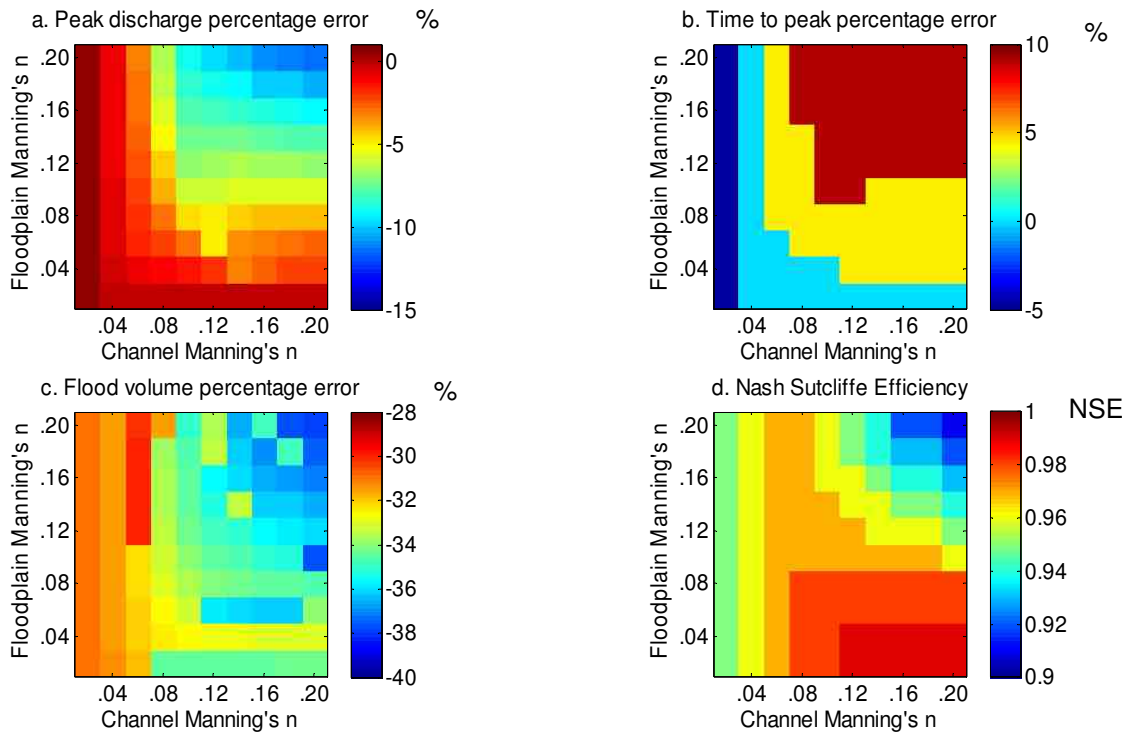


Figure 6.6 Response of hydrographs to variations in Manning's  $n$ , measured by objective functions, for the purpose of calibration: (a) Peak discharge error (%), (b) Time to peak error (%), (c) Overbank flood volume error (%) and (d) Nash Sutcliffe Efficiency (dimensionless). Values are given by the colour bar on the right of each plot. Note that in the case of (a), (b) and (c), values closer to 0 imply greater model accuracy, while in the case of (d), higher values imply better fit between observations and predictions.

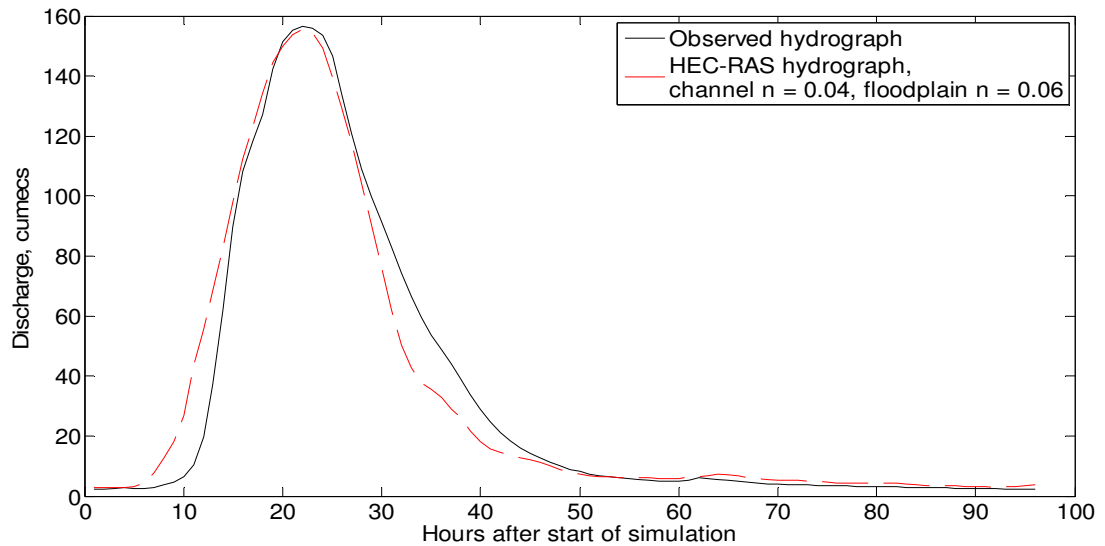


Figure 6.7 Observed hydrograph and the calibrated HEC-RAS hydrograph at the Normanby gauging station, using the optimised Manning's  $n$  values.

## 6.5.2. Comparison with *Overflow*

### 6.5.2.1. Confidence intervals

Model response	HEC-RAS confidence interval		<i>Overflow</i> confidence interval	
	Absolute	Percent	Absolute	Percent
Peak discharge	$\pm 1.07 \text{ m}^3\text{s}^{-1}$	$\pm 0.72$	$\pm 1.91 \text{ m}^3\text{s}^{-1}$	$\pm 1.83$
Time to peak	$\pm 0.19$ hours	$\pm 0.84$	$\pm 0.55$ hours	$\pm 2.32$
Overbank flood volume	$\pm 45,000 \text{ m}^3$	$\pm 0.61$	$\pm 76,000 \text{ m}^3$	$\pm 1.56$

Table 6.2 Confidence intervals around the mean of the results due to  $n$  value uncertainty (see Equation 6.5), for the hydrograph at the Normanby gauging station and using the calibrated Manning's  $n$  values for the catchment with no interventions.

The variability in the model results in response to variations in Manning's  $n$  values is given in Table 6.2 in the form of confidence intervals. The HEC-RAS results had smaller percentage confidence intervals than those of *Overflow* (Table 5.5), implying that the predictions were more precise. This suggests that over the range of Manning's  $n$  values tested, HEC-RAS was less sensitive to variations in  $n$  values than *Overflow*. This is unsurprising as the Manning equation, which is used in *Overflow* to calculate flow velocity and the effect of flow resistance, is a steady, uniform flow



approximation of the Saint Venant equations, which are used in HEC-RAS (Lane, 1998; Horritt and Bates, 2002).

### 6.5.2.2. Flow routing

Three reaches were tested in both *Overflow* and HEC-RAS with Manning's  $n$  values pertaining to; (1) the reach using the optimised  $n$  values, and; (2) flow attenuation measures (woody debris dams and riparian vegetation) in the channel and on the floodplain. The  $n$  values used for unmodified reaches with no interventions were, in *Overflow*: channel  $n = 0.35$ , floodplain  $n = 0.06$ , and in HEC-RAS: channel  $n = 0.04$ , floodplain  $n = 0.06$ . Since no observed data were available to calibrate Manning's  $n$  for flow attenuation measures,  $n$  values of 0.14 for the channel and 0.16 for the first 20 m of the floodplain immediately adjacent to the channel on each bank were selected. These values were based on previous work with Forest Research and the *Overflow* model (see section 5.2.4) (Odoni and Lane, 2010). This corresponds to channels that are heavily vegetated or contain large woody debris, and floodplains densely planted with trees (Chow, 1959).

As discussed in the description of HEC-RAS (section 6.3.3), Manning's  $n$  has a different role in the process equations of the two models. To increase  $n$  values therefore has a different physical meaning in HEC-RAS and *Overflow*. This is a limitation to the comparison of the influence of flow attenuation on each model, because it is not possible to use  $n$  values to represent the same physical processes that increase flow resistance. However, the aim of this exercise is to assess how the modelling method (*Overflow*) impacts upon the results in comparison a conceptually different model. From this perspective, it is still informative to compare the impact of increasing flow resistance in each model, in the way that is prescribed by each model's constituent equations.

In each model, the same input hydrograph was used. The model process equations route this input hydrograph through the reach of interest, to calculate a downstream hydrograph (the model output). Given the same topographic data, any difference between the input and output hydrographs can therefore be attributed to differences in model process equations. This difference can be used to quantify the effect of the flow routing equations. It is this difference between input and output hydrographs that was used to compare the process equations of the two models, *Overflow* and HEC-RAS.

The input and output hydrographs for each model run are compared in Figure 6.8 and Figure 6.9. In all cases, both HEC-RAS and *Overflow* predicted qualitatively similar hydrographs in terms of their timing and shape. However, in all model runs it was found that *Overflow* predicted an increase in peak discharge magnitude downstream, whereas HEC-RAS did not. As a result, *Overflow* predicted a higher magnitude peak discharge than HEC-RAS (Table 6.3). Given the

percentage confidence intervals (Table 6.2), this discrepancy is significant: no value of peak discharge for any given Manning's  $n$  value is compatible with both models. Therefore, the discrepancy between the two models cannot be solely to uncertainties in parameter selection.

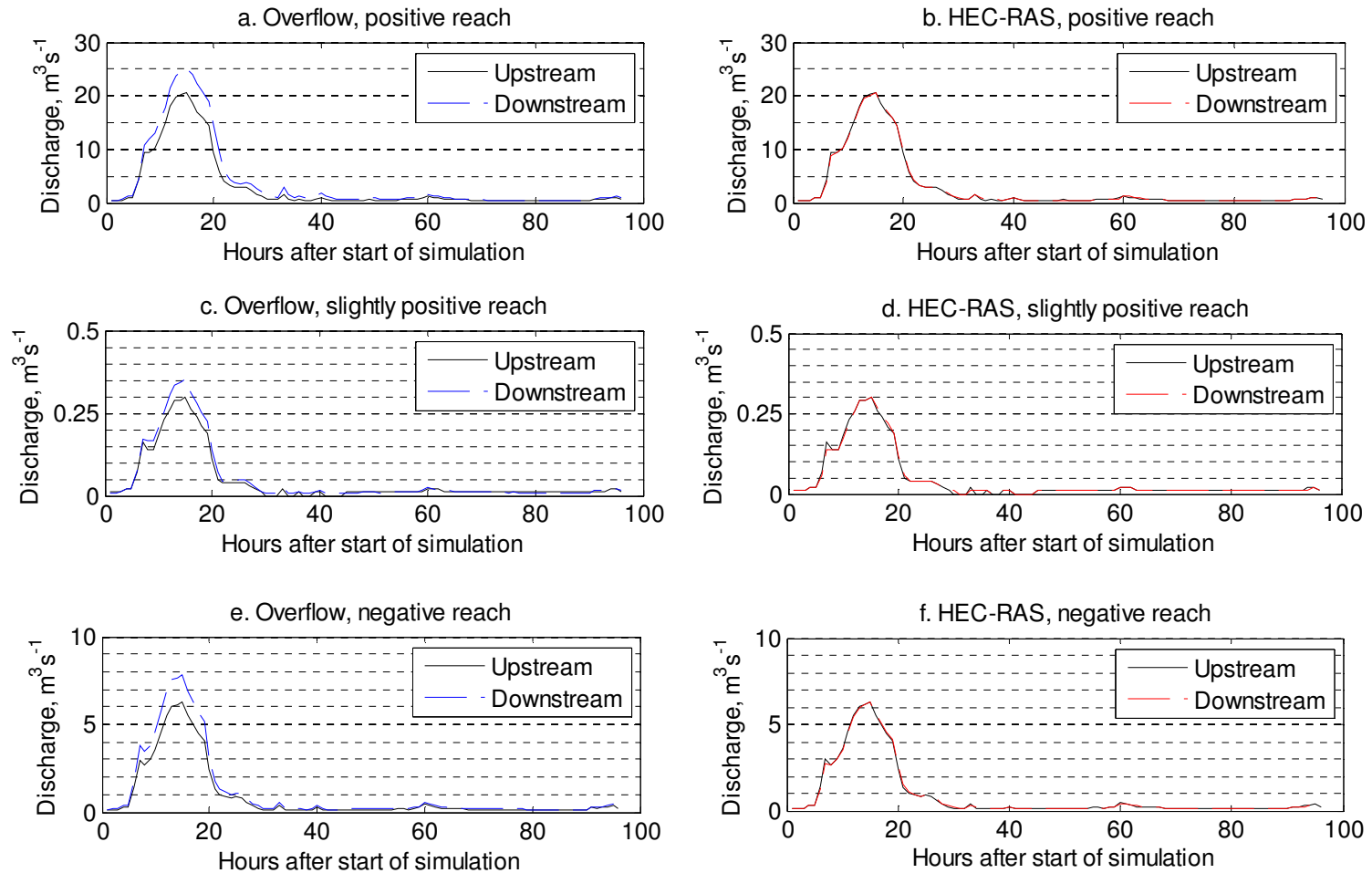


Figure 6.8 Hydrographs at the reach inlets and outlets. The upstream hydrograph was predicted by Overflow and also used as the boundary condition in HEC-RAS. The downstream hydrograph was predicted by each model using a channel Manning's  $n$  of 0.035 (Overflow) and 0.4 (HEC-RAS) and a land cover/floodplain Manning's  $n$  of 0.6 (both models).

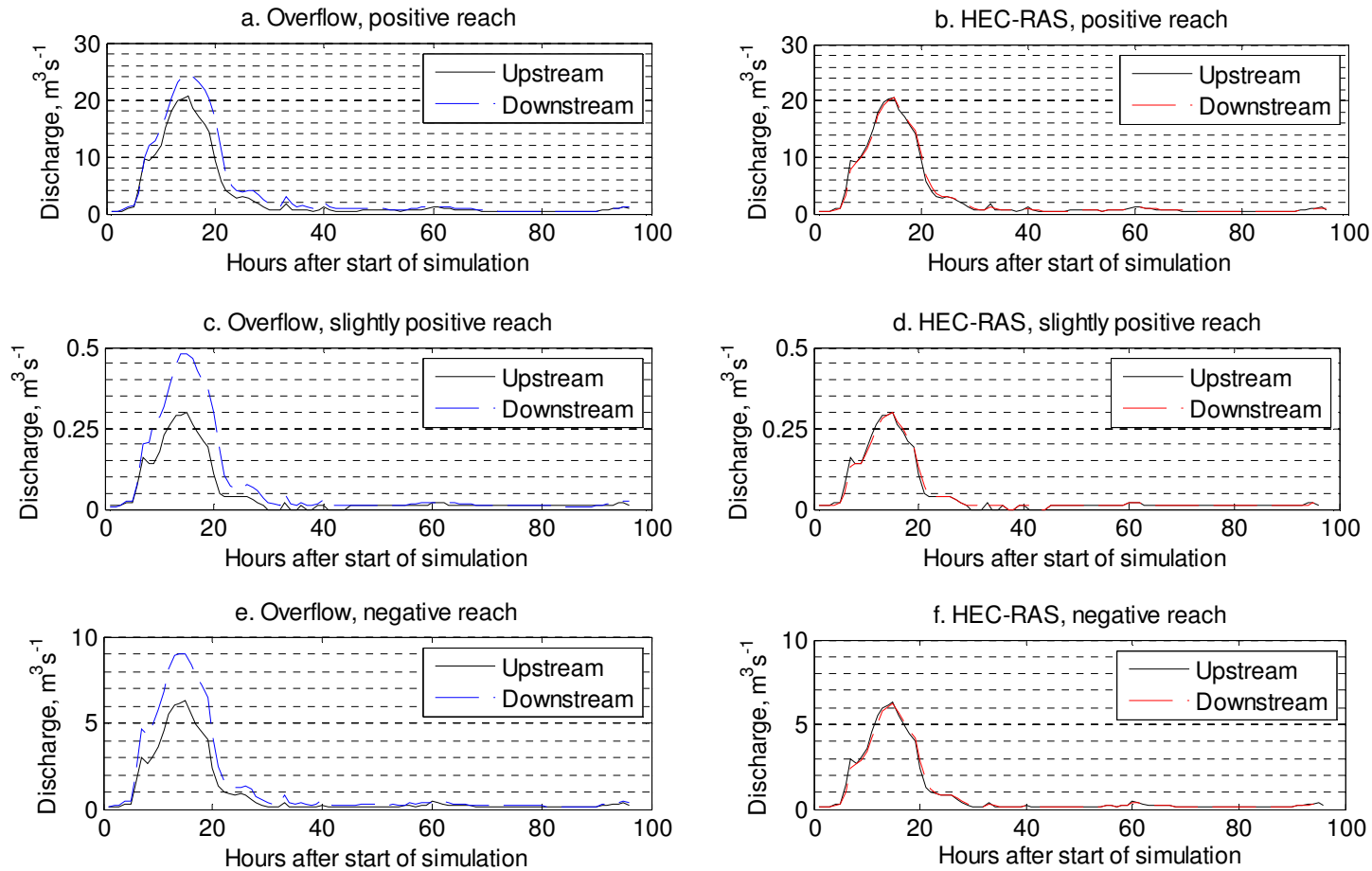


Figure 6.9 Hydrographs at the reach inlets and outlets in a situation with flow attenuation measures. The upstream hydrograph was predicted by *Overflow* and also used as the boundary condition in HEC-RAS. The downstream hydrograph was predicted by each model using a channel Manning's  $n$  of 0.14, a Manning's  $n$  of 0.16 for the first 20 m adjacent to the channel and a Manning's  $n$  of 0.6 for the rest of the floodplain.

	Positive reach		Slightly positive reach		Negative reach	
<b>No interventions</b>	4.52 m <sup>3</sup> s <sup>-1</sup>	21.96 %	0.05 m <sup>3</sup> s <sup>-1</sup>	16.67 %	1.52 m <sup>3</sup> s <sup>-1</sup>	24.36 %
<b>With interventions</b>	3.82 m <sup>3</sup> s <sup>-1</sup>	18.56 %	0.18 m <sup>3</sup> s <sup>-1</sup>	60.00 %	2.77 m <sup>3</sup> s <sup>-1</sup>	44.39 %

**Table 6.3** Difference in peak discharge between *Overflow* and HEC-RAS. The absolute difference in peak discharge was given by the *Overflow* peak discharge minus HEC-RAS peak discharge (m<sup>3</sup>s<sup>-1</sup>). The difference is also given as a percentage of the peak discharge predicted by HEC-RAS. In all cases, *Overflow* predicted a higher peak discharge than HEC-RAS.

The absolute figures for change in peak discharge are given in Table 6.4. Comparing the input and output hydrographs (Figure 6.8 and Figure 6.9) shows that the differences in peak discharge are not the result of a modification to the shape of the hydrograph. All of the downstream hydrographs peak within a very short time of the upstream input hydrographs, which is unsurprising over the relatively short reaches that were modelled. However, the downstream hydrographs predicted by *Overflow* appear to be greater in volume than the upstream input, whereas in HEC-RAS, the upstream and downstream hydrographs are similar in size.

	No intervention	With intervention
<b>Overflow positive reach</b>	4.47	3.70
<b>Overflow slight positive reach</b>	0.05	0.18
<b>Overflow negative reach</b>	1.50	2.70
<b>HEC-RAS positive reach</b>	- 0.05	- 0.12
<b>HEC-RAS slight positive reach</b>	0.00	0.00
<b>HEC-RAS negative reach</b>	- 0.02	- 0.07

**Table 6.4** Change in peak discharge downstream (m<sup>3</sup> s<sup>-1</sup>), given by the difference between the peak of the upstream and downstream hydrographs.

The discrepancy may be as a result of the different nature of the flow routing assumptions in each model. In HEC-RAS, which is a hydraulic model, the flow hydrograph at the upstream inlet of each reach is routed between successive cross sections to predict a hydrograph at the downstream outlet of the reach. In contrast, as a hydrologic model, *Overflow* routes flow overland between different model grid cells across the entire catchment surface. In the case of non-channel cells flow is routed diffusively and apportioned to each neighbouring cell according to local gradients

(see section 2.5.3.4). Therefore it is possible for water to enter the channel within the reach, from the adjacent floodplains. It is also possible for flow to arrive the furthest downstream grid cell by an overland flow route, other than the channel. As a result, the *Overflow* discharge hydrographs may account for additional overland flow, from routes other than directly upstream.

Table 6.5 shows the contributing area of the catchment at the inlet and outlet of each reach. The contributing area is the land area from which flow is routed through the reach in question. This can be found in *Overflow* using an algorithm that traces flow routing paths in reverse, which is included as a constituent part of the model (Odoni and Lane, Forthcoming).

The contributing areas at the inlet of the positive and negative reaches consisted of the area of land drained by tributaries upstream of that point, while the downstream contributing areas also included the area of land that drained into the reaches themselves. The slightly positive reach showed no increase in contributing area. This is because it is a first order reach, so there are no tributaries draining into the reach from further upstream. In each model, the upstream input hydrograph is based on the contributing area to the inlet of the reach. In *Overflow*, the downstream boundary condition is based on flow from the upstream contributing area and the additional contributing area along the reach until the downstream outlet. However, HEC-RAS routes the hydrograph from the upstream contributing area through the reach to give the downstream predicted hydrograph. HEC-RAS does not account for flow from the additional contributing area along the reach of interest.

The results in Table 6.5 demonstrate that if the upstream peak discharge (column E) is increased by the same proportion as the increase in contributing area (column D), the resulting peak discharge (column F) is broadly similar to the modelled peak discharge, predicted by *Overflow* (column G). This shows that an increase in peak discharge by the same proportion as the increase in contributing area along a reach can approximately account for the higher modelled peak discharge at the reach outlet.

However, with the available data, the contribution of the additional volume of water along the reach cannot be easily modelled in HEC-RAS in a physically meaningful way. In *Overflow*, floodplain flow is routed diffusively between cells. It is difficult to identify the volume of water that is routed overland to the reach outlet, since flow may appear in one grid cell in one timestep and reappear in an adjacent grid cell in the next timestep. However, *Overflow* currently does not allow floodplain flow to be resolved in one direction (i.e. downstream), so it was not possible to directly calculate the volume of overland flow. Although some research has attempted to combine a 2D representation of floodplain flows with a 1D hydraulic representation of the channel (e.g. Lin et al., 2006; Tayefi et al., 2007), this was not possible in the version of HEC-RAS available for use in this project. Further work may be required to isolate the relevant component of floodplain flow in *Overflow* to integrate this as a boundary condition for a hydraulic model.

A	B	C	D	E	F	G
Reach	Contributing area upstream (m <sup>2</sup> )	Contributing area downstream (m <sup>2</sup> )	Percentage increase in contributing area	Upstream peak discharge (m <sup>3</sup> s <sup>-1</sup> )	Downstream peak discharge, accounting for proportional increase in contributing area (m <sup>3</sup> s <sup>-1</sup> )	Modelled downstream peak discharge (m <sup>3</sup> s <sup>-1</sup> )
Positive	621,540	720,940	15.99	20.70	24.01	25.17
Slightly positive	15,520	15,520	0.00	0.30	0.30	0.35
Negative	194,740	265,300	36.23	6.31	8.60	7.81

**Table 6.5 Analysis of peak discharge at reach inlet and outlets in *Overflow*. Contributing area (column B and C) and modelled peak discharge (columns E and G) at the upstream and downstream boundaries of each reach are given. Column F is the downstream peak discharge increased by the same proportion as the increase in contributing area, column D (i.e. percentage increase in contributing area x upstream peak discharge).**

### 6.5.2.3. Flow attenuation

A further analysis was undertaken to examine the impact of flow attenuation interventions in each model. Given that there were discrepancies between the *Overflow* and HEC-RAS hydrographs for the same scenarios, a direct comparison between output hydrographs of the two models would contain some error relating to the different model flow routing schemes. The response of the model equations to flow attenuation interventions were again quantified by the change in peak discharge between input and output hydrographs (Table 6.6 and Figure 6.10).

The results in Table 6.6 show that for both models, the change in peak discharge was lower or more negative when Manning's  $n$  was increased. This is consistent with the results in Chapter 4 (the sensitivity analysis) and Chapter 5 (the impact of CRIMS), which showed that higher Manning's  $n$  values caused flow attenuation, which reduced downstream peak discharge magnitude.

The change in peak discharge between the upstream and downstream hydrographs was used to quantify the impact of model equations on flow hydrographs (the model response). The difference in model response with and without flow attenuation interventions was compared between the two models. However, the previous section showed that the downstream hydrographs predicted by *Overflow* and HEC-RAS differed in absolute terms. This may be due to the inclusion of diffuse, floodplain flow routing in *Overflow*. To compare the absolute values of the model hydrographs would have also included errors relating to this discrepancy, in addition to any discrepancy caused by flow attenuation. As a result, the difference in model response with and without flow attenuation interventions was calculated as a percentage of the model response. The two models were compared on this basis.

In Figure 6.10, the downstream hydrographs were used to compare the response of each model to a higher Manning's  $n$  value (a flow attenuation intervention), relative to the default Manning's  $n$  value (no intervention). Table 6.6 also shows the difference between model response with and without interventions. In absolute terms, the difference between model responses to 'a flow attenuation intervention' and 'no intervention' was greater in the case of *Overflow* than HEC-RAS. However, when standardised as a percentage of the model response to no interventions, HEC-RAS showed greater sensitivity to the inclusion of flow attenuation interventions than *Overflow*. The exception was in the slightly positive reach, where HEC-RAS did not predict any change in peak discharge in response to flow attenuation interventions, and *Overflow* detected only a small change, of  $0.13 \text{ m}^3\text{s}^{-1}$ . This suggests that *Overflow* will underpredict the impact of flow attenuation measures.



	Change in peak discharge downstream ( $\text{m}^3\text{s}^{-1}$ )		Difference between change in peak discharge	
	No intervention	With intervention	Absolute ( $\text{m}^3\text{s}^{-1}$ )	Percent
<b>Overflow positive reach</b>	4.47	3.70	- 0.77	- 17.23
<b>Overflow slight positive reach</b>	0.05	0.18	0.13	260.00
<b>Overflow negative reach</b>	1.50	2.70	1.20	80.00
<b>HEC-RAS positive reach</b>	- 0.05	- 0.12	- 0.07	140.00
<b>HEC-RAS slight positive reach</b>	0.00	0.00	0.00	0.00
<b>HEC-RAS negative reach</b>	- 0.02	- 0.07	- 0.05	250.00

Table 6.6 Differences in model response between *Overflow* and HEC-RAS, where model response is the change in peak discharge downstream. As in Table 6.4, the change in peak discharge ( $\text{m}^3\text{s}^{-1}$ ) is used as a measure of the impact of the flow routing equations on the input hydrograph, to predict the downstream output hydrograph. In this table, the difference between these measures is also given in absolute terms, and as a percentage of the case with no interventions.

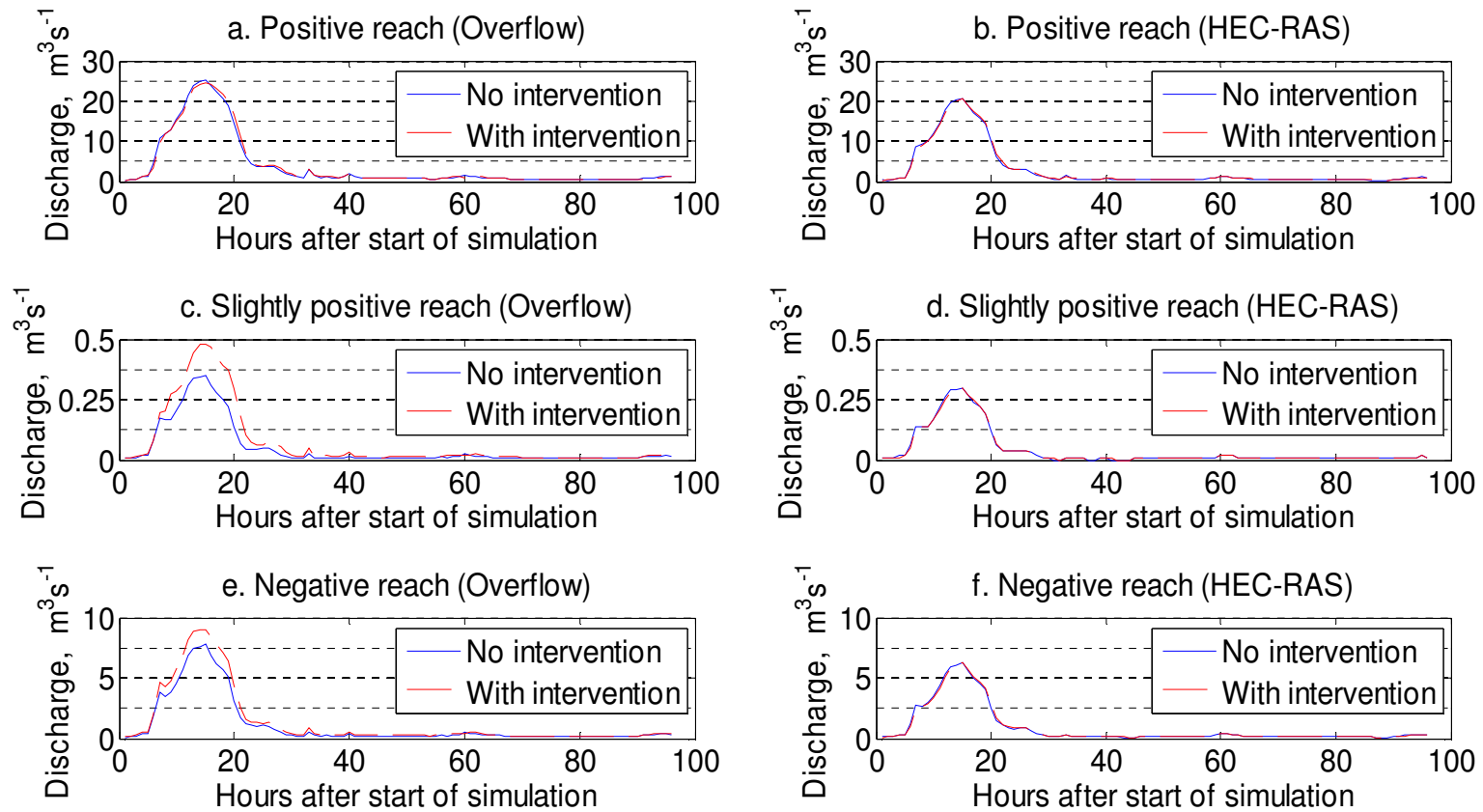


Figure 6.10 Downstream hydrographs predicted by each model, for each reach in the case of a flow attenuation intervention (higher Manning's n value).

## 6.6. Discussion

For the three reaches tested, *Overflow* compares favourably with HEC-RAS in its ability to predict the timing and general shape of the flood hydrograph. However, there are some discrepancies in predicting the magnitude of the hydrograph. In one reach, which had the greatest discrepancy, *Overflow* predicted a  $4.47 \text{ m}^3\text{s}^{-1}$  increase in peak discharge through the reach, whereas HEC-RAS predicted a  $0.05 \text{ m}^3\text{s}^{-1}$  decrease. The reason for this may relate to the different assumptions made in each model regarding flow routing. In the hydrological model, *Overflow*, water can be routed diffusively across the land surface whereas in the hydraulic model, HEC-RAS, flow is routed along the river channel in one-dimension only. It is possible to combine HEC-RAS with 2D models of floodplain flow, where the 1D HEC-RAS model is used to provide boundary conditions to the 2D model (Lin et al., 2006; Tayefi et al., 2007). However, diffuse floodplain flow routing in *Overflow* means that water can be routed between adjacent cells of the cross section used to specify the upstream boundary condition of the 1D model. In the current version of *Overflow*, challenges remain in isolating the downstream dimension of flow.

The models also showed different responses to increasing Manning's  $n$  to represent CRIMS. For two out of the three sample reaches, as a proportion of the change in peak discharge between upstream and downstream hydrographs, *Overflow* was less sensitive to an increase in  $n$  (Table 6.6). One area of uncertainty is therefore the extent to which 'roughness' (large woody debris dams and riparian vegetation) affects flow behaviour and the accuracy with which this can be represented by Manning's  $n$  (Lane, 2005).

The calculated confidence intervals showed that the HEC-RAS predictions were more precise than those of *Overflow*. Peak discharge was predicted with a confidence of  $\pm 0.72 \text{ m}^3\text{s}^{-1}$  in HEC-RAS, in comparison to  $\pm 1.83 \text{ m}^3\text{s}^{-1}$  in *Overflow*. In practical terms, HEC-RAS was much more time consuming to set up since cross sectional data and boundary conditions, once extracted from *Overflow*, had to be entered manually. The amount of cross sectional data required and the complexity of building a hydraulic model would require a prohibitive amount of time to set up for a large scale study, limiting its use at the scale of an entire catchment or its transferability to different catchments (Brooks and Tobias, 1996). However, once HEC-RAS had been set up for a river reach, it was able to perform simulations much more rapidly; HEC-RAS required around three seconds to perform each simulation, whereas *Overflow* required approximately fifteen minutes to recalculate flow velocities across each grid cell when new Manning's  $n$  values were applied.

The key limitation of this experiment is that both models are simplifications of reality. The analysis therefore does not offer a means of validating either model with respect to reality. Because the

models are conceptually different from each other, direct comparison of the magnitude of the results is uncertain. In particular, overland flow routing in *Overflow* caused an increase in hydrograph magnitude that could not be represented in HEC-RAS in a physically meaningful manner. However, HEC-RAS is an established model, which is widely used in flood studies (Tayefi et al., 2007) and has been used specifically to predict flood flows in response to large woody debris (Thomas and Nisbet, 2007). Corroboration of results between each model is informative in that both predict respond to increases in Manning's  $n$  in the same way (flow attenuation).

## 6.7. Conclusion

In previous chapters, *Overflow* was used to predict the impact of flow attenuation measures on downstream flood flows at the catchment scale, both in response to catchment-wide variations in parameter values (Chapter 4) and spatially distributed flow attenuation interventions (Chapter 5). In chapters 4 and 5, the model was evaluated based on external measures (Bates and Anderson, 2001).

Based on a sample of reaches, this chapter examined flow hydrographs at a scale that is internal to *Overflow* by comparison with a hydraulic model, HEC-RAS. The results showed the two models are capable of predicting flow hydrographs that are consistent in timing and shape. However, there was some discrepancy between *Overflow* and HEC-RAS in the magnitude of the flood hydrographs (up to  $4.52 \text{ m}^3\text{s}^{-1}$  or 60% depending on the reach tested). This discrepancy may be due to the difficulty of accounting for diffuse floodplain flow routing in HEC-RAS. Future work might focus on incorporating diffuse floodplain flow routing in *Overflow* as a boundary condition for 1D or 2D hydraulic models.

The models were compared on the basis of the change between an upstream (boundary condition) hydrograph and a downstream (predicted) hydrograph. In two out of the three reaches tested, this change was proportionally less sensitive to increases in Manning's  $n$  in *Overflow* than HEC-RAS. This suggests that *Overflow* may underpredict the impact of flow attenuation. However, the different conceptual basis for each model means that Manning's  $n$  has a different physical meaning in each. Further work might also assess the use of Manning's  $n$  itself to simulate the effects of flow attenuation caused by CRIMS. In the next and final chapter, the implications of these results will be drawn together with reference to the research objectives.

## 7. Summary and conclusions

The first chapter of this thesis argued that the pressures of climate change and floodplain development are causing flood risk in the UK to increase (Thorne et al., 2006). The need to plan flood management at the scale of entire river catchments has driven the development of reduced complexity models that are capable of simulating a wide range of intervention options (Chapter 2). Chapter 3 introduced the River Seven, North Yorkshire as a flood prone area, which is in need of strategies to mitigate flooding over large spatial scales but at low cost.

This project has used a reduced complexity hydrologic model, *Overflow*. In an assessment of the model accuracy and parameter sensitivity, the model was compared to observed measurements of the June 2007 flood event. The model was shown to replicate the observed behaviour of the River Seven catchment in a theoretically realistic manner (Chapter 4). *Overflow* was then used to predict the impact of flow attenuation measures, based on their reduction of the magnitude of downstream flood flows (Chapter 5). As a final test of *Overflow's* constituent equations, an internal evaluation (Bates and Anderson, 2001) of the model was undertaken (Chapter 6). This corroborated predictions from *Overflow* with those of a hydraulic model, HEC-RAS, at the scale of individual river reaches. This was intended to inform as to how simplifications introduced into *Overflow* compared to an established flood model. The comparison found that the model qualitatively replicated the timing and shape of the flood hydrograph, although there were some discrepancies in the peak discharge magnitude and volume of the hydrograph. This may have resulted from the inclusion of floodplain flows in *Overflow* but not HEC-RAS.

This concluding chapter draws together the results presented in this thesis, in answer to the research objectives of this project:

- (1) Quantify the impact of flow attenuation measures in isolation.
- (2) Understand the combined effects of multiple interventions.
- (3) Assess the uncertainty in the results resulting from the selection of parameter values to represent flow attenuation measures (CRIMS).
- (4) Assess the accuracy of the model representation of physical processes in relation to observed data, theoretical understanding of catchment processes and a different model conceptualisation, HEC-RAS.

This chapter summarises the research presented in this thesis and then draws conclusions to each of the research objectives in turn, before evaluating the implications of the specific methods used in the project. A final conclusion summarises the results and arguments presented in this thesis.

## 7.1. Thesis summary

Chapter 1 argued that flood risk is likely to increase as a result of future climate change (Arnell, 1998) and the ongoing development of river floodplains for homes and businesses (Pitt, 2008). These pressures have led to consideration of a wide range of strategies for flood risk management. In particular, Defra's *Making Space for Water* policy has placed an emphasis on floodwater attenuation and storage (Defra, 2004). If the volume of water is to be conserved (Equation 1.1), slowing the flow must lead to a local increase in flow width or depth. However, if flood water is retained for longer in upstream locations and is released downstream over a longer period of time, the peak magnitude of downstream flood flows will be reduced (Shaw, 1994).

Chapter 2 argues that testing the effect of flow attenuation on catchment-scale flood flows requires process-based numerical models. However, empirical data is not available at the density required to specify spatially distributed flow behaviour and flow attenuation measures. Some simplifications in process representation are also needed to reduce computation times, in order to test multiple combinations of interventions. The research objectives therefore require fast, catchment scale simulations based on spatially sparse empirical data. As a result, a reduced complexity hydrologic model, *Overflow*, was used in this project.

Chapter 3 justified the use of the River Seven and June 2007 flood as the test scenario for this project. The presence of rain and flow gauges, alongside previous research in the area by the Rural Economy and Land Use Programme (Ryedale Flood Research Group, 2008) has generated a large amount of data that was suitable for use in this project.

The Environment Agency's Catchment Flood Management Plan for the River Derwent, Yorkshire, refers to,

“Allowing the river to reconnect with the floodplain to slow the passage of water out of the area,”

(Environment Agency, 2010a: 12).

The River Seven, which is a tributary of the Derwent, is well suited to slowing or attenuating flood flows. It is a rural area, so the dispersed nature of settlements precludes hard engineering as a solution to flooding due to its high economic cost and detrimental effects downstream (Fleming, 2002). However, the catchment is characterised by a rapid response to rainfall events, so flow attenuation has the potential to disrupt the passage of flood flows. Large areas of the catchment, which are owned by the Forestry Commission, also offer the potential for temporary flood water storage (Broadmeadow and Nisbet, 2009).

The project is summarised in relation to the research objectives, defined in Chapter 1.

- (1) Quantify the impact of flow attenuation measures in isolation.

- (2) Understand the combined effects of multiple interventions.
- (3) Assess the uncertainty in the results resulting from the selection of parameter values to represent flow attenuation measures (CRIMS).
- (4) Assess the accuracy of the model representation of physical processes in relation to observed data, theoretical understanding of catchment processes and a different model conceptualisation, HEC-RAS.

### 7.1.1. Quantify the impact of flow attenuation measures in isolation

Chapter 4 evaluated the model sensitivity to parameter values. The model response was theoretically consistent with its constituent equations, which implied that the model was capable of representing (albeit a simplification of) physical processes. Of particular interest was the parameter Manning's  $n$ . Manning's  $n$  represents resistance to flow in the form of channel irregularities or obstructions (Cowan, 1956) and is related to flow velocity by the Manning equation – as  $n$  increases, velocity decreases (Manning, 1891). As  $n$  increased, the time-to-peak of the downstream hydrograph increased, which indicated slower flow velocities and flow attenuation. As a result, the volume of water was distributed over a longer period of time, so peak discharge decreased. Over a range of representative Manning's  $n$  values, peak discharge decreased from  $144.37 \text{ m}^3\text{s}^{-1}$  to  $123.49 \text{ m}^3\text{s}^{-1}$  in response to channel  $n$  and from  $179.38 \text{ m}^3\text{s}^{-1}$  to  $157.53 \text{ m}^3\text{s}^{-1}$  in response to land cover  $n$ . Although the magnitude of these reductions are uncertain, they demonstrate that increasing flow resistance resulted in flow attenuation, and that flow attenuation was associated with reductions in the magnitude of flood flows downstream.

In Chapter 5, Manning's  $n$  was used to represent reach-scale Catchment Riparian Intervention Measures (CRIMS). *Overflow* was used to predict their individual impact of a CRIM in each reach of the catchment on the downstream hydrograph. Reaches were classified into 'positive', 'neutral' or 'negative' based on their impact on downstream peak discharge. A number of reaches, mainly in the middle to lower catchment, were found to increase peak discharge. Those reaches that had a positive impact by reducing peak discharge tended to be located in the headwaters of the catchment. Thus the impact of flow attenuation measures in isolation was affected by their location in the catchment. There may be a number of physical reasons for this behaviour. By disrupting the timing of flood contributions from different tributaries, 'negative' CRIMS may cause flood hydrographs to arrive coincidentally in the main river (Lane et al., 2007b). 'Positive' CRIMS may tend to be located in the catchment headwaters where there is a greater potential to attenuate and desynchronise the timing of flow contributions to the drainage network (Odoni and Lane, 2010).

Interventions solely in the channel (LWD dams) had a greater impact than interventions that were solely overbank (riparian buffer strips). This is because flow is more likely to interact with in-

channel interventions. Flow will only be affected by overbank interventions in the locations where flow goes out-of-bank. However, a combination of channel and overbank interventions was found to have an even greater impact on downstream flood flows. In this situation, slower flow velocities within the channel led to a local increase in water depth. This increased the probability of flows exceeding the depth of the channel and interacting with overbank interventions, where further attenuation took place.

Individually however, the magnitude of the impact of CRIMS on downstream flood flows was small. Given the uncertainties in the model (section 7.1.3) it was not possible to state with any confidence the precise magnitude of the impact of a single intervention. It seems unlikely that any one intervention would make a significant contribution to peak discharge reduction downstream. For these reasons, multiple interventions were tested in combination.

### 7.1.2. Understand the combined effects of multiple, spatially distributed interventions

Testing CRIMS individually allowed those with a negative impact on downstream peak discharge to be excluded. Chapter 5 then assessed the impact of multiple, 'positive' CRIMS in various combinations of reaches. Multiple interventions caused a greater reduction in downstream peak discharge than individual interventions. With interventions in all positive reaches, *Overflow* predicted a reduction in peak discharge at Sinnington of  $6.8 \text{ m}^3\text{s}^{-1}$  (5.3 %) during the June 2007 flood event.

However, it was again found that some locations had a more beneficial impact than others: the best 20 reaches resulted in a reduction of  $4.29 \text{ m}^3\text{s}^{-1}$  (3.35 %), which was the majority of the total reduction achieved. However, some reaches that were positive in isolation became negative when used in combination with other reaches. It is possible that if flow was attenuated such that the arrival of floodwater from different tributaries became synchronised, this might contribute to an increase in the magnitude of the flood hydrograph downstream (Lane et al., 2007b). An important conclusion is that downstream flood flows are not only affected by the number of CRIMS, but also their location.

The results suggest that a combination of CRIMS may be capable of attenuating flood water to reduce downstream peak flood flows. However, the reason for using a numerical model in this investigation was that, in the 'real world', it is not practical to make observations of many different CRIM combinations during comparable flood events. If observations of CRIM impacts do not exist, then the model predictions cannot be 'proved'. In particular, Manning's  $n$  was used to represent the CRIMS, but since this is a dimensionless parameter, it is difficult to relate changes in Manning's  $n$  to empirical observations. As a result, this study and a number of others (e.g. Odoni



and Lane, 2010; Ryedale Flood Research Group, 2008; Thomas and Nisbet, 2007) have recognised that the conclusions drawn about the impact of CRIMS are subject to uncertainty. Hence, a large part of this thesis aimed to assess the uncertainty associated with *Overflow* model predictions.

### **7.1.3. Assess the uncertainty in the results resulting from the selection of parameter values to represent flow attenuation measures (CRIMS).**

An uncertainty analysis on the Manning's  $n$  values used to represent flow attenuation measures was also undertaken in Chapter 5. Manning's  $n$  values were varied within a physically reasonable range and the model response was recorded.

Variation in  $n$  values caused variations in peak discharge of up to  $\pm 0.10 \text{ m}^3\text{s}^{-1}$ . Combined with the uncertainty in the selection of rainfall rate and runoff rate parameter values, this caused a variation in peak discharge of  $0.31 \text{ m}^3\text{s}^{-1}$ . This was of similar magnitude to the impact of individual CRIMS (these gave, at most, a  $0.92 \text{ m}^3\text{s}^{-1}$  reduction in peak discharge). Individual CRIM impacts were not significantly greater than that caused by uncertainty in the selection of parameter values to represent CRIMS. Thus it could not be shown that an individual CRIM impact was significant. However, when multiple CRIMS were tested, the impact on downstream flood flows was of greater magnitude than parameter uncertainty (up to a  $6.80 \text{ m}^3\text{s}^{-1}$  reduction in peak discharge). It can be inferred that when the effects of interventions were accumulated throughout the catchment, *Overflow* was capable of discerning their effects from parameter uncertainty.

### **7.1.4. Assess *Overflow's* representation of physical processes in relation to observed data, theoretical understanding of catchment processes and a different model conceptualisation, HEC-RAS.**

In the local sensitivity analysis (section 4.4), all the parameters were subject to catchment-wide variations across a representative range of values. The analysis found nothing to suggest that the model behaviour was theoretically unrealistic in response. The model response to each parameter was consistent with the model's constituent equations, which were in turn approximations of physical processes operating in the catchment. Increases in the rainfall rate parameter, which increased the flow velocity across each model grid cell, led to a reduced time to peak and higher peak discharges. Increases to runoff rate, which increased the effective volume of water entering the model, also generated predictions of higher peak discharges. Increases to Manning's  $n$ , which represented flow resistance, caused increases in time to peak, implying reductions in flow velocity. Reductions in peak discharge also resulted, because in response to lower flow velocities, discharge was distributed over a longer period of time.

A global sensitivity analysis found that rainfall rate and runoff rate were the parameters to which the model was most sensitive, and which demonstrated the least equifinality. Using these parameters, the model was calibrated to observations by a process of optimising parameter values to match the modelled to observed hydrograph. This gave 200 parameter sets with Nash Sutcliffe Efficiency values of greater than 0.98. For each subsequent model simulation, these 200 parameter sets were used to predict 200 flood hydrographs and the mean of these hydrographs was taken as the final result.

After calibration, *Overflow* was therefore capable of accurately reproducing gauging station observations of the June 2007 flood event. The sensitivity analysis also showed that the model responded to changes in parameters in a way that was theoretically consistent with its constituent equations and hence an approximation to physical processes. This provided a baseline case against which the impact of CRIMS could be predicted. However, the analysis did not allow the magnitude of the model response to be evaluated. There was no empirical data available to do so, since the experiment required catchment scale variations in parameter values. Consequently, in Chapter 6 the impact of *Overflow's* simplifications to physical processes were assessed by comparison to a hydraulic model, HEC-RAS. Whereas previous chapters had assessed *Overflow* in terms of bulk flow measures at the catchment scale, Chapter 6 undertook an internal assessment of the model domain. This assessed the behaviour of *Overflow's* constituent equations at the reach scale.

*Overflow* was found to predict higher magnitude flood hydrographs than HEC-RAS. In the calibrated models without CRIMS, the discrepancy was up to 24.36 %. An uncertainty analysis of each model showed that the discrepancies were significant, that is, the difference in results between each model could not have been solely due to parameter uncertainty (Taylor, 1982). The difference between the two models was partly explained through the assumptions made by the different flow routing equations. HEC-RAS routes flow in one dimension, from one reach cross section to the next. *Overflow*, however, allows flow to be routed diffusively between adjacent grid cells, so water can enter the channel from the adjacent floodplains or can arrive at the reach outlet by a different route entirely.

Additionally, the different models responded in an increase in Manning's  $n$  (representing a flow attenuation measure) by different magnitudes. In each model, the change between the upstream and downstream hydrograph was used to quantify the impact of the model equations. In *Overflow*, there change between upstream and downstream hydrographs differed by up to  $1.20\text{m}^3\text{s}^{-1}$  when Manning's  $n$  was increased. HEC-RAS, at most, showed a difference of  $0.07\text{m}^3\text{s}^{-1}$ . Manning's  $n$  is incorporated into the constituent equations of *Overflow* and HEC-RAS in different ways, so  $n$  has a different physical meaning in each model. In *Overflow*,  $n$  is directly related to velocity by the Manning equation and therefore represents resistance to flow from all sources,

such as unmeasured topographic details (Lane, 2005). In HEC-RAS,  $n$  represents energy loss due to information that is not explicitly included in the one dimensional representation of the channel; for example, two dimensional variations in channel planform (Horritt and Bates, 2002). This raises uncertainties in the selection of  $n$  values to represent flow attenuation measures, which is discussed further in Project Limitations (section 7.2).

In terms of the shape and timing of the flood hydrograph at the scale of individual reaches, *Overflow* compared favourably to HEC-RAS. Discrepancies in the magnitude of the hydrographs may be a result of additional flow routing on the floodplain in *Overflow*. However, in two out of the three reaches tested, *Overflow* was shown to be less sensitive than HEC-RAS to an increase in Manning's  $n$  values. This suggests that, if anything, *Overflow* may under-predict the impact of CRIMS. The difference in how each model responded to changes in  $n$  raises uncertainty over whether the use of Manning's  $n$  to represent CRIMS is an accurate representation of the physical processes involved. This is discussed in the next section.

## 7.2. Project limitations

Other than the general uncertainties related to numerical modelling, which were outlined in Chapter 3, two limitations specific to this project are discussed. The first is the use of Manning's  $n$  to represent flow attenuation measures. The second relates to the wider applicability of the results.

### 7.2.1. Manning's $n$ and flow attenuation

The flood management measures considered in this project make use of flow attenuation to reduce the magnitude of downstream flood flows. Large woody debris dams and vegetation were selected as potential measures by which to achieve flow attenuation because they occur naturally in river channels, so they can be reinstated at low economic and environmental cost (Thomas and Nisbet, 2007). Woody debris and vegetation slow flow by generating form drag or obstructing flow entirely, with consequent energy losses (Lane and Thorne, 2007). Computing resources and process understanding allow the impact of such measures to be directly calculated (Yu and Lane, 2006a; Yu and Lane, 2006b). However, the high resolution topographic data and multidimensional dimensional models required to do so are unavailable for many catchments (Marks and Bates, 2000). As a result, most models used for flood prediction or management use the parameter, Manning's  $n$ , to represent resistance to flow (Ferguson, 2007).

Since Manning's  $n$  is used to account for unmeasured topographic data,  $n$  values are frequently not directly estimated, but are used as a means of calibrating model predictions to observations

(Lane, 2005). For example, in this project,  $n$  values for the HEC-RAS model were selected on the basis of their ability to accurately reproduce an observed flood hydrograph (Chapter 6). However, for the purposes of this research, flow attenuation measures were represented in both the *Overflow* and HEC-RAS models using high Manning's  $n$  values. In calibrating the models, efforts were made to select  $n$  values that realistically represented the river channel and catchment land surface, based on previous research in the area (Odoni and Lane, 2010) and widely used qualitative descriptions (Chow, 1959; Evans et al., 2001).

The selection of precise  $n$  values to represent flow attenuation generates variability in model results. These uncertainties are insignificant in comparison to the magnitude of peak discharge reduction achieved (Chapter 5), provided that  $n$  is a realistic representation of flow attenuation measures. This is frequently assumed to be the case in flood modelling studies (Evans et al., 2001), as in this project. However, as shown by the comparison of *Overflow* results to HEC-RAS (Chapter 6), Manning's  $n$  does not necessarily have the same physical meaning in different numerical schemes (Horritt and Bates, 2002). Different models may therefore respond in different ways to increased flow resistance, which raises uncertainties over which model most accurately represents flow behaviour in the real catchment. One area that warrants further work is the extent to which intervention measures designed to increase flow resistance can be accurately represented using a Manning's  $n$  value, or otherwise incorporated into the constituent equations of *Overflow*. For a model that is used as a predictive tool, there are often situations for which there are no observed data to check the validity of the model results (Lane and Richards, 2001). It is important to ensure that the results are based on process understanding, rather than inappropriately extrapolated statistical relationships (Lane, 2003b), to accurately quantify the effect of particular flow attenuation interventions.

### 7.2.2. Wider applicability of the results

The optimum location of interventions in catchment headwaters reinforces that of other studies (Odoni and Lane, 2010) and there is a physical argument that this should to be the case. The model is process based, so given further work (e.g. relating optimum locations for flow attenuation to channel geometry), it might be possible to extend the results into a general process-based relationship (Lane and Bates, 2000). However, this project has specifically looked at the case of the River Seven catchment during the June 2007 flood event. The results cannot necessarily be applied to other catchments, where other processes may operate affecting, for example, the timing of flood waves from different tributaries. Nor can the results necessarily be expected to hold true for all flood events, each of which will be caused by a unique combination of antecedent conditions, rainfall intensity and duration, or storm travel direction (Jackson et al., 2008). For example, Odoni and Lane (2010) found that the impact of flow attenuation measures

varied with the magnitude of the flood event, because higher magnitude floods were more likely to interact with the full range of flow attenuation interventions. However, by using the June 2007 flood, which was an event of extreme magnitude (Pitt, 2008), this project demonstrates how flow attenuation can be expected to perform in extreme conditions.

In comparison to more computationally intensive models such as HEC-RAS, *Overflow* is easy to set up and requires limited input data. As such, it can be easily transferred to other catchments and events, provided that elevation, rain gauge and flow gauge data are available. In ungauged catchments, rain and river flow data can be estimated by some other means, such as the Flood Estimation Handbook (Robson and Reed, 1999). These boundary conditions make the model representative of a particular catchment and event. Given this information, the sensitivity analysis in Chapter 4 showed that the model's process equations can be expected to behave in a theoretically realistic manner and, with calibration, give reasonably accurate results. *Overflow* is therefore a viable method that can be applied to other catchments and events, even if the specific results of this project cannot be more widely generalised. *Overflow* also has fast run times, allowing multiple scenario testing, such as testing the many possible locations for flow attenuation. It is therefore also suited to catchment scale approaches to flood risk management. This allows the downstream impacts of flood mitigation strategies to be considered, allowing strategies to be designed to benefit large areas.

### 7.3. Overall conclusions

Flood risk in the UK is subject to pressure from urban development of floodplains, which increases the number of people and properties exposed to flooding (Fleming, 2002), and climate change, which is likely to increase the magnitude and frequency of floods (Arnell, 1998). Flood management must therefore consider measures that benefit large areas of land, while minimising detrimental impacts downstream. Public concern (Ryedale Flood Research Group, 2008) and legislation such as the EU Water Framework Directive also requires flood risk management to be compatible with other uses of river and floodplain environments, such as ecology (Lane et al., 2007b).

The UK government's policy for flood risk management now focuses on 'Making Space for Water' (Defra, 2004). In practice, this involves allowing rivers to reconnect to their floodplains, where water is temporarily stored during a flood event. To achieve this often requires measures that slow, or attenuate, flow. Although the volume of water transferred through the river network is the same, if that volume is distributed over a longer period of time, then the peak magnitude of downstream flood flows will be lower.

This project has shown that flow attenuation in the River Seven catchment can contribute to reductions in downstream peak discharge, thereby reducing downstream flood risk. Introducing CRIMS (LWD dams and riparian buffer strips) into all suitable reaches led to a reduction in peak discharge of  $6.8 \text{ m}^3\text{s}^{-1}$  (5.3 %) for the June 2007 flood event. However, almost half of this reduction could be achieved with interventions in only five reaches. Some reaches therefore have greater potential to contribute to reductions in downstream flood magnitude than others. Additionally, some reaches can have a detrimental impact on downstream flood flows. This is likely to be a result of the synchronisation of the arrival of floodwater from different tributaries (Lane et al., 2007b). The best locations for flow attenuation measures tend to be in the catchment headwaters, where there is a greater potential to desynchronise flood hydrograph contributions to the main river from different tributaries.

Using a rating curve calculated by the HEC-RAS model in Chapter 6, the reduction in peak discharge corresponded to a reduction in peak water level of 0.13 m. Flow attenuation is therefore unlikely to completely protect settlements on the River Seven from flooding. However, it may mitigate flooding by reducing peak flood magnitude and provide an important contribution alongside other measures, such as local defences or flood proofing (Thomas and Nisbet, 2007). At a wider scale, similar schemes in other tributaries to the Rivers Rye and Derwent may also make a cumulative contribution to flood mitigation further downstream. However, the magnitude of peak discharge reduction should be considered within the context of *Overflow's* limitations, which this thesis has aimed to evaluate.

The impact of multiple dispersed small scale interventions requires an assessment of flood risk at the catchment scale. It also requires a consideration of flood events, which in any given location are infrequent and difficult to observe. As a result, numerical modelling is a standard method for flood prediction and management in the UK (Tayefi et al., 2007). However, because of the large spatial scales involved and the limitations on data availability, a number of assumptions and simplifications are required in the model representation of the system. This project has evaluated a reduced complexity hydrologic model, *Overflow*. After calibration, the model was capable of accurately replicating an observed flood event (June 2007). *Overflow* was also shown to behave in a theoretically realistic manner in response to variations in parameters. The model response to parameter values were consistent with its constituent equations and thus had physical explanations. This suggests that the model may be used to predict the impacts of a change to parameter values, such as increased flow resistance. The uncertainty in the model results resulting from parameter selection was significant in the case of individual flow attenuation interventions. However, the overall reduction of peak discharge achieved by multiple, spatially distributed interventions was great enough to be discerned from parameter uncertainty.

However, in the absence of empirical data to validate these predictions, the magnitude of the model response is uncertain.

It was informative to compare *Overflow* with an alternative model of the system. This allowed a comparison of how different methods of process representation responded to flood management interventions. Flood hydrographs predicted at the scale of river reaches were compared to a hydraulic model, HEC-RAS. In all cases *Overflow* predicted higher magnitude hydrographs but was less sensitive to an increase in Manning's  $n$ , which was used to represent flow attenuation. The discrepancy in hydrograph magnitude may be a result of the different constituent equations of each model. Further work may be required to assess the accuracy of flow routing calculations at a scale that is internal to *Overflow*. This is needed to ensure that the model is not over-calibrated to external measurements, to the detriment of selecting physically realistic parameter values and the internal accuracy of flow routing calculations (Bates and Anderson, 2001). Flood hydrographs at the catchment outlet must be calculated as a result of the correct internal processes (i.e. an accurate response to flow attenuation in a particular reach), if the model is to be used for process understanding or as a predictive tool, in situations in which there is no empirical data to validate the results (Lane and Richards, 2001; Kirchner, 2006).

*Overflow's* simplicity represents a trade-off between practical use and explicitly representing physical processes and boundary conditions. Model predictions must therefore be interpreted within the context of the associated uncertainties and limitations of the model. However, in practical terms, *Overflow* is quick to set up, requires comparatively little boundary condition data and can undertake rapid catchment scale simulations. This simplicity and ease of use allows it to be set up for catchment scale flood management investigations, for different events and catchments. It has therefore been successful in achieving its aims of modelling a range of flood management options and their impact on the downstream flood hydrograph, in response to the pressures placed on flood management and the needs of local people.

## References

- Acreman, M. C., Riddington, R. and Booker, D. J. (2003) "Hydrological impacts of floodplain restoration: a case study of the River Cherwell, UK." *Hydrology and Earth System Sciences* **7** (1): 75-85.
- Alexander, D. (2002) "Principles of emergency planning and management." Harpenden: Terra Publishing
- Andrews, L. C. and Phillips, R. L. (2003) "Mathematical Techniques for Engineers and Scientists." Bellingham, Washington: SPIE
- Apel, H., Aronica, G. T., Kreibich, H. and Thieken, A. H. (2009) "Flood risk analyses - how detailed do we need to be?" *Natural Hazards* **49** (1): 79-98
- Arnell, N. W. (1998) "Climate change and water resources in Britain." *Climatic Change* **39**: 83-110.
- Aronica, G., Hankin, B. and Beven, K. (1998) "Uncertainty and equifinality in calibrating distributed roughness coefficients in a flood propagation model with limited data." *Advances in Water Resources* **22** (4): 349-365.
- Atkins (2005) "Making Space for Water: Combating flood risk." Atkins. [Online] Accessed 16th October 2009, from [www.atkinsglobal.com/Images/Making space for water\\_tcm12-4105.pdf](http://www.atkinsglobal.com/Images/Making%20space%20for%20water_tcm12-4105.pdf).
- Barnes, H. H. (1967) "Roughness Characteristics of Natural Channels." US Geological Survey, Water Supply Paper 1849, [Online]. Accessed 23<sup>rd</sup> July 2010, from [http://pubs.usgs.gov/wsp/wsp\\_1849/](http://pubs.usgs.gov/wsp/wsp_1849/).
- Bates, P. D. and Anderson, M. G. (2001) "Validation of hydraulic models." In: M. G. Anderson and P. D. Bates (Eds.), *Model Validation: Perspectives in Hydrological Science*. Chichester: Wiley. pp. 325-356.
- Bates, P. D., Anderson, M. G., Price, D. A., Hardy, R. J. and Smith, C. N. (1996) "Analysis and Development of Hydraulic Models for Floodplain Flows." In: M. G. Anderson, D. E. Walling and P. D. Bates (Eds.), *Floodplain processes*. Chichester: Wiley. pp. 215-254.
- Bates, P. D., Stewart, M. D., Siggers, G. B., Smith, C. N., Hervouet, J. M., Sellin, R. H. J. and TELEMAC (1998) "Internal and External Validation of a Two-Dimensional Finite Element Code for River Flood Simulations." *Proceedings of the Institution of Civil Engineers. Water, Maritime and Energy* **130** (3): 127-141.
- Bathurst, J. C. (1988) "Flow processes and data provision for channel flow models." In: M. G. Anderson (Eds.), *Modelling Geomorphological Systems*. Chichester: Wiley. pp. 127-152.
- Beck, M. B. and Chen, J. (2000) "Assuring the Quality of Models Designed for Predictive Tasks." In: A. Saltelli, K. Chan and E. M. Scott (Eds.), *Sensitivity Analysis*. Chichester: Wiley. pp. 401-420.
- Beven, K. (1989) "Changing ideas in hydrology -- The case of physically-based models." *Journal of Hydrology* **105** (1-2): 157-172.
- Beven, K. (1996) "Equifinality and Uncertainty in Geomorphological Models." In: B. L. Rhoads and C. R. Thorn (Eds.), *Proceedings of the 27th Binghamton Symposium in Geomorphology held 27-29 September 1996*. Chichester: Wiley. pp. 289-313.



- Beven, K. and Freer, J. (2001) "Equifinality, data assimilation, and uncertainty estimation in mechanistic modelling of complex environmental systems using the GLUE methodology." *Journal of Hydrology* **249** (1-4): 11-29.
- Beven, K. J. (2000) "Uniqueness of place and process representations in hydrological modelling." *Hydrology and Earth System Sciences* **4** (2): 203-213.
- Beven, K. J. (2001) "Rainfall-Runoff Modelling: The Primer." Chichester: Wiley.
- Beven, K. J. and Binley, A. M. (1992) "The future of distributed models: calibration and uncertainty prediction." *Hydrological Processes* **6**: 279-298.
- Beven, K. J., Kirkby, M. J., Schofield, N. and Tagg, A. F. (1984) "Testing a physically-based flood forecasting model (TOPMODEL) for three U.K. catchments." *Journal of Hydrology* **69** (1-4): 119-143.
- Birol, E., Hanley, N., Koundouri, P. and Kountouris, Y. (2009) "Optimal management of wetlands: Quantifying trade-offs between flood risks, recreation, and biodiversity conservation." *Water Resources Research* **45** DOI: 10.1029/2008wr006955.
- Broadmeadow, S. and Nisbet, T. R. (2009) "Opportunity Mapping for Woodland to Reduce Flooding in the Yorkshire & Humber Region." Forest Research, Farnham. Accessed 16th March 2010, from [http://www.forestry.gov.uk/pdf/York\\_and\\_Humber\\_flooding\\_final\\_report\\_2009.pdf/\\$FILE/York\\_and\\_Humber\\_flooding\\_final\\_report\\_2009.pdf](http://www.forestry.gov.uk/pdf/York_and_Humber_flooding_final_report_2009.pdf/$FILE/York_and_Humber_flooding_final_report_2009.pdf).
- Brookes, A. (1997) "River Dynamics and Channel Maintenance." In: C. R. Thorne, R. D. Hey and M. D. Newson (Eds.), *Applied Fluvial Geomorphology for River Engineering and Management*. Chichester: Wiley. pp. 293-308.
- Brooks, R. J. and Tobias, A. M. (1996) "Choosing the best model: Level of detail, complexity, and model performance." *Mathematical and Computer Modelling* **24** (4): 1-14.
- Brown, J. D. and Damery, S. L. (2002) "Managing Flood Risk in the UK: Towards an Integration of Social and Technical Perspectives." *Transactions of the Institute of British Geographers* **27** (4): 412-426.
- Brunner, G. W. (2008) "HEC-RAS, River Analysis System Hydraulic Reference Manual." Davis, California, US Army Corps of Engineers, Hydrologic Engineering Center. [Online] Accessed 27<sup>th</sup> September 2010 from, [http://www.hec.usace.army.mil/software/hecras/documents/HEC-RAS\\_4.0\\_Reference\\_Manual.pdf](http://www.hec.usace.army.mil/software/hecras/documents/HEC-RAS_4.0_Reference_Manual.pdf)
- Burt, T. P. (1989) "Storm runoff generation in relation to the flood response of large basins." In: K. Beven and P. Carling (Eds.), *Floods: Hydrological, Sedimentological and Geomorphological Implications*. Chichester: Wiley. pp. 11-35.
- CEH (2008) "National River Flow Archive: Seven at Normanby." Centre for Ecology and Hydrology, Wallingford. Accessed 13th September 2010, from [http://www.nwl.ac.uk/ih/nrfa/station\\_summaries/027/057.html](http://www.nwl.ac.uk/ih/nrfa/station_summaries/027/057.html).
- Chau, K. W., Wu, C. L. and Li, Y. S. (2005) "Comparison of Several Flood Forecasting Models in Yangtze River." *Journal of Hydrologic Engineering* **10** (6): 485-491.
- Chevion, B., Gumiere, S. J., Le Bissonais, Y., Moussa, R. and Raclot, D. (2010) "Sensitivity analysis of distributed erosion models: Framework." *Water Resources Research* **46** (8) DOI: 10.1029/2009wr007950.
- Chow, V. T. (1959) "Open-channel hydraulics." New York: McGraw-Hill.

- Cowan, W. L. (1956) "Estimating Hydraulic Roughness Coefficients." *Agricultural Engineering* **37**: 473-475.
- Crichton, D. (2005) "Flood Risk and Insurance in England and Wales: Are there lessons to be learned from Scotland?" Technical Paper 1, Benfield Hazard Research Centre. [Online] Accessed 19th November 2008, from [http://www.abuhrc.org/Publications/Technical\\_Paper\\_1.pdf](http://www.abuhrc.org/Publications/Technical_Paper_1.pdf).
- Darby, S. E. (1999) "Effect of Riparian Vegetation on Flow Resistance and Flood Potential." *Journal of Hydraulic Engineering* **125** (5): 443-454.
- Defra (2004) "Making Space for Water. Developing a New Government Strategy for Flood and Coastal Erosion Risk Management in England." Department of Environment Food and Rural Affairs, London.
- Defra (2010) "Flood and Water Management Act,." Department for the Environment, Food and Rural Affairs, [Online]. Accessed 16th August 2010, from <http://www.defra.gov.uk/environment/flooding/policy/fwmb/key-areas.htm>.
- Downs, P. W. and Thorne, C. R. (2000) "Rehabilitation of a lowland river: reconciling flood defence with habitat diversity and geomorphological sustainability." *Journal of Environmental Management* **58**: 249-268.
- Emmett, W. W. (1978) "Overland Flow." In: M. J. Kirkby (Ed.), *Hillslope Hydrology*. Chichester: Wiley. pp. 145-177.
- Environment Agency (2007a) "Yorkshire Derwent Catchment Flood Management Plan." Environment Agency, Leeds. Accessed 16<sup>th</sup> December 2009, from [http://publications.environment-agency.gov.uk/pdf/GENE0407BMID-e-e.pdf?lang=\\_e](http://publications.environment-agency.gov.uk/pdf/GENE0407BMID-e-e.pdf?lang=_e).
- Environment Agency. (2007b) "Pickering." *2007 Summer Floods Reviews*. [Online] Accessed 30th November, 2009, from <http://www.environment-agency.gov.uk/research/library/publications/40557.aspx>.
- Environment Agency (2009) "Flooding in England: A National Assessment of Flood Risk." Environment Agency, Bristol. from <http://publications.environment-agency.gov.uk/pdf/GEHO0609BQDS-E-E.pdf>.
- Environment Agency (2010a) "Draft Derwent Catchment Flood Management Plan: Summary Report, January 2010." Environment Agency, Leeds. Accessed 26th July 2010, from <http://publications.environment-agency.gov.uk/pdf/GENE0110BRLJ-e-e.pdf>.
- Environment Agency (2010b) "The costs of the summer 2007 floods in England." *Flood and Coastal Erosion Risk Management Research and Development Programme*, Project: SC070039/R1. Environment Agency, Bristol. from <http://publications.environment-agency.gov.uk/pdf/SCHO1109BRJA-e-e.pdf>.
- Ervine, D. A., Willetts, B. B., Sellin, R. H. J. and Lorena, M. (1993) "Factors Affecting Conveyance in Meandering Compound Flows." *Journal of Hydraulic Engineering* **119** (12): 1383-1399.
- Evans, E. P., Ashley, R., Hall, J., Penning-Rowsell, E. C., Saul, A., Sayers, P., Thorne, C. R. and Watkinson, A. (2004) "Foresight, Future Flooding. Scientific Summary: Volume I, Future risks and their drivers." Office of Science and Technology, London. Accessed 1st December 2006, from [http://www.foresight.gov.uk/Previous\\_Projects/Flood\\_and\\_Coastal\\_Defence/Reports\\_and\\_Publications/Volume1/Chapter2.pdf](http://www.foresight.gov.uk/Previous_Projects/Flood_and_Coastal_Defence/Reports_and_Publications/Volume1/Chapter2.pdf).
- Evans, E. P., Pender, G., Samuels, P. G. and Escarameia, M. (2001) "Scoping study for reducing uncertainty in river flood conveyance." Environment Agency, Bristol. [Online] Accessed

- 15th December 2008, from <http://www.river-conveyance.net/ces/documents/ScopingReport2001.pdf>.
- Evans, E. P., Simm, J. D., Thorne, C. R., Arnell, N. W., Ashley, R. M., Hess, T. M., Lane, S. N., Morris, J., Nicholls, R. J., Penning-Rowsell, E. C., Reynard, N. S., Saul, A. J., Tapsell, S. M., Watkinson, A. R. and Wheeler, H. S. (2008) "An update of the Foresight Future Flooding 2004 qualitative risk analysis." London: Cabinet Office.
- Fasken, G. B. (1963) "Guide for selecting roughness coefficient "n" values for channels." US Department of Agriculture, Lincoln, Nebraska. [Online] Accessed 22nd July 2010, from [http://civil.sharif.edu/~ataie/Hydraulics\\_Course\\_Web/GUIDE%20FOR%20SELECTING%20ROUGHNESS%20COEFFICIENT%20VALUES%20FOR%20CHANNELS.pdf](http://civil.sharif.edu/~ataie/Hydraulics_Course_Web/GUIDE%20FOR%20SELECTING%20ROUGHNESS%20COEFFICIENT%20VALUES%20FOR%20CHANNELS.pdf).
- Ferguson, R. (1986) "Hydraulics and Hydraulic Geometry." *Progress in Physical Geography* **10** (1): 1-31 10.1177/030913338601000101.
- Ferguson, R. (2007) "Flow resistance equations for gravel- and boulder-bed streams." *Water Resources Research* **43** DOI: 10.1029/2006wr005422.
- Fleming, G. (2002) "Learning to live with rivers - the ICE's report to government." *Civil Engineering* **150**: 15-21.
- Fleming, G., Frost, L., Huntingdon, S., Knight, D., Law, F. and Rickard, C. (2001) "Learning to live with rivers: Final Report of the Institution of Civil Engineers' Presidential Commission to Review the Technical Aspects of Flood Risk Management in England and Wales." Institution of Civil Engineers. [Online] Accessed 17th October 2009, from <http://www.ice.org.uk/rtpdf/iceflooding.pdf>.
- Forestry Commission (2007) "Forestry and Flooding." *Regional Forestry Strategy for Yorkshire and the Humber*, Briefing Note 1. Forestry Commission. Accessed 4/2/10, from [http://www.forestry.gov.uk/pdf/forestry\\_and\\_flooding\\_Dec07.pdf/\\$FILE/forestry\\_and\\_flooding\\_Dec07.pdf](http://www.forestry.gov.uk/pdf/forestry_and_flooding_Dec07.pdf/$FILE/forestry_and_flooding_Dec07.pdf).
- Forestry Commission. (2010) "Slowing the flow at Pickering." [Online] Accessed 22/6/10, from <http://www.forestry.gov.uk/website/forestresearch.nsf/ByUnique/INFD-7YML5R>.
- Freer, J., Beven, K. and Ambrose, B. (1996) "Bayesian Estimation of Uncertainty in Runoff Prediction and the Value of Data: An Application of the GLUE Approach." *Water Resources Research* **32** (7): 2161-2173 10.1029/95wr03723.
- Green, I. R. A. and Stephenson, D. (1986) "Criteria for comparison of single event models." *Hydrological Sciences Journal* **31** (3): 395-411.
- Haestad Methods, Dyhouse, G. R., Hatchett, J. and Benn, J. (2003) "Floodplain modelling using HEC-RAS." Waterbury: Haestad Press.
- Hamby, D. M. (1994) "A review of techniques for parameter sensitivity analysis of environmental models." *Environmental Monitoring and Assessment* **32** (2): 135-154 10.1007/BF00547132.
- Hamer, B. A. and Mocke, R. (2002) "Flood risk modelling: a crisis of confidence?" *Civil Engineering* **150**: 30-35.
- Hamilton, S. (2007) "Just say NO to equifinality." *Hydrological Processes* **21** (14): 1979-1980.
- Hardy, R. J. (2008) "Geomorphology Fluid Flow Modelling: Can Fluvial Flow Only Be Modelled Using a Three-Dimensional Approach?" *Geography Compass* **2** (1): 215-234.

- Hardy, R. J., Lane, S., Ferguson, R. and Parsons, D. R. (2003) "Assessing the credibility of a series of computational fluid dynamic simulations of open channel flow." *Hydrological Processes* **17**: 1539-1560.
- Hess, T. M., Holman, I. P., Rose, S. C., Rosolova, Z. and Parrott, A. (2010) "Estimating the impact of rural land management changes on catchment runoff generation in England and Wales." *Hydrological Processes* **24** (10): 1357-1368.
- HMSO (2006) "Planning Policy Statement 25: Development and Flood Risk." DEFRA. [Online] Accessed 20<sup>th</sup> January 2009, from <http://www.communities.gov.uk/planningandbuilding/planningsystem/planningpolicy/planningpolicystatements/pps25/>
- Horritt, M. S. (2006) "A methodology for the validation of uncertain flood inundation models." *Journal of Hydrology* **326** (1-4): 153-165.
- Horritt, M. S. and Bates, P. D. (2002) "Evaluation of 1D and 2D numerical models for predicting river flood inundation." *Journal of Hydrology* **268** (1-4): 87-99.
- Houghton-Carr, H. (1999) "Flood Estimation Handbook: Volume 4, Restatement and application of the Flood Studies Report rainfall-runoff method." Wallingford: Institute of Hydrology.
- Hulme, M., Jenkins, G. J., Lu, X., Turnpenny, J. R., Mitchell, T. D., Jones, R. G., Lowe, J. A., Murphy, J. M., Hassell, D., Boorman, P., McDonald, R. and Hill, S. (2002) "Climate change scenarios for the United Kingdom: The UKCIP02 Scientific Report." Tyndall Centre for Climate Change Research, School of Environmental Sciences, University of East Anglia, Norwich.
- Hunter, N. M., Bates, P. D., Horritt, M. S. and Wilson, M. D. (2007) "Simple spatially-distributed models for predicting flood inundation: a review." *Geomorphology* **90**: 208-225.
- Intermap (2011) "NEXTMAP Britain" [Online] Accessed 12<sup>th</sup> April 2011, from [http://info.intermap.com/rs/intermap/images/INTERMAP\\_NMBritain.pdf](http://info.intermap.com/rs/intermap/images/INTERMAP_NMBritain.pdf)
- Ivanović, R. F. and Freer, J. E. (2009) "Science versus politics: truth and uncertainty in predictive modelling." *Hydrological Processes* **23** (17): 2549-2554
- Jackson, B. M., Wheeler, H. S., McIntyre, N. R., Chell, J., Francis, O. J., Frogbrook, Z., Marshall, M., Reynolds, B. and Solloway, I. (2008) "The impact of upland land management on flooding: insights from a multiscale experimental and modelling programme." *Journal of Flood Risk Management* **1** (2): 71-80.
- JBA Consulting (2008a) "Rating Check File: 10. Sinnington." *Rye and Derwent Forecasting Model Report, 2007s2545*. JBA Consulting, Skipton.
- JBA Consulting (2008b) "Rating Check File: 7. Normanby." *Rye and Derwent Forecasting Model Report, 2007s2545*. JBA Consulting, Skipton.
- Johnson, C., Penning-Rowsell, E. and Tapsell, S. (2007) "Aspiration and reality: flood policy, economic damages and the appraisal process." *Area* **39** (2): 214-223.
- Johnson, R. (2007) "Flood Planner: A Manual for the Natural Management of River Floods." WWF Scotland. [Online] Accessed 17<sup>th</sup> October 2007, from [http://www.wwf.org.uk/filelibrary/pdf/floodplanner\\_web.pdf](http://www.wwf.org.uk/filelibrary/pdf/floodplanner_web.pdf)
- Kirchner, J. W. (2006) "Getting the right answers for the right reasons: Linking measurements, analyses, and models to advance the science of hydrology." *Water Resources Research* **42** DOI: 10.1029/2005wr004362.
- Konikow, L. F. and Bredehoeft, J. D. (1992) "Ground-water models cannot be validated." *Advances in Water Resources* **15** (1): 75-83.

- Knighton, D. (1998) "Fluvial Forms and Processes." London: Arnold
- Lane, S. N. (1998) "Hydraulic modelling in hydrology and geomorphology: a review of high resolution approaches." *Hydrological Processes* **12** (8): 1131-1150.
- Lane, S. N. (2003a) "More floods, less rain? Changing hydrology in a Yorkshire context." In: M. Atherden (Eds.), *Global Warming in a Yorkshire Context*. York: PLACE Research Centre.
- Lane, S. N. (2003b) "Numerical modelling in physical geography: understanding, explanation and prediction." In: N. J. Clifford and G. Valentine (Eds.), *Key Methods in Geography*. London: Sage. pp. 263-290.
- Lane, S. N. (2005) "Roughness - time for a re-evaluation?" *Earth Surface Processes and Landforms* **30** (2): 251-253.
- Lane, S. N. (2008) "Slowing the floods in the UK Pennine Uplands...a case of Waiting for Godot?" *Journal of Practical Ecology and Conservation*, 2008. [Online] Accessed 14<sup>th</sup> December 2009 from <http://knowledge-controversies.ouce.ox.ac.uk/Ryedale2/documents/usefuldocuments/Lane.pdf>
- Lane, S. N. and Bates, P. D. (2000) "Introduction." In: P. D. Bates and S. N. Lane (Eds.), *High Resolution Flow Modelling in Hydrology and Geomorphology*. Chichester: Wiley. pp. 1-14.
- Lane, S. N., Bradbrook, K. F., Richards, K. S., Biron, P. A. and Roy, A. G. (1999) "The application of computational fluid dynamics to natural river channels: three-dimensional versus two-dimensional approaches." *Geomorphology* **29** (1-2): 1-20.
- Lane, S. N., Morris, J., O'Connell, P. E. and Quinn, P. F. (2007b) "Managing the rural landscape." In: C. R. Thorne, E. P. Evans and E. C. Penning-Rowsell (Eds.), *Future Flooding and Coastal Erosion Risks*. Chichester: Wiley. pp. 297-319.
- Lane, S. N., Reaney, S. M. and Heathwaite, A. L. (2009) "Representation of landscape hydrological connectivity using a topographically driven surface flow index." *Water Resources Research* **45** (W08423) DOI: 10.1029/2008WR007336.
- Lane, S. N. and Richards, K. S. (2001) "The 'Validation' of Hydrodynamic Models: Some Critical Perspectives." In: M. G. Anderson and P. D. Bates (Eds.), *Model Validation: Perspectives in Hydrological Science*. Chichester: Wiley. pp. 413-438.
- Lane, S. N., Tayefi, V., Reid, S. C., Yu, D. and Hardy, R. J. (2007a) "Interactions between sediment delivery, channel change, climate change and flood risk in a temperate upland environment." *Earth Surface Processes and Landforms* **32** (3): 429-446.
- Lane, S. N. and Thorne, C. R. (2007) "Fluvial Systems and Processes." In: C. R. Thorne, E. P. Evans and E. C. Penning-Rowsell (Eds.), *An update of the Foresight Future Flooding 2004 qualitative risk analysis*. London: Cabinet Office. pp. 83-92.
- Lane, S. N. and Thorne, C. R. (2007) "River Processes." In: C. R. Thorne, E. P. Evans and E. C. Penning-Rowsell (Eds.), *Future flooding and coastal erosion risks*. London: Thomas Telford. pp. 82-99.
- Legates, D. R. and McCabe, G. J., Jr. (1999) "Evaluating the Use of Goodness-of-Fit Measures in Hydrologic and Hydroclimatic Model Validation." *Water Resources Research* **35** (1): 233-241
- Leopold, L. B. and Maddock, T. (1953) "The Hydraulic Geometry of Stream Channels and Some Physiographic Implications." *US Geological Survey Professional Paper 252*. [Online] Accessed 16<sup>th</sup> January 2010, from <http://eps.berkeley.edu/people/lunaleopold/>

- Limerinos, J. T. (1970) "Determination of the Manning Coefficient From Measured Bed Roughness in Natural Channels." *US Geological Survey Water-Supply Paper 1898-B*.
- Lin, B., Wicks, J. M., Falconer, R. A. and Adams, K. (2006) "Integrating 1D and 2D hydrodynamic models for flood simulation." *Water Management* **159** (1): 19-25.
- Lopes, L. F. G., Do Carmo, J. S. A., Vitor Cortes, R. M. and Oliveira, D. (2004) "Hydrodynamics and water quality modelling in a regulated river segment: application on the instream flow definition." *Ecological Modelling* **173** (2-3): 197-218.
- Manning, R. (1891) "On the flow of water in open channels and pipes." *Transactions of the Institute of Civil Engineers* **20**: 161-207.
- Marks, K. and Bates, P. D. (2000) "Integration of high-resolution topographic data with floodplain flow models." *Hydrological Processes* **14**: 2109-2122.
- Marrington, S. (2010) "Outline Specification for the Construction of Large Woody Debris Dams." Pickering, Forest Research, Unpublished Work.
- McCuen, R. H. (1973) "The role of sensitivity analysis in hydrologic modeling." *Journal of Hydrology* **18** (1): 37-53.
- McCuen, R. H., Knight, Z. and Cutter, A. G. (2006) "Evaluation of the Nash--Sutcliffe Efficiency Index." *Journal of Hydrologic Engineering* **11** (6): 597-602.
- Mendenhall, W., Beaver, R. J. and Beaver, B. M. (2009) "Introduction to Probability and Statistics." Belmont: Brooks/Cole.
- Morris, J., Posthumus, H., Trawick, P., Hess, T., Neville, D., Philips, E. and Wysoki, M. (2008b) "Impacts of summer 2007 floods on rural communities in England." Cranfield University; Commission for Rural Communities. Accessed 17th October 2009, from <http://www.ruralcommunities.gov.uk/publications/impactsofsummer2007floodsonruralcommunitiesinengland>.
- Morton, A. (1993) "Mathematical Models: Questions of Trustworthiness." *The British Journal for the Philosophy of Science* **44**: 659-674.
- Mulligan, M. (2002) "Modelling Catchment Hydrology." In: J. Wainwright and M. Mulligan (Eds.), *Environmental Modelling: Finding Simplicity in Complexity*. Chichester: Wiley. pp. 107-122.
- Mulligan, M. and Wainwright, J. (2002) "Modelling and Model Building." In: J. Wainwright and M. Mulligan (Eds.), *Environmental Modelling: Finding Simplicity in Complexity*. Chichester: Wiley. pp. 7-74.
- Murphy, J., Sexton, D., Jenkins, G., Boorman, P., Booth, B., Brown, K., Clark, R., Collins, M., Harris, G. and Kendon, L. (2009) "UKCP09 Climate Change Projections." UK Climate Impacts Programme, [Online]. Accessed 18th August 2010, from <http://ukclimateprojections.defra.gov.uk/content/view/824/500/>.
- Nash, J. E. and Sutcliffe, J. V. (1970) "River flow forecasting through conceptual models part I -- A discussion of principles." *Journal of Hydrology* **10** (3): 282-290.
- Nisbet, T. R. and Broadmeadow, S. (2003) "Opportunity mapping for trees and floods: final report to the Parrett Catchment Project Wet Woodland Group."
- O'Callaghan, J. F. and Mark, D. M. (1984) "The extraction of drainage networks from digital elevation data." *Computer Vision, Graphics, and Image Processing* **28**: 323-344.
- Odoni, N. A. (2007) "Exploring equifinality in a landscape evolution model." *Ph.D. Thesis*, University of Southampton.

- Odoni, N. A. and Lane, S. N. (2010) "Assessment of the impact of upstream land management measures on flood flows in Pickering Beck using Overflow." Forestry Commission, [Online]. Accessed 6th August 2010, from [http://www.forestry.gov.uk/pdf/Pickering\\_crim\\_report\\_April\\_2010.pdf/\\$FILE/Pickering\\_crim\\_report\\_April\\_2010.pdf](http://www.forestry.gov.uk/pdf/Pickering_crim_report_April_2010.pdf/$FILE/Pickering_crim_report_April_2010.pdf).
- Odoni, N. A. and Lane, S. N. (Forthcoming) "Development of the OVERLOW distributed model for testing catchment-wide land management interventions to reduce flood risk: (1) model conception and testing." *Hydrological Processes*.
- Odoni, N. A. and Lane, S. N. (In preparation) "Knowledge-Theoretic Models in Hydrology."
- Pappenberger, F., Beven, K., Horritt, M. and Blazkova, S. (2005) "Uncertainty in the calibration of effective roughness parameters in HEC-RAS using inundation and downstream level observations." *Journal of Hydrology* **302** (1-4): 46-69.
- Parrott, A., Brooks, W., Harmar, O. and Pygott, K. (2009) "Role of rural land use management in flood and coastal risk management." *Journal of Flood Risk Management* **2** (4): 272-284.
- Perrin, C., Michel, C. and Andréassian, V. (2001) "Does a large number of parameters enhance model performance? Comparative assessment of common catchment model structures on 429 catchments." *Journal of Hydrology* **242** (3-4): 275-301.
- Pinter, N. and Heine, R. A. (2005) "Hydrodynamic and morphodynamic response to river engineering documented by fixed-discharge analysis, Lower Missouri River, USA." *Journal of Hydrology* **302** (1-4): 70-91.
- Pitt, M. (2008) "*The Pitt Review: Learning Lessons from the 2007 Floods*." London: Cabinet Office. [Online] Accessed 30th November 2008, from [http://archive.cabinetoffice.gov.uk/pittreview/thepittreview/final\\_report.html](http://archive.cabinetoffice.gov.uk/pittreview/thepittreview/final_report.html).
- Planchon, O. and Darboux, F. (2001) "A fast, simple and versatile algorithm to fill the depressions of digital elevation models." *Catena* **46**: 159-179.
- Posthumus, H., Hewett, C. J. M., Morris, J. and Quinn, P. F. (2008) "Agricultural land use and flood risk management: Engaging with stakeholders in North Yorkshire." *Agricultural Water Management* **95** (7): 787-798.
- Quinn, P. F., Beven, K., Chevallier, P. and Planchon, O. (1991) "The prediction of hillslope flow paths for distributed hydrological modelling using digital terrain models." *Hydrological Processes* **5**: 59-79.
- Raven, E. K., Lane, S. N., Ferguson, R. I. and Bracken, L. J. (2009) "The spatial and temporal patterns of aggradation in a temperate, upland, gravel-bed river." *Earth Surface Processes and Landforms* **34** (9): 1181-1197.
- Rhoads, B. L. and Thorn, C. R. (1996) "Towards a Philosophy of Geomorphology." In: B. L. Rhoads and C. R. Thorn (Eds.), *Proceedings of the 27th Binghamton Symposium in Geomorphology, 27-29th September 1996*. Chichester: Wiley. pp. 115-144.
- Rice, S. (2003) "Sampling in geography." In: N. J. Clifford and G. Valentine (Eds.), *Key methods in geography*. London: Sage. pp. 223-248.
- Richards, K. (1996) "Samples and Cases: Generalisation and Explanation in Geomorphology." In: B. L. Rhoads and C. R. Thorn (Eds.), *Proceedings of the 27th Binghamton Symposium in Geomorphology, 27-29 September 1996*. Chichester: Wiley. pp. 171-190.
- Robson, A. J. and Reed, D. (1999) "Flood Estimation Handbook: Volume 3, Statistical Procedures for Flood Frequency Estimation." Wallingford: Institute of Hydrology.

- Romanowicz, R. and Beven, K. (1998) "Dynamic real-time prediction of flood inundation probabilities." *Hydrological Sciences Journal* **43** (2): 181-196.
- Ryedale Flood Research Group (2008) "Making Space for People: Involving Local Knowledge in Flood Risk Research and Management in Ryedale, Yorkshire." [Online] Accessed 28th October 2009, from [http://knowledge-controversies.ouce.ox.ac.uk/ryedaleexhibition/Making\\_Space\\_for\\_People.pdf](http://knowledge-controversies.ouce.ox.ac.uk/ryedaleexhibition/Making_Space_for_People.pdf).
- Saltelli, A., Ratto, M., Andres, T., Campolongo, F., Cariboni, J., Gatelli, D., Saisana, M. and Tarantola, S. (2008) "Global Sensitivity Analysis. The Primer." Chichester: Wiley.
- Samuels, P. G. (1990) "Cross-section location in 1-D models." *International Conference on River Flood Hydraulics*, Wallingford, 17th - 20th September 1990. Chichester: Wiley. 339-350
- Sanchez, S. M. (2006) "Work smarter, not harder: Guidelines for designing simulation experiments." In: M. E. Kuhl, N. M. Steiger, F. B. Armstrong and J. A. Joines (Eds.), *Proceedings of the 2005 Winter Simulation Conference*. pp. 69-82.
- Sear, D. A., Newson, M. D. and Brookes, A. (1995) "Sediment-related river maintenance: The role of fluvial geomorphology." *Earth Surface Processes and Landforms* **20** (7): 629-647.
- Shaw, E. M. (1994) "Hydrology in Practice." London: Chapman & Hall.
- Shreve, R. L. (1966) "Statistical Law of Stream Numbers." *The Journal of Geology* **74** (1): 17-37.
- Smith, J. and Smith, P. (2007) "Environmental Modelling: An Introduction." Oxford: Oxford University Press.
- Stover, S. C. and Montgomery, D. R. (2001) "Channel change and flooding, Skokomish River, Washington." *Journal of Hydrology* **243** (3-4): 272-286.
- Tayefi, V., Lane, S. N., Hardy, R. J. and Yu, D. (2007) "A comparison of one- and two-dimensional approaches to modelling flood inundation over complex upland floodplains." *Hydrological Processes* **21** (23): 3190-3202.
- Taylor, J. R. (1982) "An introduction to error analysis: the study of uncertainties in physical measurements." Mill Valley, Calif: University Science Books.
- Thomas, H. and Nisbet, T. R. (2007) "An assessment of the impact of floodplain woodland on flood flows." *Water and Environment Journal* **21**: 114-126.
- Thorn, C. E. (2003) "The Critical Role of 'Qualitative Thought' in Physical Geography and Geomorphological Research." In: N. J. Clifford and G. Valentine (Eds.), *Key Methods in Geography*. London: Sage. pp. 249-262.
- Thorne, C., Evans, E. and Penning-Rowsell, E., Eds. (2006) "Future flooding and coastal erosion risks." London: Thomas Telford.
- Van Huffel, S. and Vandewalle, J. (1991) "The Total Least Squares Problem: Computational Aspects and Analysis." Philadelphia: Society for Industrial and Applied Mathematics.
- von Lany, P. H. and Palmer, J. (2007) "River engineering responses." In: C. R. Thorne, E. P. Evans and E. C. Penning-Rowsell (Eds.), *Future flooding and coastal erosion risks*. London: Thomas Telford. pp. 375-391.
- Werritty, A. (2006) "Sustainable flood management: oxymoron or new paradigm?" *Area* **38** (1): 16-23
- Whatmore, S. J. and Landström, C. (2009) "Manning's N - Putting Roughness to Work." In: M. Morgan and P. Howlett (Eds.), *How well do facts travel?* Cambridge: Cambridge University Press. pp. 111-135.



- Wheater, H. S. (2006) "Flood hazard and management: a UK perspective." *Philosophical Transactions of the Royal Society of London A* **364**: 2135-2145.
- Wilcox, A. C., Nelson, J. M. and Wohl, E. E. (2006) "Flow resistance dynamics in step-pool channels: 2. Partitioning between grain, spill, and woody debris resistance." *Water Resources Research* **42** DOI: 10.1029/2005wr004278.
- Wilcox, A. C. and Wohl, E. E. (2006) "Flow resistance dynamics in step-pool stream channels: 1. Large woody debris and controls on total resistance." *Water Resources Research* **42** DOI: 10.1029/2005wr004277.
- Wilson, E. M. (1990) "Engineering Hydrology." Basingstoke: Palgrave Macmillan.
- Wohl, E. E. (1998) "Uncertainty in Flood Estimates Associated with Roughness Coefficient." *Journal of Hydraulic Engineering* **124** (2): 219-223.
- Wu, C. F. J. and Hamada, M. (2000) "Experiments: planning analysis and parameter design optimization." Chichester: Wiley.
- Wydoski, R. S. and Wick, E. J. (2000) "Flooding and Aquatic Ecosystems." In: E. E. Wohl (Eds.), *Inland Flood Hazards: Human, riparian, and aquatic communities*. Cambridge: Cambridge University Press. pp. 238-270.
- Young, P., Parkinson, S. and Lees, M. (1996) "Simplicity out of complexity in environmental modelling: Occam's razor revisited." *Journal of Applied Statistics* **23**: 165-210.
- Yu, D. and Lane, S. N. (2006a) "Urban fluvial flood modelling using a two-dimensional diffusion-wave treatment, part 1: mesh resolution effects." *Hydrological Processes* **20** (7): 1541-1565.
- Yu, D. and Lane, S. N. (2006b) "Urban fluvial flood modelling using a two-dimensional diffusion-wave treatment, part 2: development of a sub-grid-scale treatment." *Hydrological Processes* **20** (7): 1567-1583.

## Appendix 1: Index of Manning's $n$ values

Manning's  $n$  values and associated descriptions from:

Chow, V. T. (1959) "Open-channel hydraulics." New York, McGraw-Hill, pp. 109-113.

Excerpts relevant to the channel and land cover types of the River Seven (natural channels and floodplains) are given.

Type of Channel and Description	Minimum	Normal	Maximum
<b>Natural streams</b>			
1. Clean, straight, full stage, no rifts or deep pools	0.025	0.030	0.033
2. Same as above, but more stones and weeds	0.030	0.035	0.040
3. Clean, winding, some pools and shoals	0.033	0.040	0.045
4. Same as above, but some weeds and stones	0.035	0.045	0.050
5. Same as above, lower stages, more ineffective slopes and sections	0.040	0.048	0.055
6. Same as '4', but more stones	0.045	0.050	0.060
7. Sluggish reaches, weedy, deep pools	0.050	0.070	0.080
8. Very weedy reaches, deep pools, or floodways with heavy stand of timber and underbrush	0.075	0.100	0.150
<b>Floodplains</b>			
a. Pasture, no brush			
1. Short grass	0.025	0.030	0.035
2. High grass	0.030	0.035	0.050
b. Cultivated areas			
1. No crop	0.020	0.030	0.040
2. Mature row crops	0.025	0.035	0.045
3. Mature field crops	0.030	0.040	0.050

Type of Channel and Description	Minimum	Normal	Maximum
c. Brush			
1. Scattered brush, heavy weeds	0.035	0.050	0.070
2. Light brush and trees, in winter	0.035	0.050	0.060
3. Light brush and trees, in summer	0.040	0.060	0.080
4. Medium to dense brush, in winter	0.045	0.070	0.110
5. Medium to dense brush, in summer	0.070	0.100	0.160
d. Trees			
1. Dense willows, summer, straight	0.110	0.150	0.200
2. Cleared land with tree stumps, no sprouts	0.030	0.040	0.050
3. Same as above, but with heavy growth of sprouts	0.050	0.060	0.080
4. Heavy stand of timber, a few down trees, little undergrowth, flood stage below branches	0.080	0.100	0.120
5. Same as above, but with flood stage reaching branches	0.100	0.120	0.160

## Appendix 2: Frequently used terms and definitions.

<b>Boundary conditions</b>	Data that constrain the model equations to a particular place and period of time (e.g. observations of a particular flow event).
<b>Calibration</b>	The process of adjusting parameter values to obtain a better match between model predictions and observations.
<b>Catchment</b>	The area of land that drains through a particular point. In the case of this project, the area of land drained by the River Seven at Normanby.
<b>CRIM</b>	‘Catchment Riparian Intervention Measure’; a term used to define interventions in the river channel or adjacent floodplain designed to cause flow attenuation.
<b>Cumecs</b>	An abbreviation for ‘cubic metres per second’ ( $\text{m}^3\text{s}^{-1}$ ), the units in which discharge is measured.
<b>Discharge</b>	The volume of water passing through a point over a given period of time. Measured in $\text{m}^3\text{s}^{-1}$ .
<b>DEM</b>	An acronym for ‘Digital Elevation Model’, a digital representation of the topography and elevation of the land surface.
<b>Effective rainfall</b>	In <i>Overflow</i> , the net rainfall after subtraction of evaporation or infiltration losses. This is used to calculate the volume of water routed overland.
<b>Equifinality</b>	The concept that there may be many parameter values or models for the same catchment and event, which give acceptable predictions.
<b>Large woody debris (LWD) dam</b>	Woody material, such as tree trunks and branches, which may naturally or artificially form a dam across the channel. LWD dams increase flow resistance and are represented in this project by a Manning’s $n$ value of 0.14.
<b>Main effects test</b>	A simulation of the impact of variations in an individual parameter or other input on the modelled response.
<b>Monte Carlo</b>	Multiple model simulations, each with a randomly chosen parameter set, in which each parameter is selected from a uniform distribution across the range of feasible values for that parameter.
<b>NSE</b>	‘Nash Sutcliffe Efficiency’. An objective function used to quantify the difference between two hydrographs.

<b>OAT sampling</b>	'One-at-a-time' sampling in which each parameter value is varied in turn, so that any change in model outputs can be attributed solely to that parameter.
<b>Optimisation</b>	The process of finding a parameter set that gives the 'best-fit' of model predictions to observations.
<b>Parameter</b>	A constant in the model equations. Parameters are often selected by a process of calibration and, as such, may be used to account for unknown processes and data.
<b>Parameter space</b>	The range of feasible values that parameters can take.
<b>PDF</b>	'Probability density function'. A plot of the likelihood that a particular model result will occur in response to a particular parameter value.
<b>Rating curve</b>	A statistical relationship between discharge and stage at a given point in a river. Many gauging stations only regularly measure stage, so rating curves are used to predict discharge from stage measurements.
<b>Reach</b>	A stretch of river channel between its confluence with one tributary and the next, or in the case of a first order channel, from its source to its confluence with the next tributary.
<b>Response surface</b>	The relationship between model inputs, e.g. parameter values, and the model response, e.g. a statistical function.
<b>Riparian buffer strip</b>	Overbank vegetation that occurs alongside the river channel and increases flow resistance. Represented by a Manning's $n$ value of 0.16 for the first 20 m either side of a reach.
<b>Sensitivity analysis</b>	An assessment of the variability in model results caused by variability (or uncertainty) in the selection of values for particular parameters.
<b>Stage</b>	Depth of water above the river channel bed. Measured in metres.
<b>Uncertainty analysis</b>	An assessment of how uncertainty in parameter selection propagates to uncertainty in model results.
<b>Validation</b>	An evaluation of a model by comparison with observed data.
<b>Verification</b>	An evaluation of whether a model solves its constituent equations correctly.